PATHWAYS TO PERCEPTION

Aidan T. Williams

PATHWAYS TO PERCEPTION

Sexual differentiation and pheromone communication in parasitoid wasps

Aidan T. Williams

Propositions

1. The driving force behind the evolution of eusociality in Hymenoptera is pheromonal complexity in parasitoid wasps.
   (this thesis)

2. *Drosophila* is not a panacea for deciphering pheromone communication.
   (this thesis)

3. Institutional collaboration in academia is a double-edged sword.

4. Increasing pressure to innovate conflates the concepts of conjecture, hypothesis and theory in academic research.

5. Curbing overconsumption in society means fighting against our inherent instincts.

6. Discourse on gender identity benefits from scientific input on sex determination.

Propositions belonging to the thesis, entitled

Pathways to Perception: Sexual differentiation and pheromone communication in parasitoid wasps

Aidan Thomas Williams
Wageningen, 9 January 2026

Pathways to Perception

Sexual differentiation and pheromone communication in parasitoid wasps

Aidan Thomas Williams

Thesis committee

Promotor
Prof. Dr Marcel Dicke
Professor of Entomology
Wageningen University & Research

Co-promotor
Dr Eveline C. Verhulst
Associate professor in Entomology
Wageningen University & Research

Other members
Prof. Dr J. C. Billeter, University of Groningen
Prof. Dr C. H. J. van Oers, Wageningen University & Research
Prof. Dr A. T. Groot, University of Amsterdam
Dr N. E. Fatouros, Wageningen University & Research

This research was conducted under the auspices of the C.T. de Wit Graduate School for Production Ecology & Resource Conservation

Pathways to Perception

Sexual differentiation and pheromone communication in parasitoid wasps

Aidan Thomas Williams

Thesis

submitted in fulfilment of the requirements for the degree of doctor

at Wageningen University

by the authority of the Rector Magnificus,

Prof. Dr C. Kroeze,

in the presence of the

Thesis Committee appointed by the Academic Board

to be defended in public

on Friday 9 January 2026

at 1 p.m. in the Omnia Auditorium.

Aidan Thomas Williams
Pathways to Perception: Sexual differentiation and pheromone communication in parasitoid wasps
237 pages

PhD thesis, Wageningen University, Wageningen, the Netherlands (2026)
With references, with summary in English

ISBN: 978-94-6534-011-1
DOI: 10.18174/681123

Table of contents

Chapter 1

General introduction

Chemical signalling and pheromones

Chemical signalling involves sending and receiving chemical information in the form of infochemicals (Dicke & Sabelis, 1988). It is the oldest and most universal form of communication and occurs at all levels of biological organization (Wilson, 1970). This includes the regulation of cells and organs within plants and animals as well as the ecological interactions between individual organisms. Semiochemicals comprise a whole range of chemical substances. One such group comprises the pheromones (from Greek *pherein* to bear and *hormōn* to stimulate), which have evolved in one individual to elicit a behavioural response in another individual of the same species (Wyatt, 2014). Although chemical signalling has been recognized in animals for some time, it was the German biochemist Adolf Butenandt who was the first to identify a pheromone (bombykol) in 1959 (Butenandt *et al*., 1961). Since this discovery, research has identified pheromones throughout the animal kingdom, ranging from algae, yeasts and bacteria to crustaceans, fish and mammals (Wyatt, 2014). But also, significantly, in insects.

Pheromone communication in insects

The most sophisticated form of pheromone communication can arguably be found in insects. Edward O. Wilson and William Bossart divided insect pheromones into two types: releasers and primers (Wilson & Bossert, 1963). Releasers are pheromones that elicit a specific and immediate behavioural response, whereas primers induce long-term physiological responses. Releaser pheromones are not only known as sex attractants, but are also utilized for a range of other functions, such as aggregation, dispersion, alarm, tracking, marking, egg-laying, recruitment and for brood- and cast-recognition (Wyatt, 2014). Insect pheromones are produced in various specialized secretory glands distributed throughout the body (Tillman *et al*., 1999). There is evidence that most insect pheromones evolved from chemical precursor compounds that were either metabolic by-products or had a non-communicative function (Stökl & Steiger, 2017). These precursor compounds originate from normal metabolic pathways, such as fatty-acid and isoprenoid synthesis (Tillman *et al*., 1999). This sender-precursor hypothesis predicts that pheromones can evolve from any compound that is released by one individual and detected by another of the same species.

Compounds evolve into pheromones when the receiver is able to detect the biochemistry of the compound and to associate it with a specific condition, such as the identity and presence of the sending individual (Steiger *et al*., 2011; Wyatt, 2014). Insects have evolved specialized sensory organs and chemosensory receptors to perceive pheromones. Darwin was one of the first to recognize the pheromone-detecting capabilities of the antennae of male moths (Darwin, 1871). A number of male moths have evolved elaborate bipectinate antennae that are more sensitive to lower quantities of the female sex pheromone. The great flexibility of the insect olfactory system means that any type of chemical compound can be detected and potentially evolve into a pheromone (Wyatt, 2014). Sensitivity to these chemosensory stimuli

can therefore evolve to exploit chemical compounds that possess a signal value to the receiver. If perceiving these compounds leads to greater reproductive success or survival, sexual selection can work on improving selectivity and sensitivity in the receiver, and increasing pheromone production in the sender. This process ultimately results in assortative mating and sexual dimorphism, where mate choice is based on sender-receiver preferences (Buchinger & Li, 2023; Johansson & Jones, 2007; Steiger & Stökl, 2014).

Sexual differentiation in pheromone communication

The process of sexual differentiation literally means the development of differences between sexes of the same species. This process leads to sexual dimorphism, where males and females exhibit dissimilar morphological traits other than their sexual organs. Sexual differentiation in pheromone communication determines the sex-specific behavioural and physiological responses to pheromones. Males and females may produce different pheromones and have distinct chemosensory receptors to perceive them, or they may produce the same pheromone and have the same receptor, but a sexually dimorphic neural circuit to process the information. Sexual differentiation in these traits is regulated by the sex-determination pathway (**Figure 1**) (Billeter *et al*., 2006a; Rideout *et al*., 2006; Ferveur *et al*., 1997; Savarit & Ferveur, 2002). This pathway is initiated by a primary signal, which is transduced by instructor genes to a conserved splicing factor required for sexual differentiation (Saccone, 2022). While primary signals are extremely diverse among insect species, genes further downstream are widely conserved in terms of their function and position in the cascade (Gamble & Zarkower, 2012; Sánchez, 2008; Wilkins, 1995). Accordingly, most insect species share a common sex-determination mechanism, comprising a conserved binary switch or splicing-factor gene, called *Transformer* (*Tra*), and the transcription-factor gene, *Doublesex* (*Dsx*) (Verhulst *et al*., 2010b; Verhulst & van de Zande, 2015). Instructive primary signals either turn *Tra* ON for female differentiation or OFF for male differentiation (Bopp *et al*., 2014).

The sex-determination pathway in insects

In most insects, the ON-OFF regulation of *Tra* results from its sex-specific alternative splicing (Bopp *et al*., 2014). Only female-specific splicing of *Tra* mRNA (*TraF*) yields a functional protein (TRA), whereas in males a non-functional truncated protein is produced (Verhulst *et al*., 2010b). The primary instructor signals that regulate the splicing of *Tra* are extremely diverse and species-specific. Examples of these signals include the X-linked signal elements (XSEs) communicating the X-chromosome dose in *Drosophila*, piwi-interacting RNA (piRNA) in Lepidoptera and *Wasp overruler of masculinization* (*Wom*) in *Nasonia* (**Figure 1**) (Laslo *et al*., 2023).

Transformer functions as a splicing factor of the conserved gene *Dsx* and has been shown to splice other genes, such as *Fruitless* (*Fru*) in *Drosophila melanogaster*. The pre-mRNA of *Dsx* and *Fru* is a target for the TRA protein, which is only present in females and regulates female-

specific splicing, resulting in female differentiation. In males, the absence of the TRA protein results in male-specific splicing of *Dsx* and *Fru* pre-mRNA and consequently in male differentiation (Ryner *et al*., 1996; Verhulst *et al*., 2010b) Both male- and female-specific splicing of *Dsx* result in functional DSX proteins, whereas in *D. melanogaster* it has been shown that only male-specific splicing of *Fru* results in a functional FRU protein (Ryner *et al*., 1996).

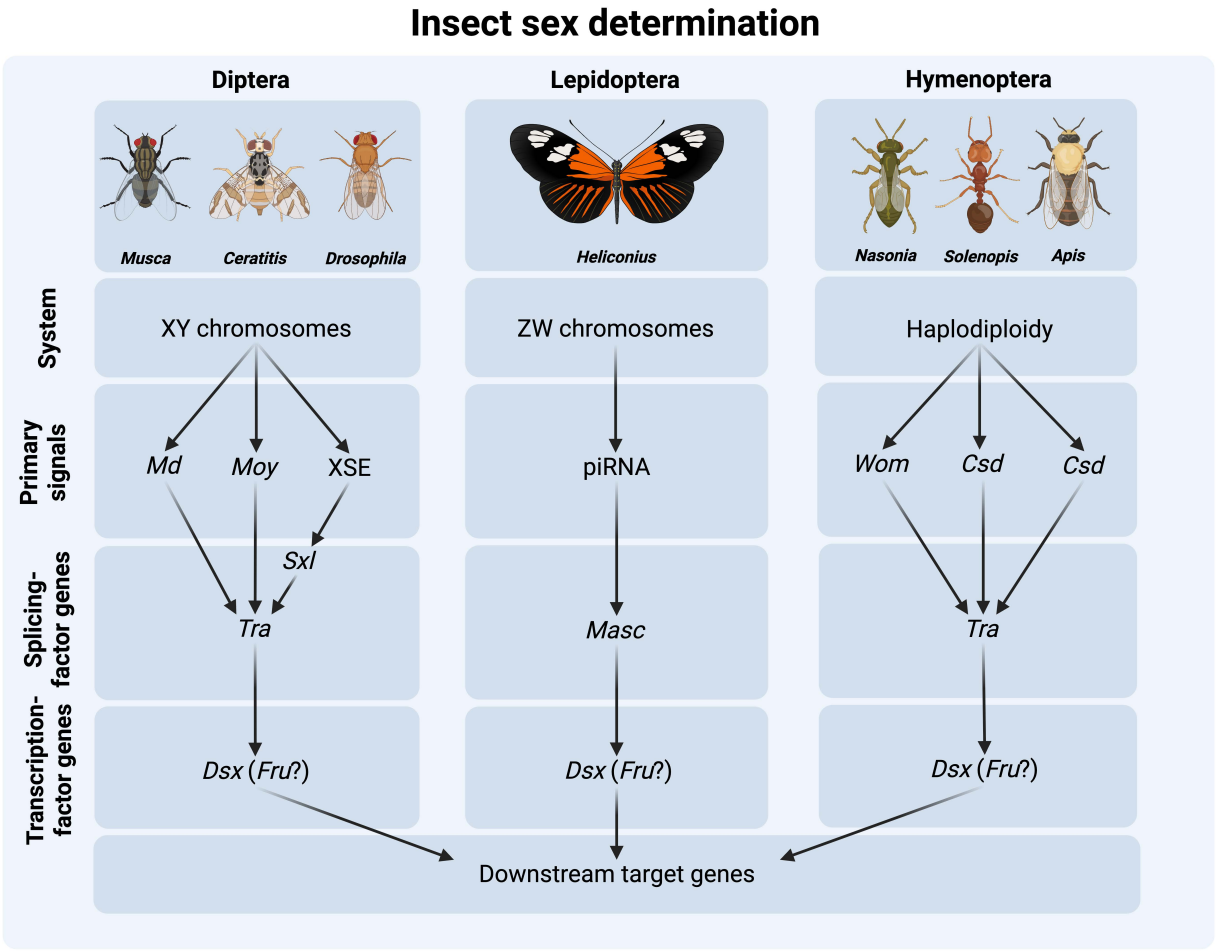

Figure 1: The sex-determination pathway in insects.
Insects possess different sex-determination systems, such as XY chromosomes in Diptera, ZW chromosomes in Lepidoptera and haplodiploidy in Hymenoptera. The upstream signalling elements in these systems vary widely among insects. The primary instructor signals are the sex-determining signals. These include *Male determiner* (*Md*), *Maleness-on-the-y* (*Moy*), X-linked signal elements (XSEs), piwi-interacting RNA (piRNA), *Wasp overruler of masculinization* (*Wom*) and *Complementary sex determiner* (*Csd*). Primary signals are transduced to conserved splicing-factor genes, *Transformer* (*Tra*) in Diptera and Hymenoptera and *Masculinizer* (*Masc*) in Lepidoptera. The splicing factors TRA and MASC regulate the splicing of *Doublesex* (*Dsx*) and potentially *Fruitless* (*Fru*). *Dsx* and *Fru* encode for transcription factors that activate or repress the sex-biased expression of downstream genes.

The transcription-factor genes *Dsx* and *Fru* have been shown to regulate morphological and behavioural sexual differentiation in insects. These transcription factors either activate or repress the sex-biased expression of their target genes by binding to *cis*-regulatory elements (Neville *et al*., 2014; Verhulst & van de Zande, 2015). *Doublesex* regulates the sexual identity of cells when required, by determining their function and morphology in both males and

females (Verhulst & van de Zande, 2015). *Fruitless*, on the other hand, plays a male-specific role in *D. melanogaster* (Demir & Dickson, 2005; Gailey *et al*., 2006). Both genes are important for regulating biosynthesis, chemoreception and neural circuits in insect pheromone communication (Bray & Amrein, 2003; Kimura *et al*., 2008; Kurtovic *et al*., 2007; Shirangi *et al*., 2009; Sun *et al*., 2023a; Zhou *et al*., 2014). It can therefore be postulated that sexual dimorphism in the production and perception of pheromones is attributed to the sex-specific regulation of genes by DSX and FRU.

Focus area and knowledge gap

Given the significant role that DSX and FRU play in regulating biosynthesis, chemoreception and neurodevelopment in pheromone communication, research on how these transcription factors regulate these pathways has primarily been limited to the model organism *Drosophila*. However, this species utilizes a so-called dedicated labelled-line system to perceive and process pheromones (Keesey & Hansson, 2021; Kurtovic *et al*., 2007). Other insects, including Hymenoptera, have evolved a combinatorial-coding system to discriminate pheromones (Brandstaetter & Kleineidam, 2011; Carcaud *et al*., 2015; Couto *et al*., 2017, 2023; d'Ettorre *et al*., 2017; Galizia & Rössler, 2010; Joerges *et al*., 1997; Marty *et al*., 2025; McKenzie *et al*., 2016; McKenzie & Kronauer, 2018; Sandoz *et al*., 2007; Wang *et al*., 2008; Yamagata *et al*., 2006; Zube *et al*., 2008).

Previous research in Diptera and Lepidoptera provides evidence that these insects perceive pheromones through dedicated neural circuits, called labelled lines (Galizia, 2014; Haverkamp *et al*., 2018; Hildebrand & Shepherd, 1997; Keesey & Hansson, 2021; Kurtovic *et al*., 2007; Touhara & Vosshall, 2009). The pheromone receptors in these species are narrowly tuned to the individual components of a pheromone blend and correspond to specialized glomeruli in the antennal lobe, for example the macroglomerular complex in male moths. It has been asserted that this labelled-line coding system has typically evolved for processing those compounds with a high ecological relevance, such as pheromones (Haverkamp *et al*., 2018; Keesey & Hansson, 2021). However, labelled lines are not a prerequisite for processing pheromones, as other insects use broadly tuned receptors for specific pheromone compounds that activate multiple glomeruli in the antennal lobe.

Pheromone coding in Hymenoptera utilizes a system in which a single pheromone compound can activate combinations of pheromone receptors and glomeruli (Brandstaetter & Kleineidam, 2011; Carcaud *et al*., 2015; Couto *et al*., 2017, 2023; d'Ettorre *et al*., 2017; Galizia & Rössler, 2010; Joerges *et al*., 1997; Marty *et al*., 2025; McKenzie *et al*., 2016; McKenzie & Kronauer, 2018; Sandoz *et al*., 2007; Wang *et al*., 2008; Yamagata *et al*., 2006; Zube *et al*., 2008). This system is called combinatorial coding and has evolved to meet the increased demand for olfactory discrimination to negotiate their intricate life histories, such as parasitoidism and sociality. Hymenoptera are examples of insects with pheromone blends that display a high degree of complexity, in particular in their cuticular hydrocarbon (CHC) profiles.

CHCs are long-chain lipids found on the cuticle of insects and function as desiccation barriers and pheromones (Chung & Carroll, 2015). They comprise an extensive range of compounds that vary in number and position of methyl groups, saturation and chain length (Kather & Martin, 2015). Combinatorial coding is utilized in Hymenoptera to process their complex pheromone blends (Brandstaetter & Kleineidam, 2011; Couto *et al*., 2017, 2023; d'Ettorre *et al*., 2017; Marty *et al*., 2025; McKenzie *et al*., 2016; McKenzie & Kronauer, 2018). However, how this coding system evolves at the molecular level of sex determination remains unknown in these species. Elucidating these genetic mechanisms would therefore provide a more complete picture of the forces driving evolutionary transitions in insect pheromone communication.

Thesis objective

The main objective of this thesis is to elucidate the genetic mechanisms by which sexual differentiation regulates pheromone communication of the parasitoid wasp *Nasonia vitripennis*. I investigated the role that sex determination plays in regulating pheromone production and perception in this model species. For this, I silenced the genes responsible for male and female differentiation with RNA interference (RNAi): *Dsx* in males and *Tra* in females. I first determined the function of these genes in regulating pheromone perception by analysing the development of sensilla on the insect antennae with scanning electron microscopy, the formation of glomeruli in the antennal lobe with neural-tracing protocols and the downstream neurodevelopmental genes involved. I then turned to pheromone production and utilized state-of-the-art gas chromatography mass-spectrometry (GC-MS) to identify sexual dimorphism in the CHC profile and the downstream biosynthetic genes involved.

Study system

Nasonia vitripennis

Nasonia vitripennis (Hymenoptera: Pteromalidae), commonly known as the jewel wasp, is one of four closely related species of the *Nasonia* genus (Darling, 1990). It is a generalist ectoparasitoid of the pupae of various fly hosts, such as blowflies, flesh flies and houseflies (Raychoudhury *et al*., 2010). Like all other Hymenoptera, *N. vitripennis* has a haplodiploid mating system, in which males develop from unfertilized haploid eggs and females from fertilized diploid eggs (Whiting, 1967). Its haplodiploid genetics, short generation time, laboratory tractability and availability of closely related species has made it a suitable model species among parasitoid wasps (Werren & Loehlin, 2009b). Consequently, *N. vitripennis* has been used in genetic research for more than half a century (Werren & Loehlin, 2009b; Whiting, 1967) and is one of the best understood species in the area of chemical communication (Mair & Ruther, 2019). The genome of *N. vitripennis* has also been fully sequenced and annotated (Benetta *et al*., 2020; Werren *et al*., 2010), and the growing body of genetic resources makes it an ideal system for analysing how pheromone communication has evolved (Lynch, 2015).

Chemical ecology of *N. vitripennis*

Numerous studies have identified a whole range of pheromones used by *N. vitripennis* at various stages of its life cycle (Mair & Ruther, 2019; Niehuis *et al*., 2011, 2013). Males use an abdominal sex pheromone to scent-mark territories and attract females after emerging from the host (Ruther *et al*., 2007). They subsequently recognize females as potential mating partners based on their CHC profile (Steiner *et al*., 2006). The female CHC profile elicits courtship in males, during which the male releases an oral sex pheromone from its mandibular glands to induce receptivity in the female (Van den Assem, 1980). Females discriminate between conspecific and heterospecific males based on differences in this oral sex pheromone. After copulation, the male performs post-copulatory courtship, causing a switch in female olfactory preference (Ruther *et al*., 2007, 2010; Ruther & Hammerl, 2014). Mated females are no longer attracted to the male abdominal sex pheromone and switch to host-seeking behaviour. Host-habitat cues are subsequently used by females to locate potential hosts. Females then assess host quality through chemical inspection with their ovipositor (Blaul & Ruther, 2011; Frederickx *et al*., 2014; King & Rafai, 1970).

Sex determination in *N. vitripennis*

With its genome fully sequenced and annotated, *N. vitripennis* has emerged as the genetic model for all parasitoid wasps (Benetta *et al*., 2020; Werren *et al*., 2010). The *Tra* and *Dsx* genes in this species have been identified and characterized as orthologs of *Tra* and *Dsx* in *Drosophila* (Oliveira *et al*., 2009; Verhulst *et al*., 2010a). This indicates that these genes have a similar role in the sex-determination cascade of both species. The *Fru* gene and its splice variants have also been identified in *N. vitripennis* (Bertossa *et al*., 2009), but it remains unproven whether this gene is spliced by *Tra*. Male and female *N. vitripennis* are easily distinguishable based on sexually dimorphic traits, such as leg and antennal pigmentation and wing size. Studies have shown that silencing *Dsx* in males causes feminization by suppressing the sexual signal for male differentiation (Wang *et al*., 2022a). This results in males developing female-like characteristics, including dark leg and antennal pigmentation and longer wings. Females do not develop the reverse phenotypic effects after silencing *Dsx*, although the efficiency of RNAi in these tests was low (Wang *et al*., 2022a). Conversely, silencing *Tra* in females results in male-specific splicing of *Dsx* and suppresses the signal for female differentiation, causing morphological masculinization (Verhulst *et al*., 2010a). Studies have also shown that *Dsx* regulates the production of various pheromones that affect both male and female mating behaviour (Wang *et al*., 2022b). I will now further delineate the research objectives of my thesis in the following paragraphs.

Thesis outline

Insects have evolved specialized sensory systems and neural circuits to perceive and process pheromones within a dynamic olfactory environment. In **Chapter 2**, I present a comprehensive literature review, in which I reflect on the diversity of chemosensory adaptations that have evolved to increase the sensitivity to sex pheromones. I also explore the underlying sex-determination mechanisms that regulate sexually dimorphic neural-circuit development. I specifically focus on the insect antennal lobe, the primary olfactory-processing centre, and discuss differences in the development of olfactory glomeruli between insect orders.

Hymenoptera have evolved sexually dimorphic adaptations in their olfactory system to process complex pheromone blends. These adaptations include specialized sensilla on the antennae, an expansion in the olfactory-receptor repertoire and an increase in the number of antennal-lobe glomeruli. In **Chapter 3**, I focus on sexual dimorphism in the olfactory system of *N. vitripennis* and the role of the sex-determination genes *Tra* and *Dsx*. I analyse the sex-specific regulation of olfactory sensilla and the organization of glomeruli in the antennal lobe.

In insects, there is a one-to-one relationship between the number of olfactory receptor genes and the number of glomeruli in the antennal lobe (Couto *et al*., 2005; Fishilevich & Vosshall, 2005; Kurtovic *et al*., 2007; Vosshall, 2000). Olfactory receptor genes are expressed in olfactory sensory neurons (OSNs). Hymenoptera depend heavily on OSN innervation for glomerular development. In **Chapter 4**, I analyse the function of *Olfactory-receptor co-receptor* (*Orco*), a conserved chemosensory gene downstream of *Dsx*, which is known to play an important role in glomerular development in Hymenoptera.

Parasitoid wasps have evolved some of the most complex CHC profiles among insects. Species such as *N. vitripennis* depend on CHCs for close-range pheromone communication. However, knowledge on the genetic mechanisms regulating sexual dimorphism in the CHC profile has predominately been limited to the model organism *Drosophila*, which uses a different coding system to process pheromones. In **Chapter 5**, I investigate how the sex-determination pathway generates sexual dimorphism in the CHC profile of *N. vitripennis*. For this, I focus on the specific function of TRA, the splicing factor of *Dsx* (and possibly of *Fru*).

Sexual dimorphism in the insect CHC profile originates from the sex-specific regulation of biosynthetic genes. The enzymes that these genes encode convert fatty-acid precursors into CHC compounds and evolve relatively rapidly between closely related species. In **Chapter 6**, I investigate a group of such rapidly evolving biosynthetic genes downstream of *Dsx*. I analyse the role that these genes play in generating sexual dimorphism in the CHC profile of *N. vitripennis* and in producing pheromones for mate recognition.

In **Chapter 7**, I interpret the key findings of this thesis and contextualize them within the existing body of knowledge on insect sexual differentiation. I reflect on the experimental research carried out for this thesis and discuss how the process of sexual differentiation, neurodevelopment and biosynthesis are closely interlinked with the evolution of pheromone communication in parasitoids. I also discuss how sexual differentiation is integral to the evolution of pheromone communication in Hymenoptera, specifically to the combinatorial coding of pheromones in these species. I finalize this chapter by elaborating on the implications and future directions of my research within the areas of evolutionary developmental biology, neuroethology and biological control.

Acknowledgements

I am grateful for the feedback on this chapter provided by Eveline Verhulst and Marcel Dicke.

Chapter 2

A unique sense of smell: development and evolution of a sexually dimorphic antennal lobe – a review

Aidan Williams[1], *Eveline Verhulst*[1] & *Alexander Haverkamp*[1]

[1]Laboratory of Entomology, Wageningen University, PO Box 16,
6700 AA Wageningen, the Netherlands

Entomologia Experimentalis et Applicata, 2022, *170* (4), 303-318
DOI: https://doi.org/10.1111/eea.13145

Abstract

Pheromones are pivotal to sexual communication in insects. These chemical signals are processed by sexually dimorphic circuits in the antennal lobe (AL) of the insect brain. However, there is limited understanding of how these circuits form during AL development. Our review addresses this issue by comparing how circuits develop throughout the growth processes of peripheral and deutocerebral neurons in various insect orders. Olfactory sensory neurons (OSNs) expressing novel pheromone receptors are eligible candidates to initiate new sexually dimorphic circuits when these OSNs survive programmed cell death and match the physiological properties of pheromone-sensing sensilla. The probability of these OSNs forming new glomeruli is largely determined by the degree of glia-OSN interactions and projection neuron (PN) prepatterning. The relative contribution of either of these processes determines the degree of evolutionary neuroplasticity, which is particularly prevalent in those species with complex ALs lacking specific macroglomerular structures. The extent of sexual dimorphism is determined by sex-determination genes, such as *Doublesex* and *Fruitless*, that regulate factors inducing OSN programmed cell death. Currently, these mechanisms are largely unexplored. This review, therefore, aims to provide a solid foundation for ongoing research into the evolution of AL sexual dimorphism and formation of pheromone circuits in the light of insect sex determination.

Introduction

Well-defined neural circuits in the invertebrate nervous system have long served as model systems to address fundamental questions in neuroscience (Kandel, 2001; Masse *et al*., 2009). The insect antennal lobe (AL), in particular, possesses highly specialized and well-defined neural circuits ideal for examination. In this review, we will assess how developmental processes in this brain region contribute to the evolution of sexually dimorphic pheromone circuits within insects.

Insect neurobiologists have long been fascinated by the curious anatomy of the AL, not only by its synaptic organization, but also by the functional properties of its neurons. Each AL neuron has a defined role in processing information. When combined, these neurons reconstruct the complex olfactory world of an insect (Hansson & Anton, 2000). The extensive variety in neuronal composition and AL organization reflects numerous lifestyle and behavioural adaptations to chemical environments (Boeckh & Tolbert, 1993; Chou *et al*., 2010a; Spletter *et al*., 2010; Kollmann *et al*., 2016). The AL is the primary olfactory-processing centre where olfactory sensory neurons (OSNs) from the antennae form synapses with projection neurons (PNs) of higher brain centres to produce spherical neuropils, called olfactory glomeruli (**Figure 1**). These can range from hundreds of microglomeruli as found in locusts (Ignell *et al*., 2001) to voluminous glomerular islets as seen in moths (Anton & Homberg, 1999). In addition to these inter-taxonomic variations, insect ALs also show sexual dimorphism in the structure, number, and volume of glomeruli, which in turn adds to the diversification of insect species (Arnold *et al*., 1985; Kondoh *et al*., 2003; Roselino *et al*., 2015; Rospars & Hildebrand, 2000). Sex-specific pheromonal glomeruli, for example, are finely tuned to process spatiotemporal information of a limited number of compounds (Agarwal & Isacoff, 2011). The question remains how these sexually dimorphic differences evolve within the conventional blueprint of AL development.

Records show that the insect brain and, more specifically, the process of insect olfaction have been the source of intrigue among biologists for at least the past 200 years. The French biologist Félix Dujardin was not only the first to identify the mushroom bodies (*corpora pedunculata*) in Hymenoptera and to consider them as the seat of insect intelligence, he also produced revealing illustrations of the honeybee brain that include globular structures we now know as antennal lobes (Dujardin, 1850). These dense AL masses at the base of insect antennae were later described by Leydig (1864) and Rabl-Rückhard (1875) as non-nucleated cells. However, it was Dietl (1876) who more correctly classified these structures as olfactory bodies. In an unpublished communication (1874) to the Kielers Physiologische Vereins, the German amateur neurobiologist Johann Flögel also drew attention to the fact that these structures are indeed not cells. Flögel was the first to discover that the ALs are composed of small ball-like elements (Flögel, 1878) or, in his words, *Geruchskörper* (scent bodies). He also identified tracts connecting the ALs to the calyces of the mushroom bodies and observed a

proportional relationship between the size of the calyx and the number of AL scent bodies. Four years later, Bellonci (1883) went on to name these 'scent bodies' olfactory glomeruli (*Glomeruli olfactorii*) and also made the significant assertion that the olfactory lobes and glomeruli in lower vertebrates are homologous to the ALs and glomeruli in insects.

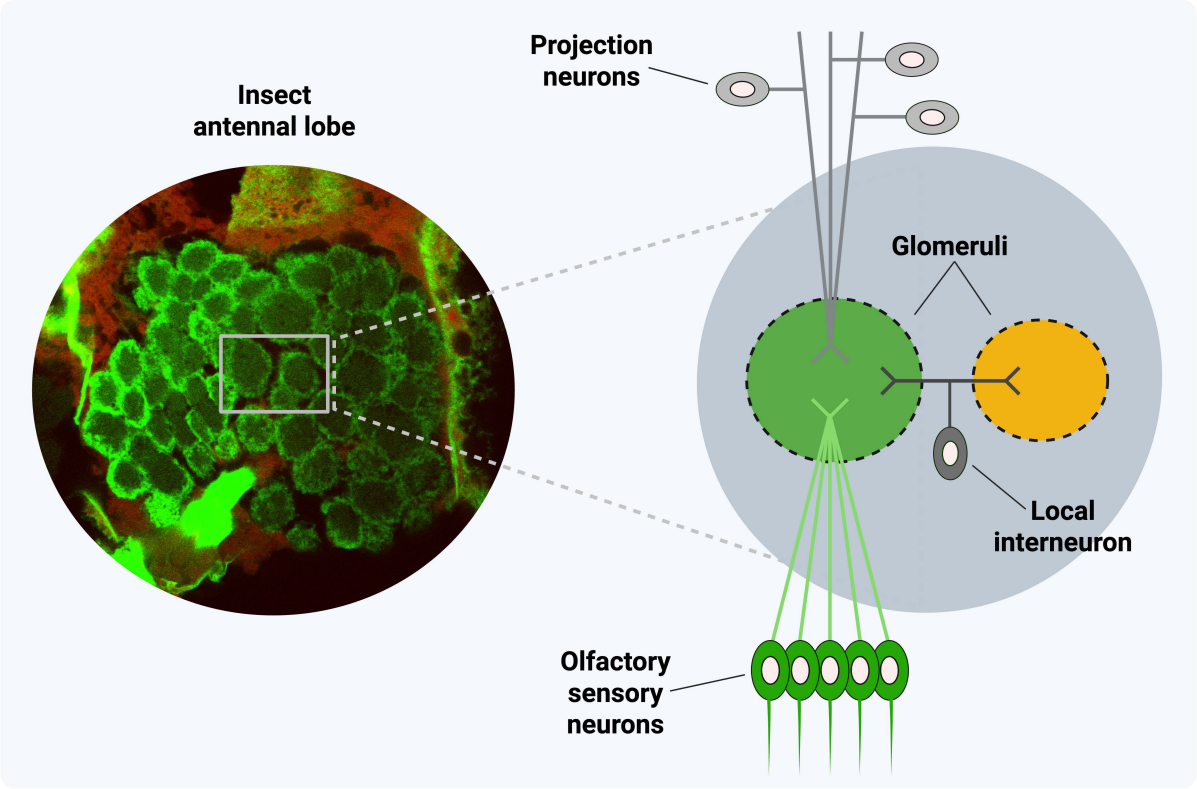

Figure 1: Overview of the insect antennal lobe (AL) and the neuronal composition of olfactory glomeruli. A glomerulus is composed of olfactory sensory neurons (OSNs), projection neurons (PNs), and local interneurons (LNs).

The term 'glomerulus' was next mentioned in the illustrated studies of French neuroanatomist Henri Viallanes, who used the word in his paper on the locust brain (Viallanes, 1887). Viallanes proposed a new classification of the insect brain, appointing the AL and the antennal and accessory nerves to the deutocerebrum. He also confirmed Flögel's observations of neuronal tracts connecting the AL to the cups of the mushroom bodies. A decade later, F.C. Kenyon verified these connections by using Golgi's method of silver chromate staining and determined the production of olfactory glomeruli through tuft-like terminations of afferent antennal fibres (Kenyon, 1896). These are the first steps in identifying glomeruli as distinct olfactory-processing units in the insect AL.

The earliest accounts of AL sexual dimorphism in insects coincide with the discovery of enlarged glomeruli. In 1924, F. Bretschneider was the first to describe conspicuous sex-specific glomeruli in moths. He observed that male oak egger moths display several enlarged glomeruli where the antennal nerve fibres enter the AL (Bretschneider, 1924). Koontz &

Schneider (1987) later identified these enlarged glomeruli in males as processing neuropils for female sex pheromones. Since Bretschneider's discovery, similar enlarged glomeruli have been determined in other insect species: cockroaches (Boeckh *et al*., 1987; Jawlowski, 1948; Neder, 1959), bees (Arnold *et al*., 1984; Brockmann & Brückner, 2001), ants (Kleineidam *et al*., 2005; Nishikawa *et al*., 2008), flies (Kondoh *et al*., 2003), and moths (Anton & Homberg, 1999). More recently, this glomerular mass was coined a 'macroglomerulus' for a single glomerulus (Boeckh & Boeckh, 1979) and a 'macroglomerular complex' (MGC) for multiple glomeruli (Hildebrand *et al*., 1980). Functional subdivisions have been identified in the MGC as separate pheromone-processing regions (Hansson *et al*., 1991), demonstrating how sex-specific glomeruli have evolved to process pheromone blends.

Glomerular development depends on the growth processes of OSNs and deutocerebral neurons, following a genetically fixed programme. Olfactory sensory neurons expressing specific pheromone receptors project their axons to sexually dimorphic glomeruli or glomerular clusters (Hansson *et al*., 1992). Projection neurons, on the other hand, connect the glomeruli through conserved tracts to the higher brain centres in the lateral protocerebrum. This connectivity occurs almost universally in insects and constitutes a genetic ground plan for connecting glomeruli (Strausfeld *et al*., 2009), although the precise molecular mechanisms underlying the development of sexually dimorphic AL circuits have yet to be fully determined. Research, however, has revealed that sex-specific glomeruli develop in response to sex-determination transcription-factor genes, such as *Doublesex* (*Dsx*) and *Fruitless* (*Fru*) (Cachero *et al*., 2010; Kimura *et al*., 2008; Zhou *et al*., 2014). These sex-specific mechanisms are integrated in AL development and could drive the evolution of novel sexually dimorphic circuits.

In this review, we examine and evaluate the current consensus on the evolution of AL sexual-dimorphism and pheromone processing. We analyse developmental principles, from receptor expression and sensillum specialization to AL synaptic innervation, and compare their relative contribution to the glomerular development in various species. We assess how specialized sensilla give rise to novel OSN-glomeruli associations and how OSN-afferents are sorted through pioneering sensory neurons. We subsequently look at how the intricate interactions between OSN sorting, glia proliferation, and PN patterning are related to glomerular development. Each OSN expresses olfactory receptors (ORs) that form functional sensing units with the highly conserved *Olfactory-receptor co-receptor* (*Orco*) gene. The role of the latter in glomerular development is also discussed in this review. Sex-determination mechanisms are finally evaluated to present a framework for ongoing research into these processes at different levels of AL development.

Sexually dimorphic antennae

It can be a daunting task for a diminutive invertebrate to navigate a complex chemical world, continuously being confronted by an infinite number of odour blends. As a result, insects have evolved remarkable peripheral adaptations to filter background noise and transduce relevant cues to reliable signals (Hansson & Stensmyr, 2011). The olfactory-receptor repertoire has evolved from very few receptors in primitive arthropods to a highly divergent receptor superfamily that is specifically adapted to an insect's chemical environment (Clyne *et al*., 1999; Missbach *et al*., 2014; Robertson *et al*., 2010). An insect's distinct environment is perceived by specific receptor repertoires, which aid insects in fulfilling behaviour crucial to their survival (Carey *et al*., 2010; Gardiner *et al*., 2008; Stensmyr *et al*., 2003), such as finding mates, foraging for food, and selecting suitable oviposition sites. Olfactory receptors are expressed in OSNs that are encapsulated by specialized sensory organs, the antennal sensilla (Zacharuk, 1980). These small hair-like structures protruding from the antennal cuticle are efficiently equipped to capture and transport chemical compounds to the OSN membrane (Steinbrecht, 1997).

The striking morphological diversity of insect sensilla makes it possible to classify them into types, the most common of which are trichoid (hair-like) (**Figure 2A**), placoid (plate-like) (**Figure 2C**), basiconic (cone-like), and coeloconic (peg-like) (Schneider & Steinbrecht, 1968). Chemosensing sensilla are further subdivided according to the presence of pores (Steinbrecht, 1997), where uniporous sensilla are responsible for contact chemoreception or gustation and multiporous sensilla for olfaction. The diverse shapes and distributional patterns of sensilla reflect diverse sensory modalities and occasionally take the form of extreme specialized morphologies (Schneider, 1964). Sensillum specialization for pheromone detection can sometimes be visible, even to the naked eye, and gives rise to conspicuous sexual dimorphisms in the shape and size of antennae (Steinbrecht, 1987). However, there can also be distinct sexually dimorphic differences in the number and distribution of sensillum types (**Figure 2A, 2C**), which exemplify sexual differences in olfactory life histories. Or, simply put, a sex-specific sensillum repertoire to perform sex-specific behaviour.

Antennal sexual dimorphism is epitomized in certain moth species. Male saturniid moths, for example, possess conspicuous trichoid sensilla to reflect their predisposition to trace odours of female mates. Up to 50,000 of these pheromone-detecting sensilla utilize much of the antennal surface area to maximize detection of the female's volatile pheromone (Boeckh *et al*., 1960). A predominance of a certain sensillum increases the number of receptors tuned to the specific pheromone and improves antennal sensitivity by lowering the response threshold to the pheromone molecules (Kaissling & Priesner, 1970). Similar quantitative adaptations, though less visually apparent, have also been observed in Hymenoptera species, as in the greatly increased number of pore plates in drone honeybees (Esslen & Kaissling, 1976). These pore plates contain OSNs expressing general food receptors as well as specific receptors for

the queen substance and scent-gland odours (Nasonov's gland) (Kaissling & Renner, 1968; Vareschi, 1971). The pore plates bear a close structural relationship with trichoid sensilla (*sensilla trichodea curvata*) in *Formica* ants, which are basically pore plates lifted from the antennal cuticle (Walther, 1981). It would appear that in Hymenoptera both types can transmute into each other and therefore share common developmental features. Such a bimodal relationship could be regulated through a sex-differentiating switch mechanism, repressing one morphological state while activating the other. Silencing transcription-factor genes such as *Dsx*, or changing this gene's sex-specific splicing, could therefore result in a reversion to either placoid or trichoid morphology (**Chapter 3**).

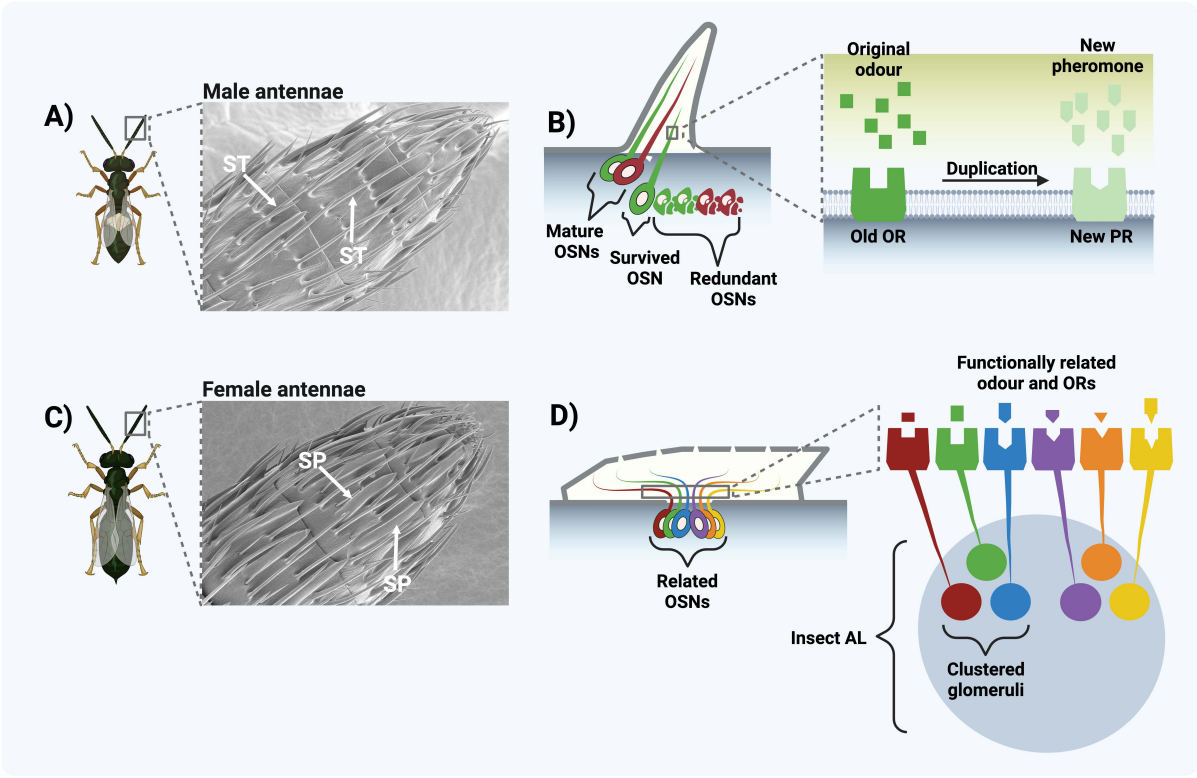

Figure 2: Sexual dimorphism in olfactory sensilla and glomerular arrangement in a parasitoid wasp.
A: Olfactory sensilla of a male parasitoid wasp highlighting the presence of sensilla trichodea (ST). **B:** Cross section of a trichoid sensillum, comprising two mature functional olfactory sensory neurons (OSNs) and one OSN that has survived programmed cell death. Redundant OSNs are eliminated through programmed cell death during neural development. OSNs surviving programmed cell death are eligible candidates to evolve novel pheromone receptors (PRs) from olfactory receptors (ORs) through gene duplication. **C:** Olfactory sensilla of a female parasitoid wasp, highlighting the higher abundance of sensilla placodea (SP) relative to the male. **D:** Cross section of a placoid sensillum, comprising six functionally related OSNs. The OSNs possess ORs that bind to functionally related odours. ORs specializing in a specific subset of odours correspond to clustered glomerular regions in the insect antennal lobe (AL).

Sensillum sexual dimorphism, while numerically conspicuous in one taxon, can be obscurely visible in others and still determine important chemosensory properties. Male and female *Bombyx mori* moths differ slightly in the number of trichoid sensilla (Steinbrecht, 1970), but differ quite significantly in the properties of the two OSNs in the trichoids. In males, these

OSNs respond to the pheromones bombykol and bombykal, whereas in females these OSNs are unresponsive to these substances (Kaissling *et al*., 1978). Transgenetic studies have expressed the moth's bombykol receptor in 'empty neurons' from *Drosophila* basiconic sensilla, but observed a low sensitivity compared to the native trichoid sensilla on the moth's antennae (Syed *et al*., 2010). However, expression of the moth's bombykol receptor in the *Drosophila* trichoid system yielded a sensitivity comparable to the moth's native trichoids, suggesting this to be a more suitable habitat for the moth's bombykol receptor. Pheromone sensitivity of OSNs therefore seems to be closely associated with the structural, biochemical, and biophysical properties of their corresponding sensillum. Specialized subpopulations of pheromone-sensing neurons are located in specialized sensilla specifically programmed for pheromone detection (Ha & Smith, 2006). These sensillum-specific neural subpopulations not only differ between sexes, but also show a functional and topographical segregation in the AL (**Figure 2D**).

A specialized sensillum subsystem

Antennal lobe architecture depends on the variety of sensillum morphologies. Chemosensing sensilla and their corresponding OSNs are often distinctly distributed on antennal segments (de Bruyne *et al*., 2001; Stocker, 2001; Vosshall *et al*., 1999) and can be traced simultaneously to distinct regions of the AL (Couto *et al*., 2005; Gao *et al*., 2000; Grabe *et al*., 2016). The major pheromone-sensing neurons in *Drosophila* are located in specific trichoid sensilla, which are marginally more abundant in males (Xu *et al*., 2005). The pheromone-sensing neurons of these trichoids respond to the courtship volatile *cis*-vaccenyl acetate (cVA) (Van der Goes van Naters & Carlson, 2007) and project their axons to two sexually dimorphic glomeruli (Datta *et al*., 2008), which are also significantly larger in males (Kondoh *et al*., 2003). In the cockroach *Periplaneta americana*, basiconic sensilla project OSNs to an MGC composed of two immediately adjacent glomeruli (Watanabe *et al*., 2012). Likewise, in the hawkmoth *Manduca sexta*, OSNs from male-specific trichoid sensilla project their axons exclusively towards the MGC (Christensen *et al*., 1995). The axons from trichoids on the dorsal side of the moth's antennae are projected towards the medial region, whereas axons from ventral trichoids project towards lateral areas. Finally, social Hymenoptera species typically utilize a sensillum subsystem for perceiving colony cues and pheromones, as well as odours associated with foraging (Couto *et al*., 2017; Kropf *et al*., 2014; Ozaki *et al*., 2005). Sensory neurons capable of detecting these compounds are typically located in basiconic sensilla usually present in only one of the sexes.

Whatever strategy is used, it is evident that numerous insects employ a specialized sensillum subsystem containing distinctive physiological features that corresponds to spatially segregated glomeruli in the AL, whether these form an MGC or a cluster of regular glomeruli. This functional correspondence between a sensillum, OSN and glomerulus results in a functional segregation of pheromonal and non-pheromonal afferents in the antennae,

although further research needs to be carried out to determine how this segregation actually takes place and which molecular mechanisms are responsible for it. Before entering the AL, OSNs are actively sorted in the antennae through interactions with peripheral glia cells (Sen *et al*., 2005). In *Drosophila*, the majority of these glia cells originate from pioneering sensory neurons specified by the *Atonal* transcription-factor gene. These sensory neurons are the first to permeate the antennal lobe during development (Jhaveri *et al*., 2000). The glia cells wrap the OSN tracts into three distinct fascicles before exiting the antennae and entering the AL. Loss of *Atonal* function disrupts OSN segregation from all chemosensing sensilla (c. 1,000 neurons in *Drosophila*) and glomerular patterning fails to materialize (Jhaveri & Rodrigues, 2002). Once firmly established, excess OSN afferents are eliminated from a sensillum through programmed cell death (Sen *et al*., 2004) (**Figure 2B**). Any neuron that has survived this process has the potential to integrate into pre-existing olfactory circuits and form novel sensillum-receptor glomerular associations (Prieto-Godino *et al*., 2020). These surviving neurons have the potential to evolve into novel sexually dimorphic pheromone circuits.

Sexually dimorphic antennal lobe

In terms of task assignment, structure and composition, the AL is surprisingly unique. In terms of its development, it is rather ambiguous. Its uniqueness is manifested in the diversity of distinct glomeruli, with each having its own olfactory identity. In moths, honeybees and fruit flies, each glomerulus has its own identifiable shape and position in the fixed organizational structure of the AL (Rospars, 1988; Rospars & Chambille, 1989). Rospars & Chambille were the first to determine this fixed organizational structure in cockroach species (Chambille *et al*., 1980; Chambille & Pierre Rospars, 1985; Rospars & Chambille, 1981). In addition to a unique appearance, each glomerulus possesses a unique neuronal composition based on the total number of innervating OSNs and the synapses they form with local interneurons (LNs) and PNs (Grabe *et al*., 2016). This unique neuronal composition determines glomerular size, which in turn determines sensory specialization and the contribution of processed odour compounds to behavioural relevance (Dekker *et al*., 2006; Linz *et al*., 2013). Highly significant ecological cues, such as sex pheromones, are usually processed by labelled lines: single glomeruli that receive few lateral inputs from LNs, but display a relatively high number of PNs (Grabe *et al*., 2016). The low degree of lateral processing in these glomeruli enables fast innate responses towards sex pheromones. General odours, however, elicit broader AL response patterns, called combinatorial codes, which require computational input from multiple interconnected glomeruli. In this way, distinct processing channels are formed from different neuronal compositions, being either broadly tuned or narrowly tuned to odour compounds (Christensen & Hildebrand, 2002; Haverkamp *et al*., 2018; Sachse *et al*., 1999). It remains unclear, however, how these coding systems are established throughout AL development, how developmental changes can result in novel labelled lines, and to what extent combinatorial coding contributes to pheromone processing in different insect orders.

Pheromone processing in the AL is not an isolated task. Insect pheromones interact with additional cues in the AL to modulate important reproductive decisions. Food odours trigger *Drosophila* males to deposit the pheromone 9-tricosene on rotting fruit, which promotes aggregation and mediates female oviposition decisions (Lin *et al*., 2015). Food odours also enhance male attractiveness as females become more receptive when food is sensed in conjunction with the male pheromone cVA (Lebreton *et al*., 2015). At the AL level, food odours enhance activation of the cVA-responsive glomerulus (DA1) and this effect is mediated through lateral excitation from neighbouring glomeruli (Das *et al*., 2017). Similar interactions are also found in the AL between moth pheromones and plant volatiles (Reddy & Guerrero, 2004), the latter of which are capable of masking or synergizing the pheromone response from a male moth's MGC (Chaffiol *et al*., 2012; Deisig *et al*., 2012; Namiki *et al*., 2008). Although extensive interaction in flies and moths occurs at the glomerular level, pheromone processing in the AL of these insects still follows a dedicated labelled-line system (Haverkamp *et al*., 2018). Hymenoptera, however, form an exception to insect orders that use a specialized labelled-line system.

In species such as ants, honeybees and wasps, pheromones can play a role other than sexual attraction and may favour a combinatorial-coding strategy instead (Carcaud *et al*., 2015). These species utilize olfactory subsystems, consisting of glomerular clusters innervated by uniglomerular PNs (Kropf *et al*., 2014). Honeybees possess two olfactory subsystems, innervated separately by two different PN tracts (Galizia & Rössler, 2010). While queen and brood pheromones are processed by either of these tracts, all pheromone components are capable of eliciting a combinatorial code in both subsystems (Carcaud *et al*., 2015). Ants, bees and wasps also use a conserved cluster innervated by basiconic-associated OSNs for the coding of colony cues, pheromones and odours associated with foraging (Couto *et al*., 2017; Nakanishi *et al*., 2010; Ozaki *et al*., 2005). The parasitoid wasp *Nasonia vitripennis* possesses a highly sexually dimorphic AL (c. 185 glomeruli in males and c. 225 glomeruli in females), which is arranged in sex-specific clusters likely to be used for processing pheromones and/or host odours (**Chapter 3**). These dimorphic clusters are currently being investigated in the light of sex-determination mechanisms to ascertain whether silencing sex-determination genes leads to a sex-reversal in glomerular organization. Silencing these genes in *Drosophila* does not lead to a significant change in glomerular organization (Stockinger *et al*., 2005). However, because Hymenoptera use a different strategy to process pheromones, it is likely that glomerular development is more intricate in these species.

A prepatterned outline?

To understand the developmental evolution of pheromone-processing glomeruli, we need to dissect their neurophysiological properties and elucidate neurogenetic mechanisms. Across almost all insect taxa, the number of AL glomeruli approximates the number of genes that encode olfactory-receptor proteins. Most OSNs express only one or rarely two OR genes

(Clyne *et al*., 1999; Silbering *et al*., 2011; Vosshall *et al*., 1999), and the axons of neurons expressing the same OR gene converge in the same glomerulus (Couto *et al*., 2005; Fishilevich & Vosshall, 2005; Gao *et al*., 2000; Silbering *et al*., 2011; Vosshall, 2000). These functional relationships have been coined the one-neuron-one-receptor and one-receptor-one-glomerulus principles. Each OR has a specific chemoreceptive field, being broadly or narrowly tuned to specific odour compounds, and these tuning properties are inherited by their corresponding glomeruli (Hallem & Carlson, 2006). Convergent projections to specific glomeruli therefore create a topographic olfactory map, as witnessed in *Drosophila*, and the identity of a glomerulus should therefore be closely associated with OSNs expressing a specific OR gene. However, the genetic mechanisms for glomerular development are not the same as those generating different types of ORs: silencing an OR gene does not eliminate OSN connectivity or glomerular formation in *Drosophila* (Dobritsa *et al*., 2003; Elmore *et al*., 2003; Goldman *et al*., 2005; Ray *et al*., 2007). In fact, a prototypic AL has already formed in the fly well before ORs are expressed and before OSNs have innervated their corresponding glomeruli (Jefferis *et al*., 2004).

Projection neurons are the first to reach the AL and their dendrites develop to establish protoglomeruli. In *Drosophila*, PNs are prespecified by lineage and birth order to form synapses with specific incoming OSNs and therefore to transmit specific olfactory information (Jefferis *et al*., 2001). Glomerulus-specific PNs prepattern their target region at the onset of *Drosophila* pupation before OSN arrival (**Figure 3**), suggesting olfactory circuits are formed through synaptic recognition of OSNs by the resident PNs (Jefferis *et al*., 2004). This stage of prespecification may be used to hardwire glomerular identity, enabling stereotypical behaviour towards sex pheromones. Within 18 hours of puparium formation, after pioneering sensory neurons permeate the AL, OSNs converge on their target glomerulus and connect with PNs. Molecular mechanisms, such as the adhesion molecules N-cadherin and Dscam, enable class-specific OSN axon sorting (Goyal *et al*., 2019; Zhu & Luo, 2004) and synaptogenesis is initiated after OSNs recognize PN dendritic cues (Zhu *et al*., 2006). Although PNs are necessary for correct patterning of the AL in *Drosophila*, it has been demonstrated that glomeruli in *Manduca* also form after individual PN clusters are surgically removed (Oland & Tolbert, 1998). In this species, the AL template of protoglomeruli is stabilized through glia-cell proliferation.

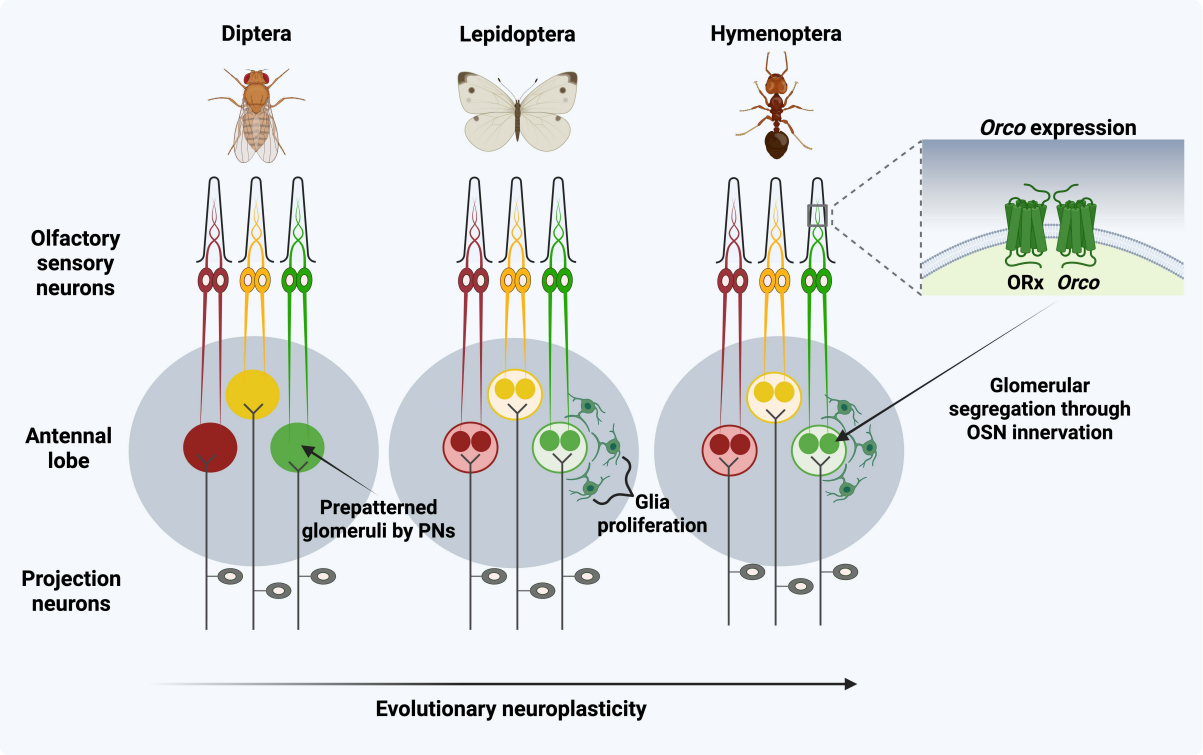

Figure 3: Concept of antennal lobe development in three insect orders.
In *Drosophila*, projection neuron (PN) prepatterning is crucial for forming stable glomeruli, whereas refinement through glia proliferation and olfactory sensory neuron (OSN) innervation play a lesser role. In Lepidoptera, however, glomeruli are also able to form after PNs are surgically removed and after transplanting the antennae between sexes. Glia proliferation and OSN innervation play a bigger role in glomerular refinement in these species. In Hymenoptera, OSN innervation is crucial for refining glomerular structure. These innervations are necessary for protoglomeruli to divide and form the glomerular organization of the adult AL. Expression of the *Olfactory-receptor co-receptor* (*Orco*) gene in OSNs plays an important role in this developmental process. The process of OSNs refining glomerular development makes modifications in glomerular structure more likely to occur and therefore increases the degree of evolutionary neuroplasticity.

Glia and OSNs: effective team players?

Glia cells play a crucial role in the induction of glomeruli formation through reciprocal interaction with innervating OSNs (Oland & Tolbert, 2011). The glia cells first form a ring around the immature AL neuropil, after which they are stimulated by ingrowing axons to migrate around the protoglomeruli and form glomerular envelopes (Oland & Tolbert, 1987). These glia-cell walls act as important boundaries to the protoglomeruli for incoming OSNs to initiate synaptic interactions with PNs. Research on the relative contribution of glia towards glomerular development has focused specifically on the comparison between *Manduca* and *Drosophila*. In the former, glia cells form thick glomerular boundaries that are essential for the formation of stable glomeruli (Tolbert *et al*., 2004). Delayed or incomplete development of glia cells in the *Manduca* AL can result in the misrouting of pheromone-specific OSNs and incomplete glomerular segregation of the MGC (Rössler *et al*., 2000). Glia cells in *Drosophila*, however, form rather weak boundaries and are unlikely to play a significant role in either

axonal sorting or glomerular isolation (Oland *et al*., 2008). Moreover, glia processes are also extended well after glomeruli have formed and therefore play a minor role in glomerular stabilization (Jefferis *et al*., 2004; Oland *et al*., 2008). Taken together, the glomerular structure in *Drosophila* appears to be determined primarily by a prespecified PN pattern, whereas in *Manduca* OSN-glia interactions appear to be paramount for forming stable glomeruli, reshaping the innervation patterns of the initial PNs (Jefferis *et al*., 2004; Oland & Tolbert, 2011) (**Figure 3**). Locusts, to give a further example, employ a microglomerular design (Ignell *et al*., 2001) and add additional glomeruli to the AL after each moulting event (Ochieng *et al*., 2000), while PNs remain constant as the locust ages (Anton *et al*., 2002). It would be interesting to investigate how glia affect AL formation of these species and how signals from innervating OSNs cause further proliferation.

Transplanting insect antennae

A good example of primary glomerular development is illustrated in the experiments using antennae transplanted between different sexes of the hawkmoth *M. sexta* (Kalberer *et al*., 2010; Rössler *et al*., 1999; Schneiderman *et al*., 1982). These experiments involve removing the antennal imaginal discs of late-instar caterpillars of one sex and replacing them with an antennal imaginal disc of the opposite sex. During metamorphosis, the insects that have undergone this procedure then develop antennae according to the sex of the donor insect. Interestingly, the OSNs from these transplanted antennae also significantly reshape the AL of the recipient. In Lepidoptera, the male AL is characterized by the MGC, which consists of axons from pheromone-sensing neurons (PSNs) arriving from the antenna, LNs that process the antennal signals and PNs that transfer the pheromone signal to higher brain centres (Hansson *et al*., 1991; Reisenman *et al*., 2011). The female AL, on the other hand, contains two lateral large female-specific glomeruli (latLFG), which respond to different plant volatiles (Reisenman *et al*., 2004). If a male antennal imaginal disc is transplanted onto a female *M. sexta*, the male pheromone-sensing neurons will induce the formation of a male MGC instead of the latLFG, stimulating the female LNs and PNs, which are already present in the AL, to adapt to these altered glomeruli (Rössler *et al*., 1999; Schneiderman *et al*., 1982).

In a number of cases, these gynandromorphic females also show oviposition behaviour in response to stimulation with an artificial pheromone blend, indicating that the newly formed connections between the male OSNs and the female PNs actually trigger the same behavioural circuits as would normally be activated by the OSNs innervating the latLFG (Schneiderman *et al*., 1986). However, these results also indicate that there is no OSN/PSN-specific recognition by the PNs. Which OSN will connect to the waiting PNs simply depends on the specific location to which the neurons are guided by glia cells. This of course begs the question which mechanisms are employed by the glia cells to sort the arriving OSNs. Activation of the epidermal growth factor receptor (EGFR) along with Fasciclin II and Neuroglian, members of the immunoglobulin superfamily of cell-adhesion molecules (IgSF

CAMs) in the axons of the arriving OSNs, play an important role in guiding these neurons to the right location in the developing AL (Gibson & Tolbert, 2006). On the glia side, fibroblast growth factor receptors (FGFRs) are crucial for the development of the axon sorting zone (Gibson *et al*., 2012). However, it has yet to be established how the axons of specific OSNs are guided to a certain protoglomerulus. Interestingly, the *Olfactory-receptor co-receptor* (*Orco*) gene, which is required for normal activity of the olfactory receptors, is not necessary for the correct development of the AL in *Manduca* or *Drosophila* (Fandino *et al*., 2019; Ryba *et al*., 2020).

Independent of the specific mechanism, the role glia cells play in the formation of the olfactory glomeruli does pose a potential problem for the evolution of new olfactory circuits. Novel OSN types can arise through duplication events in OR genes and through the survival of OSNs during metamorphosis, which would otherwise be destined for programmed cell death (Prieto-Godino *et al*., 2020) (**Figure 2B**). How then are glia cells able to recognize these new OSN types in order to induce the formation of a new glomerulus? In *Drosophila*, OSNs expressing genetically similar ORs often project to neighbouring glomeruli, which would suggest that OSN types arising through gene duplication might initially be sorted to the same or adjacent locality in the AL (Couto *et al*., 2005; Prieto-Godino *et al*., 2020). From an evolutionary perspective, glia cells would ultimately have to recognize the novel OSN populations as such and initiate a budding process, through which glomeruli with a similar response spectrum would form in close proximity to each other, comparable to that of the pheromone-detecting glomeruli in the majority of insect species (Hansson & Stensmyr, 2011). However, given the fact that the total number of OSNs will be limited by the surface area of the antenna, and assuming that the number of PNs does not arise proportionally with the number of novel OSN types, new glomeruli will lead to a reduction in the size of the existing AL structures. Over time, pheromone components could increase and take on additional roles beyond sexual communication, which would then result in rewiring of PSNs to make a switch from a labelled-line system to combinatorial coding. This pheromone-coding switch ultimately leads to a loss of distinct MGCs in the AL, which might help to explain the absence of these structures in many Hymenoptera species.

Olfactory-receptor co-receptor and the loss of glomeruli

Although *Drosophila* glomerular formation is generally not affected by genetically eliminating OR genes, it appears the opposite is true in Hymenoptera where *Orco* is concerned (Trible *et al*., 2017). Insect OR proteins form a complex with ORCO, a highly conserved co-receptor, which localizes the OR to the dendritic membrane (Jones *et al*., 2005). The colocalized OR-ORCO complex is essential for signal transduction, enabling OSN polarization after receptor binding of olfactory ligands (Larsson *et al*., 2004). Studies carried out on *Orco* null mutants of ants revealed that these ants showed a loss of OSNs and a dramatic reduction (c. 82%) in the number of glomeruli (Trible *et al*., 2017). As a consequence, these mutant ants demonstrated

significant deficiencies in social behaviour, including an inability to recognize nestmates, follow pheromone trails, recognize general odorants and forage for food. Conspecific communication was similarly impaired, resulting in unsuccessful mating and a significantly reduced fitness (Yan *et al*., 2017). *Olfactory-receptor co-receptor* expression in OSNs is therefore required for the development of pheromone-detecting glomeruli in the hymenopteran AL. All Hymenoptera employ two AL olfactory subsystems, each of which has a PN tract that projects to either the mushroom body or the lateral horn (Couto *et al*., 2016; Rössler & Zube, 2011). Both subsystems can process information from pheromones, but extract different odorant properties before transmitting signals to the higher brain centres (Brill *et al*., 2013; Carcaud *et al*., 2015; Rössler & Brill, 2013). This demonstrates that pheromone processing requires both subsystems to cooperate in parallel (Carcaud *et al*., 2015). Glomeruli in the *Orco* mutant ants were indeed lacking glomerular clusters from both subsystems, which explains the malfunction of social behaviour in these ants.

Loss of *Orco* in non-Hymenoptera species leads to impaired pheromone sensitivity, but does not cause severe anatomical changes in glomerular organization (Ryba *et al*., 2020). Knocking out *Orco* diminishes pheromone detection in *M. sexta* (Fandino *et al*., 2019), *B. mori* (Liu *et al*., 2017), *Spodoptera littoralis* (Koutroumpa *et al*., 2016) and *Locusta migratoria* (Li *et al*., 2016), but has little effect on the structure of the AL. Loss of *Orco* also has no significant impact on the *Drosophila* AL, with essentially no difference in the number and organization of glomeruli (Ryba *et al*., 2020). In Hymenoptera, however, ORs and *Orco* are expressed before the onset of glomerular formation. It is therefore likely that, through *Orco*, OSNs play a more important role in refining glomerular identity after PNs have prepatterned the glomerular structure. The remaining glomeruli in the *Orco* mutant ants failed to segregate normally (Yan *et al*., 2017), indicating the significance of *Orco* and OSNs in elaborating AL complexity (**Figure 3**). Hymenoptera have evolved an expansive olfactory-receptor repertoire, which is reflected in large ALs and elaborate mushroom bodies. A parasitic or social lifestyle might have favoured flexible developmental processes, which enabled combinatorial coding adaptations for cognitive-demanding tasks, such as spatial learning and host foraging. Pheromone processing might have initially followed a labelled-line strategy in ancestral species, but eventually evolved and developed into a combinatorial-coding strategy that favours elaborate ALs. Research should therefore be carried out to investigate this transition by making phylogenetic comparisons and elucidating neurogenetic mechanisms.

Sex determination and the birth of neurons

Molecular basis of sex determination in insects

In most insects, sexual differentiation is initiated by the action of two highly conserved transcription-factor genes: *Dsx* (reviewed in Verhulst & van de Zande, 2015) and *Fru* (reviewed in Sato & Yamamoto, 2020). In *D. melanogaster* and many other holometabolous insects, the transcripts of both genes are sex-specifically spliced into the female splice-variant

by the upstream splicing factor Transformer (TRA) and Transformer-2 (TRA-2), whereas in males TRA is not functionally present to splice *Dsx* and *Fru* and both are spliced by default into the male-specific splice-variants (Bopp *et al*., 2014; Cline & Meyer, 1996; Geuverink & Beukeboom, 2014; Heinrichs *et al*., 1998; Ryner *et al*., 1996; Verhulst *et al*., 2010b). Both male- and female-specific *Dsx* isoforms are required for sexual differentiation (Baker & Ridge, 1980), whereas only the male-specific *Fru* isoforms are required for the development of neural pathways for male courtship behaviour (Gill, 1963; Ito *et al*., 1996; Ryner *et al*., 1996) and the female-specific *Fru* isoforms are assumed to have no function (Taylor *et al*., 1994). Von Philipsborn *et al*. (2014) investigated four major *Drosophila Fru* splice variants and attempted to correlate the cellular and behavioural function of each *Fru* isoform. Here, however, we refer to all male-specific *Fru* protein isoforms as *Fru*.

In previous overviews of sex determination and differentiation in *Drosophila*, *Dsx* is shown to be required for morphological differentiation and *Fru* to be the master control gene required for shaping the brain centres for male sexual behaviour (Demir & Dickson, 2005; Ito *et al*., 1996; Manoli *et al*., 2005; Ryner *et al*., 1996). We now know, however, that this distinction is not that strict and that *Dsx* and *Fru* are both needed to regulate courtship behaviour in males (Billeter *et al*., 2006b; Villella *et al*., 2006; Rideout *et al*., 2007; Shirangi *et al*., 2006; Villella & Hall, 1996), whereas for sexual behaviour in females only *Dsx* is required (Zhou *et al*., 2014). The role of *Fru* in controlling brain organization for male sexual behaviour in other insects is largely unknown. Despite this, recent research suggests that in basal hemimetabolous insects, *Fru* is not sex-specifically spliced and is not likely to be involved in neural sex determination (Watanabe, 2019). However, even in *Drosophila*, all neuronal clusters expressing *Dsx* are either sex-specific or sexually dimorphic and none are sexually monomorphic (Nojima *et al*., 2021). This suggests that AL development and the resulting behaviour in males and females could be predominantly controlled by *Dsx*.

Fruitless and/or Doublesex regulate neuronal growth and development

Sex-specific splicing of *Fru* is highly complex in both Diptera and Hymenoptera (Bertossa *et al*., 2009; Heinrichs *et al*., 1998), due to the use of different promoters and alternative splicing. Only transcripts originating from the first, most distal, promoter are sex-specifically spliced by *Tra* and *Tra-2*, whereas transcripts from the other promoters are non-sex-specifically spliced (Bertossa *et al*., 2009; Heinrichs *et al*., 1998). In *Drosophila*, both male and female *Fru* mRNA expression is observed in the central nervous system (CNS) (Usui-Aoki *et al*., 2000), with about 2% of the CNS cells expressing male-specific *Fru* at peak expression approximately two days into pupal development (Baker *et al*., 2001; Lee *et al*., 2000). Only in males, however, are FRU proteins expressed in the CNS, whereas in females FRU proteins are not expressed here (Usui-Aoki *et al*., 2000). In males, these *Fru* expressing cells are organized into c. 20 groups (Lee *et al*., 2000). One of these clusters, termed mAL, is located just above the AL and contains 30 neurons in males and five neurons in females (Kimura *et al*., 2005), and is thought to be involved in pheromone input integration (Yamamoto, 2007). The cell-

death inducing *Grim*, *Head involution defective* (*Hid*) and *Reaper* (*Rpr*) genes appear to regulate the number of interneurons in the mAL under repressive control of FRU (**Figure 4**). In females, the majority of these mAL neurons are destined to die due to the absence of FRU, as ectopic FRU protein expression in females inhibits the death of these mAL neurons (Kimura *et al*., 2005). In summary, FRU in *Drosophila* inhibits cell death in males and regulates male-specific morphology of the mAL neurites, whereas in females, absence of FRU leads to programmed cell death and female-specific development of the few remaining mAL neurites (Kimura *et al*., 2005; Yamamoto, 2007).

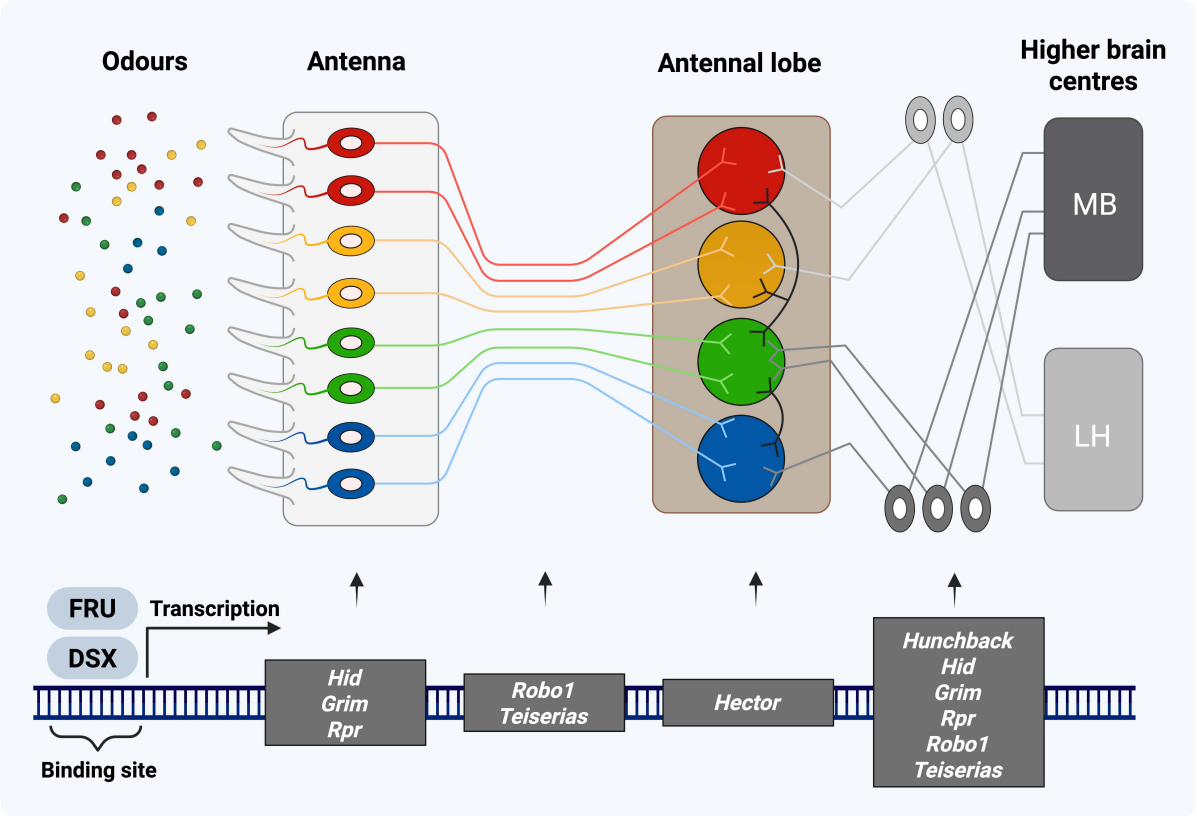

Figure 4: Concept showing the target genes of Doublesex (DSX) and Fruitless (FRU) affecting sexual dimorphism in the insect olfactory system.
The transcription-factor proteins DSX and FRU affect developmental processes in different regions of the olfactory system by regulating various downstream target genes, from the antennae to the antennal lobe and on to the higher brain centres of the mushroom body (MB) and lateral horn (LH).

Programmed cell death is not the only mechanism employed in *Drosophila* to regulate the number of neurons. *Dsx* is expressed earlier than *Fru* in the CNS (Lee *et al*., 2002) and controls abdominal neural stem-cell proliferation on a sex-specific basis (Taylor & Truman, 1992). Four of these abdominal neural stem cells express *Dsx*, but female-specific *Dsx* induces programmed cell death of these neural stem cells in conjunction with the Hox gene *Abdominal-B* (Ghosh *et al*., 2019). Male-specific *Dsx*, however, regulates a continued proliferation into late third-instars, resulting in neurons crucial for male mating behaviour (Billeter *et al*., 2006b; Taylor & Truman, 1992).

A combined action of *Fru* and *Dsx* has been shown in the birth and death of the P1 neuronal cluster (Kimura *et al*., 2008). In males, this P1 cluster expresses *Fru* in about 20 neurons and extends from the AL to the lateral horn. *Fruitless* is needed for correct neurite arborization of these neurons in the lateral horn to initiate courtship (Kimura *et al*., 2008). Both male-specific *Dsx* and *Fru* are required for the correct number of P1 cells, as loss of either of them leads to a reduction in these cells (Kimura *et al*., 2008). In females, female-specific *Dsx* is involved in the active removal of the P1 cluster from the female brain by programmed cell death, again involving *Grim*, *Hid* and *Rpr* (Kimura *et al*., 2008). Three other neuronal clusters express *Dsx* and are candidates for female-specific behaviour (Zhou *et al*., 2014). Two of these clusters (pCd and PC1) respond to the male-specific pheromone, cVA, to promote female receptivity (Zhou *et al*., 2014). Overall, *Dsx* and *Fru* appear to regulate the birth and death of olfactory neurons by targeting the programmed-cell-death-inducing factors *Grim*, *Hid* and *Rpr*. The same mechanisms potentially regulate OSN survival rate and the formation of novel OSN circuits described by Prieto-Godino *et al*. (2020).

Fruitless target genes involved in neuron differentiation and signalling

Fruitless target genes are involved in changes in dendritic arborization: the ipsilateral neurite in the mAL is present in males but absent in females, and the branching of the contralateral neurite differs between males and females (Kimura *et al*., 2005). The potential FRU downstream target, the transcription-factor gene *Hunchback*, has been shown to be required for male-specific branching of the contralateral neurites (Goto *et al*., 2011), whereas the FRU target *Robo1*, an axon-guidance gene, normally inhibits ipsilateral neurite development in females. Its expression, however, is repressed by FRU in males, resulting in ipsilateral neurite development (Ito *et al*., 1996). Recently, another FRU target gene has been identified, *Teiresias*, which is required for feminization of the neurite patterns, possibly by interacting with *Robo1* in females, and is repressed by FRU in males (Sato *et al*., 2020). The potential FRU target *Hector*, a novel putative G protein-coupled receptor (GPCR) gene, is found in a subset of AL glomeruli that are innervated by *Fru*-expressing PNs. Signalling through this GPCR in PNs is essential for male courtship behaviour (Li *et al*., 2011). It would be interesting to investigate whether the combined action of *Robo1*, *Teiresias* and *Hector* similarly regulate the correct targeting of OSN axons to the AL (**Figure 4**).

Fruitless and/or Doublesex rewire olfactory brain circuits

The male pheromone cVA has opposite effects in male and female *Drosophila*. It inhibits male-male mating behaviour, but promotes courtship and receptivity in females through the action of the Or67d receptor (Kurtovic *et al*., 2007). It has been shown that this single OSN class is capable of switching sex-specific behaviour in response to cVA (Kurtovic *et al*., 2007). The Or67d OSNs project to the DA1 glomerulus in the AL of both males and females (Manoli *et al*., 2005; Stockinger *et al*., 2005). The OSNs innervating DA1 then synapse male-specifically with PNs that project to the lateral horn under control of FRU, whereas in females, DA1 PNs

show a female pattern of axonal arbours in the lateral horn (Datta *et al*., 2008). The Or67d OSNs and the PNs both express *Fru*, but show no sexual dimorphism (Datta *et al*., 2008; Kurtovic *et al*., 2007). This would suggest that the olfactory input can be the same for both sexes, but the processing of this information in the lateral horn occurs sex-specifically. Kohl *et al*. (2013) builds on the work of Cachero *et al*. (2010) and shows that indeed two populations of lateral-horn neurons, aSP-f and aSP-g, have sex-specific dendritic arborization and reroute pheromone information to create a bidirectional switch. Male-specific FRU protein is required for the male form of the circuit switch by connecting the aSP-f neurons to the circuit and disconnecting the aSP-g neurons (Kohl *et al*., 2013). A similar circuit controlled by DSX and FRU switches between courtship and aggression in *Drosophila* males (Koganezawa *et al*., 2016). More recently, an additional circuit was identified in *Drosophila* that processes distinct sex-specific inputs, which converges on the *Dsx*-expressing anterior dorsal neuron (aDN) cluster, which in turn relays them to sex-specific outputs (Nojima *et al*., 2021). This cluster has sexually dimorphic dendritic arborizations, receiving inputs from visual PNs in males and predominantly olfactory PNs in females. The aDNs in females connect to an egg-laying circuit, whereas in males they play a role in motion detection during courtship, enabling them to locate and track a moving female (Nojima *et al*., 2021). In conclusion, only minimal sex-specific changes to higher brain order neurons would seem to be sufficient to elicit dramatic differences in sex-specific behaviour (Kohl *et al*., 2013; Nojima *et al*., 2021). Taken together, *Dsx* and *Fru* are essential for connecting and disconnecting AL PNs with higher brain order neurons to form circuits for sex-specific behaviour.

Conclusions

Sexual dimorphism in the AL is determined by genetically fixed growth processes of peripheral and deutocerebral neurons, but the relative contribution of these processes vary across insect orders. The first stages of inducing sexually dimorphic pheromone circuits are most likely set at the periphery through the expression of novel pheromone receptors in specialized sensilla. Neurons that succeed in surviving programmed cell death are eligible candidates for novel pheromone circuits. If these functional 'surviving' neurons match the right biochemical properties of their specific sensillum, a new olfactory pathway might be maintained if the novel OSN types are matched by similar expansions in the number of novel pheromone compounds. Pioneering sensory neurons sort the newly formed afferents of these surviving neurons to the AL and corresponding glomerulus. From an evolutionary perspective, an increase in the number of sensilla in one sex would not only simultaneously increase the number of these functional surviving neurons, but also the volume of the corresponding glomerulus and sensitivity to the pheromone component. It would be interesting to see whether the same processes of OSN-programmed cell death contribute to the reduction of glomerular volume and to the loss of redundant glomeruli in one sex, amplifying the degree of sexual dimorphism over evolutionary time. Such a phenomenon could occur in species that have evolved extreme differences in sex-specific tasks, such as in colony-forming insects or differences in reproductive roles.

The probability for the establishment of sexually dimorphic glomeruli seems to be largely determined by the degree of glia-OSN interactions and PN prepatterning. The relative contribution of either of these two processes determines the degree of evolutionary neuroplasticity. Transplanting male antennae onto female moths will form a male MGC even in the presence of female PNs, suggesting that signals induced by OSNs play a significant role in glia proliferation in these species. It remains to be investigated, however, what these signals are composed of and how glia cells sort incoming OSNs. Although genetically similar, novel OSNs might initially be sorted to the same glomerulus in the AL, but ultimately can be guided to a different location by glia cells and evolve into new glomeruli. The greatest degree of evolutionary neuroplasticity in this process is expected to have occurred in species with complex ALs lacking any specific macroglomerular structures. Hymenoptera integrate pheromone processing into combinatorial codes composed of glomerular clusters instead of MGCs that represent labelled lines. New glomeruli in these species may have initially emerged from a macroglomerulus and evolved into glomerular clusters after pheromone blends increased in complexity. Pheromone receptors would be excellent candidates to investigate this latter instance, given that previous studies have already determined the significant role the *Olfactory-receptor co-receptor* (*Orco*) plays in glomerular formation.

Different outcomes of sexual dimorphism are determined through sex-determination mechanisms, which are able to operate at various levels throughout AL development. The

transcription-factor genes *Dsx* and *Fru* can specify which neuron types are expressed and are needed for correct neurite arborization. Differential regulation of factors inducing programmed cell death determines the birth and death of olfactory neurons. Surviving neurons with beneficial properties can be favoured over evolutionary time and upregulated through sex-determination transcription factors by inhibiting the process of programmed cell death. Understanding the full significance of these transcription factors on AL development is still very much in its infancy, and the large majority of research has been carried out on *Drosophila*. This review can therefore serve as a foundation on which to initiate research into sexual dimorphism in the AL in light of sex-determination transcription factors.

In addition to providing a deeper understanding of the evolutionary processes involved, specific knowledge of pheromones and pheromone circuits can also have broad environmental and societal benefits. In agriculture and horticulture, sex pheromones are widely used as a tool to control insect pests and disease vectors, for example through mate disruption, but also serve as a potential means to attract biological control agents. Research into neuronal mechanisms of pheromone communication in parasitoid Hymenoptera is still in its infancy, whereas these species are crucial for maintaining ecosystem stability. In the same way, pollinating Hymenoptera fulfil essential ecosystem services and utilize complex pheromone-coding systems that require further research. Sex-determination processes play an important role in these and other insect species and may have significant developmental consequences for pheromone-processing circuits. Integrating sex determination in AL development therefore provides an opportunity to research these concepts and their numerous beneficial applications.

Acknowledgments

We are grateful to the staff of the Wageningen Electron Microscopy Centre for the production of scanning electron microscopy images of insect antennal sensilla. This work is partly financed by a VIDI grant (016.Vidi.189.099) of the Dutch Research Council (NWO) to Eveline Verhulst and an NWO VENI grant (016.Veni.192.116) to Alexander Haverkamp.

Minor modifications have been made to the original published article.

Chapter 3

Doublesex and *Transformer* shape neuronal differentiation in parasitoid olfaction

Aidan Williams[1], *Hans Smid*[1] *& Eveline Verhulst*[1]

[1]Laboratory of Entomology, Wageningen University, PO Box 16, 6700 AA Wageningen, the Netherlands

Abstract

Sex-specific behaviour in insects originates from differences in the peripheral and central nervous system that are regulated by conserved transcription factors at the bottom of the sex-determination pathway. Initiation of sexual behaviour in male and female insects is predominately determined by sex pheromones. These pheromones are perceived by sex-specific peripheral sensory organs and subsequently processed by sex-specific signalling pathways in the brain. Olfactory sensory neurons in sensilla transmit pheromonal information to the antennal lobe, the first odour-processing centre in the insect brain. Olfactory glomeruli in the antennal lobe then translate this information into an olfactory code. Sex-specific differences in the olfactory system are manifested in the form of sexual dimorphism of the sensilla and in the organization of glomeruli. Our knowledge of the genetic basis of these sex-specific differences, however, is limited to only a few species, such as *Drosophila*, even though the way transcription factors regulate these differences across species is highly diverse. More research is therefore needed to elucidate both the function of sex-determination transcription factors in regulating sexual dimorphism in the olfactory system across species and how these transcription factors in turn affect sex-specific behaviour. We used the model species *Nasonia vitripennis* to analyse the role that the sex-determination genes *Transformer* (*Tra*) and *Doublesex* (*Dsx*) have in determining behavioural responses towards sex pheromones and how such responses correspond to morphological differences in olfactory sensilla and in the organization of glomeruli in the antennal lobe. We silenced *NvTra* and *NvDsx* expression with dsRNA to masculinize females and feminize males before analysing the behavioural responses of these silenced wasps towards sex pheromones in an olfactometer bioassay. We observed that *Tra*-silenced females were no longer attracted to the male abdominal pheromone, whereas *Dsx*-silenced males acquired a preference for the male-specific pheromone blend. In addition, morphological differences were also observed in the olfactory sensilla on the antennae of these silenced specimens. Subsequent antennal tracing revealed a difference in the number of sex-specific glomeruli between males and females and that these glomeruli are regulated through *NvTra* in a clustered arrangement. This is the first study that confirms the conserved role that sex-determination transcription factors have in regulating sexual dimorphism in the olfactory system and sexual behaviour of parasitoid wasps.

Introduction

Insects rely on chemical communication for expressing their behaviour, such as finding mates, food sources and oviposition sites (Cardé & Baker, 1984; Wyatt, 2014). The complex chemical world of an insect consists of infinite odour blends forming its olfactory environment, also known as an odourscape (Conchou *et al*., 2019), from which relevant ecological cues are extracted. This requires acute sensory adaptations that are specifically tuned to filter out background noise and translate relevant cues into behavioural output (Hansson & Stensmyr, 2011; Haverkamp *et al*., 2018). A prime example of these adaptations is found in the sensory system where sexual-selection pressures act on the ability to detect host cues and sex pheromones optimally. For example, many female insects have evolved sensory adaptations, such as specialized receptors (Van der Goes van Naters & Carlson, 2007) used to detect sex pheromones produced by potential mating partners (Baker, 2002; Leary *et al*., 2012). Males, conversely, exploit these female adaptations by evolving pheromone signals specifically tuned to pheromone receptors to increase their mating opportunities (Stökl & Steiger, 2017). Sexual-selection forces act specifically on pheromone communication systems, inducing evolutionary shifts in pheromone composition and perception and lead to the evolution of sex-specific behaviour (Cao *et al*., 2023; Leary *et al*., 2012; Smadja & Butlin, 2009; Van Schooten *et al*., 2020). Sex-specific neural circuits then translate sex-pheromone information into sexual behaviour (Asahina, 2018; Auer & Benton, 2016; Manoli *et al*., 2013; Stowers & Logan, 2010), although our understanding of these processes between circuits and behaviour is currently limited to *Drosophila* (Yamamoto & Koganezawa, 2013). The way in which selection pressures act on molecular mechanisms regulating sex-specific circuits remains a significant unanswered question in the evolution of insect chemical communication.

Pheromone perception is initiated in the peripheral nervous system, through various receptors in the insect antennae. The antennae are enveloped in a variety of cuticular protrusions, called olfactory sensilla, which contain the dendrites of olfactory sensory neurons (OSNs) (Zacharuk, 1980). Sensilla come in different types, such as trichoid (hair-like), placoid (plate-like), basiconic (peg-like) and coeloconic (cone-like) (Keill, 1999; Schneider & Steinbrecht, 1968). Each type possesses a unique set of OSNs that express a subset of olfactory receptors (ORs) (Ai *et al*., 2010; Hallem & Carlson, 2006b; Kurtovic *et al*., 2007; Suh *et al*., 2004). Chemical compounds enter an olfactory sensillum through numerous pores, after which odorant binding proteins carry these compounds to the ORs on the OSN membrane (Leal, 2013; Vogt *et al*., 1991). The chemical ligand will bind to the OR, which is then activated and triggers the depolarization of the OSN. The axons of the OSNs expressing ORs project to a densely packed neuropil called the antennal lobe (AL) in the insect brain (Homberg *et al*., 1989). This brain region consists of numerous spheroid structures, called glomeruli, which pre-process olfactory information (Hansson & Anton, 2000). The morphology of a glomerulus is largely determined by the innervation of the OSNs (Grabe *et al*., 2016) and can vary in shape, volume and number between sexes and species (Arnold *et*

al., 1985; Kondoh *et al*., 2003; Roselino *et al*., 2015; Rospars & Hildebrand, 2000). Each OSN usually expresses a single OR and innervates a single glomerulus, a process referred to as the one-receptor-one-glomerulus principle (Fishilevich & Vosshall, 2005; Vosshall, 2000). OSNs that detect similar odours form separate neural classes, which are located in different sensilla. These classes project to distinct domains in the AL, resulting in a glomerular olfactory map (Couto *et al*., 2005; Gao *et al*., 2000; Grabe *et al*., 2016). Differential regulation of OSNs can therefore lead to novel neural circuits and a change in sex-specific behaviour (Hansson & Stensmyr, 2011; Ignell *et al*., 2001). Consequently, the sensillum-OSN-glomerulus relationship and the molecular mechanisms that regulate these intricate circuits are of particular interest to help us gain a better understanding of the evolution of insect chemical communication. To date, these developmental processes have received limited attention within neurogenetic research.

Neural circuits for sex pheromone perception are regulated by transcription factors of the sex-determination pathway (Bray & Amrein, 2003; Datta *et al*., 2008; Kimura *et al*., 2008; Sun *et al*., 2023a; Zhou *et al*., 2014). Sex determination in insects begins with a primary instructor signal that is transduced by a genetic switch called *Transformer (Tra)* (Bopp *et al*., 2014). Female splicing of *Tra* leads to female splicing of the downstream transcription-factor genes *Doublesex* (*Dsx*) and *Fruitless* (*Fru*), resulting in female differentiation, whereas in the absence of *Tra*, these factors are spliced male-specifically by default (Verhulst *et al*., 2010b). The sex-specific proteins of *Dsx* and *Fru* regulate the sex-biased expression of genes for the development of sexually dimorphic traits (Manoli *et al*., 2013; Verhulst & van de Zande, 2015). They do so by targeting DNA binding sites, so called *cis*-regulatory elements, and consequently activate or repress downstream genes (Clough *et al*., 2014; Neville *et al*., 2014; Vernes, 2014). Initially, DSX was considered to be exclusively a regulator of sex-specific morphological development, while FRU was thought to mediate sex-specific behaviour, as identified in *Drosophila melanogaster*. Emerging evidence now shows that DSX coordinates with FRU to regulate neurons for the initiation of sexual behaviour (Kimura *et al*., 2008; Siwicki & Kravitz, 2009). Research on sex-specific circuits, on the other hand, has primarily focused on *Drosophila*, in which *Fru* plays a dominant role. Nevertheless, this model species shows relatively little sexual dimorphism in the olfactory system compared to other species, such as Hymenoptera (Nishikawa *et al*., 2008; Roselino *et al*., 2015; Streinzer *et al*., 2013). Moreover, the role *Dsx* plays in regulating circuits for pheromone communication in these species has primarily been ignored.

Parasitoid wasps, such as *Nasonia*, are perfect model systems to study DSX regulation of pheromone communication. *Nasonia* are gregarious endoparasitoid wasps that parasitize the pupae of Cycloraphous flies (Barrass, 1960; Darling, 1990; Raychoudhury *et al*., 2010). *Nasonia vitripennis* in particular is one of the most studied insects in the areas of parasitoid behaviour and chemical ecology, and has been a parasitoid model species for over half a century (Mair & Ruther, 2019; Whiting, 1967). *Nasonia vitripennis* males use a blend of

abdominal long-range pheromones to attract females. These consist of the major components (4R,5R)- and (4R,5S)-5-hydroxy-4-decanolide (HDL-RR and HDL-RS) and the minor synergistic component, 4-methylquinazoline (4-MeQ) (Ruther *et al*., 2007, 2011). Female short-range cuticular hydrocarbons are used for mate recognition and eliciting courtship (Steiner *et al*., 2006), during which males use an oral pheromone to induce female receptivity for copulation (Ruther *et al*., 2010; Van den Assem, 1980). After mating, females switch to host-seeking behaviour and seek out host-habitat odours (Frederickx *et al*., 2014; Ruther *et al*., 2007, 2010; Ruther & Hammerl, 2014; Steiner & Ruther, 2009). In addition, sex-specific sensilla have been identified on male and female antennae (Wibel *et al*., 1984). Consequently, *N. vitripennis* is one of the best understood model species in the area of chemical ecology and the growing body of genetic resources makes it an ideal model system for studying the genetic regulation of parasitoid pheromone communication. The sex-determination pathway, including *Dsx* and *Fru*, has also been elucidated for *N. vitripennis* (Bertossa *et al*., 2009; Oliveira *et al*., 2009; Verhulst *et al*., 2010a; Zou *et al*., 2020) and DSX has been shown to regulate morphological differentiation at various life stages (Guerra, 2024; Wang *et al*., 2022a) and the production of certain male pheromones responsible for eliciting specific mating behaviour (Wang *et al*., 2022b). Silencing *Dsx* in males reduced the production of long- and short-range pheromones, and affected the receptivity response in females. However, it remains unclear whether *Dsx* is also responsible for regulating the *Nasonia* peripheral and central nervous systems for perceiving these pheromones.

The aim of this current study was to determine the roles of *Dsx* and *Tra* in regulating the olfactory system of the parasitoid *N. vitripennis* for sex-specific pheromone communication in both behaviour and perception. We silenced *Dsx* and *Tra* expression in late larval males and females respectively and investigated: (1) the behavioural response towards sex pheromones; (2) the development and distribution of olfactory sensilla on the antennae; and (3) the number and organization of antennal-lobe glomeruli. Based on previous studies (Guerra, 2024; Wang *et al*., 2022b), we hypothesized to find feminization in males in these three areas after silencing *Dsx* and masculinization in females after silencing *Tra*. Our study sets the foundation for further research into identifying genes targeted by DSX and TRA that are involved in sex-specific pheromone communication. Parasitoid wasps are invaluable for the biological control of agricultural pests. A thorough understanding of their olfactory system, therefore, is necessary to help us fully utilize their effectiveness and for implementing integrated pest-management strategies.

Materials & Methods

Nasonia rearing

The experiments were performed on the AsymCX laboratory strain of *N. vitripennis* (Werren *et al*., 2010). The AsymCX wasps were reared on *Calliphora vomitoria* host pupae (Kreikamp & Zn, Hoevelaken, the Netherlands) that had been stored at 4°C for a maximum duration of four weeks. Virgin *N. vitripennis* females were placed together with host pupae in polystyrene rearing vials to produce male-only offspring (100% males) and mated females were used to produce mainly female offspring (90% females). The AsymCX wasps were reared in accordance with the protocol for strain maintenance set out by Werren & Loehlin (2009a). The shorter rearing procedure of this protocol was chosen to ensure efficient timing of the experiments by incubating the vials in an incubator at a constant temperature of 25°C using a 16-hour light, eight-hour dark cycle. This enabled the brood to develop rapidly and emerge after approximately two weeks.

Synthesis and micro-injection of *NvDsx* and *NvTra* dsRNA

We used the MEGAscript RNAi Kit (Thermo Fisher, Waltham, MA, USA) to generate *NvDsx* and *NvTra* dsRNA from *Nasonia* cDNA. A non-sex-specific *NvTra* fragment of 452 bp was synthesized in a PCR using the GoTaq Flexi DNA polymerase (Promega, Madison, WI, USA) and the designed primers Nv_Tra_RNAi_F1 (5'-CGAGACATCAGTTAGAAGAT-3') and Nv_Tra_RNAi_R1 (5'-GTCTTGTGGTCCTATGAAAC-3'). For *NvDsx*, we generated dsRNA using the primers Nv_Dsx_U_RNAi_F (5'-CCAAGAGGCAGCAAATTATG-3') and Nv_Dsx_U_RNAi_R (5'-GTTATACGCCGCATGGCTAC-3'), producing a 457 bp amplicon corresponding to a sequence common to all male and female *NvDsx* isoforms. These PCR products were amplified in two separate PCRs to add T7 promotors [TAATACGACTCACTATAGGG] to either end of the amplicon. The resulting two templates were then used in separate PCR reactions to transcribe both sense and antisense RNA molecules in accordance with the MEGAscript RNAi Kit (Ambion, Austin, TX, USA) protocol (16 hours at 37°C). *Gfp* dsRNA was used as an exogenous control in our behavioural experiments and was generated from the pOPINEneo-3C-GFP vector (Addgene plasmid #53534; https://www.addgene.org/53534/; RRID: Addgene_53534). Amplification by PCR using GoTaq Flexi DNA polymerase (Promega) with the primers GFP_RNAi_F (5'-GTGACCACCTTGACCTACG-3') and GFP_RNAi_R (5'-TCTCGTTGGGGTCTTTGCT-3') produced a 460 bp amplicon, which covered 64% of the Emerald GFP CDS.

The synthesized dsRNA was measured for its purity and concentration on a spectrophotometer (DeNovix, DS-11 FX, Wilmington, Delaware, USA) and subsequently diluted with RNase-free water to a concentration of 4 µg/µl and injected in *N. vitripennis* larvae to silence *NvDsx* (*Dsx*-i) and *NvTra* (*Tra*-i). By doing so, we injected dsRNA before the onset of adult brain development, which typically takes place during the insect pupal phase (Tissot & Stocker, 2000). *NvDsx* dsRNA was injected in male and female fourth-instar larvae

(L4) six days post oviposition, and *NvTra* dsRNA was injected in female third-instar larvae (L3) four days post oviposition. The L3 larvae were specifically chosen for injecting *NvTra* dsRNA to enable sufficient time for the sex-specific splicing of *NvDsx* to develop masculinized morphologies. The larvae were aligned on a 1x phosphate-buffered saline (PBS) agar plate and injected with a mixture of 4.5 µl dsRNA and 0.5 µl food dye in their posterior using a FemtoJet 4i microinjection pump (Eppendorf, Hamburg, Germany) according to the protocol set out by Lynch & Desplan (2006) and Werren *et al*. (2009). The L3 larvae were returned to a parasitized host to continue feeding until pupation, whereas the L4 larvae were allowed to pupate on the agar plate. To ensure consistency, the parasitized hosts for the L3 larvae were prepared one day before the dsRNA injections by enabling female *N. vitripennis* to oviposit their eggs in the anterior of the fly pupae. The eggs were removed after 24 hours and the *NvTra* dsRNA-injected L3 larvae were placed inside the host to continue development. All dsRNA-injected larvae were incubated at 25°C until the emergence of adult wasps after pupation.

RNA extraction and cDNA synthesis

We extracted RNA from wasp pupae and adults to generate cDNA for assessing dsRNA efficiency. We used male pupae three days post-larval injection to analyse *NvDsx* expression, using *Gfp*-i males as a control. Female adults, on the other hand, were used to analyse *NvTra* expression, using wild-type males and females as controls. Wasp pupae and adults were individually collected and stored at −80°C until RNA was extracted. Five individuals per treatment group were pooled in Eppendorf tubes, each forming a replicate. The entire body of wild-type and dsRNA-treated males and females was used for isolating RNA. The frozen bodies were ground up and homogenized with a sterile pellet pestle in an Eppendorf tube. Total RNA was then extracted from all the replicates within a treatment group either with the RNA lysis buffer in accordance with the column-based protocol of the ZR Tissue & Insect RNA MicroPrep Kit (Zymo Research, Irvine, CA, USA) or with Trizol (Invitrogen, Carlsbad, CA, USA), according to the manufacturer's instructions. RNA was then quantified with a spectrophotometer (DeNovix, DS-11 FX, Wilmington, Delaware, USA). One µg of total RNA was used to synthesize cDNA using the 5x TransAmp buffer of the SensiFAST cDNA Synthesis Kit (Bioline Reagents Ltd, London, UK) containing a mixture of anchored oligo(dT) and random hexamer primers. The resulting cDNA was used for reverse transcription quantitative real-time PCR (RT-qPCR) and reverse transcription PCR (RT-PCR) procedures.

Reverse transcription quantitative real-time PCR on *NvDsx*

RT-qPCR was performed with a solution of 2 µl of cDNA diluted 1:16 and a 400 nM SensiFAST SYBR Lo-ROX mix (Bioline Reagents Ltd, London, UK) on a BIORAD Real-Time PCR Detection System (Veenendaal, the Netherlands). *NvDsx* was amplified with the primers Fq_cDSX_OD1 (5'-GCGAGTGCGAGTTCAGATAC-3') and Rq_cDSX_OD (5'-TCCTCATTTCCATCAGCATCTCG-3'). Elongation factor 1 alpha (EF1α) was used as a reference gene with the primers Nv_EF-

1a_qPCR_F (5'-CACTTGATCTACAAATGCGG-3') and Nv_EF-1a_qPCR_R (5'-GAAGTCTCGAATTTCCACAG-3'). The qPCR thermocycling conditions were 95°C 3'; 39x 95°C 15'', 55°C 30'', 72°C 30'', followed by a post-melt curve to check the degree of non-specific amplification. Raw fluorescence data generated by the CFX Manager software (v3.1) was baseline-corrected manually in the same software. We used the delta-delta Ct method ($2^{-\Delta\Delta Ct}$) to calculate relative gene expression (Livak & Schmittgen, 2001), in which delta-delta Ct is the calculated difference in cycle threshold values of housekeeping genes and reference samples. dsRNA efficiency was calculated using MS Excel and the data was analysed with a Wilcoxon rank-sum test in RStudio (v2024.12.1+563, Posit PBC).

Splice-variant analysis of *NvTra* and *NvDsx* after *Tra*-i

Sex-specific fragments of *NvTra* and *NvDsx* in dsRNA-injected and control females were analysed through RT-PCR. Five µl of a 100-fold cDNA dilution was used for this procedure. For sex-specific splicing of *NvTra*, we used the amplification primers Nv_Tra_F2 (5'-GACCAAAAGAGGCACCAAAA-3') and Nv_Tra_R3 (5'-GGCGCTCTTCCACTTCAAT-3'), located at exon 2 and 3 respectively, yielding a single 228 bp fragment in females and three fragments of 514, 460 and 282 bp in males depending on their age (Verhulst *et al*., 2010a). We used the primer pair A14_Nvit_DsxU_F2 (5'-TGAGCAATAACAACAGCAACAG-3') and Nv_DsxM_RNAi_R1 (5'-TCGGAGAAGATTGGCAGAAC-3') to amplify the male and female splice forms *NvDsxM1* and *NvDsxF* respectively, and the primer pair A14_Nvit_DsxU_F1 (5'-ACGGTTTGGCTACCATTGGC-3') and Nv_DsxM_R (5'-TAGTAGACGCTCTCTTTGGG-3') to amplify the male splice forms *NvDsxM2* and *NvDsxM3* (Wang *et al*., 2022a). *EF1α* was used as a reference gene with the primers NvEF1a_F1a and NvEF1a_R1a. The PCR thermocycling conditions were 95°C 3'; 35x 95°C 30'', 55°C 30'', 72°C 45''. The PCR fragments were analysed on a 2% non-denaturing agarose gel stained with ethidium bromide.

Olfactometer bioassay

We tested the response of dsRNA-injected males and females to the male long-range abdominal pheromone blend (HDL-RR, HDL-RS and 4-MeQ) in a linear acrylate olfactometer, based on an experimental setup utilized by Ruther *et al*. (2008) and modified to incorporate airflow. The olfactometer was divided into three six-centimetre zones: the central part representing a neutral zone and the two ends representing a control and test zone. The airflow was provided by a Stimulus Air Controller CS-55 (Ockenfels Syntech GmbH, Buchenbach, Germany) and was charcoal filtered and humidified before entering both ends of the olfactometer. The airflow was controlled by flowmeters (Dwyer RMA-11-SSV) and channelled through the olfactometer via Teflon tubes at a rate of 20 ml/min, which resulted in a linear velocity of 0.42 cm/s. Synthetic compounds (provided by Joachim Ruther) of the male abdominal pheromone blend were dissolved in dichloromethane and pipetted onto a filter paper strip measuring 2x4 cm. The following pheromone treatments were tested: 400 ng/µl HDL vs solvent control for males and 400 ng/µl HDL + 5 ng/µl 4-MeQ vs solvent control

for females. The 4-MeQ component is essential for females since it has a synergizing effect on the attractiveness of the HDL component (Ruther *et al*., 2008). Following application, the dichloromethane was allowed to evaporate for two minutes before the filter papers were inserted into Teflon tubes connected to the control and test zones. Individual wasps were subsequently inserted into the neutral zone with an aspirator. The residence time in the control and test zone was recorded for five minutes per individual with a timer. The timer was paused when the individual entered the neutral zone. After every five replicates, the filter paper was replaced and the olfactometer was turned 180 degrees to correct for possible unforeseen side bias. After each experiment, the olfactometer was cleaned with detergent and dried by forcing compressed air through the tubes. The above-mentioned procedure was used to determine the preference of *Gfp*-i females (n = 17) for a mixture of 400 ng/µl HDL + 5 ng/µl 4-MeQ vs the solvent control. We subsequently repeated this test for *Tra*-i (n = 25) and *Dsx*-i (n = 27) females. We then determined the preference of *Gfp*-i males (n = 20) for 400 ng/µl HDL vs the solvent control and repeated this test for *Dsx*-i males (n = 22). The difference in mean residence time between the control and test zones after five minutes was analysed with a Wilcoxon signed-rank test of the Coin package in RStudio (v2024.12.1+563, Posit PBC). Zone preference of *Tra*-i and *Dsx*-i individuals after five minutes was compared with the *Gfp*-i control and analysed with Pearson's Chi-squared test with Yates's continuity correction.

Scanning electron microscopy of antennal sensilla

Wild-type and dsRNA-injected wasps were sedated and decapitated on a CO_2 pad and the heads were transferred to a clean glass vial with ice-cold 2% glutaraldehyde (Sigma-Aldrich) in a 0.5M sodium cacodylate buffer (pH = 7.4, Merck Schuchardt). After two hours of fixation, the wasps were rinsed three times in a 0.5M sodium cacodylate buffer and post-fixated for one hour in 1% OsO_4 (Agar Scientific) in a 0.5M sodium cacodylate buffer, followed by five rinsing cycles in water. The specimens were subsequently incubated overnight in CCl_4 at room temperature and then subjected to three short boiling cycles in fresh CCl_4 before being transferred to 100% ethanol. The specimens were then supercritically dried to remove liquid from their bodies to prevent damage caused by changes in surface tension and sputtered with a 12 nm layer of iridium to prepare them for visualization with a FEI Magellan 400 scanning electron microscope (SEM) at 2kV. Scanning electron micrographs were made of the antennae and analysed with the Fiji package of ImageJ2 (v2.9.0/1.53t). The length, width and surface area of every flagellar subsegment was measured and used to calculate the total surface area of the entire flagellum. The total number of sensilla was then counted and the sensillum density was calculated by dividing the total number of sensilla by the total surface area of the flagellum. The following types of sensilla were subsequently identified based on the classifications of Slifer (1969) and Wibel *et al*. (1984): *sensilla trichodea*, *sensilla chaetica*, *sensilla placodea* and *sensilla basiconica*. The individual types were quantified using the Multi-point tool in ImageJ2 and analysed for sex-specific morphological differences. The length and width of the trichoid and placoid sensilla were measured using the Region of Interest (ROI) manager of ImageJ2 and differences in the pore density of the pore plates on

the placoid sensilla were visualized. Differences in the basiconic capitate sensilla were determined by counting the number of ridges on the sensillum peg. All data was analysed with a Wilcoxon rank-sum test of the Coin package in RStudio (v2024.12.1+563, Posit PBC).

Anterograde tracing of the antennal lobe

We performed anterograde tracing of antennal OSNs to visualize AL morphology of wild-type and dsRNA-injected wasps in accordance with the protocol adopted by Smid *et al*. (2003). Antennal backfills were performed by severing the left antenna of cold-sedated wasps between the flagellum and the pedicel. The wasp bodies were then immobilized in commercial modelling dough, with the head and amputated antenna protruding. A tapered glass microcapillary filled with a 2.5% Biotin-Dextran (B9139, Sigma-Aldrich, St. Louis, MO, USA) solution was placed over the pedicel and the specimens were incubated at 4°C for four hours. The backfilled specimens were subsequently decapitated and the heads were fixated in freshly dissolved 4% formaldehyde in a 0.1M PBS solution (pH 7.2) at 4°C overnight. The heads were then briefly washed once in 70% ethanol and four times in 1x PBS to remove residual formaldehyde. The brains were dissected in PBS in transparent glass staining blocks and dehydrated in a graded series of ethanol (90%, 96% and 100%), followed by a 50-50% ethanol/xylene solution and finally 100% xylene. The specimens were then rehydrated in a graded series of ethanol (100%, 96%, 90%, 70%, 50% and 30%) and finally PBS. The brains were further permeabilized in a 0.05% collagenase/PBS solution for one hour and incubated in a solution of phosphate-buffered saline with Triton X-100 (PBS-T) and 1% bovine serum albumin (BSA) at room temperature (RT) for one hour. A Streptavidin-Alexa Fluor 488 conjugate (S32354, Invitrogen, Waltham, MA, USA) and propidium iodide (P1304MP, Invitrogen) were subsequently added to the PBS-T-BSA solution in a 1:50 and 1:200 dilution, respectively. After incubation for ten hours, the brains were washed in three cycles of PBS and PBS-T and dehydrated again in a graded series of ethanol (30%, 50%, 70%, 90%, 96%, 3x 100%), followed by a 50-50% ethanol/xylene solution and finally 100% xylene. Finally, the brains were mounted on individual microscope slides in Dibutyl phthalate Polystyrene Xylene (DPX, 06522, Sigma-Aldrich).

Confocal microscopy and antennal lobe 3D reconstruction

The mounted brain specimens were examined with a Zeiss LSM510 confocal laser scanning microscope (Zeiss, Jena, Germany). The excitation light was provided by an argon ion laser (458, 488 and 514 nm). The laser was fitted with a band-pass emission filter set at 488 nm to excite the Alexa Fluor 488 stain and with a long-pass emission filter set at 560 nm to excite the propidium iodide stain. The ALs were scanned using either the 40x or 63x Plan-Neofluar NA 1.3 oil-immersion objective at a resolution of 2048 x 2048 pixels at 8-bits. Z-stacks were scanned side by side with approximately 20% oversampling (i.e. 20% overlapping of the optical sections on the Z-axis). The resulting image stacks were then merged into datasets and AL glomerular organization was analysed using 3D-visualization software (AMIRA 5.4.2.,

Visage Imaging). Individual glomeruli were manually segmented in each optical section by assigning voxels to discrete elements representing 3D space. A unique label was then assigned to each specific glomerulus, resulting in a 3D array of voxels, where each voxel was individually labelled as either a glomerulus or belonging to the background. Only ALs with pronounced and well-defined glomeruli were used to determine the number of glomeruli from the completed segmentations. The total number of individual glomeruli was then calculated by counting all the unique glomerular labels and analysed for significant differences between treatment groups with a Wilcoxon rank-sum test of the Coin package in RStudio (v2024.12.1+563, Posit PBC). We then used the Resample module to enlarge the resolution for subsequent 3D-surface reconstructions. From these datasets, we created 3D-surface reconstructions of the ALs with the SurfaceGen and Unconstrained Smoothing modules. These 3D reconstructions enabled glomerular morphology to be viewed from any angle, which made it possible to visualize discrepancies in glomerular structures between wild-type and dsRNA-injected males and females.

Results

dsRNA efficiency following *Tra*-i and *Dsx*-i

We assessed *NvTra* dsRNA efficiency by analysing the sex-specific splicing of *NvTra* and *NvDsx* in wild-type and *Tra*-i samples. Wild-type males and females in our study showed normal male- or female-specific splicing of *NvTra* and *NvDsx* (**Figure 1A-1C**), as observed previously by Oliveira *et al*. (2009) and Verhulst *et al*. (2010a). Conversely, silencing *Tra* in females resulted in both male- and female-specific splicing of *NvTra* (**Figure 1A**). In addition, these samples also showed both male- and female-specific splice forms of *NvDsx* (**Figure 1B, 1C**). The reference gene EF1α showed a constant expression pattern in all wild-type and dsRNA-injected samples (**Figure 1D**).

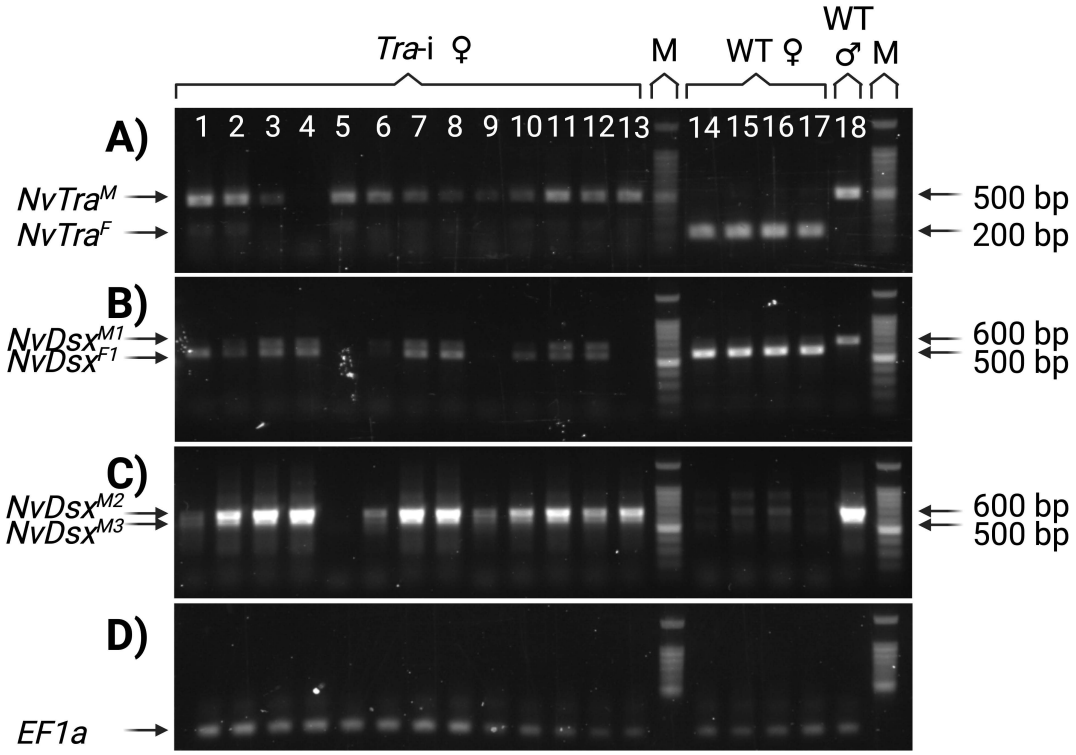

Figure 1: Sex-specific splicing of *NvTra* after dsRNA treatment.
A-D: Gel electrophoresis showing sex-specific splicing of *NvTra* and *NvDsx* in females after *Tra*-i. Lanes 1 to 13 represent *NvTra* dsRNA-injected females, lanes 14 to 17 represent wild-type females and lane 18 a wild-type male. M is a 100-bp molecular-weight size marker. The samples in lanes 5 and 13 contained contamination, which hampered *NvTra* amplification. Arrows mark male- and female-specific splicing of *NvTra* and *NvDsx*. **A:** Sex-specific splicing patterns of *NvTra*, amplified with the NvTra_F2 and NvTra_R3 primers. **B-C:** Sex-specific splicing patterns of *NvDsx*, showing the three male-specific splice forms (*NvDsxM1*, *NvDsxM2* and *NvDsxM3*) and the female-specific splice form (*NvDsxF1*). **D:** The *EF1α* reference gene was expressed in all samples.

The *Tra*-i females that exhibited both male- and female-specific splicing also developed a male-like phenotype. The antennae and femora, in particular, had significantly lighter pigmentation compared to wild-type females, and wing morphology also showed an intermediate state between wild-type males and females. Normally, the forewings of wild-type females extend well beyond the abdominal tip (Wang *et al*., 2022a), whereas the

forewings of *Tra*-i females extended to or marginally beyond the abdominal tip. The *Tra-i* females that expressed these male-like phenotypes confirmed successful *NvTra* knockdown and were selected for our subsequent experiments.

We also assessed the efficiency of *NvDsx* dsRNA with RT-qPCR (**Figure 2, Supplementary Table 1**). We silenced *NvDsx* in L4 male larvae and sampled these *Dsx*-i males (n = 8) three days later as white-stage pupae to assess *NvDsx* expression. We observed a ~35% reduction of *NvDsx* expression relative to *Gfp*-i males (n = 8), although this reduction was not significant (Wilcoxon rank-sum test, W = 14, p = 0.06). However, silencing *NvDsx* in males also resulted in female-like phenotypes, including dark pigmentation on the femora, tibiae and antennae, as previously observed by Wang *et al*. (2022a). Again, forewing morphology showed an intermediate state between wild-type males and females. The *Dsx*-i males that expressed these female-like phenotypes likewise confirmed successful *NvDsx* knockdown and were also selected for our subsequent experiments.

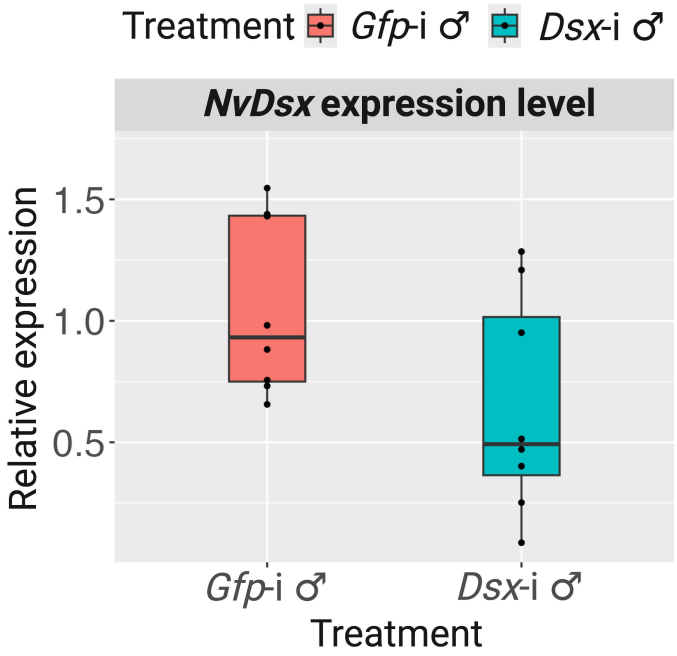

Figure 2: Relative expression of *NvDsx* after dsRNA treatment.
Normalized relative expression of *NvDsx* in males after *Dsx*-i. Relative quantification of *NvDsx* expression in *Dsx*-i males shows a ~35% reduction relative to the *Gfp*-i control (W = 14, p = 0.06). The significance of the difference between the *Gfp-i* control and *Dsx*-i males was analysed with a Wilcoxon-rank sum test. Significance levels: NS = not significant.

Sex-pheromone preference following *Tra*-i and *Dsx*-i

We tested the preference (**Figure 3A**) and residence time (**Figure 3B**) of dsRNA-injected *N. vitripennis* males and females in an olfactometer bioassay containing the male abdominal pheromone ((4R,5R)- and (4R,5S)-5-hydroxy-4-decanolide and 4-methylquinazoline) (**Supplementary Table 2**).

All females were subjected to the HDL+4-MeQ components of the male abdominal pheromone. We found that *Gfp*-i females silenced at the L3 stage (n = 17) spent significantly more time in the pheromone zone than in the control zone (Wilcoxon signed-rank test, Z = 2.7693, p < 0.01). In total, 88% of the *Gfp*-i females showed a preference for the pheromone zone. This indicates that silencing *Gfp* in females did not affect their ability to perceive the male abdominal pheromone. *Tra*-i females silenced at the L3 stage (n = 25), on the other hand, spent a relatively similar amount of time in both the pheromone zone and control zone (Z = 0.47087, p = 0.63). In total, 48% of the *Tra*-i females showed a preference for the pheromone zone (Pearson's Chi-squared test, χ^2 = 5.4902, p < 0.05). This result indicates that NvTRA regulates factors downstream of the sex-determination pathway to activate female perception of the male abdominal pheromone. Conversely, *Dsx*-i females treated at the L4 stage (n = 27) spent significantly more time in the pheromone zone than in the control zone (Z = 4.0848, p < 0.001). In total, 96% of the *Dsx*-i females showed a preference for the pheromone zone (χ^2 = 0.17535, p = 0.67). This indicates that NvDSX is not involved in regulating female perception of the abdominal pheromone and that other factors regulated by *NvTra* must be responsible.

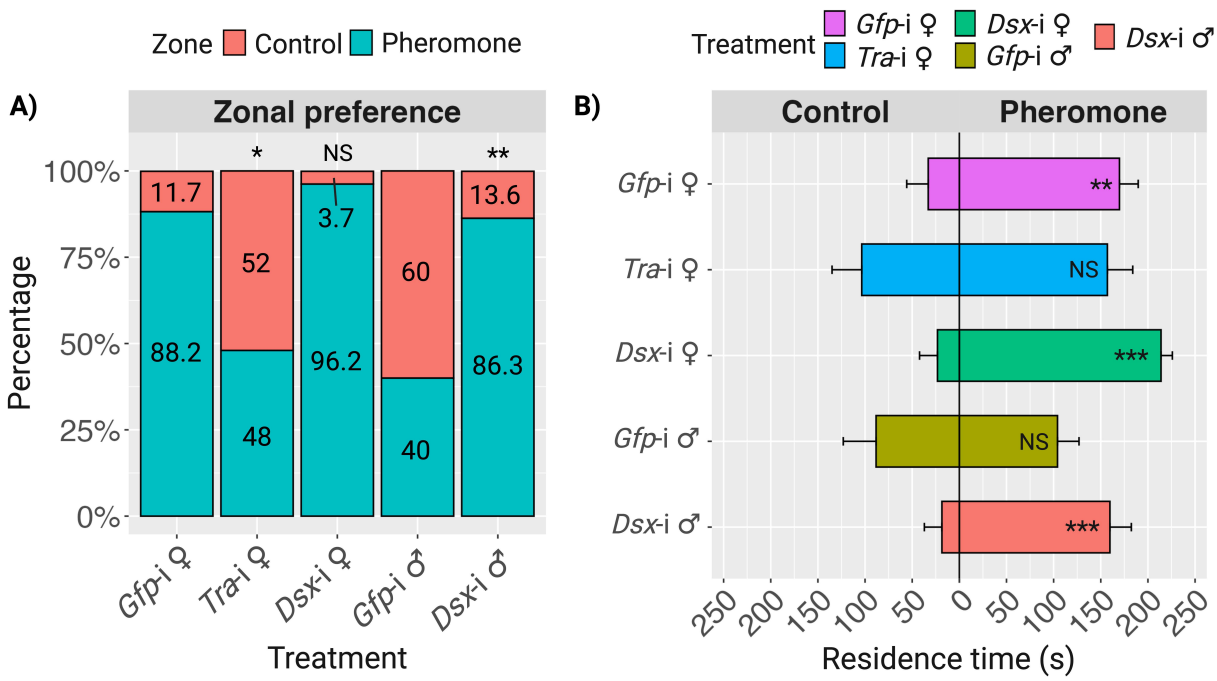

Figure 3: Zonal preference and residence time of dsRNA-injected male and female *N. vitripennis* in an olfactometer bioassay containing the male abdominal pheromone.

A: Percentage of dsRNA-injected and control (*Gfp*-i) individuals showing a preference for either the solvent control (depicted in red) or the male abdominal pheromone (HDL+4-MeQ for females and HDL for males) (depicted in blue). Preferences of *Tra*-i and *Dsx*-i individuals were compared with their respective *Gfp*-i control treatment and analysed for significant differences with a Pearson's Chi-squared test. **B:** Mean residence time of dsRNA-injected and control (*Gfp*-i) individuals in the olfactometer zones after five minutes observation. Significant differences in mean residence time spent in the olfactometer zones were analysed with a Wilcoxon signed-rank test. Significance levels: *** = p < 0.001, ** = p < 0.01, * = p < 0.05 and NS = not significant.

All males were subjected to the HDL component of the male abdominal pheromone. *Gfp*-i males silenced at the L4 stage (n = 25) spent a relatively similar amount of time in both the pheromone zone and control zone (Z = 0.39019, p = 0.69). In total, 40% of the *Gfp*-i males showed a preference for the pheromone zone. This confirms their indifference to the male abdominal pheromone and therefore indicates their inability to perceive this pheromone. Conversely, *Dsx*-i males silenced at the L4 stage (n = 25) spent significantly more time in the pheromone zone than the control zone (Z = 3.4256, p < 0.001). In total, 86% of the *Dsx*-i males showed a preference for the pheromone zone (χ^2 = 8.7734, p < 0.01). These results demonstrate that silencing *NvDsx* in males activates chemosensory processes, enabling them to perceive the male abdominal pheromone.

Differential expression of olfactory sensilla following *Tra*-i and *Dsx*-i

Antennae of *N. vitripennis*

We used scanning electron microscopy to map the antennae of wild-type (control) and dsRNA-injected males and females. The antenna of *N. vitripennis* consists of a radicula, scape, pedicel and flagellum (**Figure 4A**). The flagellum consists of two anellar segments, eight funicular segments and a clava of two segments (**Figure 4B, 4C**). We measured the length and width of each flagellar segment and calculated the mean length and surface area of the entire flagellum (**Supplementary Table 3**). The wild-type male flagellum had a mean length of 605±35 µm (mean±sd) compared to 712±45 µm in wild-type females (Wilcoxon rank-sum test, Z = 3.2404, p < 0.01). The mean surface area of the entire flagellum was 21426±2577 μm^2 in wild-type males and 24134±2278 μm^2 in wild-type females (Z = 2.4303, p < 0.05). *Dsx*-i males developed a 10% longer flagellum (671±60 µm, Z = 2.1924, p < 0.05) than wild-type males, but maintained a similar surface area (Z = −0.5684, p = 0.63). Conversely, compared to wild-type females, the flagellum of *Tra*-i females did not differ in length (Z = 0.3873, p < 0.69) or surface area (Z = 0.7746, p = 0.43).

We classified the sensilla of males and females in accordance with Slifer (1969) and Wibel *et al*. (1984) on the basis of morphological characteristics such as size, shape, ultrastructure and basal socket. Accordingly, we identified and analysed four main types of sensilla: *sensilla trichodea*, *sensilla chaetica*, *sensilla placodea* and *sensilla basiconica* (**Figure 5A-5F, Supplementary Table 4**).

Sensillum number and density

Wild-type males (n = 7) and females (n = 8) showed sexual dimorphism in the total number of sensilla on the flagellum (**Figure 4B, 4C**): wild-type males possessed 277±18 sensilla compared to 373±21 in wild-type females (Z = 3.2433, p < 0.01). However, despite the difference in surface area, no significant difference in sensillum density was found (**Figure 6B**; Z = 1.7359, p = 0.08). *Dsx*-i males (n = 6), on the other hand, showed no significant difference in the total number of sensilla (**Figure 6A**; Z = 1.7166, p = 0.08) nor in sensillum density (**Figure 6B**; Z =

1.7143, p = 0.08), whereas *Tra*-i females (n = 6) developed 9.78% more sensilla (**Figure 6A**; 410±28, Z = 2.1971, p < 0.05), while maintaining a similar sensillum density (Z = 0.6455, p = 0.51).

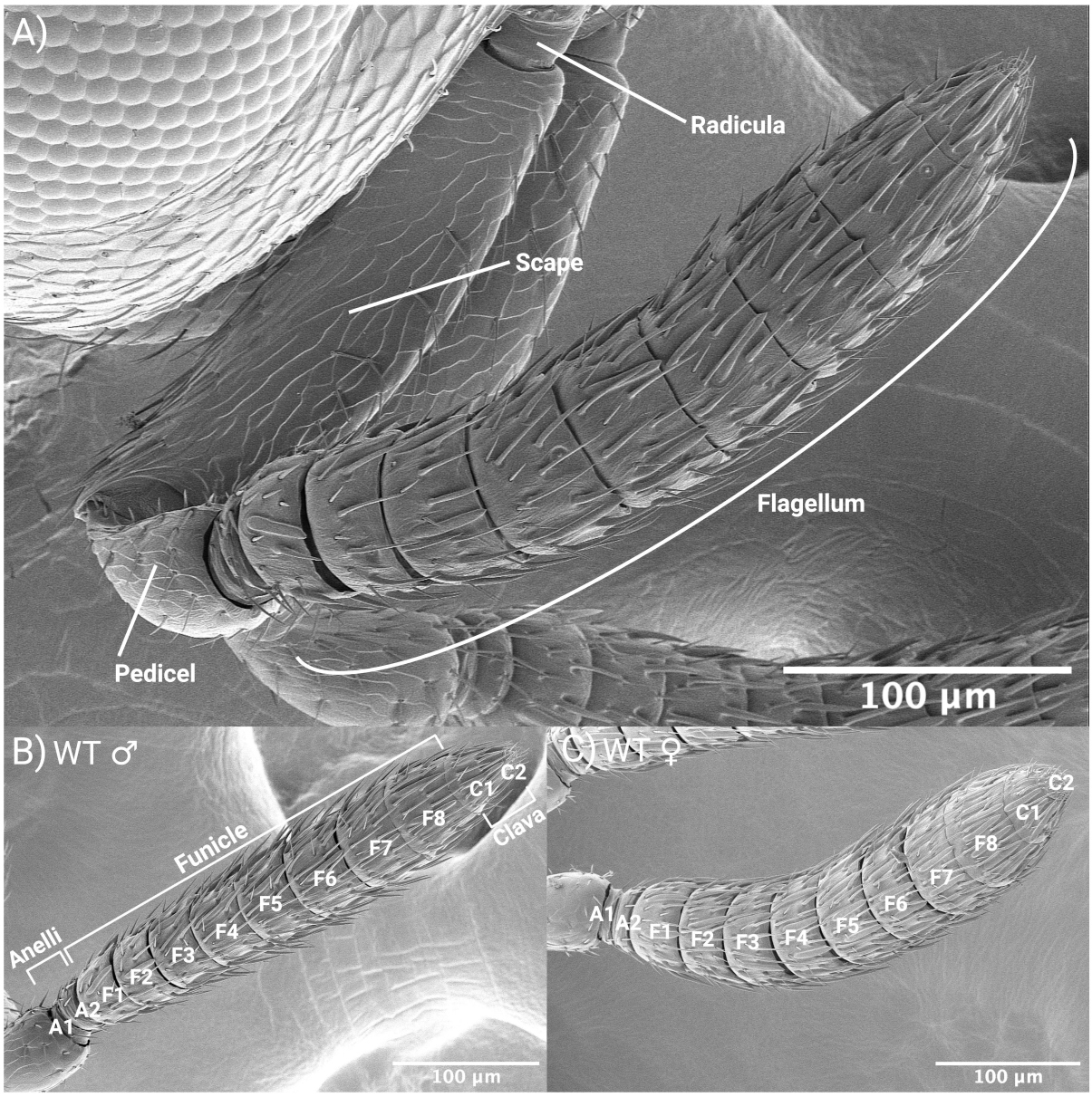

Figure 4: Scanning electron micrographs of *N. vitripennis* antennae.
A: Morphology of wild-type (WT) *N. vitripennis* antennae, consisting of the radicula, scape, pedicel and flagellum segments. **B-C:** Overview of antennal segmentation in wild-type males and females: flagellum consisting of two anelli (A1-A2), eight funicular segments (F1-F8) and a clava of two segments (C1-C2).

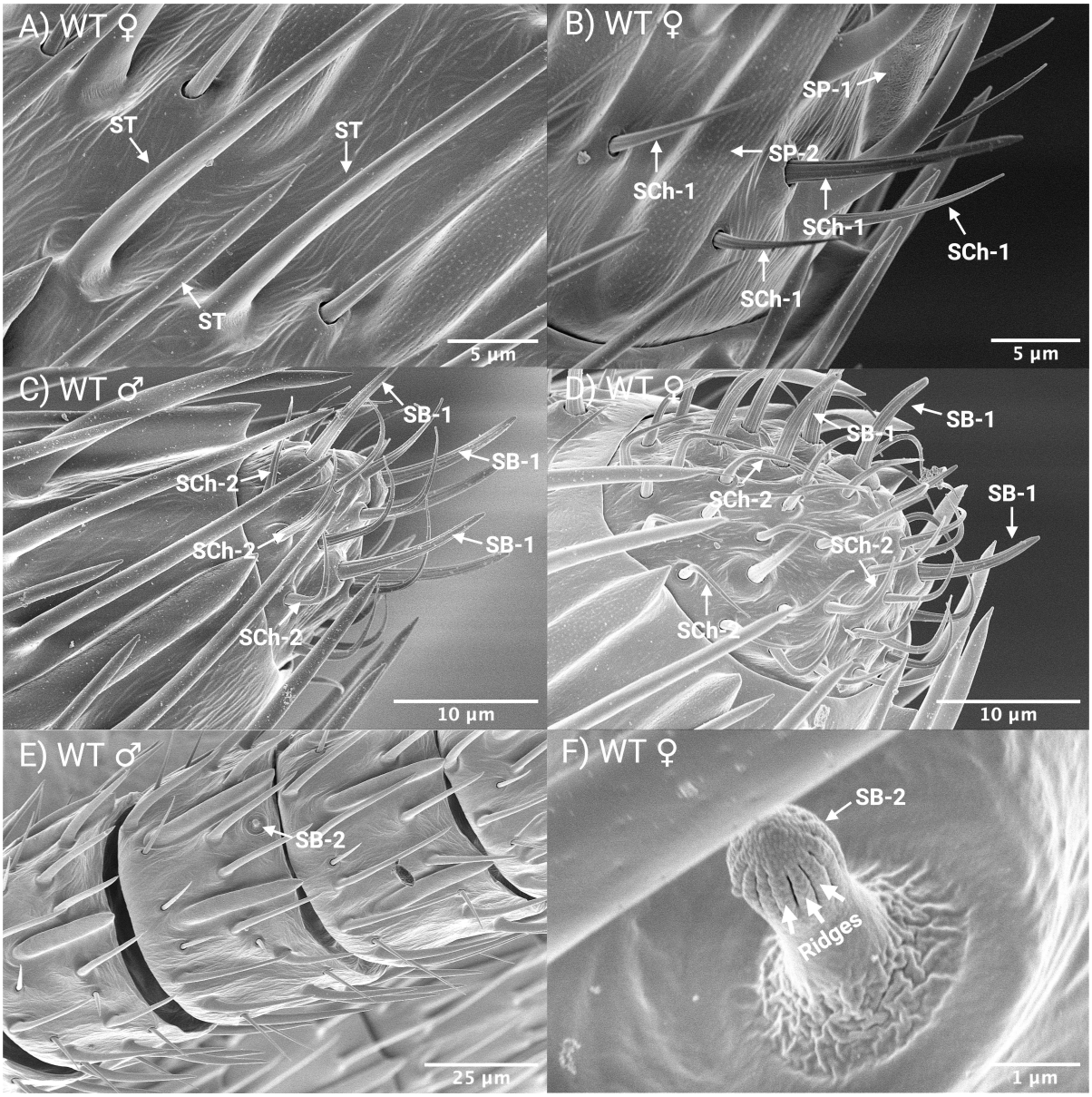

Figure 5: Scanning electron micrographs of different types of sensilla on wild-type male and female *N. vitripennis* antennae.

A-F: Magnified view of wild-type (WT) male and female segments showing the ultrastructure of different sensillum types. **A:** Hair-like *sensilla trichodea* (ST) with pores distributed along the hairs. **B:** *Sensilla chaetica* subtype 1 (SCh-1) and *sensilla placodea* subtypes 1 (SP-1) and 2 (SP-2) with distinct differences in pore density. **C-D:** Magnified view of the male and female antennal clava showing *sensilla chaetica* subtype 2 (SCh-2) with a curved structure and *sensilla basiconica* subtype 1 (SB-1) in a generally clustered arrangement with a single pore on the tip. **E-F:** Ultrastructure of *sensilla basiconica* subtype 2 (SB-2) showing a peg-like structure and a bulbous head containing a sex-specific number of ridges.

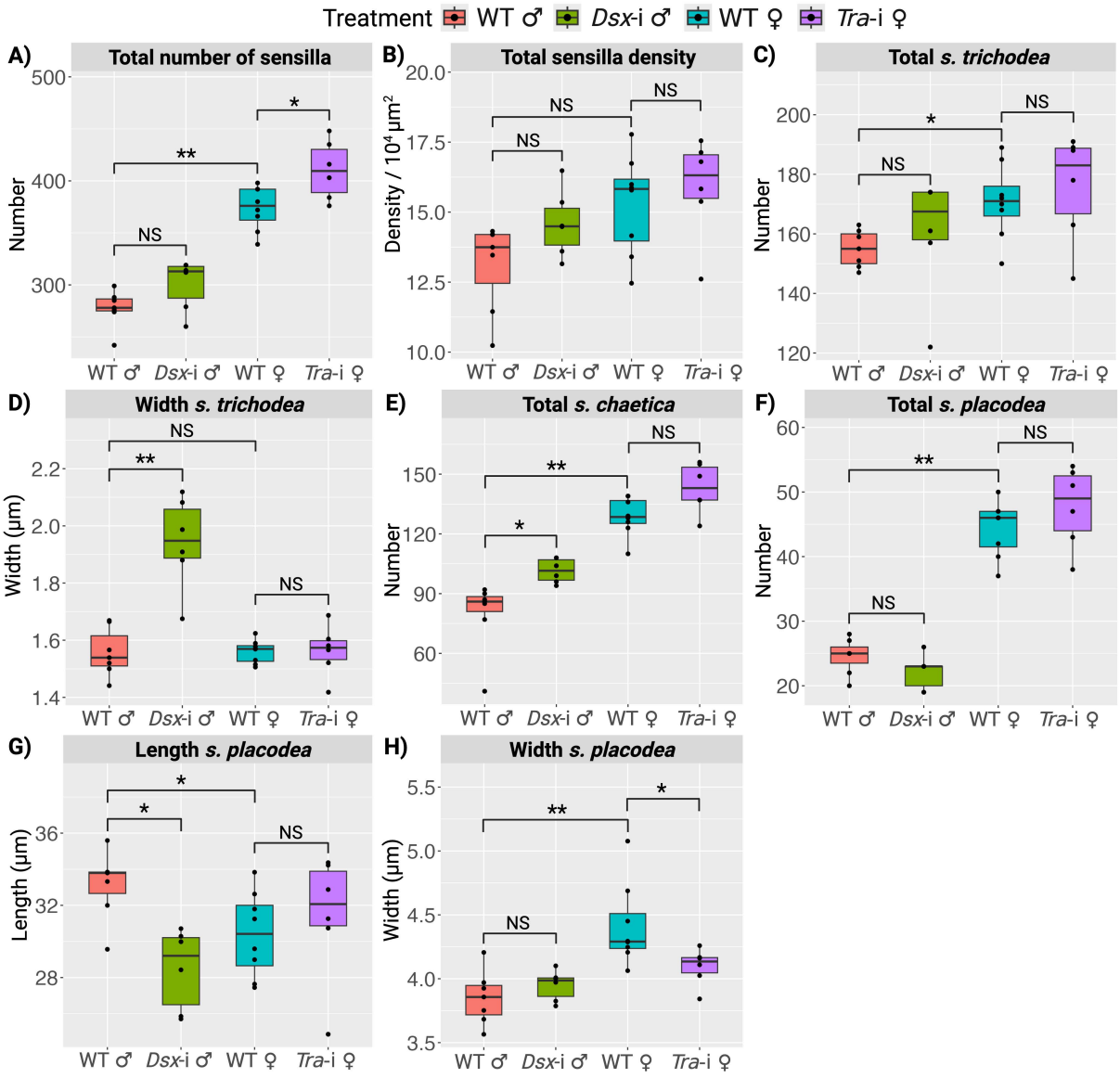

Figure 6: Morphological analysis of *N. vitripennis* antennal sensilla after dsRNA treatment.
A: Wild-type (WT) females possessed significantly more sensilla than wild-type males. *Tra*-i females developed significantly more sensilla than wild-type females. **B:** No significant difference was detected in sensillum density between wild-type males and females. There was also no significant difference found in sensillum density in *Dsx*-i males and *Tra*-i females compared to their wild-type counterparts. **C:** Wild-type females possessed significantly more *sensilla trichodea* than wild-type males, whereas no significant change was detected in the number in *Dsx*-i males and *Tra*-i females compared to their wild-type counterparts. **D:** *Dsx*-i males developed significantly wider *sensilla trichodea* than wild-type males. There was no significant change in trichoid width in *Tra*-i females compared to wild-type females. **E:** Wild-type females and *Dsx*-i males developed significantly more sensilla chaetica than wild-type males. **F:** Wild-type females possessed significantly more *sensilla placodea* than wild-type males, whereas no significant change was detected in the number in *Dsx*-i males and *Tra*-i females compared to their wild-type counterparts. **G:** Wild-type males possessed significantly longer *sensilla placodea* than wild-type females, whereas in *Dsx*-i males these sensilla were significantly shorter than in wild-type males. There was no significant difference in placoid length between *Tra*-i females and wild-type females. **H:** Wild-type females possessed significantly wider *sensilla placodea* than wild-type males, whereas in *Tra*-i females these sensilla were significantly thinner than in wild-type females. There was no significant difference in placoid width between *Dsx*-i males and wild-type males. Significant differences in the number, density, length and width were analysed with a Wilcoxon rank-sum test. Significance levels: ** = $p < 0.01$, * = $p < 0.05$ and NS = not significant.

Sensilla trichodea

The antennae of *N. vitripennis* possess a large number of multiporous hair-like sensilla, which were classified by Slifer (1969) as “thin-walled pegs” and by Wibel *et al*. (1984) as “thin-walled chemoreceptors”. The morphology of these hair-like sensilla corresponds closely to what has been identified in other parasitoid wasps as *sensilla trichodea* (Dweck, 2009; Onagbola & Fadamiro, 2008). Each trichoid sensillum emerges from the cuticle without a socket, has a smooth surface and is covered in multiple small pores (**Figure 5A**). These tapered sensilla are distributed between the placoid sensilla on nine flagellar segments (**Figure 4B, 4C**: F1-C1) in both males and females and are 28.21±2.01 µm long and 1.55±0.06 µm wide at the base.

Wild-type males possessed 155±6 trichoid sensilla compared to 170±13 in wild-type females (**Figure 6C**; $Z = 2.4303$, $p < 0.05$). However, there was no significant difference in overall trichoid density (**Supplementary Figure 1A**; $Z = -0.98545.5$, $p = 0.32$). After silencing, neither *Dsx*-i males nor *Tra*-i females showed a significant difference in the number of trichoid sensilla compared to wild-type males and females (**Figure 6C**; $Z = 1.3666$, $p = 0.17$ and $Z = 0.84007$, $p = 0.40$, respectively), and likewise in trichoid density (**Supplementary Figure 1A**; $Z = 0.85832$, $p = 0.39$ and $Z = -0.6455$, $p = 0.51$, respectively).

Wild-type males and females showed sexual dimorphism in the morphology of trichoid sensilla. In males, these sensilla were 26.91±1.38 µm long compared to 29.34±1.82 µm in females (**Supplementary Figure 1B**; $Z = 2.1988$, $p < 0.05$). After silencing, *Dsx*-i males developed significantly wider (24.71%) trichoid sensilla compared to wild-type males (1.94±0.16 µm and 1.55±0.08 µm, respectively) (**Figure 6D**; $Z = 3$, $p < 0.01$). These modified trichoid sensilla were particularly widened at the base, with a number of them attaching to the antennal cuticle along the sensillum length and showing a proliferation of pore formation towards the base (**Figure 7A-7D**). From these results, it is evident that these sensilla have developed into an intermediate state between a trichoid and a placoid, which indicates that *NvDsx* in males regulates the development of these types of sensilla.

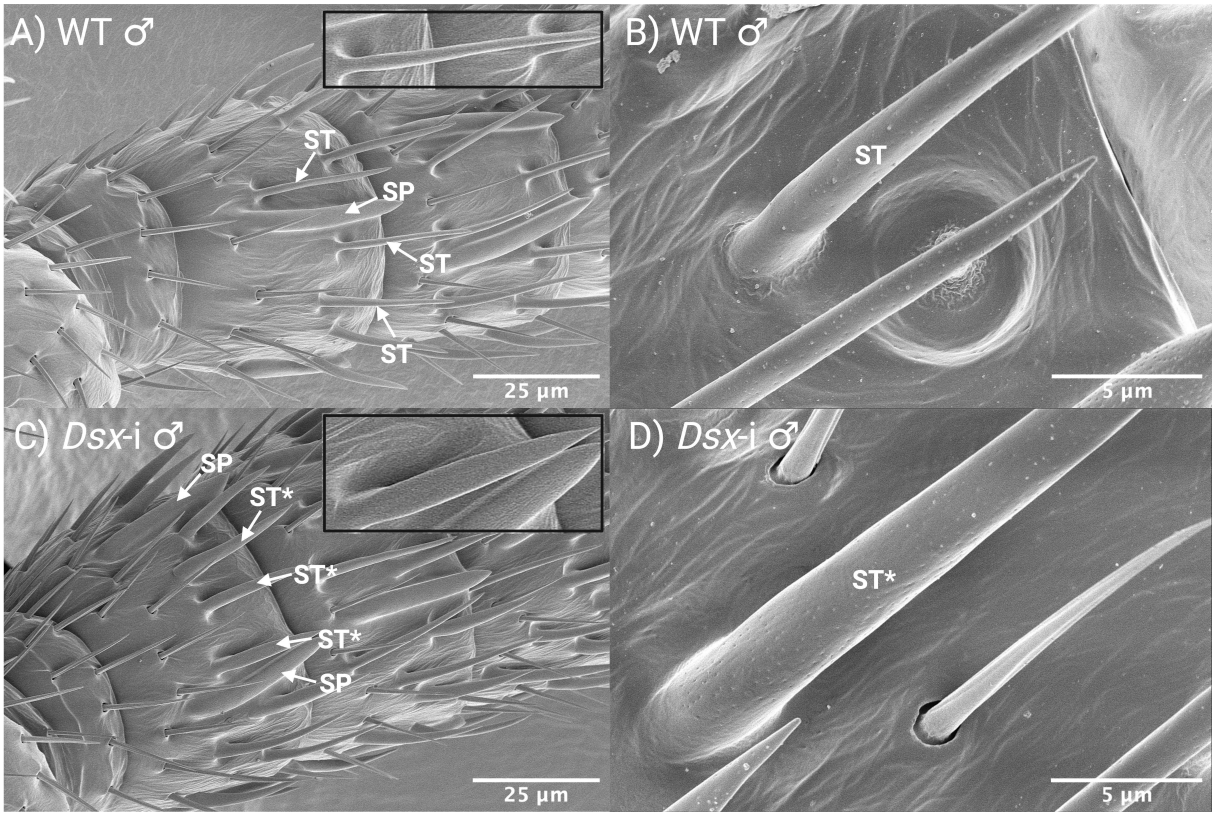

Figure 7: Scanning electron micrographs showing morphological differentiation in trichoid sensilla on male *N. vitripennis* antennae after silencing *NvDsx.*

A: Wild-type (WT) male showing *sensilla trichodea* (ST) and *sensilla placodea* (SP). Insert shows a magnified example of a wild-type male trichoid. **B**: Ultrastructure of a wild-type male trichoid. **C:** *Dsx*-i male showing widened trichoids (ST*) adjacent to placoids (SP). Insert shows a magnified example of a widened trichoid. **D**: Ultrastructure of a widened trichoid, showing a proliferation of pore formation towards the base.

Sensilla chaetica

The second most abundant sensilla on the antennae of *N. vitripennis* are classified by both Slifer (1969) and Wibel *et al*. (1984) as "tactile hairs". However, in other parasitoid wasps, these hair-like sensilla are consistent with what have been identified as *sensilla chaetica* (Dweck & Gadallah, 2008; Liu *et al*., 2024). They form straight or curved hair-like tapered structures arising from a cuticular pit and have a grooved surface that lacks pores. There are two subtypes of *sensilla chaetica* (SCh-1 and SCh-2). Subtype SCh-1 represents a straight or slightly curved hair (**Figure 5B**) and is the most abundant of the two. It is distributed between the placoids on 11 flagellar segments (**Figure 4B, 4C**: A1-C1) in both males and females. Subtype SCh-2 is curved at approximately 90 degrees (**Figure 5C, 5D**) and is present on the antennal tip (**Figure 4B, 4C**: C2). The lack of pores on both subtypes of *sensilla chaetica* indicates that these sensilla have a mechanosensory function.

In total, wild-type males possessed 79±18 *sensilla chaetica* compared to 128±10 in wild-type females (**Figure 6E**; $Z = 3.2433$, $p < 0.01$). There was a significant difference in overall chaetica density (**Supplementary Figure 1C**; $Z = 3.0089$, $p < 0.01$). After silencing, *Dsx*-i males

developed a 27.32% increase (101±6.05) in *sensilla chaetica* compared to wild-type males (**Figure 6E**; Z = 3.0041, p < 0.01) and possessed a higher density of this sensillum (**Supplementary Figure 1C**; Z = 2.5714, p < 0.05). However, the number of these sensilla remained unaffected in *Tra*-i females (**Figure 6E**; Z = 1.8114, p = 0.07). This indicates that *NvDsx* in males regulates the development of *sensilla chaetica* in *N. vitripennis*.

Sensilla placodea

The third most abundant sensilla on the antennae of *N. vitripennis* are classified by Slifer (1969) as "plate organs" and by Wibel *et al*. (1984) as "multiporous plate sensilla". In parasitoid wasps, these sensilla are referred to as *sensilla placodea* (Dweck, 2009; Onagbola & Fadamiro, 2008). Although the etymology of the term "placoid" denotes a flat plate-like structure, in *N. vitripennis* and other parasitoid wasps, placoid sensilla have a flattened, elongated morphology and are attached to the antennal cuticle along the majority of the sensillum's body and covered in pores (**Figure 5B**). There are three sex-specific subtypes of *sensilla placodea* (**Figure 8**; SP-1 and SP-2 in females and SP-3 in males), which are dimorphic in shape and are arranged more or less regularly on nine flagellar segments (**Figure 4B, 4C**: F1-C1) in both males and females. The presence of pores indicates that these sensilla have a chemosensory function.

Wild-type males possessed 24±3 placoid sensilla compared to 44±4 in wild-type females (**Figure 6F**; Z = 3.2579, p < 0.01). There was also a significant difference in overall placoid density (**Supplementary Figure 1D**; Z = 3.2404, p < 0.01). After silencing, neither *Dsx*-i males nor *Tra*-i females showed a significant difference in the number of placoid sensilla compared to wild-type males and females (**Figure 6F**; Z = −1.4466, p = 0.14 and Z = 1.2981, p = 0.19, respectively), and likewise in placoid density (**Supplementary Figure 1D**; Z = −0.7868, p = 0.43 and Z = 0.45284, p = 0.65, respectively).

Wild-type males and females show sexual dimorphism in the length and width of sex-specific placoid subtypes (Wibel *et al*., 1984). Wild-type male placoid sensilla were 33.13±1.89 µm long and 3.85±0.21 µm wide, compared to 30.39±2.34 µm long and 4.41±0.32 µm wide in wild-type females (**Figure 6G, 6H**; Z = −2.2008, p < 0.05 and Z = 3.1246, p < 0.01, respectively). After silencing, *Dsx*-i males developed significantly shorter (28.49±2.24 µm) placoids compared to wild-type males (**Figure 6G**; Z = −2.575, p < 0.05), but were not significantly affected in the width (Z = 1.2857, p = 0.19). Conversely, *Tra*-i females developed significantly thinner (4.09±0.14 µm) placoids (**Figure 6H**; Z = −2.3238, p < 0.05), but were not significantly affected in the length (Z = 1.0328, p = 0.30). These dimorphic differences in geometric measurements correspond to the presence of the placoid subtypes described by Wibel *et al*. (1984) and indicate that the morphology of these subtypes is regulated by NvDSX and NvTRA.

Wibel *et al*. (1984) also pointed out that these sex-specific subtypes differed in pore density (**Figure 8B, 9B and 9C**). Accordingly, wild-type males possess one sex-specific subtype (SP-3)

with a density of 15 pores/µm^2 (**Figure 8B**), whereas wild-type females possess two sex-specific subtypes (SP-1 and SP-2) with a density of 20 pores/µm^2 and 9 pores/µm^2, respectively (**Figure 9B, 9C**). These sex-specific differences in pore density were visually discernible from our scanning electron micrographs (**Figure 8A-8E, 9A-9F)**). After silencing *NvDsx* in males, we observed that these specimens developed a female-specific SP-1-type (**Figure 8D**) alongside an SP-3-type placoid (**Figure 8E**). Conversely, after silencing *NvTra* in females, we observed that these specimens developed a male-specific SP-3-type placoid (**Figure 9F**) alongside a female-specific SP-2-type placoid (**Figure 9E**). This indicates that both *NvDsx* and *NvTra* regulate the development of these sex-specific placoid subtypes in *N. vitripennis* and that these subtypes have a sex-specific olfactory function.

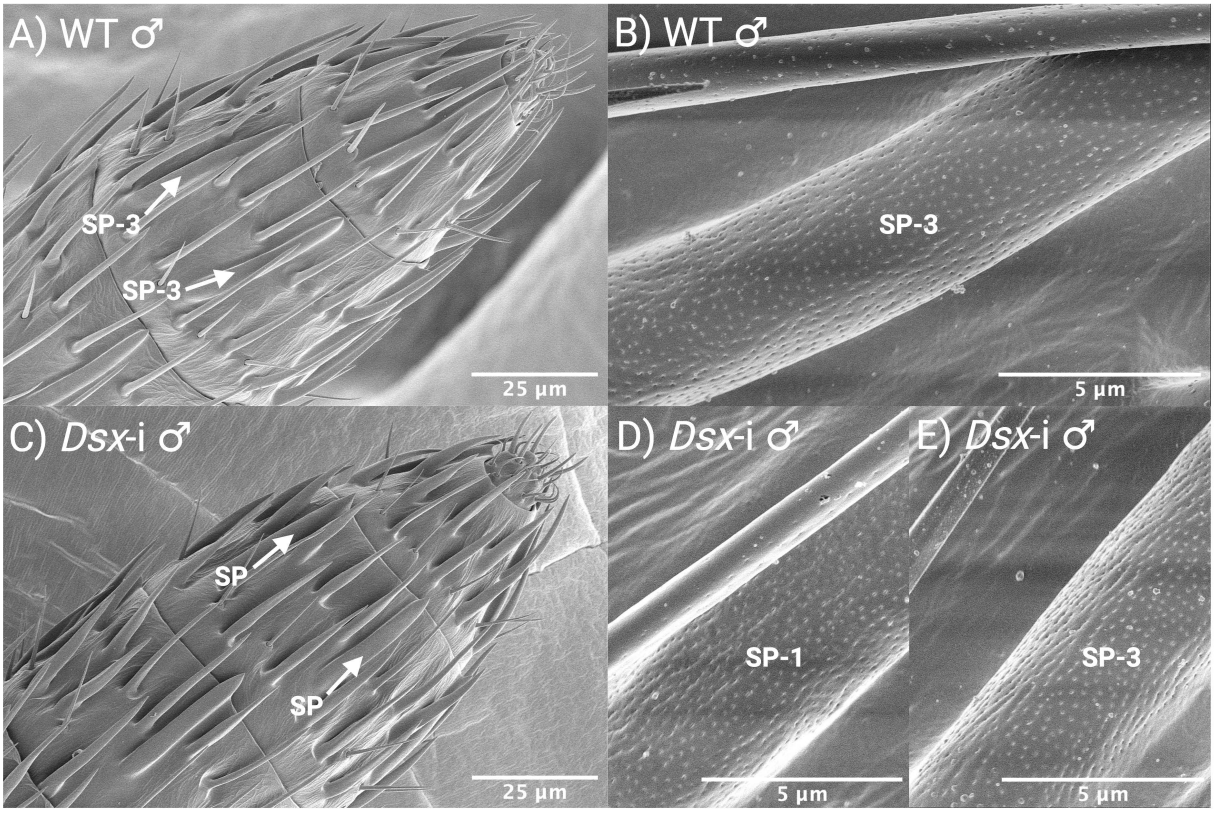

Figure 8: Scanning electron micrographs showing morphological differentiation in placoid sensilla on male *N. vitripennis* antennae after silencing *NvDsx*.

A-B: Wild-type (WT) male showing male-specific subtype 3 placoids (SP-3). **B:** Ultrastructure of a wild-type male SP-3. **C-E:** *Dsx*-i male showing female-specific subtype 1 placoids (SP-1) and male-specific subtype 3 placoids (SP-3). **D-E:** Ultrastructure of a *Dsx*-i male SP-1 and SP-2.

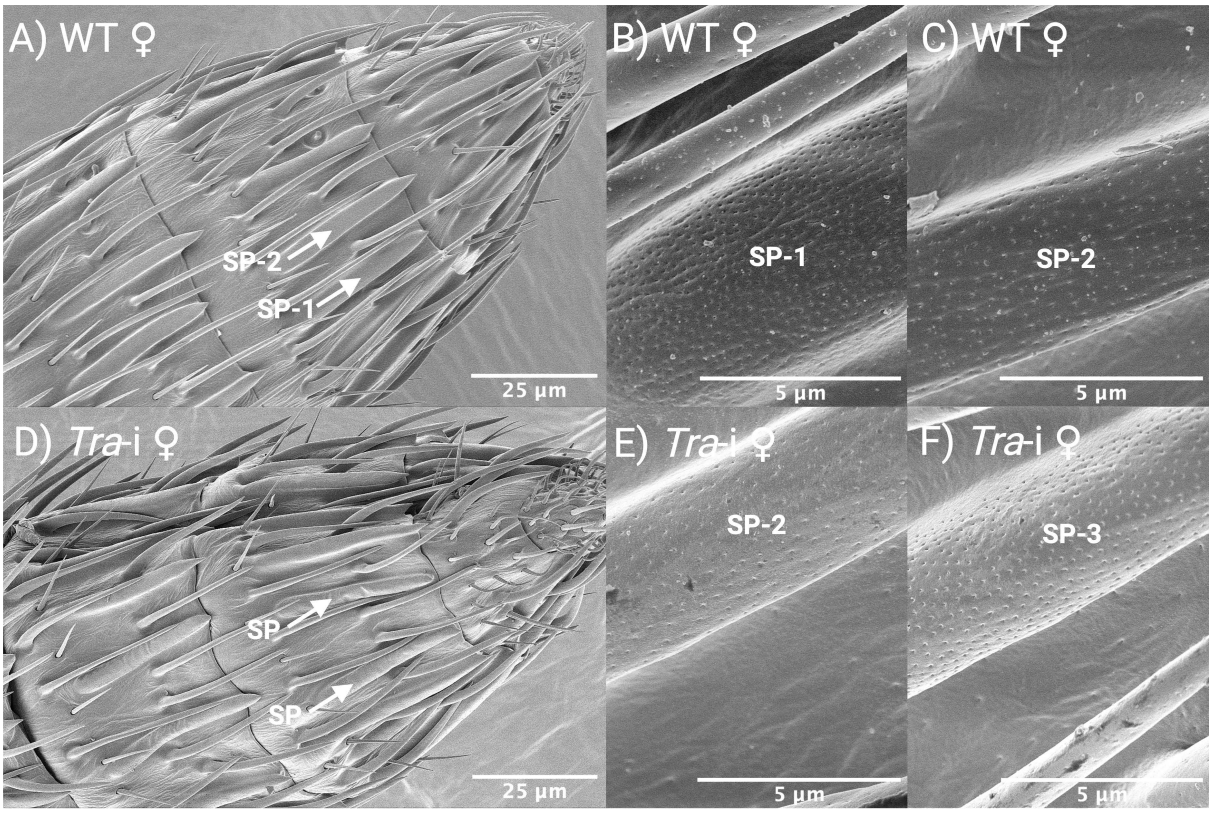

Figure 9: Scanning electron micrographs showing morphological differentiation in placoid sensilla female *N. vitripennis* antennae after silencing *NvTra*.
A-C: Wild-type (WT) female showing female-specific subtype 1 and 2 placoids (SP-1 and SP-2). **B-C:** Ultrastructure of a wild-type female SP-1 and SP-2. **D-F:** *Tra*-i female showing male-specific subtype 3 placoids (SP-3) and female-specific subtype 2 placoids (SP-2). **E-F:** Ultrastructure of a *Tra*-i female SP-2 and SP-3.

Sensilla basiconica

The least abundant sensilla on the antennae of *N. vitripennis* are classified by Slifer (1969) as "thick-walled pegs" and by Wibel *et al*. (1984) as "thick-walled chemoreceptors". The morphology of these peg-like sensilla correspond closely to what are identified in other parasitoid wasps as *sensilla basiconica* (Dweck, 2009; Onagbola & Fadamiro, 2008). These sensilla are sturdy peg-like structures that emerge from a pit or socket on the antennal cuticle. There are two subtypes of *sensilla basiconica* (SB-1 and SB-2).

Subtype SB-1 represents a slightly curved and grooved, uniporous peg (**Figure 5C, 5D**) located on both segments of the antennal clava (**Figure 4B, 4C**: C1-C2). The morphology and location on the antennal clava indicates that this subtype functions as a contact sensillum for sensing both host chemicals and non-volatile pheromones (Silva *et al*., 2016). Sex-specificity in SB-1 was observed in the number (max. seven in males and max. ten in females) and the distribution (**Figure 5C, 5D**; predominantly clustered in females and more dispersed in males) (Wibel *et al*., 1984). Due to variation in the angle of the scanned antennae, we were unable to determine the exact number of this subtype and potential differences between wild-type and dsRNA-treated specimens.

Subtype SB-2 represents a mushroom-shaped capitated peg arising from a pit, with a pronounced ridged head (**Figure 5E, 5F**) and a spiralling distribution on the antennal segments F3-F8 in wild-type males and F3-C1 in wild-type females (Wibel *et al*., 1984). The function of this subtype remains elusive, but it has been suggested to play a role in hygro- or thermoreception (Onagbola & Fadamiro, 2008; Pettersson *et al*., 2001; Wcislo, 1995; Wibel *et al*., 1984). Sex-specificity in SB-2 sensilla has previously been observed in the number of pegs on the antennae of wild-type males and females (Wibel *et al*., 1984). However, we were unable to confirm potential differences in the number between wild-type and dsRNA-treated specimens due to variations in the angle of the scanned antennae. Sexual dimorphism was observed in the number of ridges on this subtype: invariably 12 in wild-type males and 11-15 in wild-type females. After silencing *NvDsx* in males, SB-2 sensilla developed 13 ridges, corresponding to the morphology of wild-type female SB-2 sensilla. The number of ridges in *Tra*-i females, however, remained unaffected. This indicates that NvDSX regulates sexual dimorphism in the ultrastructure of this subtype and represses variation in the number of ridges of this subtype in males.

Antennal lobe morphological differentiation following *Tra*-i and *Dsx*-i

Nasonia vitripennis antennal-lobe anatomy

We performed anterograde tracing of antennal OSNs to analyse the glomerular organization of the AL in wild-type and dsRNA-injected males and females. Anterograde tracing was performed by backfilling severed antennae with the tracer Biotin-Dextran, which interacted with the streptavidin-Alexa Fluor 488 (AF488) conjugate. The AF488 signal visualized the AL glomerular morphology in fluorescent green in the confocal image stacks (**Figure 10A**). The glomerular neuropil is surrounded by glia cells, which were stained with propidium iodide (PI) in fluorescent blue (**Figure 10B**).

The antennal OSNs enter the AL on the ventral side via the antennal nerve (**Figure 10A, 11A and 12A**), which in turn separates into numerous smaller tracts that innervate the various glomerular regions of the AL (**Figure 11B, 12B**). We defined the glomeruli based on the fluorescent AF488 signal from the Biotin-Dextran-backfilled OSNs in combination with the auto-fluorescence of the glomeruli and used the surrounding glia cells as a counterstain. Individual glomeruli are globular in form and are organized as a continuous outer layer on the AL (**Figure 11B-11C, 12B-12C**). This layer is one or two glomeruli thick and surrounds a fibrous core comprising OSN tracts that innervate the glomeruli. We segmented all individual glomeruli before making 3D reconstructions of the AL in both wild-type and dsRNA-injected males and females (**Figure 10C-10F**). Both the confocal stacks and the 3D reconstructions showed sexual dimorphism in the overall glomerular morphology of the AL, which was oblate in wild-type males (**Figure 10C, 11A**) and more spherical in wild-type females (**Figure 10E, 12A**), although these differences may be due to the scanning angle and/or mounting factors.

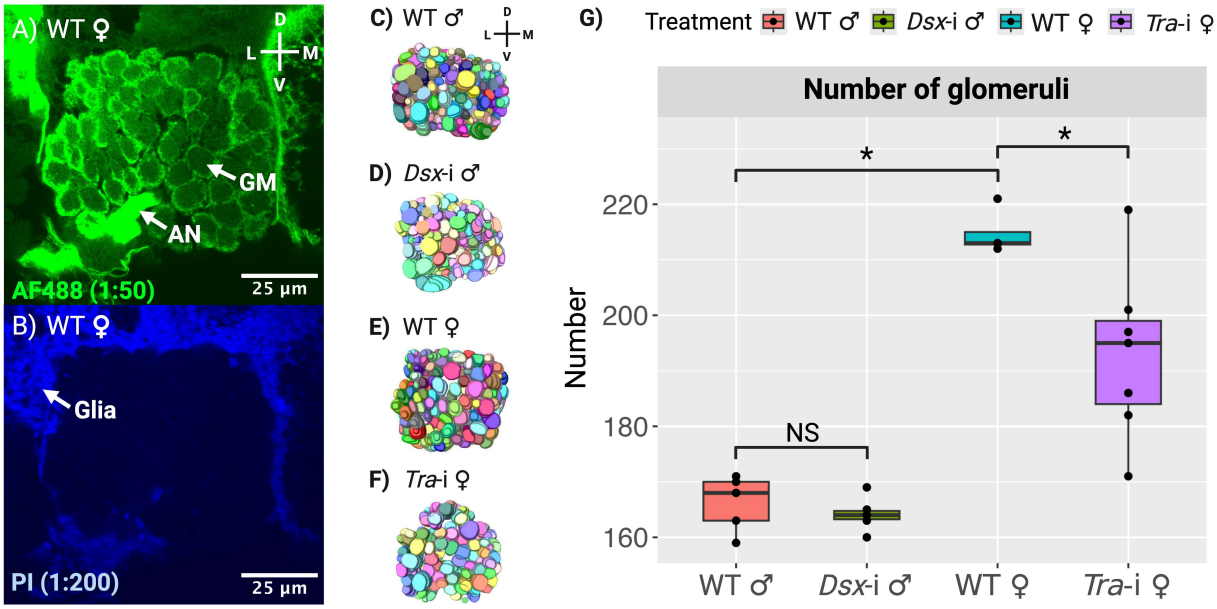

Figure 10: Anterograde tracing of the *N. vitripennis* antennal lobe (AL).
A: Staining of the Biotin-Dextran-backfilled OSNs with streptavidin-Alexa Fluor 488 (AF488) conjugate. The OSN axons enter the AL via the antennal nerve (AN) and innervate the glomeruli (GM). The fluorescent AF488 signal is predominantly visible in the cortical layer of the glomeruli and in a number of fibres in the glomerular core. **B:** Counterstain with 1:200 diluted propidium iodide (PI) of the glia cells surrounding the AL glomerular neuropil. **C-F:** AL 3D reconstructions of a wild-type (WT) male, *Dsx*-i male, wild-type female and *Tra*-i female, showing the segmented glomeruli and morphological changes after *Dsx*-i and *Tra*-i. **G:** Number of glomeruli in male and female *N. vitripennis* treated with *NvDsx* and *NvTra* dsRNA, respectively. Wild-type males and females show sexual dimorphism in the number of glomeruli. *Dsx*-i males show no significant difference in the number of glomeruli compared to wild-type males, whereas *Tra*-i females show a significant reduction in the number of glomeruli compared to wild-type females. Significant differences in the number of glomeruli were analysed with a Wilcoxon rank-sum test. Significance levels: * = $p < 0.05$ and NS = not significant.

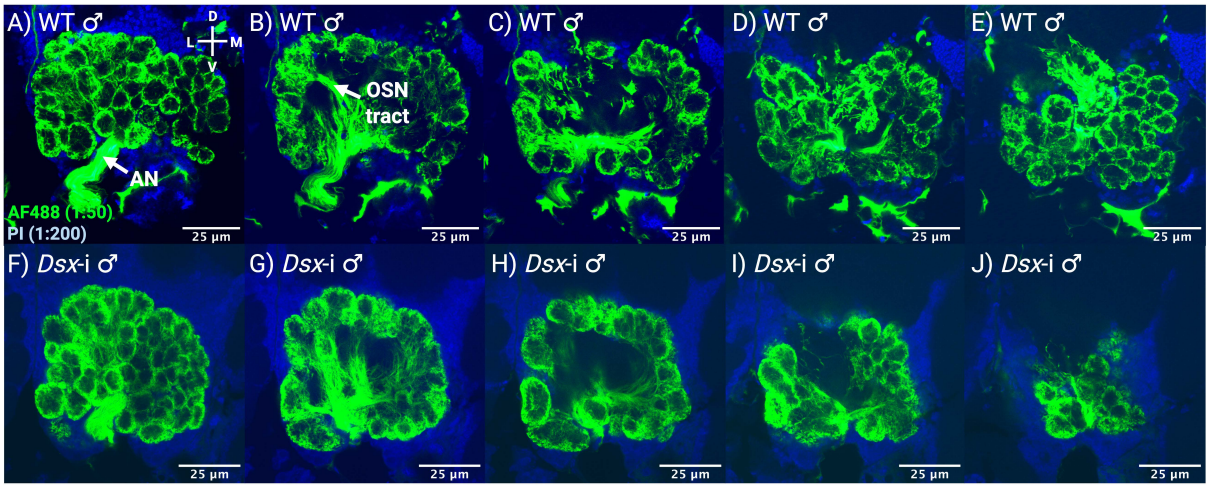

Figure 11: Optical sections and 3D reconstructions of the glomeruli in the AL of *N. vitripennis*.
A-J: Confocal stacks of the glomerular neuropil morphology of wild-type (WT) males and *Dsx*-i males (represented in rows) showing various sections of the AL from anterior to posterior. *Dsx*-i males show morphological variation compared to wild-type males.

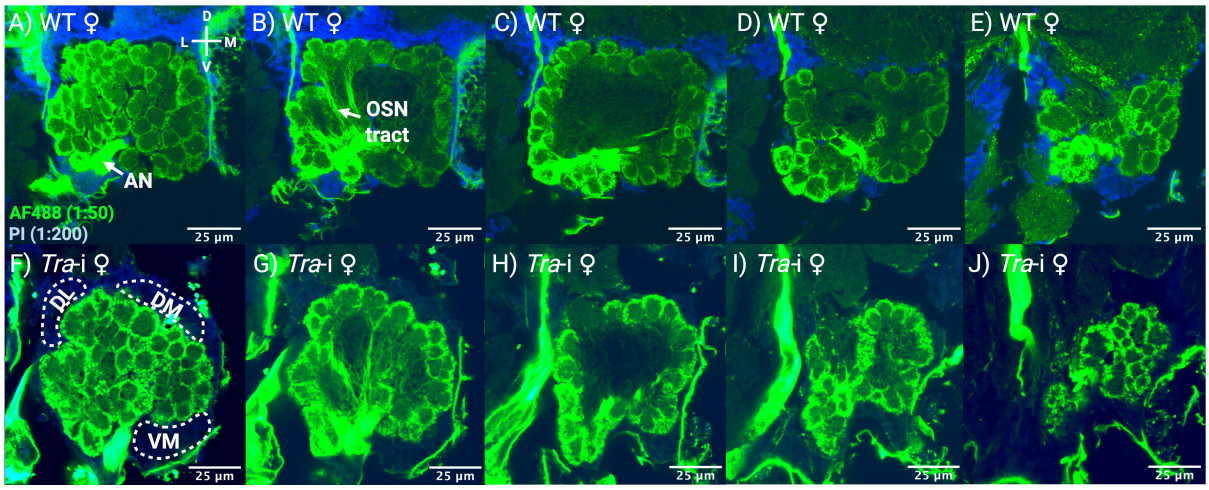

Figure 12: Optical sections and 3D reconstructions of the glomeruli in the AL of *N. vitripennis*.
A-J: Confocal stacks of the glomerular neuropil morphology of wild-type (WT) females and *Tra*-i females (represented in rows) showing various sections of the AL from anterior to posterior. Differences in glomerular neuropil morphology between *Tra*-i females and wild-type females were due to the absence of female-specific glomerular clusters at the ventromedial (VM), dorsomedial (DM) and dorsolateral (DL) sections of the AL in *Tra*-i females.

Changes in the number of sex-specific glomeruli following *Tra*-i and *Dsx*-i

We used the 3D-reconstructed ALs (**Figure 10C-F**) to count the total number of glomeruli in wild-type and dsRNA-treated specimens (**Figure 10G, Supplementary Table 5**). The number of glomeruli is sexually dimorphic between wild-type males and females. Wild-type males (n = 4) possessed 167±5 glomeruli compared to 214±4 in wild-type females (n = 4) (**Figure 10G**; Wilcoxon rank-sum test, $Z = 2.4598$, $p < 0.05$). Variation in the number of glomeruli was low between individual male and individual female specimens. Wild-type males possessed between 159 and 171 glomeruli and wild-type females between 212 and 224. 3D reconstructions were also used to count the total number of glomeruli in *Dsx*-i males and *Tra*-i females. After silencing, *Dsx*-i in males (n = 6) did not significantly affect the number of glomeruli (**Figure 10G**; $Z = -0.64193$, $p = 0.52$). However, *Tra*-i females (n = 7) developed 10% fewer glomeruli (193±15) compared to wild-type females (**Figure 10G**; $Z = -2.0835$, $p < 0.05$). This indicates that NvTRA regulates other downstream factors than *NvDsx*, such as *NvFru,* to control the number of female-specific glomeruli. Differences in the number of glomeruli between individual *Tra*-i females are likely attributable to slight variations in the amount and timing of *NvTra* dsRNA injected in the specimens.

Changes in glomerular neuropil morphology following *Dsx*-i and *Tra*-i

The confocal stacks and 3D reconstructions of our specimens enabled us to visualize changes to the glomerular neuropil after *Dsx*-i and *Tra*-i. Although there was no significant difference in the number of glomeruli between *Dsx*-i and wild-type males, the glomerular neuropil of the *Dsx*-i specimens did show morphological variation (**Figure 10C-10D, 11A-11J**). We also

detected a difference in glomerular neuropil morphology between *Tra*-i and wild-type females (**Figure 10E-10F, 12A-12J**), which corresponds to the absence of female-specific glomerular clusters in the *NvTra*-silenced specimens (**Figure 12F**).

Identification of female-specific glomerular clusters following *Tra*-i

We used a well-defined *Tra*-i specimen to confirm the absence of four female-specific glomerular clusters (**Figure 12F-12J, 13**) by assigning landmark glomeruli according to the procedure of Smid *et al*. (2004). A cluster of approximately ten glomeruli present in the ventromedial section of wild-type females was absent in the *Tra*-i specimen (**Figure 13A-13B**, in blue). Only the glia cells that were stained with propidium iodide were visible at the location of the missing cluster (**Figure 12F**). Two clusters were also visibly absent in the dorsomedial and dorsolateral sections of this specimen (**Figure 12F**), although it was not possible to assign landmark glomeruli to identify specific glomeruli in these clusters. Finally, a cluster of approximately 13 glomeruli in the lateral-dorsolateral section of wild-type females was absent in our specimen (**Figure 13C-13D**). These 13 glomeruli were located in close proximity to a relatively large glomerulus (**Figure 13C**, in blue).

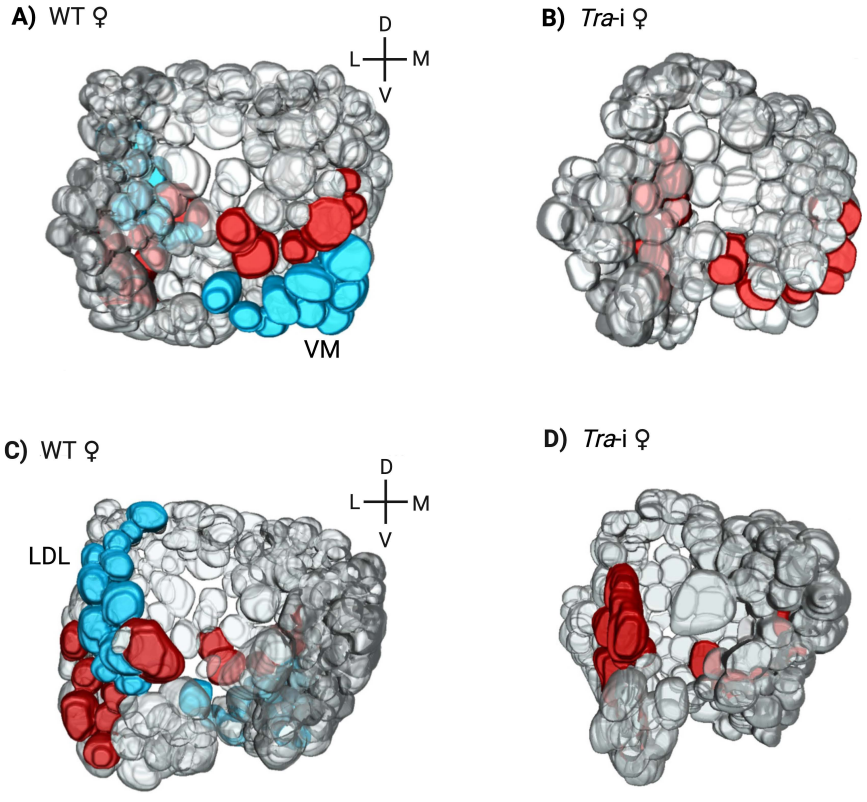

Figure 13: Comparison of glomerular clusters in wild-type and *Tra*-i females.
A-D: 3D reconstructions of the glomerular neuropil morphology of wild-type (WT) females (**A** and **C**) and *Tra*-i females (**B** and **D**). **A** and **B** show the anterior view; **C** and **D** show the posterior view. Female-specific glomerular clusters present in wild-type females (indicated in blue) are absent in *Tra*-i females. Landmark glomeruli (indicated in red) were used to identify these female-specific glomerular clusters. Accordingly, we identified a female-specific cluster in the ventromedial (VM) section (**A**) and a female-specific cluster in the lateral-dorsolateral (LDL) section (**C**) of the wild-type female AL.

These results indicate that NvTRA regulates downstream factors to form these sex-specific glomerular clusters and that these clusters have a female-specific olfactory function. NvDSX*,* on the other hand, is not involved in regulating glomerular morphological differentiation in males, indicating that other factors downstream of *NvTra* are responsible for this process.

Discussion

In the evolution of chemical communication, insects have developed specialized neural circuits to perceive pheromones. However, the sex-determination genes and their mechanisms involved in shaping these sex-specific circuits remain elusive. We studied the role that *NvTra* and *NvDsx* play in regulating sexual dimorphism of the olfactory system in *N. vitripennis* for pheromone communication, by focusing on behaviour, sensilla development, the morphology of the antennal lobe and the organization of glomeruli. We successfully used dsRNA to silence *NvDsx* and *NvTra* expression in males and females, respectively. *Dsx*-i males were feminized by reducing *NvDsx* expression, whereas *Tra*-i females were masculinized by reducing *NvTra* expression and changing the female-specific splicing of *NvDsx* to male-specific splicing.

Silencing these genes altered pheromone-mediated behaviour in both males and females. Normally, only wild-type females are attracted to the male abdominal pheromone. After silencing, however, *Dsx*-i males became attracted to the HDL component of this pheromone and *Tra*-i females became indifferent. We also determined changes in the type, number and morphology of olfactory sensilla in both silenced males and females, including the development of intermediate forms. These changes corresponded to modifications in the number and organization of glomeruli of the respective antennal lobes. Moreover, although *NvDsx* did not appear to be a determining factor, *NvTra* did have a clear effect on the number and organization of glomeruli, indicating that factors downstream of *NvTra* are responsible for determining this process. As a result, our study confirms for the first time that sexual dimorphism in the olfactory system of parasitoids and conserved elements of the sex-determination cascade are responsible for pheromone-mediated behaviour in these insects and opens up new avenues for identifying the downstream factors involved.

In the area of pheromone-mediated behaviour, our study shows that silencing *NvDsx* and *NvTra* changed how the male abdominal pheromone was perceived. The male abdominal pheromone consists of two components. The first, HDL (Ruther *et al*., 2007; Steiner & Ruther, 2009), is used to attract potential females, and the second, 4-MeQ, is used to ward off male competitors (Ruther *et al*., 2008). Wild-type males do not normally respond to the HDL component of their own pheromone blend (Ruther *et al*., 2011), which we confirmed with the *Gfp*-i individuals. After silencing, however, we determined that *Dsx*-i males were significantly attracted to the HDL component. Conversely, wild-type females are normally attracted to the male-specific HDL component, but became indifferent to this pheromone after silencing *NvTra*. It is likely that this effect is caused by DSX-M expression, as silencing *NvTra* masculinizes *NvDsx* splicing, although FRU-M or other unidentified factors downstream of *NvTra* could also influence this process. A previous study confirmed that DSX-M regulates the production of the male abdominal pheromone (Wang *et al*., 2022b) and our study has further demonstrated that DSX-M represses chemosensory processes responsible for perceiving this pheromone in males. In the case of *Tra*-i females, on the other hand, although

it remains ambiguous which factors are specifically responsible for the loss of pheromone attractiveness, it is likely that DSX-M is similarly involved. Future studies should therefore focus on identifying these factors downstream of *NvTra* and elaborate on the specific chemosensory genes responsible for inducing pheromone-mediated behaviour.

Olfactory sensilla on the antennae are responsible for detecting information in the form of odours, such as cues for host identification as well as pheromones for mate recognition, sex discrimination and courtship. Both males and females possess a unique set of sensilla to enable sex-specific odour perception.

We confirmed that the sensilla in *N. vitripennis* are sexually dimorphic in number and morphology as a result of NvDSX and NvTRA regulation. After silencing *NvDsx* and *NvTra*, we observed specific changes in the number and morphology of trichoid and placoid sensilla, the latter of which could be differentiated into sex-specific types based on pore density. Interestingly, *Dsx*-i males developed an intermediate type of sensillum between a trichoid and a placoid. This intermediate sensillum with both trichoid- and placoid-like characteristics was particularly widened at the base of the hair and was attached to the antennal cuticle along the length of the sensillum similar to a placoid. Since we confirmed that wild-type females possess significantly more placoids than wild-type males, it is plausible that these intermediate types in *Dsx*-i males were developing from trichoids into female-specific placoids. We also confirmed two sex-specific placoid subtypes (SP-1 and SP-2) in wild-type females, whereas wild-type males possess only one subtype (SP-3). After silencing, we observed that *Dsx*-i males developed a female-specific SP-1 subtype together with a male-specific SP-3 subtype. Conversely, *Tra*-i females developed a male-specific SP-3 subtype together with a female-specific SP-2 subtype. This indicates that silencing *NvDsx* and *NvTra* resulted in an intermediate phenotype, but not a complete reversal of sex-specific placoid development, probably attributable to variable expression levels in our silenced specimens. Our results therefore show that factors downstream of *NvTra* regulate sexual dimorphism in trichoid and placoid development. We can conclude that DSX-M expression plays a role in trichoid development in males, whereas it remains ambiguous whether the placoid changes we observed in females are regulated by NvDSX or other factors spliced by NvTRA.

The developmental fate of a sensillum type is determined by a so-called sensory organ precursor (SOP). During development, the SOP is selected from cells that express proneural genes through a process that requires Notch signalling (Barad *et al*., 2011; Troost *et al*., 2023). The selected SOP subsequently undergoes asymmetric division and the sensillum fate is then determined by two classes of proneural transcriptional activators: the Ato class (the *Atonal* and *Amos* genes) for olfactory sensilla (Goulding *et al*., 2000; Gupta & Rodrigues, 1997; Jhaveri *et al*., 2000; zur Lage *et al*., 2003) and the AS-C class (the *Achaete*, *Scute* and *Lethal of scute* genes) for gustatory and mechanosensory sensilla (Gómez-Skarmeta *et al*., 2003). Although it remains unclear how DSX and TRA are involved in regulating these genetic

pathways, *Dsx* is expressed in SOPs to control the number of gustatory bristles in *Drosophila* (Luecke *et al*., 2022). It does so by enhancing the activity of proneural genes, such *Pox-Neuro*, which then determine the developmental fate of either gustatory or mechanosensory bristles (Luecke *et al*., 2022). Although this mechanism is responsible for regulating gustatory sensilla in *Drosophila* and gustatory sensilla are not affected by NvDSX or NvTRA in *N. vitripennis*, we hypothesize that *NvDsx* is expressed in olfactory SOPs to regulate sexual dimorphism in trichoid and placoid olfactory sensilla in this species. It would therefore be interesting to analyse how transcription factors of the *Ato* class are regulated by NvDSX and NvTRA to determine how these sensilla develop in *N. vitripennis*.

The life histories of males and females determine the receptive capacity of their respective sensory systems and the development of their neural circuits. This in turn is reflected in the number of respective glomeruli needed to process olfactory information for olfactory-mediated behaviour within their respective life histories and as a result in sexual dimorphism in the morphology of the antennal lobe. We confirmed that the glomeruli in *N. vitripennis* are sexually dimorphic in number and morphology as a result of NvTRA regulation. We visualized the ALs using antennal backfills with Biotin-Dextran, which traces the OSNs to their corresponding glomeruli. After silencing, we confirmed a reduction in the number of glomeruli in *Tra*-i females. No significant change, however, was detected in the number of glomeruli in *Dsx*-i males, although the AL structure of these specimens showed morphological variation. We also succeeded in demonstrating NvTRA regulation of glomerular neuropil organization, which corresponded to the absence of glomerular clusters in *Tra*-i females. Different sensillum types possess distinct classes of OSNs, which project to distinct clusters of glomeruli in the antennal lobe (Couto *et al*., 2005; Gao *et al*., 2000; Grabe *et al*., 2016). Consequently, we hypothesize that the development of sex-specific glomerular clusters in *Nasonia* females is dependent on the axonal growth and synaptic projections of the OSNs.

Distinct classes of OSNs located in different types of sensilla require specific genetic mechanisms for determining axonal growth and synaptic projections to corresponding glomeruli (Evans & Bashaw, 2010). In *Drosophila*, SOPs in the antennae produce distinct OSN classes that express different levels of the *Patched* receptor, which subsequently determine OSN axon sensitivity to *Hedgehog* expression in the AL (Chou *et al*., 2010b). During axon growth, cell surface proteins, such as semaphorins and cell adhesion molecules (CAMs), also ensure that OSNs project to their corresponding glomeruli (Araújo & Tear, 2003), although it remains unclear how *Tra* and its downstream factors, *Dsx* and *Fru*, are involved in this process. In *Drosophila*, *Dsx* is expressed in subsets of neurons and these project to sexually dimorphic glomeruli (Datta *et al*., 2008; Kondoh *et al*., 2003; Manoli *et al*., 2013; Stockinger *et al*., 2005). Previous research has also found that *Dsx* and *Fru* are expressed in gustatory sensory neurons to promote the process of axon midline-crossing in *Drosophila* by directly or indirectly regulating *Robo* signalling (Mellert *et al*., 2010). Accordingly, DSX-F inhibited midline-crossing in females, whereas FRU-M promoted this process in males. It would therefore also be

interesting to investigate whether similar mechanisms are involved in regulating the observed sex-specificities in the female AL in *Nasonia*.

Compared to other insect orders, the development of the hymenopteran AL appears to be dependent on the function of ORs (Chen *et al*., 2021; Trible *et al*., 2017; Yan *et al*., 2017). The functioning of insect ORs is dependent on the expression of the *Olfactory-receptor co-receptor* (*Orco*), which acts as an obligatory chaperone and olfactory tuning factor (Benton *et al*., 2006; Getahun *et al*., 2013). The absence of *Orco* would hamper the expression of ORs in OSN dendrites (Larsson *et al*., 2004). Recent research in ants and honeybees also shows that disrupting *Orco* significantly reduced the number of glomeruli in these Hymenoptera species (Chen *et al*., 2021; Trible *et al*., 2017; Yan *et al*., 2017), whereas in Diptera and Lepidoptera species the number remained unaffected (DeGennaro *et al*., 2013; Fan *et al*., 2022; Fandino *et al*., 2019; Larsson *et al*., 2004; Sun *et al*., 2020). This makes *Orco* an interesting candidate for determining whether NvTRA regulates this gene for directing OSN axons to the sex-specific clusters of glomeruli in the female AL in *Nasonia*. In addition to OSNs, glomerular development is also determined by projection neurons, interneurons and neuroglia (Hansson & Anton, 2000; Oland *et al*., 2008). Neuroglia in particular, play a crucial role in guiding OSN axons in the antennae to clusters of glomeruli (Jhaveri *et al*., 2000; Rössler *et al*., 1999). Research has also shown that neuroglia develop from the AL and create an axon-sorting zone before the OSNs enter the AL (Gibson *et al*., 2012; Oland *et al*., 2008). It would therefore be interesting to study how neuroglia affect AL development in *Nasonia* and how sex-determination transcription factors play a role in this process.

Our study is the first to establish sexual dimorphism in the olfactory system of a parasitoid model species and to provide evidence on the role of NvDSX and NvTRA in regulating the olfactory system for pheromone-mediated behaviour. After silencing *NvDsx* and *NvTra*, we determined the sex-specific regulation of olfactory sensilla and AL glomeruli for perceiving sex-specific olfactory signals for inducing pheromone-mediated behaviour. Our results indicate that NvDSX in males regulates proneural genes in olfactory SOPs to develop olfactory sensilla and that NvTRA in females regulates OSNs for developing sex-specific glomeruli. Future studies should investigate which factors downstream of *NvTra* are responsible for shaping the sex-specific glomerular clusters in *Nasonia* females. *Fru* is a very promising candidate for this due to its role in forming neural circuits in *Drosophila* (Bray & Amrein, 2003; Kimura *et al*., 2008; Kohl *et al*., 2013; Zhou *et al*., 2014) and the fact that sex-specific splice forms of this gene have already been identified in *Nasonia,* including a transcript exclusively present in females (Bertossa *et al*., 2009). Another promising candidate is the recently identified *Glubschauge* (*Glu*) gene, which is responsible for determining sexual dimorphism in the eyes of *Apis mellifera* (Netschitailo *et al*., 2023).

The sex-specificities we identified in the olfactory system of *Nasonia* can serve as a template for future studies aimed at determining neural circuits for parasitoid pheromone-mediated

behaviour, such as sex discrimination, mate recognition, courtship and foraging for hosts. We therefore recommend pursuing our results further in experiments that include functionally analysing downstream genetic pathways, identifying pheromone-sensitive sensilla through single-sensillum recordings and tracing OSN projections from these sensilla to their corresponding glomeruli. The placoid and trichoid sensilla regulated by NvDSX and NvTRA in males and females, respectively, would be ideal targets for these experiments as we expect the OSNs of these sensilla to project to sex-specific glomeruli. Understanding the sex-specific regulation of the sensillum-OSN-glomerulus relationship will greatly advance our knowledge on the genetic mechanisms and neural developmental pathways that determine the evolution of neural circuits for pheromone perception in hymenopterans and in parasitoids in particular. Future research into these processes in *Nasonia* will help further elucidate the chemosensory mechanisms responsible for parasitoid olfactory behaviour and enable it to be utilized for biological control purposes.

Acknowledgements

We would like to thank Jimmie Zeelenberg for his help in carrying out quantitative and morphometric analysis of the SEM micrographs in ImageJ2 and Anna Haaring for her help in carrying out preliminary studies on pheromone-mediated behaviour after RNA interference. We also thank Joachim Ruther for providing us with the synthetic components of the *N. vitripennis* male abdominal pheromone. We are grateful for the feedback on this chapter provided by Marcel Dicke.

Supplementary information

Supplementary Table 1: Relative expression of *NvDsx* after RNAi.
Relative expression of *NvDsx* calculated using the delta-delta Ct method. EF1α was used as a reference gene. This table can be accessed online at:
https://git.wur.nl/aidan.williams/chapter3/-/blob/main/Supplementary_Table_1.csv?ref_type=heads

Supplementary Table 2: Olfactometer behavioural-assay data.
Average residence time measured for *Gfp*-i, *Dsx*-i and *Tra*-i specimens in a olfactometer containing the male abdominal pheromone and control solvent dichloromethane. For each specimen, the preference for either the abdominal pheromone or control solvent is noted. This table can be accessed online at:
https://git.wur.nl/aidan.williams/chapter3/-/blob/main/Supplementary_Table_2.csv?ref_type=heads

Supplementary Table 3: Length and surface area of the antennae.
The length and surface area of the antennae measured in wild-type, *Dsx*-i and *Tra*-i specimens. This table can be accessed online at:
https://git.wur.nl/aidan.williams/chapter3/-/blob/main/Supplementary_Table_3.csv?ref_type=heads

Supplementary Table 4: Counts and morphometric measurements of the antennal sensilla.
Total number, density, average length and width of the different sensilla types analysed in wild-type, *Dsx*-i and *Tra*-i specimens. This table can be accessed online at:
https://git.wur.nl/aidan.williams/chapter3/-/blob/main/Supplementary_Table_4.csv?ref_type=heads

Supplementary Table 5: Number of glomeruli in the antennal lobe.
Total number of glomeruli after segmentation of the antennal lobe in wild-type, *Dsx*-i and *Tra*-i specimens. This table can be accessed online at:
https://git.wur.nl/aidan.williams/chapter3/-/blob/main/Supplementary_Table_5.csv?ref_type=heads

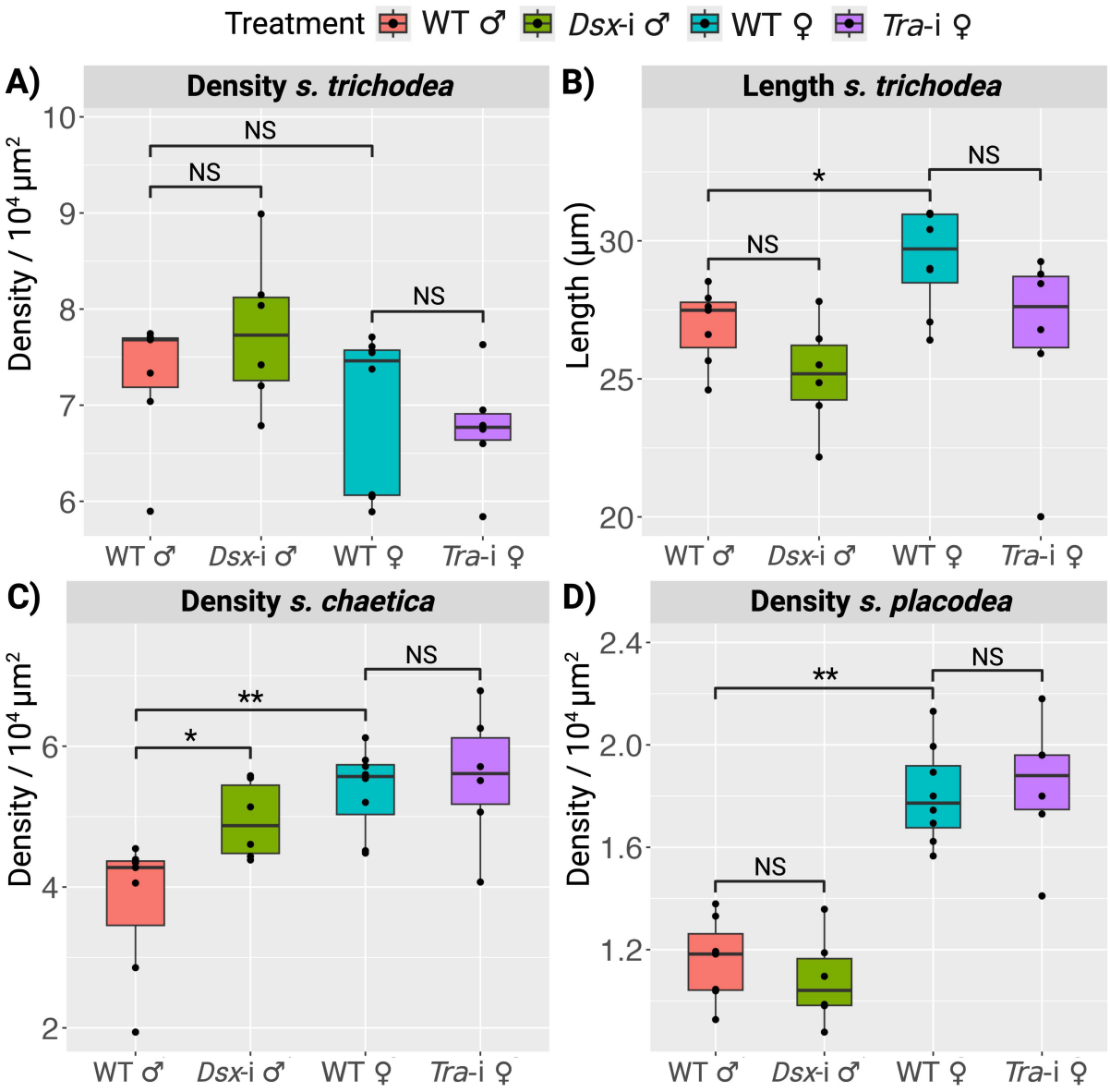

Supplementary Figure 1: Morphological analysis of *N. vitripennis* antennal sensilla after dsRNA treatment. **A:** No significant difference was detected in trichoid density between wild-type (WT) males and females. There was also no significant difference found in trichoid density in *Dsx*-i males and *Tra*-i females compared to their wild-type counterparts. **B:** Wild-type females possessed significantly longer trichoids, whereas there was no significant change in trichoid length in *Dsx*-i males and *Tra*-i females compared to their wild-type counterparts. **C:** Wild-type females and *Dsx*-i males developed a significantly higher *sensilla chaetica* density than wild-type males. There was no significant change in *sensilla chaetica* density in *Tra*-i females compared to wild-type females. **D:** Wild-type females possessed a significantly higher *sensilla placodea* density than wild-type males. There was no significant difference found in *sensilla placodea* density in *Dsx*-i males and *Tra*-i females compared to their wild-type counterparts. Significant differences in the density and length were analysed with a Wilcoxon rank-sum test. Significance levels: ** = $p < 0.01$, * = $p < 0.05$ and NS = not significant.

Chapter 4

Silencing *Orco* transforms antennal-lobe morphology in the parasitoid *Nasonia vitripennis*

Aidan Williams[1] *& Eveline Verhulst*[1]

[1]Laboratory of Entomology, Wageningen University, PO Box 16, 6700 AA Wageningen, the Netherlands

Abstract

Parasitoid wasps need to process complex habitat cues and pheromone signals to navigate their natural environment. Consequently, they have evolved an expansive olfactory-receptor repertoire and a corresponding antennal-lobe (AL) glomerular morphology in the brain. Non-parasitoid Hymenoptera depend on the *Olfactory-receptor co-receptor* (*Orco*) for the proper innervation and development of AL glomeruli by olfactory sensory neurons (OSNs). Unlike in *Drosophila*, in which glomerular morphology is fixed, research has shown that disrupting *Orco* in non-parasitoid Hymenoptera results in the inability of the AL neuropil to differentiate into multiple glomeruli. However, it remains unclear whether *Orco* expression is also necessary for glomerular differentiation in the AL of parasitoid wasps. We hypothesize that a similar mechanism is also responsible for determining the number and morphology of glomeruli in these species, resulting in the degree of AL complexity necessary for their parasitoid odour-mediated behaviour. We analysed the function of the *Orco* gene in *Nasonia vitripennis* by silencing its expression with dsRNA at the late larval stage. We subsequently analysed AL development by backfilling the antennae with Biotin-Dextran to trace OSN projections to the glomeruli. Following AL 3D reconstruction, we determined a dramatic change in glomerular organization, including a reduction in glomerular number and an increase in individual glomerular and AL volume. Our study provides a solid basis for future research that aims to link AL glomerular development and the evolution of parasitoid olfaction to the specific functioning of the *Orco* gene.

Introduction

Within Hymenoptera species, parasitoid wasps are important natural enemies of many agricultural pests and have therefore been the focus of much research, especially concerning their chemical communication (Mair & Ruther, 2019; Polaszek & Vilhemsen, 2023). To navigate their natural environments, parasitoids need to process complex chemical blends, such as cuticular hydrocarbons for eliciting courtship (Kühbandner *et al*., 2012; Mair *et al*., 2017; Weiss *et al*., 2015; Würf *et al*., 2020) and odours for locating and assessing potential hosts (Haverkamp *et al*., 2018; Meiners *et al*., 2003). This intricate life history serves as a driver for the evolution of enhanced cognitive mechanisms to discriminate such odours. The olfactory receptors (ORs) in particular have evolved rapidly in parasitoids and their hymenopteran relatives (Legan *et al*., 2021; McKenzie *et al*., 2016; McKenzie & Kronauer, 2018; Robertson *et al*., 2010; Zhou *et al*., 2015) and this has resulted in the increased number and morphological complexity of glomeruli in the antennal lobe (AL) (Arnold *et al*., 1985; Das & Fadamiro, 2013; Groothuis *et al*., 2019; McKenzie *et al*., 2016; Smid *et al*., 2003; Zube & Rössler, 2008). In the previous chapter, we determined the role of the sex-determination transcription-factor genes *Doublesex* (*Dsx*) and *Transformer* (*Tra*) in regulating sexual dimorphism in the AL of *Nasonia vitripennis*. Sexual differentiation is therefore a major contributor to sexual dimorphism in the number of ORs and glomeruli in parasitoids. However, we only have limited knowledge of the downstream genetic pathways responsible for inducing these sex-specific differences in the olfactory system of these species.

The number of AL glomeruli corresponds to the number of expressed functional ORs in the insect antennae (Couto *et al*., 2005; Fishilevich & Vosshall, 2005; Kurtovic *et al*., 2007; Vosshall, 2000). Each glomerulus is innervated by olfactory sensory neurons (OSNs) expressing the same OR gene. Each glomerulus is therefore defined as a unique functional unit with a specific odour response (Ai *et al*., 2010; Hallem & Carlson, 2006; Kurtovic *et al*., 2007; Suh *et al*., 2004). This functional correspondence between OR, OSN and glomerulus creates a topographic odour-response pattern and allows for novel glomerular circuits to arise through evolutionary shifts in the OR repertoire (Williams *et al*., 2022). Changes in the number of glomeruli should therefore arise from genes involved in regulating OR expression and OSN-glomerular projection. Numerous transcription factors have been identified that regulate OSN development (Komiyama & Luo, 2006; Li *et al*., 2016), such as DSX and FRU. These transcription factors target neurodevelopmental pathways to specify insect neural circuits (Bray & Amrein, 2003; Datta *et al*., 2008; Kimura *et al*., 2008; Zhou *et al*., 2014). However, the target genes and downstream mechanisms through which these transcription factors operate remain poorly understood. One potential target that has received particular attention is the *Olfactory-receptor co-receptor* (*Orco*), a gene required for the function of all insect ORs (Larsson *et al*., 2004; Nakagawa *et al*., 2012; Nichols *et al*., 2011; Pask *et al*., 2011).

Orco has been identified as a chaperone gene for insect ORs (Larsson *et al*., 2004). Unlike in mammals, insect ORs are unable to function independently and require *Orco* for their

expression within OSN dendrites. Accordingly, ORs couple with ORCO to form a heteromeric complex, which then functions as a ligand-gated cation channel for binding odour compounds (Nakagawa *et al*., 2012; Nichols *et al*., 2011; Pask *et al*., 2011) (**Figure 1**). The binding of odours activates the OR via a metabotropic pathway. This in turn activates ORCO and sensitizes the OR, enabling the insect to provide fine-tuned responses to a wide range of odours at different concentration levels (Getahun *et al*., 2013). As a result, *Orco* is an important supporting and tuning component for insect ORs and its disruption leads to the loss of insect OR-mediated perception. Studies that disrupted *Orco* in various insect species confirmed a major loss in olfactory sensitivity towards a broad range of odours, greatly hampering odour-guided behaviour, such as short-distance orientation, host detection, pheromone perception and social communication (DeGennaro *et al*., 2013; Koutroumpa *et al*., 2016; Larsson *et al*., 2004; Li *et al*., 2016; Liu *et al*., 2017; Trible *et al*., 2017; Wang, 2023; Yan *et al*., 2017). Parasitoid wasps lacking *Orco* expression have also been shown to exhibit impaired mating and host-searching behaviour (Zhang *et al*., 2023).

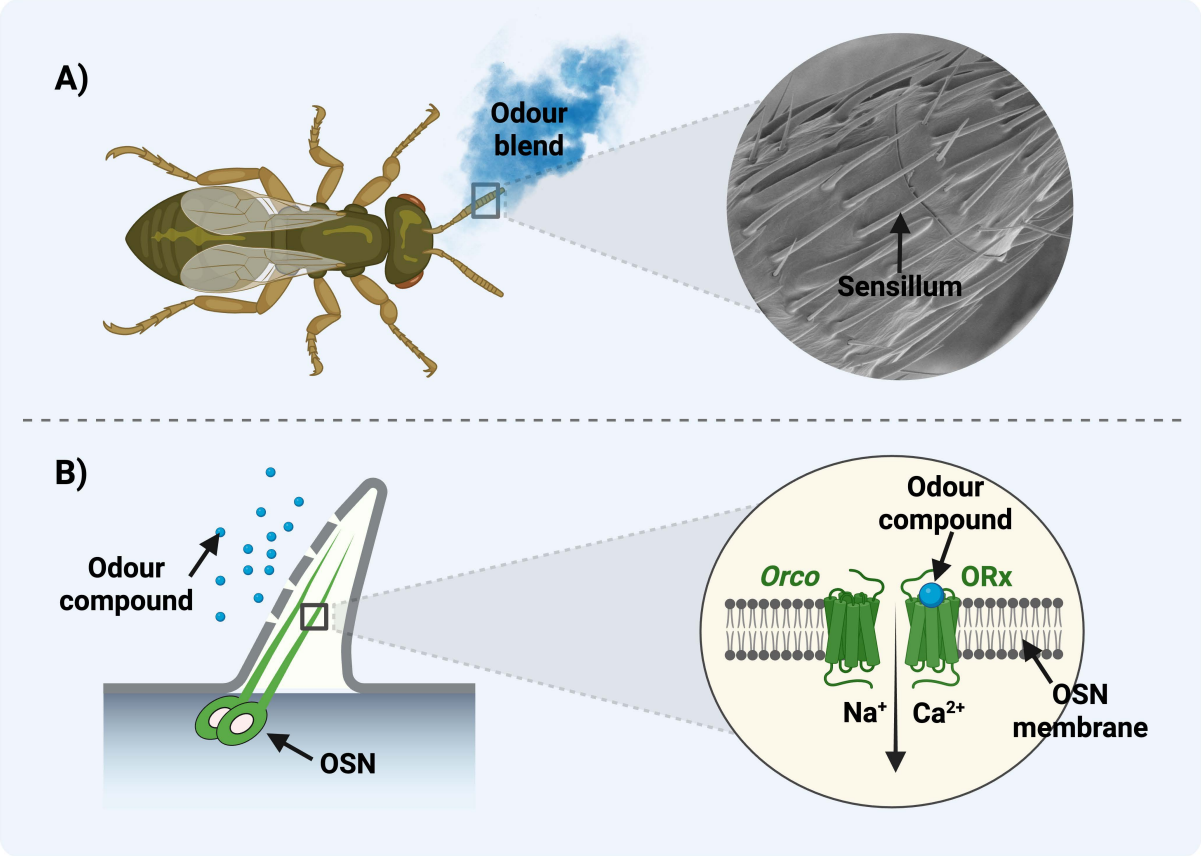

Figure 1: The function of *Orco* in insects.
A: Odours are detected by the antennae, which are covered by numerous olfactory sensilla. **B:** *Orco* is expressed in the membrane of OSN dendrites located in olfactory sensilla and ORCO is necessary for the functioning of ORs and OSNs.

Recent studies on Hymenoptera have demonstrated striking neuroanatomical changes after disrupting *Orco* (Chen *et al*., 2021; Trible *et al*., 2017; Yan *et al*., 2017). In ant species, this disruption impaired OSN development and caused a dramatic reduction in the number of AL glomeruli. Interestingly, such anatomical changes following *Orco* disruption have not been encountered in non-hymenopteran insects, although these did show severe impairment in olfactory function (DeGennaro *et al*., 2013; Koutroumpa *et al*., 2016; Larsson *et al*., 2004; Li *et al*., 2016; Liu *et al*., 2017). This would indicate that the *Orco*-dependent mechanism for AL development is specific to Hymenoptera by incorporating OSN activity for glomerular formation. *Orco* expression therefore enables OSNs to play a crucial role in AL differentiation in these species, resulting in the proper separation of proto-glomeruli into multiple glomeruli (Chen *et al*., 2021; Trible *et al*., 2017; Yan *et al*., 2017).

We hypothesized that the same *Orco*-dependent mechanism applies to AL development in parasitoid Hymenoptera and that this mechanism interacts with the sex-determination pathway to form glomerular circuits for sex-specific odour-mediated behaviour. In addition to determining the role of the transcription factor NvDSX and its splicing factor NvTRA in regulating sexual dimorphism in the AL of *N. vitripennis,* recent research has also confirmed the reduced expression of *Orco* (*NvOrco*) in *N. vitripennis* in a transcriptomic survey after silencing *NvDsx* (Rougeot *et al*., 2025). Our aim was therefore to analyse the function of *NvOrco* in the development of the *N. vitripennis* AL by silencing this gene with RNA interference at the late larval stage and subsequently backfilling the antennae of these specimens with Biotin-Dextran to trace OSN projections to AL glomeruli. Ultimately, our research will help gain a better understanding of the neurodevelopmental mechanisms facilitating the evolution of the intricate life history of parasitoid wasps.

Materials & Methods

Nasonia rearing

We used the lab strain AsymCX of *N. vitripennis* to silence *Orco* expression with dsRNA. The AsymCX wasps were reared on *Calliphora vomitoria* pupae obtained as larvae from a commercial manufacturer (Kreikamp & Zn, Hoevelaken, the Netherlands). The fly larvae were reared in Lignocel 9S (JRS) wood fibre at room temperature and stored refrigerated at 5°C for a maximum duration of four weeks once they pupated. After they emerged and had mated, individual female wasps were placed together with a single host pupa in glass vials for 24 hours. Mated *N. vitripennis* females produce an offspring ratio of approximately 90% females and 10% males. After 24 hours, we followed the rearing protocol for strain maintenance as set out by Werren & Loehlin (2009a). This involves incubating the parasitized pupae in an incubator at a constant temperature of 25°C for six days using a 16-hour light, eight-hour dark cycle. The incubated pupae were subsequently dissected and fourth-instar wasp larvae (L4) were collected in their grey-gut stage to inject *Orco* dsRNA.

Synthesis of *NvOrco* dsRNA and microinjection

We used the MEGAscript RNAi Kit (Thermo Fisher, Waltham, MA, USA) to generate *NvOrco* dsRNA from *N. vitripennis* cDNA. A non-sex-specific *NvOrco* fragment of 302 bp was synthesized in a PCR based on exon 1 of *NvOrco* using the GoTaq Flexi DNA polymerase (Promega, Madison, WI, USA) and the primers F_RNAi_Or1_ [CCTGATGATGGAGAGCGACG] and R_RNAi_Or1_[CGATCCTCTTGACCGACTCG] designed in Geneious Prime (Dotmatics, Boston, MA, USA). This PCR product was amplified in two separate PCRs to add T7 promotors [TAATACGACTCACTATAGGG] to either end of the amplicon. The resulting two templates were then used in separate PCR reactions to transcribe both sense and antisense RNA molecules in accordance with the MEGAscript RNAi Kit protocol (16 hours at 37°C). *Gfp* dsRNA was used as an exogenous control and was generated from the pOPINEneo-3C-GFP vector (Addgene plasmid #53534; https://www.addgene.org/53534/; RRID: Addgene_53534). Amplification by PCR using GoTaq Flexi DNA polymerase with the primers GFP_RNAi_F (5'-GTGACCACCTTGACCTACG-3') and GFP_RNAi_R (5'-TCTCGTTGGGGTCTTTGCT-3') produced a 460 bp amplicon, which covered 64% of the Emerald GFP CDS.

The synthesized dsRNA was measured for its purity and concentration on a spectrophotometer (DeNovix, DS-11 FX, Wilmington, Delaware, USA) and subsequently diluted with RNase-free water to a concentration of 4 µg/µl and injected in *N. vitripennis* larvae to silence *NvOrco* (*Orco*-i). By doing so, we injected dsRNA before the onset of adult brain development, which typically takes place during the insect pupal phase (Tissot & Stocker, 2000). *NvOrco* dsRNA was injected in female L4 larvae after six days post oviposition. The larvae were aligned on a 1x phosphate-buffered saline (PBS) agar plate and a mixture of 4.5 µl dsRNA and 0.5 µl food dye was injected in their posterior using a FemtoJet 4i microinjection pump (Eppendorf, Hamburg, Germany) according to the protocol set out by

Lynch & Desplan (2006) and Werren *et al*. (2009). The L4 larvae were subsequently allowed to pupate on the agar plate. All dsRNA-injected larvae were incubated at 25°C until they pupated to the black-pupal stage after six days. Female wasp pupae were then collected based on sex-specific traits (forewing size and presence/absence of the ovipositor) and kept separate in glass vials. The eclosed *Gfp*-i and *Orco*-i specimens were used in our neural tracing experiment.

Anterograde tracing of olfactory sensory neurons

We performed anterograde tracing of antennal OSNs to visualize AL morphology of *Gfp*-i and *Orco*-i females in accordance with the protocol adopted by Smid *et al*. (2003). Antennal backfills were performed by severing the right antenna of cold-sedated wasps between the flagellum and the pedicel. The wasp bodies were then immobilized in commercial modelling dough, with the head and amputated antenna protruding. A tapered glass microcapillary filled with a 3% Biotin-Dextran (B9139, Sigma-Aldrich, St. Louis, MO, USA) solution was placed over the pedicel and the specimens were incubated at 4°C for four hours. The backfilled specimens were subsequently decapitated and the heads were fixated in freshly dissolved 4% formaldehyde in a 0.1M PBS solution (pH 7.2) at 4°C overnight. The heads were then briefly washed once in 70% ethanol and four times in 1x PBS to remove residual formaldehyde. The brains were subsequently dissected in PBS in transparent glass staining blocks and dehydrated in a graded series of ethanol (90%, 96% and 100%), followed by a 50-50% ethanol/xylene solution and finally 100% xylene. The specimens were then rehydrated in a graded series of ethanol (100%, 96%, 90%, 70%, 50% and 30%) and finally PBS. The brains were further permeabilized in a 0.05% collagenase/PBS solution for one hour and incubated in a solution of phosphate-buffered saline with Triton X-100 (PBS-T) and 1% bovine serum albumin (BSA) at room temperature for one hour. A Streptavidin-Alexa Fluor 488 conjugate (S32354, Invitrogen, Waltham, MA, USA) and TO-PRO-3 (T3605, Invitrogen) were subsequently added to the PBS-T-BSA solution in a 1:50 and 1:1000 dilution, respectively. After incubation for ten hours, the brains were washed in three cycles of PBS and PBS-T and dehydrated again in a graded series of ethanol (30%, 50%, 70%, 90%, 96%, 3x 100%), followed by a 50-50% ethanol/xylene solution and finally 100% xylene. The brains were then mounted on individual microscope slides in Dibutyl phthalate Polystyrene Xylene (DPX, 06522, Sigma-Aldrich).

Analysing the effect of *Orco*-i on AL morphology

The mounted brain specimens were examined with a Zeiss LSM710 confocal laser scanning microscope (Zeiss, Jena, Germany). The excitation light was provided by an argon ion laser (458, 488 and 514 nm). The laser was fitted with a band-pass emission filter set at 488 nm to excite the Alexa Fluor 488 stain and with a long-pass emission filter set at 560 nm to excite the TO-PRO3 stain. All ALs were scanned using the 63x Plan-Neofluar NA 1.3 oil-immersion objective at a resolution of 1024 x 1024 pixels at 8-bits. The pixel area of the specimens ranged

between 0.06 x 0.06 and 0.49 x 0.49 lm^2 and had a Z-axis of 0.8 µm for detailed scans of the AL. The resulting image stacks were then merged into datasets and AL glomerular organization was analysed using 3D-visualization software (AMIRA 5.4.2., Visage Imaging). A total of six *Orco*-i and five *Gfp*-i females were selected for analysis in AMIRA based on superior confocal image quality. Individual glomeruli were manually segmented in each optical section by assigning voxels to discrete elements representing 3D space. A unique label was then assigned to each specific glomerulus, resulting in a 3D array of voxels, where each voxel was individually labelled as either a glomerulus or belonging to the background. The total number of individual glomeruli was then calculated by counting all the unique glomerular labels. We then used the Resample module to enlarge the resolution for subsequent 3D-surface reconstructions. From these datasets, we created 3D-surface reconstructions of the ALs with the SurfaceGen and Unconstrained Smoothing modules. These 3D reconstructions were used to calculate the total AL and glomerular volume and enabled glomerular morphology to be viewed from any angle, making it possible to visualize discrepancies in glomerular structures between *Gfp*-i and *Orco*-i females. All data was analysed for significant differences between the *Gfp*-i and *Orco*-i treatment with a Wilcoxon rank-sum test in RStudio (v2024.12.1+563, Posit PBC).

Results

Morphological differentiation in the *Orco*-i AL

We performed anterograde tracing of antennal OSNs to analyse the glomerular organization of the AL in *Gfp*-i and *Orco*-i females. Anterograde tracing was performed by backfilling severed antennae with the tracer Biotin-Dextran, which interacted with the streptavidin-Alexa Fluor 488 (AF488) conjugate. The AF488 signal visualized the AL glomerular morphology in fluorescent green in the confocal image stacks (**Figure 2A, 2D**). The glomerular neuropil is surrounded by glia cells, which were stained with TO-PRO-3 in fluorescent blue (**Figure 2A, 2D**). We segmented all individual glomeruli before making 3D reconstructions of the AL in both *Gfp*-i and *Orco*-i females.

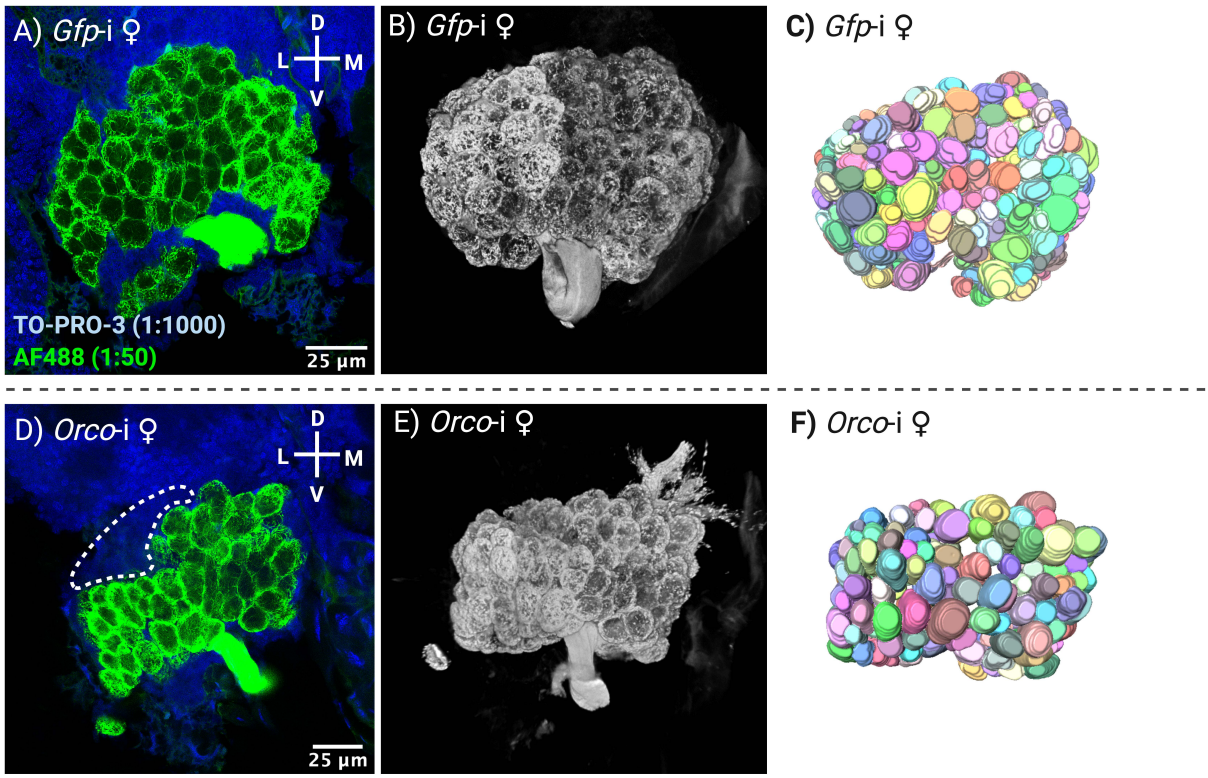

Figure 2: Anterograde tracing of the *N. vitripennis* AL after *Gfp*-i and *Orco*-i.
A: Staining of the Biotin-Dextran-backfilled OSNs in the *Gfp*-i female AL with streptavidin-Alexa Fluor 488 (AF488) conjugate (in green). Counterstain with 1:1000 diluted TO-PRO-3 of the glia cells surrounding the AL glomerular neuropil (in blue). **B:** 3D representation of the *Gfp*-i female AL through volume rendering. **C:** 3D reconstruction of the *Gfp*-i female AL showing the organization of the segmented glomeruli. **D:** *Orco*-i female AL showing the absence of a large glomerular cluster (indicated by dashed line). **E:** 3D representation of the *Orco*-i female AL through volume rendering. **F:** 3D reconstruction of the *Orco*-i female AL showing the organization of the segmented glomeruli.

The stained *Gfp*-i AL shared similar characteristics in glomerular neuropil organization to the wild-type female AL analysed in **Chapter 3** (**Figure 3A-3J**). The optical sections and 3D reconstructions of the *Orco*-i AL, on the other hand, showed clear morphological differences in glomerular neuropil organization compared to the *Gfp*-i AL (**Figure 2, 3F-3O**). There was,

however, a degree of variability in these *Orco*-i specimens, which was likely attributable to slight variations in the amount and timing of *NvOrco* dsRNA injected in the specimens. We also observed the absence of large glomerular clusters in the *Orco*-i AL compared to the *Gfp*-i AL (**Figure 2D, 3K**) and conjecture that this is the cause of the observed morphological differences in these specimens. Only the glia cells that were stained with TO-PRO-3 were visible at the location of the absent clusters. The overall glomerular structure, however, remained unchanged as a continuous outer layer on the AL surrounding a fibrous core of OSN tracts innervating the glomeruli (**Figure 3M**). These results indicate that *NvOrco* is responsible for regulating glomerular morphological differentiation in the *Nasonia* AL.

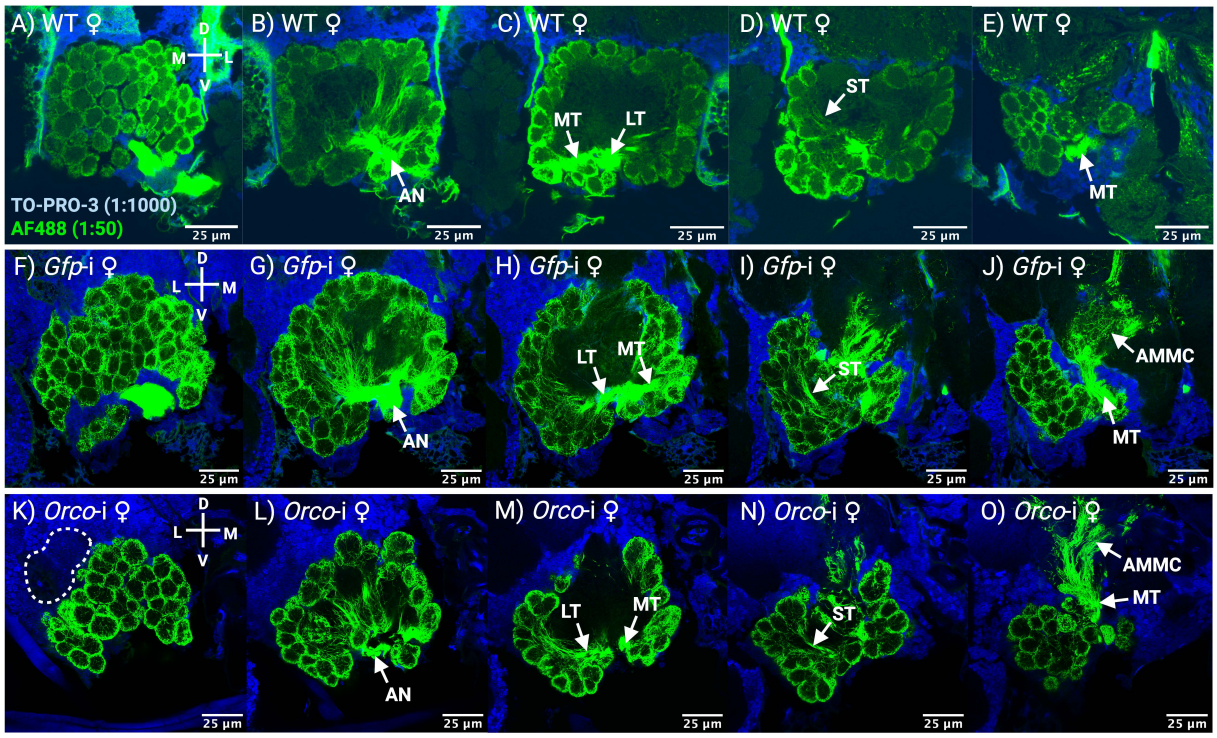

Figure 3: Optical sections of the glomeruli in the AL of female *N. vitripennis* after *Gfp*-i and *Orco*-i.
A-O: Confocal stacks of the glomerular neuropil morphology of wild-type (WT), *Gfp*-i and *Orco*-i females (represented in rows) showing various sections of the AL from anterior to posterior (AN = antennal nerve; LT and MT = lateral tract and medial tract of the antennal nerve; ST = subtracts; AMMC = antennal mechanosensory and motor centre). **A-J:** Similar glomerular organization between the wild-type and *Gfp*-i female AL. **F-O:** Morphological differences in glomerular organization between the *Gfp*-i and *Orco*-i female AL. **K:** *Orco*-i female AL showing the absence of a large glomerular cluster (indicated by dashed line). **C, H and M:** The antennal nerve bifurcates into a lateral tract and medial tract in all AL specimens. **D, I and N:** The lateral tract and medial tract divide into multiple subtracts innervating separate glomerular domains in all AL specimens. **E, J and O:** Antennal nerve also innervates the AMMC at the posterior of all AL specimens.

Silencing *NvOrco* decreases the number of glomeruli

We used the 3D-reconstructed ALs to count the total number of glomeruli in *Gfp*-i (n = 5) and *Orco*-i (n = 6) specimens. The mean number of glomeruli in wild-type females described in **Chapter 3** was similar to the number of glomeruli found in *Gfp*-i females. *Orco*-i females developed 17% fewer glomeruli compared to *Gfp*-i females. The mean number of glomeruli

was 200±8 (mean±sd) in *Gfp*-i compared to 166±12 in *Orco*-i females (**Figure 4A, Supplementary Table 1**; Wilcoxon rank-sum test, W = 30 , p < 0.01). Variation in the number of glomeruli was greater between individual *Orco*-i specimens compared to *Gfp*-i specimens. The number of glomeruli in *Gfp*-i females ranged between 187 and 207 and between 151 and 183 in *Orco*-i females. These results show that *Orco*-i in females decreases the number of glomeruli, which indicates that *NvOrco* is essential for the development and maintenance of AL glomeruli in *N. vitripennis*.

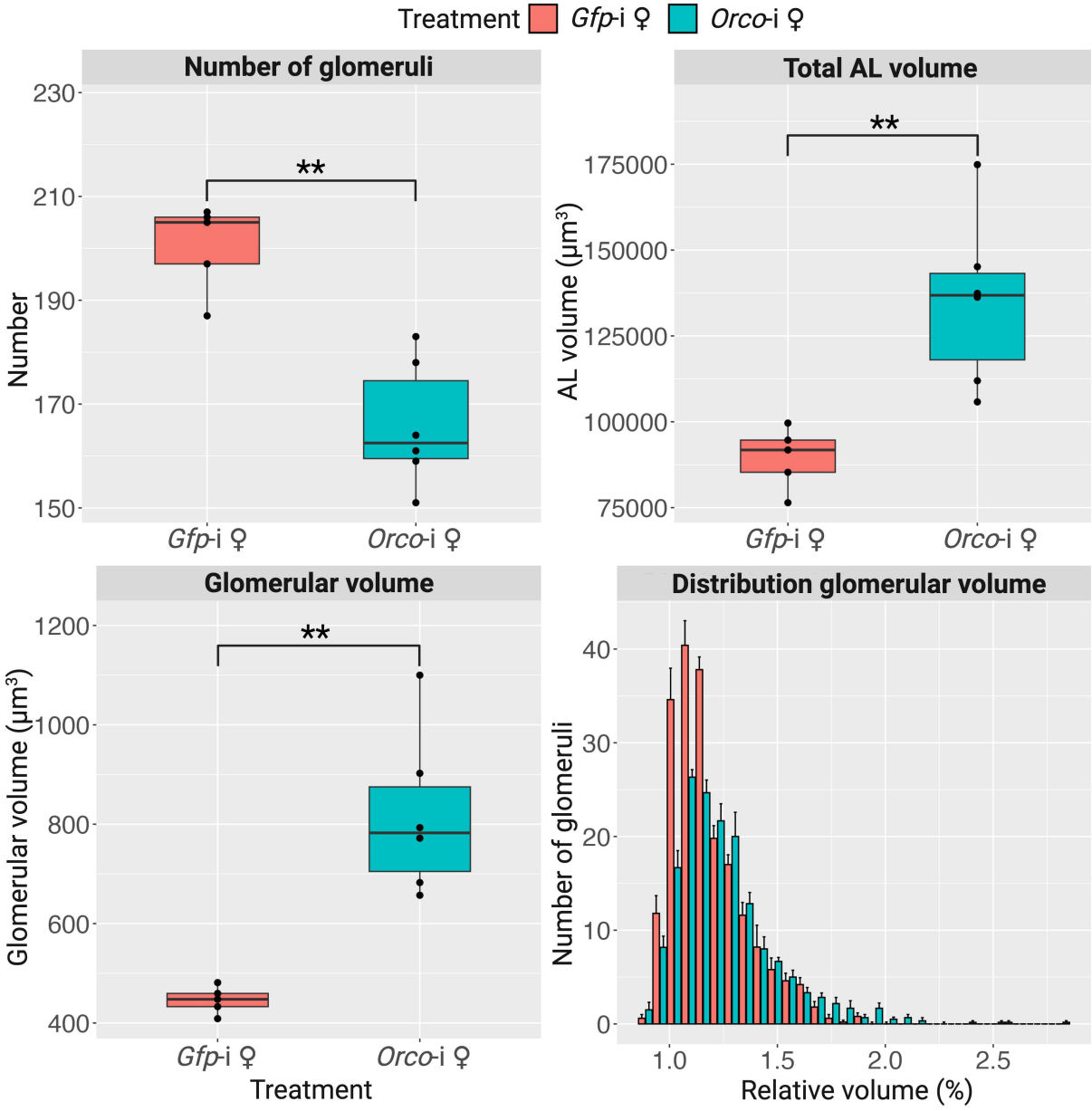

Figure 4: Morphological analysis of AL glomeruli after *Gfp*-i and *Orco*-i.
A: Number of glomeruli in *Gfp*-i and *Orco*-i females. *Orco*-i females show a significant reduction in the number of glomeruli compared to *Gfp*-i females. **B:** Total AL volume of *Gfp*-i and *Orco*-i females. *Orco*-i females show a significant increase in the total AL volume. **C:** Glomerular volume of *Gfp*-i and *Orco*-i females. *Orco*-i females show a significant increase in the volume of individual glomeruli. Significant differences in the number and volume were analysed with a Wilcoxon rank-sum test. Significance levels: ** = p < 0.01. **D:** Frequency distribution of glomerular volumes of *Gfp*-i and *Orco*-i females, showing that a greater proportion of glomeruli in *Orco*-i females consume a relatively higher volume of the AL compared to *Gfp*-i females.

Silencing *NvOrco* increases the volume of the AL and glomeruli

We also used the 3D-reconstructed ALs to calculate the total AL and glomerular volume (**Supplementary Table 1 and 2**). We found that the mean average AL volume of *Orco*-i females was consistently higher compared to *Gfp*-i females. The mean AL volume was 89,559±8,035 μm^3 in *Gfp*-i females (n = 5) compared to 135,241±24,843 μm^3 in *Orco*-i females (n = 6) (**Figure 4B, Supplementary Table 1**; Wilcoxon rank-sum test, W = 0 , $p < 0.01$). This reflects a 50% increase in the total AL volume of *Orco*-i females compared to *Gfp*-i females and would therefore indicate that a decrease in *NvOrco* expression in OSNs increases AL volume in *N. vitripennis*. Variation in the total AL volume was greater between individual *Orco*-i specimens compared to *Gfp*-i specimens. The total AL volume in *Gfp*-i females ranged between 76,430 μm^3 and 99,623 μm^3 and between 105,785 μm^3 to 174,890 μm^3 in *Orco*-i females. We also found that the mean average glomerular volume of *Orco*-i females was consistently higher compared to *Gfp*-i females. The mean glomerular volume was 446±31 μm^3 in *Gfp*-i females compared to 817±163 μm^3 in *Orco*-i females (**Figure 4C, Supplementary Table 1**; Wilcoxon rank-sum test, W = 0 $p < 0.01$). This represents an 83% increase in the glomerular volume of *Orco*-i females compared to *Gfp*-i females and would therefore indicate that a decrease in *NvOrco* expression also increases the volume of individual glomeruli. The frequency distribution of the glomerular volumes showed that a greater proportion of glomeruli in *Orco*-i females consumed a relatively higher volume of the AL compared to *Gfp*-i females (**Figure 4D**).

Discussion

Recent research has shown that disrupting *Orco* in non-parasitoid Hymenoptera hampers OSNs to innervate the AL neuropil for protoglomerular structures to differentiate into multiple glomeruli in adults (Chen *et al*., 2021; Trible *et al*., 2017; Yan *et al*., 2017). We postulate that a similar mechanism is responsible for shaping the number and morphological organization of AL glomeruli in parasitoid Hymenoptera. Our aim was to determine the role that *Orco* plays in the development of the AL in *Nasonia vitripennis*, by silencing this gene with dsRNA at the fourth-instar larval stage before the onset of OR expression and the innervation of glomeruli by OSNs (Tissot & Stocker, 2000). Reduced *NvOrco* expression resulted in dramatic neuro-anatomical changes in AL glomerular organization, including a decrease in the number of glomeruli and an increase in the total AL and glomerular volume. Our results corroborate previous studies that demonstrated the unique function of *Orco* in Hymenoptera for AL glomerular development (Chen *et al*., 2021; Trible *et al*., 2017; Williams *et al*., 2022; Yan *et al*., 2017). We can now conclude for the first time that *Orco* expression serves as a crucial mechanism in parasitoid Hymenoptera for OSNs to innervate and organize the AL glomerular neuropil.

After silencing *NvOrco* and *Gfp* in *N. vitripennis* females, we carried out antennal backfills with Biotin-Dextran to trace OSNs to the AL neuropil for analysing glomerular organization. We subsequently made 3D reconstructions of the AL of these backfilled specimens and determined the number of glomeruli. Both wild-type and *Gfp*-i females possess approximately 225 glomeruli (see **Chapter 3**), which corresponds to the number of functionally expressed ORs in *N. vitripennis* (Robertson *et al*., 2010). After silencing *NvOrco*, we determined a decrease in the number of glomeruli, in line with previous studies that disrupted *Orco* in non-parasitoid Hymenoptera, such as ants and honeybees (Chen *et al*., 2021; Trible *et al*., 2017; Yan *et al*., 2017). Our results therefore demonstrate that *Orco* is also necessary in parasitoid Hymenoptera for OSNs to innervate their corresponding glomerular targets and for determining the number of glomeruli in the AL. In species such as *Drosophila*, in which the glomeruli are determined by projection neurons prior to OSN innervation (Jefferis, 2005), *Orco* has been shown to play no role in AL development (Larsson *et al*., 2004), In Hymenoptera species, however, we can now confirm that *Orco* is essential for OSN innervation and consequently the formation of glomeruli. Nevertheless, it remains unclear how this regulatory mechanism functions in these species. Our results enable future research on parasitoid and other Hymenoptera to focus on determining the genetic pathways that recruit *Orco* for regulating OSN projections and for determining the number of glomeruli in the AL.

We also confirmed that silencing *Orco* affects glomerular volume in *N. vitripennis*. After 3D reconstruction, we determined a 50% increase in the total AL volume and an 80% increase in glomerular volume in our *Orco*-i specimens. One would expect that a decrease in the number of glomeruli would also result in a decrease in AL and glomerular volume. This would reflect

previous studies that disrupted *Orco* in ants (Trible *et al*., 2017; Yan *et al*., 2017) and honeybees (Chen *et al*., 2021) and found a decrease in these volumes. These studies on formids, however, also found a major decrease in OSNs innervating the glomeruli after knocking out *Orco* at the embryonic stage, whereas our study silenced *Orco* at the larval stage. Moreover, another recent study also showed that OSNs were unable to survive in the absence of this gene (Sieriebriennikov *et al*., 2024). This indicates that OSN and glomerular development could depend on whether *Orco* is modified or silenced, and on the precise timing of these procedures. The absence of OSNs in ants impeded the innervation of the glomeruli, which in turn resulted in a decrease in AL and glomerular volume. Silencing *Orco* in our specimens, on the other hand, did not impede OSN survival and therefore resulted in a hyperinnervation of the remaining glomeruli and consequently an increase in AL and glomerular volume. Our results therefore pave the way for future studies to investigate the relationship between OSN survival, glomerular innervation and AL development in parasitoids.

Our results also demonstrate that parasitoids utilize *Orco* for the correct differentiation of glomeruli. The differentiation of glomeruli in insects is regulated through synaptic interactions between OSNs, projection neurons and glia cells (Oland & Tolbert, 2011). These interactions form a rough template of protoglomeruli during the development of the AL. Prior to innervating the AL, OSN axons are bundled by glia cells in the antennae and are organized at a so-called axon sorting zone before arriving at their glomerular targets in the AL (Rössler *et al*., 1999). The OSNs subsequently interact with ensheathing glia that form glomerular envelopes (Oland & Tolbert, 1987). We hypothesize that in parasitoids *Orco* expression is required in OSNs to interact with glia cells to form stable glomeruli and to promote the differentiation of protoglomeruli into smaller glomeruli (**Figure 5**). These smaller glomeruli could initially be present as microglomeruli in the developing, undifferentiated protoglomerulus, similar to the microglomeruli observed in some Orthoptera species, where they are targeted separately by OSNs and projection neurons (Ignell *et al*., 2001). It would therefore also be interesting to address how *Orco* influences the interactions between OSNs, glia cells and other AL neurons for the differentiation of glomeruli in the AL.

Our 3D-reconstructed *Orco*-i specimens showed a degree of variation in morphology, number and volume of glomeruli. This is likely due to variation in the amount of injected *NvOrco* dsRNA causing different levels of *NvOrco* expression between our specimens. This is also demonstrated by the fact that the decrease in the number of glomeruli in our *Orco*-i specimens was not uniform. Our results therefore indicate that *NvOrco* functions as a general mechanism in OSNs for establishing the organization of glomeruli. This process draws comparisons with the *Hedgehog* signalling mechanism identified in *Drosophila*, where this gene is required to induce and maintain the expression of the *Patched* receptor in subsets of OSNs (Chou *et al*., 2010b). Different expression levels of *Patched* then determine the sensitivity of OSN axons to *Hedgehog* signals derived from the AL, resulting in the spatial

coordination of OSNs and their glomerular targets (Chou *et al*., 2010b). *Orco* expression in *Drosophila* marks the final step in this process (Sanchez *et al*., 2016), but has no further influence on the final morphology of the AL in this species (Larsson *et al*., 2004). This indicates that the OSNs in Hymenoptera rely more on *Orco* for fine-tuning glomerular organization, whereas *Drosophila* depends on the molecular processes preceding the expression of this gene.

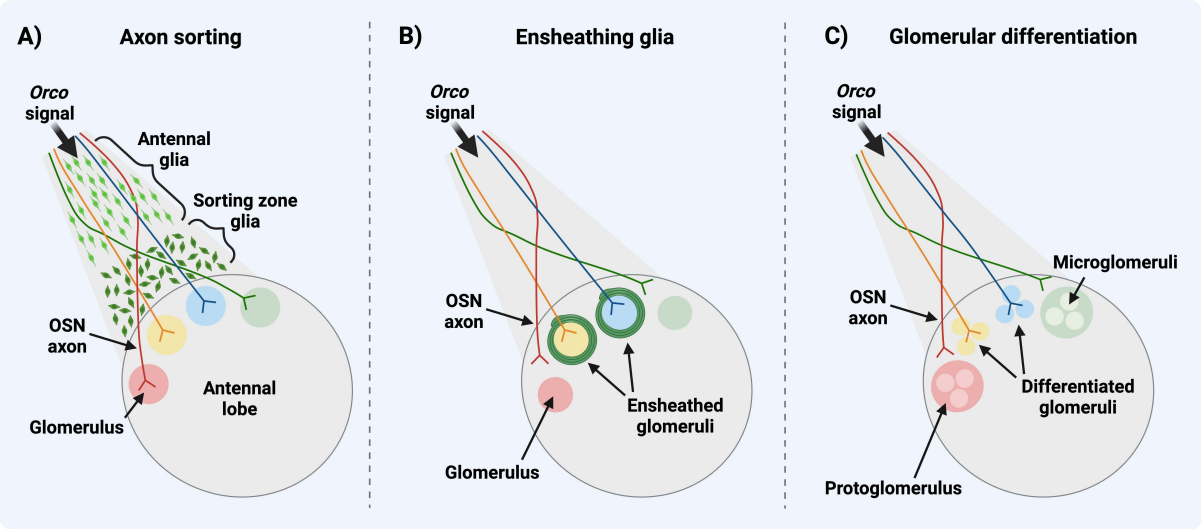

Figure 5: Hypothetical scenarios of *Orco* shaping AL glomerular formation.
Three scenarios in which *Orco* could contribute to the formation of AL glomeruli. **A:** OSNs interact with antennal and sorting zone glia for the correct innervation of glomeruli in the AL (Oland & Tolbert, 2011; Rössler *et al*., 1999). **B:** OSNs interact with ensheathing glia that stabilize glomeruli in the AL (Oland & Tolbert, 1987). **C:** OSNs are necessary for the correct differentiation of protoglomeruli (possessing numerous microglomeruli) into multiple glomeruli.

Our study is the first to determine the developmental effects of *Orco* on glomeruli in parasitoid wasps. After silencing *NvOrco* in L4 larvae, we determined dramatic morphological changes in the AL, including a decrease in the number of glomeruli and an increase in AL and glomerular volume. In social Hymenoptera, such as ants, *Orco* has been shown to be an essential component for facilitating OSN projection to specific glomeruli (Trible *et al*., 2017; Yan *et al*., 2017). Our results can now verify that *Orco* is also necessary in parasitoid OSNs for innervating their glomerular targets and for fine-tuning glomerular organization. We recommend pursuing our results further to investigate which downstream genes of *Orco* are responsible for these processes. Genes influencing OSN projections and OSN-glia interactions are potential targets for these studies. Furthermore, the glomeruli of *N. vitripennis* are sexually dimorphic in number and are regulated by the sex-determination splicing factor TRA. Silencing this gene results in a decrease in the number of glomeruli in females and the loss of glomerular clusters, comparable to our *Orco*-i specimens. This would make *Orco* a promising target of sex-determination transcription factors for regulating sexual dimorphism in the

parasitoid AL. We recommend investigating whether *Orco* interacts with these transcription factors and, if so, at which developmental stage these interactions take place.

Our results have paved the way for future research into the developmental role of *Orco* in parasitoids. Previous studies on other Hymenoptera species have already determined how the absence of *Orco* modifies glomerular organization, but have not looked at the specific mechanisms involved in OSN development (Chen *et al*., 2021; Trible *et al*., 2017; Yan *et al*., 2017). The intricate life history of parasitoids and other Hymenoptera serves as a driver for the evolution of enhanced cognitive mechanisms, such as the increased number of OR genes (Legan *et al*., 2021; McKenzie *et al*., 2016; McKenzie & Kronauer, 2018; Robertson *et al*., 2010; Zhou *et al*., 2015) and glomeruli (Arnold *et al*., 1985; Das & Fadamiro, 2013; Groothuis *et al*., 2019; McKenzie *et al*., 2016; Smid *et al*., 2003; Zube & Rössler, 2008) compared to other insect orders, such as Diptera and Lepidoptera. The increase in these cognitive mechanisms should therefore correspond to an increase in the production of OSNs, although the underlying developmental and molecular processes remain unclear. Our research now provides a neurophysiological foundation for future research into the specific function of *Orco* in these processes. *Orco* clearly plays an important role in the relationship between OSNs and AL development and this is crucial for the regulation of olfactory behaviour. In ants, *Orco* was found to significantly influence social behaviour and reproduction, indicating the importance of this gene for perceiving pheromones (Trible *et al*., 2017; Yan *et al*., 2017). In parasitoids, moreover, *Orco* is essential for inducing mating and host-searching behaviour (Zhang *et al*., 2023). Understanding the relationship between OSNs and AL development will therefore provide us with new insight into how this gene shapes glomerular organization and its role in forming neural circuits involved in odour-mediated behaviour. Knowledge of the specific neurodevelopmental genes and neural circuits involved in parasitoid host-searching behaviour can be implemented into selective breeding strategies optimizing parasitoids as biological control agents for integrated pest-management solutions.

Acknowledgements

We would like to thank Lex Koekkoek for his help in carrying out the segmentation and morphometric analysis of antennal-lobe glomeruli in AMIRA. We are also grateful for the feedback on this chapter provided by Marcel Dicke.

Supplementary information

Supplementary Table 1: Number and volumetric data of *Gfp*-i and *Orco*-i specimens.
Table showing the number of glomeruli and the total antennal lobe and glomerular volume in *Gfp*-i and *Orco*-i specimens.

Treatment	Total glomerular count	Total antennal lobe volume (µm^3)	Average glomerular volume (µm^3)
***Gfp*-i L4 female**	206	94664.80	459.54
***Gfp*-i L4 female**	207	99623.03	481.27
***Gfp*-i L4 female**	187	76430.51	408.72
***Gfp*-i L4 female**	205	91785.60	447.73
***Gfp*-i L4 female**	197	85292.57	432.96
***Orco*-i L4 female**	161	105785.39	657.05
***Orco*-i L4 female**	178	137398.96	771.9
***Orco*-i L4 female**	159	174890.29	1099.94
***Orco*-i L4 female**	151	136275.04	902.48
***Orco*-i L4 female**	164	111951.18	682.63
***Orco*-i L4 female**	183	145149.84	793.17

Supplementary Table 2: Raw volumetric data of the segmented *Gfp*-i and *Orco*-i specimens.
Volumes are calculated for each glomerulus (denoted as 'material') based on the amount of assigned voxels. This table can be accessed online at:
https://git.wur.nl/aidan.williams/chapter4/-/blob/main/Supplementary_Table_2.csv?ref_type=heads

Chapter 5

Transformer feminizes the cuticular hydrocarbon profile in the parasitoid *Nasonia vitripennis*

Aidan Williams[1], Markus Meißner[2], Tamara Pokorny[2], Joachim Ruther[2] & Eveline Verhulst[1]

[1]Laboratory of Entomology, Wageningen University, PO Box 16, 6700 AA Wageningen, the Netherlands

[2]Institute of Zoology, University of Regensburg, Universitätsstrasse 31, 93053 Regensburg, Germany

Abstract

Sex pheromones are used by insects as chemical signals to identify and choose mating partners of the opposite sex. This chapter focuses on pheromone production and in particular the genetic pathway that regulates pheromone sexual dimorphism. Sexual dimorphism in pheromones is regulated by transcription factors of the sex-determination pathway. One such group of sexually dimorphic pheromones are the cuticular hydrocarbons (CHCs), which are utilized by insects for close-range sexual communication. Transformer (TRA) is a conserved splicing factor in the sex-determination pathway that has been shown to regulate sexual dimorphism in CHC production. However, research into the mechanism by which this specific factor regulates insect CHC production has been limited to the model species *Drosophila* and has yet to be investigated in species with more complex CHC profiles. In this chapter, we confirmed the function of *Tra* in regulating sexual dimorphism in the CHC profile of the parasitoid *Nasonia vitripennis*. We determined that silencing *NvTra* at the larval stage masculinized the adult female CHC profile by changing the relative composition of CHC compounds from female-specific to male-specific. Masculinization of the female CHC profile also affected male mating behaviour, as demonstrated in the decreased duration of the time that males spent mounting and attempting to copulate with *NvTra*-silenced female specimens. We conclude that *NvTra* plays a crucial role in feminizing the CHC profile of *N. vitripennis* during pupal development, resulting in the production of CHCs for eliciting male mating behaviour. Moreover, our results now enable us to turn to identifying the downstream sex-determination transcription factors and corresponding male and female biosynthetic genes for producing sexually dimorphic CHCs.

Introduction

Attracting and recognizing the opposite sex is a critical aspect of animal sexual communication. Sex pheromones are chemicals specifically used to signal the species and sexual identity of individuals, which in turn needs to be correctly perceived by a mating partner to induce a behavioural response (Wyatt, 2014). The chemical information conveyed by sex pheromones influences the process of mate choice by advertising the quality of a potential mating partner (Johansson & Jones, 2007). Sex-pheromone specificity is therefore paramount, as any change in chemical composition can determine the outcome of mating decisions. As a result of sexual selection, insects have evolved sexually dimorphic pheromones and the cognate receptors to reinforce reproductive isolation (Buchinger & Li, 2023; Johansson & Jones, 2007; Ritchie & Noor, 2004; Smadja & Butlin, 2009; Steiger & Stökl, 2014; Svensson, 1996). In **Chapters 3 and 4**, we discussed the potential genetic mechanisms regulating sexual dimorphism in insect pheromone perception. We will now focus on pheromone production and in particular the genetic pathway that regulates pheromone sexual dimorphism. Conserved transcription factors of the sex-determination pathway regulate sexual differentiation in pheromone production (Chertemps *et al*., 2006, 2007; Ferveur *et al*., 1997; Jallon *et al*., 1988; Pei *et al*., 2021; Sun *et al*., 2023a; Tompkins & McRobert, 1989, 1995; Waterbury *et al*., 1999). These transcription factors regulate the sex-biased expression of biosynthetic genes, which in turn determine the composition of sex pheromones and contribute to reproductive isolation (Shirangi *et al*., 2009). Understanding how sexual differentiation regulates pheromone production is therefore necessary to elucidate the evolution of sexual dimorphism in insect pheromone communication.

Cuticular hydrocarbons (CHCs) have long been the primary focus of research into the genetic regulation of insect sex pheromones (Chung & Carroll, 2015; Holze *et al*., 2021; Wang *et al*., 2025). These long-chain carbon chemicals form a major component of the insect waxy layer on the cuticle (Blomquist *et al*., 1987; Lockey, 1988), preventing desiccation while also serving as pheromones for close-range sexual communication (Chung *et al*., 2014; Chung & Carroll, 2015). Moreover, the chemical biology and genetic regulation of CHCs provide an ideal model to study the evolution of sexually dimorphic pheromones. Not only are CHCs chemically diverse, but many closely related insect species have evolved a diversity of sexually dimorphic CHC profiles (Buellesbach *et al*., 2013; Dembeck *et al*., 2015; Kather & Martin, 2015; Oliveira *et al*., 2011). Studies on the mating systems of these species have also shown that sexually dimorphic CHCs play an essential role for attracting potential mating partners, while also inducing behaviour such as aggregation, aggression, courtship and copulation (Billeter & Wolfner, 2018; Ferveur, 2005; Leonhardt *et al*., 2016; Mair & Ruther, 2019). The specific CHC compounds that induce such behaviour have diverged among closely related insect species and this in turn has contributed to assortative mating and reproductive isolation (Billeter *et al*., 2009; Buellesbach *et al*., 2013; Chung & Carroll, 2015; Coyne *et al*., 1994). Research has identified the genes and corresponding enzymes involved in the insect CHC biosynthetic

pathway, which appear to be highly conserved and involve metabolizing fatty-acid precursors by fatty-acid synthases, elongases, desaturases, reductases and decarbonylases (Blomquist & Bagnères, 2010; Blomquist & Ginzel, 2021; Chung & Carroll, 2015; Holze *et al*., 2021; Howard & Blomquist, 2005). However, research on how sex determination regulates the CHC biosynthetic pathway has primarily been limited to the model organism *Drosophila*.

Cuticular hydrocarbons are among the first insect sex pheromones shown to be regulated by the sex-determination pathway. The CHCs of the model species *Drosophila melanogaster* are sexually dimorphic (Ferveur, 1997). In *Drosophila*, females produce the long-chain dienes (CHCs with double bonds), 7,11-heptacosadiene (7,11-HD) and 7,11-nonacosadiene (7,11-ND), whereas males produce larger amounts of the monoenes (monounsaturated CHCs), 7-tricosene (7-T) and 7-pentacosene (7-P). The female-specific dienes, 7,11-HD and 7,11-ND, are known as aphrodisiac molecules, which elicit courtship in males, whereas the male-specific monoenes, 7-T and 7-P, have the opposite effect (Ferveur & Sureau, 1996; Savarit *et al*., 1999; Scott & Jackson, 1988). The production of these CHCs is known to be regulated by genes of the sex-determination pathway (Chertemps *et al*., 2006, 2007; Ferveur *et al*., 1997; Jallon *et al*., 1988; Sun *et al*., 2023a; Tompkins & McRobert, 1989, 1995; Waterbury *et al*., 1999). In these studies, mutations in the *Sex-lethal* (*Sxl*), *Transformer* (*Tra*), *Transformer-2* (*Tra-2*) and *Doublesex* (*Dsx*) genes were seen to masculinize the CHC profile of females. Conversely, ectopic expression of *Sxl*, *Tra* and the female splice form of *Dsx* in males feminized the CHC profile. How these genes are involved in regulating CHC biosynthesis in other insects remains unknown.

Transformer is a central component of sex determination in most insects (Verhulst *et al*., 2010b). This splicing factor functions as a binary switch in the sex-determination pathway by regulating the sex-specific splicing of *Dsx* and *Fruitless* (*Fru*) (Bopp *et al*., 2014; Verhulst *et al*., 2010b). The sex-specific splicing of *Dsx* and *Fru* transcripts results in male and female transcription factors necessary for sex-specific development, pheromone production and behaviour (Verhulst & van de Zande, 2015). The function of TRA as a splicing factor of *Dsx* is conserved in most insects and has been shown to affect the production of sexually dimorphic CHCs (Savarit & Ferveur, 2002). Ectopic expression of *Tra* in *Drosophila* males resulted in the expression of female-specific CHC biosynthesis genes (Chertemps *et al*., 2006, 2007). The central role that *Tra* plays in the sex-determination pathway of most insects (Verhulst *et al*., 2010b) makes it an ideal candidate gene for investigating the evolution of sexual dimorphism in the CHC profile, not only in *Drosophila*, but also in species that use different pheromone-coding systems, such as Hymenoptera.

Hymenoptera, including ants, bees and wasps, have evolved a wide-ranging diversity of CHC profiles (Kather & Martin, 2015). However, only very limited research has been carried out into the role that sex determination plays in regulating the CHC biosynthetic pathway in these species. Parasitoid Hymenoptera, such as the model species *Nasonia vitripennis*, produce

some of the most complex CHC profiles, comprising a wide variety of methyl-branched alkanes (Kather & Martin, 2015). It has been shown that CHCs function as mate-recognition signals in *Nasonia*, enabling males to direct courtship to conspecific mating partners (Steiner *et al*., 2006; Sun *et al*., 2023b). As a result, all four *Nasonia* species have evolved sexually dimorphic CHC profiles (Buellesbach *et al*., 2013; Niehuis *et al*., 2011), suggesting a potential role of TRA and its downstream targets. Recent studies on *N. vitripennis* have shown that *Dsx,* a splicing target of TRA, regulates the sex-specific biosynthesis of alkenes (Wang *et al*., 2022b). Silencing *Dsx* in males decreased the absolute quantities of these alkenes and induced courtship between wild-type males and the silenced males. These alkenes therefore function as pheromones in *N. vitripennis* to inhibit male-male courtship.

This study focused on determining the function of TRA in regulating sexual differentiation in the CHC profile of *N. vitripennis*. We determined the function of *NvTra* by silencing this gene at the third-instar larval stage of females and analysing the relative composition of CHCs with GC-MS and multivariate analyses. Silencing *NvTra* at the third-instar larval stage with RNA interference (RNAi) induces masculinization by changing the alternative splicing of *Dsx* and other sex-determination transcription-factor genes from female-specific to male-specific. We therefore also analysed whether silencing *NvTra* in females affected the absolute quantities of alkenes. We hypothesized that *NvTra*-silenced females develop a male-specific CHC phenotype that affects the mating behaviour of males. Our study was able to establish that NvTRA plays an essential role in the sex-specific splicing of transcription factors that regulate female differentiation in the CHC profile of *N. vitripennis*.

Materials & Methods

Nasonia rearing

We used the lab strain AsymCX of *N. vitripennis* to silence *NvTra* expression with dsRNA. AsymCX was reared on *Calliphora vomitoria* pupae obtained as larvae from a commercial manufacturer (Kreikamp & Zn, Hoevelaken, the Netherlands). The fly larvae were left to pupate in sawdust at room temperature for three to four days and were subsequently stored at 4°C for a maximum duration of four weeks after pupation. Once they emerged, individual female wasps were placed together with a single host pupa in glass vials for 24 hours. This ensured the consistent development of our lab strains in terms of body size and CHC production. Virgin female wasps were used to produce male-only offspring (100% males) and mated females were used to produce mainly female offspring (90% females). After 24 hours, we followed the rearing protocol for *Nasonia* strain maintenance as set out by Werren & Loehlin (2009a). This protocol involved incubating the parasitized pupae at a constant temperature of 25°C using a 16-hour light, eight-hour dark cycle. The male and female offspring were subsequently used in our dsRNA and behavioural experiments.

Synthesis of *NvTra* dsRNA

We used the MEGAscript RNAi Kit (Thermo Fisher, Waltham, MA, USA) to generate *NvTra* dsRNA from *N. vitripennis* cDNA. *Nasonia vitripennis* cDNA and *NvTra* dsRNA were synthesized in line with the protocols set out in **Chapter 3**. A non-sex-specific *NvTra* fragment of 452 bp was synthesized in a PCR using the GoTaq Flexi DNA polymerase (Promega, Madison, WI, USA) and the designed primers Nv_Tra_RNAi_F1 (5'-CGAGACATCAGTTAGAAGAT-3') and Nv_Tra_RNAi_R1 (5'-GTCTTGTGGTCCTATGAAAC-3'). The PCR product was amplified in two separate PCRs to add T7 promotors [TAATACGACTCACTATAGGG] to either end of the amplicon. The resulting two templates were then used in separate PCR reactions to transcribe both sense and antisense RNA molecules in accordance with the MEGAscript RNAi Kit protocol (16 hours at 37°C). *Gfp* dsRNA was used as an exogenous control in our chemical and behavioural experiments and was generated from the pOPINEneo-3C-GFP vector (Addgene plasmid #53534; https://www.addgene.org/53534/; RRID: Addgene_53534). Amplification by PCR using GoTaq Flexi DNA polymerase (Promega) with the primers GFP_RNAi_F (5'-GTGACCACCTTGACCTACG-3') and GFP_RNAi_R (5'-TCTCGTTGGGGTCTTTGCT-3') produced a 460 bp amplicon, which covered 64% of the Emerald GFP CDS. The synthesized dsRNA was measured for its purity and concentration on a spectrophotometer (DeNovix, DS-11 FX, Wilmington, Delaware, USA) and subsequently diluted with RNase-free water to a concentration of 4 µg/µl and injected in third-instar *N. vitripennis* larvae to silence *NvTra* (*Tra*-i).

Micro-injection of *NvTra* dsRNA

NvTra and *Gfp* dsRNA was injected in female third-instar larvae (L3) four days post oviposition. This was carried out before the onset of adult oenocyte development and CHC production that occur during the pupal stage (Carlson *et al*., 1999; Johnson & Butterworth, 1985; Lawrence & Johnston, 1982). The L3 larvae were specifically chosen for injecting *NvTra* dsRNA to allow sufficient time for *Dsx* to revert to default male-specific splicing. The larvae were aligned on a 1x phosphate-buffered saline (PBS) agar plate and a mixture of 4.5 µl dsRNA and 0.5 µl food dye was injected in their posterior using a FemtoJet 4i microinjection pump (Eppendorf, Hamburg, Germany) according to the protocol set out by Lynch & Desplan (2006) and Werren *et al*. (2009). The L3 larvae were subsequently returned to a parasitized host to continue feeding until pupation. The parasitized hosts for the L3 larvae were prepared one day before the dsRNA injections, by enabling female *N. vitripennis* to oviposit in the anterior of the fly pupae. The eggs were removed from the host after 24 hours and replaced by the *NvTra* dsRNA-injected larvae, which were then able to continue development. The dsRNA-injected larvae were incubated at 25°C until pupation. Female specimens were then collected based on sex-specific traits (forewing size and presence/absence of the ovipositor) and kept separate for chemical and behavioural analysis.

As indicated in **Chapter 3**, *Tra*-i females develop a male-like phenotype, such as lighter pigmentation on the antennae and femora, as well as a wing morphology intermediate between wild-type males and females. Our PCR analysis in **Chapter 3** showed that these *Tra*-i females expressed both male- and female-specific splice forms of *NvTra* and *NvDsx,* confirming that *NvTra* was successfully silenced. On the basis of these results, we selected *Tra*-i females with similar male-like phenotypes for our chemical and behavioural experiments.

Chemical analysis

GC-MS and CHC identification

We analysed the adult CHC profile of *Tra*-i females and compared this with the CHC profile of wild-type males, wild-type females and *Gfp*-i females. Wasps of these treatment groups were collected at the black pupal stage and kept separate in 1.5 ml Eppendorf tubes (Eppendorf, Hamburg, Germany) with perforated caps. The wasps were freeze-killed at −20°C 48 hours after emergence. We then extracted the CHCs by immersing individual wasps in a 15 µl *n*-hexane solution in a 300 µl glass insert (Klaus Trott Chromatographie-Zubehör, Kriftel, Germany) for 30 minutes. The *n*-hexane solution contained 150 ng squalane (2,6,10,15,19,23-hexamethyltetracosane) used as the internal standard. The extracts were then transferred to a vial containing a 150 µl insert before being injected into a GC-MS for CHC analysis. We first calculated the linear retention indices of CHCs by injecting a Kovats standard mixture containing *n*-alkanes. We subsequently injected 2 µl of the extracted samples in splitless mode with an automated injector (AOC-20i, Shimadzu, Duisburg, Germany) into a gas

chromatograph coupled to a single quadrupole mass spectrometer (GCMS-QP 2010 Plus (Shimadzu, Duisburg, Germany). The GC-MS setup was equipped with a BPX5 column (60 m x 0.25 mm x 0.25 µm; SGE Analytical Science Europe, Milton Keynes, UK) using helium as a carrier gas at a constant flow rate of 30 cm per second. The column temperature profile started at 150°C, increasing 2°C per minute to the final temperature of 300°C, which was maintained for 30 minutes. The mass spectrometer was operated in electron-ionization mode at 70 eV and was set at a mass-to-charge ratio of 30-600 m/z. CHCs were subsequently identified according to their linear retention indices and the mass spectra provided by the total ion count chromatograms. Moreover, the methyl group position in methyl-branched alkanes was identified according to the fragmentation patterns in the mass spectra.

Data analysis

CHC peak detection, integration, identification and quantification were carried out using the Postrun Analysis modules of the Shimadzu GCMS solution software (v4.45, Shimadzu, Duisburg, Germany). All peaks were integrated manually and overlapping compounds were separated based on fragment ion chromatograms (**Supplementary Table 1**). We analysed differences in the relative CHC composition of our treatment groups by calculating the relative peak areas of CHCs. The relative peak areas were calculated by dividing individual CHC peak areas by the total CHC peak area. This procedure generated standardized proportional data for multivariate analysis. Peaks were excluded from further analysis if they contributed less than 0.1% to the total peak area. Common non-CHC lipids, such as cholesterol, were also excluded from further analysis.

A pivot table of the proportional data was created with Microsoft Excel 2019 (v16). For multivariate analysis, the data was first square-root transformed to mitigate the influence of large CHC peaks. We subsequently performed a Non-metric Multidimensional Scaling (NMDS) analysis to visualize the different CHC profiles of our treatment groups. The NMDS analysis was applied on a triangular matrix of the transformed data using Bray-Curtis-distances with 99 restarts. An Analysis of Similarity (ANOSIM) was then performed to test for significant differences between the distinct groups identified by the NMDS analysis. The ANOSIM value R ($1 > R > -1$) indicates the degree of separation between groups, ranging from no separation (0) to maximum separation (1). Negative values (to −1) indicate that separation is higher within groups than between them. We also calculated Similarity Percentages (SIMPER) to determine the contribution of each CHC peak to the overall Bray-Curtis dissimilarity between the treatment groups. The Bray-Curtis coefficient was used to quantify dissimilarity in the relative CHC composition between the treatment groups by taking into consideration the total number and relative peak area of CHC compounds. The SIMPER analysis first calculates the average similarities between every pair-wise comparison and then calculates the average dissimilarity, which typically ranges between 0% and 100%, or alternatively between 0 and 1. If both treatment groups share the same number of CHCs, with the same relative peak areas, their dissimilarity will be zero. A 50% cut-off was set to include only the CHCs that made a

significant contribution to the average Bray-Curtis dissimilarity. All multivariate analyses were performed using Primer (v6, Primer-E, Plymouth, USA) (Clarke, 1993; Clarke & Gorley, 2006).

Absolute CHC quantities (in ng) were obtained by relating the peak area of each compound with the internal standard. We focused on the absolute quantities of the alkenes Z7-C31ene, Z7-C33ene, Z9-C31ene and Z9-C33ene, which are regulated by the sex-determination pathway (Wang *et al*., 2022b) and function as pheromones in higher quantities in male *N. vitripennis* for inhibiting male-male courtship. Significant differences in alkene absolute quantities were analysed with a Kruskal-Wallis H test and Bonferroni-corrected Wilcoxon rank-sum tests in RStudio (v2024.12.1+563, Posit PBC).

Behavioural tests

Mating trials with *Tra*-i females

We conducted behavioural assays to verify that silencing *NvTra* in females affected male mating behaviour. Accordingly, we tested the mating responses of males to *Tra*-i females, using *Gfp*-i females as a control. Virgin *Tra*-i females were presented to newly emerged virgin (0-48 hours old) wild-type males in a glass vial (7.5 cm length, 1 cm diameter). We then observed four distinct elements of male mating behaviour: (1) searching time (the time the male spent finding the female, from the start of the observation until the male mounted the female); (2) mounting time (the time the male spent performing courtship on the female; (3) copulation time (the time the male spent copulating with the female); and (4) post-copulation time (the time the male spent remounting the female after copulation, until the male dismounted). Our observations of male mating behaviour started immediately after transferring a female wasp to a vial containing a male and discontinued if a male proved unsuccessful in finding the female within five minutes. After each experiment, we calculated the mating success rate as the percentage of males that copulated with a female. Significant differences in male mating behaviour were analysed using a Bonferroni-corrected Wilcoxon rank-sum test of the Coin package in RStudio (v2024.12.1+563, Posit PBC). Significant differences in mating success were analysed using a Pearson's Chi-squared test with Yates's continuity correction.

Male mate recognition of *Tra*-i females

We also conducted behavioural assays to verify that changes in the CHC profile of *Tra*-i females affected mate recognition for males. We tested the mating responses of wild-type virgin (0-48 hours old) males to the CHCs of *Tra*-i and *Gfp*-i females in a mating chamber in accordance with Mair *et al*. (2017). The silenced females were freeze-killed in liquid nitrogen before the experiment and used as dummies to minimize potential mating signals (e.g. behavioural or vibrational signals), except for CHCs (Buellesbach *et al*., 2013, 2018). The female dummies were then presented to the newly emerged virgin wild-type males in an acrylic mating chamber (ø10 mm) covered with a glass microscope slide and placed on a glass

plate. Male mating behaviour was then analysed under a stereomicroscope. Males typically show mating behaviour in response to female CHCs by mounting and copulating with the females. For mounting behaviour, we observed the amount of time a male spent positioning and performing courtship (i.e. head nodding, antennal sweeping and wing twitching, etc.) on a female dummy. For copulation behaviour, we observed the amount of time a male spent attempting to copulate with the female dummy. We recorded the cumulative time of this behaviour for five minutes. After testing six replicates, the acrylic mating chamber was cleaned with detergent (TORK mild liquid soap, 420501) and the glass plate with 70% ethanol. Significant differences in male mating behaviour were analysed using a Bonferroni-corrected Wilcoxon rank-sum test of the Coin package in RStudio (v2024.12.1+563, Posit PBC). Significant differences in copulation attempts were analysed using a Pearson's Chi-squared test with Yates's continuity correction.

Results

Identification and relative composition of CHCs

We conducted a GC-MS analysis to investigate the relative CHC composition of our four treatment groups: wild-type males (n = 10), wild-type females (n = 10), *Gfp*-i females (n = 10) and *Tra*-i females (n = 10). Our analysis identified 95 individual CHCs on the basis of their linear retention indices and diagnostic ions (**Figure 1A**). The identified compounds comprised CHCs with a chain length between 29 and 37 C-atoms and included straight-chain *n*-alkanes, methyl-branched alkanes (MB-alkanes) and alkenes (**Table 1**). MB-alkanes (87 in total) made up the vast majority of the identified CHCs (**Figure 1A**). The MB-alkanes comprised 28 monomethyl alkanes, 41 dimethyl alkanes, 16 trimethyl alkanes and two tetramethyl alkanes. In addition, we also identified a total of four *n*-alkanes and four alkenes.

We calculated the mean relative peak area for each CHC to compare the CHC composition between our treatment groups (**Table 1**). We then compared the mean relative peak areas of CHCs between wild-type males and wild-type females. Males showed a larger relative peak area of CHCs consisting of dimethyl alkanes (52.83% vs 44.55%), trimethyl alkanes (6.73% vs 3.33%) and alkenes (3.49% vs 0.29%) (**Figure 1B**). In total, 13 dimethyl alkanes (46.23% of total male CHC peak area) and 12 trimethyl alkanes (6.32% of total male CHC peak area) showed a larger relative peak area when compared to wild-type females (**Table 1**). Males also showed a larger relative peak area of MB-alkanes with a carbon chain length of 30, 31, 32 and 35 C-atoms (**Figure 1C**), as well as MB-alkanes with the first methyl branch positioned on the 3rd, 5th, 6th and 7th C-atom (**Figure 1D**). Wild-type females, on the other hand, possessed a larger relative peak area of CHCs consisting of *n*-alkanes (10.19% vs 5.81%), monomethyl alkanes (39.11% vs 28.84%) and tetramethyl alkanes (1.15%) (**Figure 1B**). In total, three *n*-alkanes (9.80% of total female CHC peak area), 14 monomethyl alkanes (26.44% of total female CHC peak area) and two tetramethyl alkanes (1.04% of total female CHC peak area) showed a larger relative peak area when compared to wild-type males (**Table 1**). Females also showed a larger relative peak area of MB-alkanes with a carbon chain length of 29, 33 and 37 C-atoms (**Figure 1C**), as well as MB-alkanes with the first methyl branch positioned on the 9th, 11th, 13th, 15th and 17th C-atom (**Figure 1D**).

Silencing *NvTra* affected the relative peak area of CHCs in females when compared to the *Gfp*-i control (**Figure 1B-D**). *Tra*-i females showed an increase in the relative peak area of dimethyl alkanes (48.72% vs 40.93%), trimethyl alkanes (5.12% vs 2.87%) and alkenes (1.43% vs 0.47%), whereas *n*-alkanes (6.71% vs 9.72%), monomethyl alkanes (34.13% vs 38.54%) and tetramethyl alkanes (0.86% vs 1.52%) decreased (**Figure 1B**). In total, 15 dimethyl alkanes (34.60% of total *Tra*-i CHC peak area), 12 trimethyl alkanes (4.42% of total *Tra*-i CHC peak area) and all four alkenes (1.43% of total *Tra*-i CHC peak area) showed a larger relative peak area when compared to the *Gfp*-i control (**Table 1**). Moreover, *Tra*-i females showed an increase in the relative peak area of MB-alkanes with a carbon chain length of 30, 31, 32, 35

and 37 C-atoms, whereas MB-alkanes with a carbon chain length of 29 and 33 C-atoms decreased (**Figure 1C**). *Tra*-i females also showed an increase in MB-alkanes with the first methyl branch positioned on the 5th, 6th and 7th C-atom (**Figure 1D**). However, MB-alkanes with the first methyl branch positioned on the 3rd, 9th, 11th, 13th, 15th and 17th C-atom decreased (**Figure 1D**). In the following section, we present the results of the multivariate analyses that show significant differences in the relative composition of CHCs between our four treatment groups.

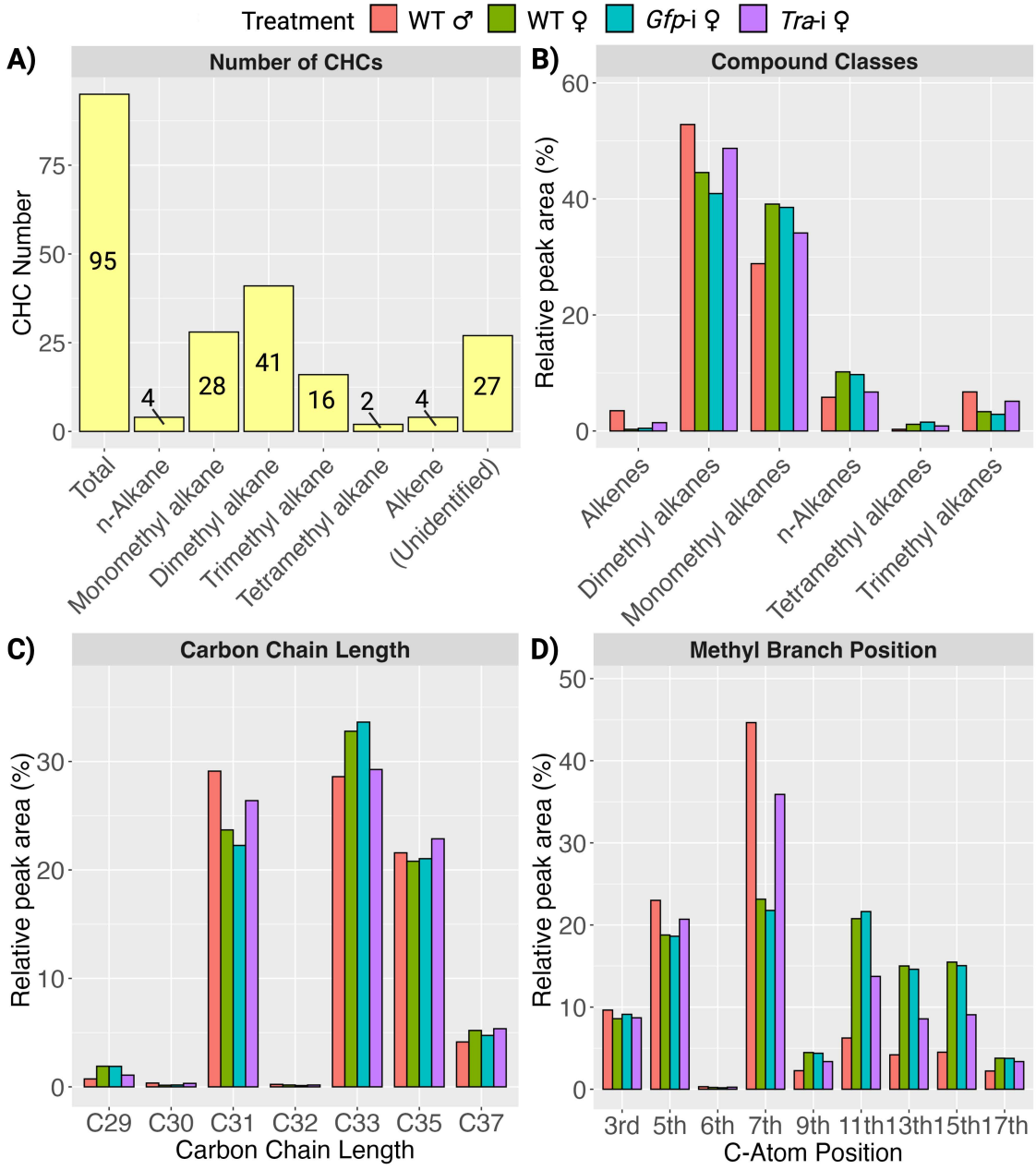

Figure 1: Relative peak area of identified CHCs in our four treatment groups.
We calculated the mean relative peak area for each CHC to determine differences in the CHC relative peak areas between the treatment groups. Relative peak areas were calculated by dividing individual CHC peak areas by the total CHC peak area. **A:** Number of individual CHC compounds identified by the GC-MS analysis. **B:** Relative peak area (in %) of the CHC classes in the treatment groups. **C:** Relative peak area of CHCs based on the carbon chain length. **D:** Relative peak area of MB-alkanes based on the C-atom position of the first methyl branch.

Table 1: Mean and standard deviation of CHC relative peak area (in %) in wild-type (WT) males, wild-type females, *Gfp*-i females and *Tra*-i females.

CHCs were identified according to their Linear Retention Index (LRI) and diagnostic ions. Relative peak areas were calculated by dividing individual CHC peak areas by the total CHC peak area. Only the peaks that contributed > 0.1% to the total peak area within a treatment group are listed. The letter *x* denotes that the methyl-group position could not be determined due to low abundance of the compound.

Peak	LRI	Compound Name	Diagnostic Ions	CHC Relative Peak Area (%)			
				WT ♂	WT ♀	*Gfp*-i ♀	*Tra*-i ♀
1	**2900**	C29	408	0.34 ± 0.08	1.74 ± 0.11	1.68 ± 0.14	0.58 ± 0.07
2	**2931**	11-MeC29	407 (M-15), 168/169, 280/281	0.01 ± 0.01	0.12 ± 0.01	0.17 ± 0.02	0.04 ± 0.01
3	**2933**	9-MeC29	407 (M-15), 140/141, 308/309	0.04 ± 0.01	0.09 ± 0.01	0.09 ± 0.01	0.03 ± 0.00
4	**2939**	7-MeC29	407 (M-15), 112/113, 336/337	0.38 ± 0.10	1.22 ± 0.07	1.16 ± 0.06	0.66 ± 0.06
5	**2948**	5-MeC29	407 (M-15), 84/85, 364/365	0.14 ± 0.03	0.28 ± 0.01	0.25 ± 0.02	0.19 ± 0.02
6	**2972**	3-MeC29	393 (M-29)	0.02 ± 0.01	0.05 ± 0.00	0.09 ± 0.02	0.03 ± 0.01
7	**2977**	7,x-DiMeC29	421 (M-15), 112/113, 350/351	0.14 ± 0.03	0.14 ± 0.01	0.13 ± 0.02	0.13 ± 0.01
8	**3000**	C30	422	0.21 ± 0.03	0.45 ± 0.05	0.46 ± 0.02	0.31 ± 0.02
9	**3039**	7-MeC30	422 (M-15), 112/113, 350/351	0.27 ± 0.04	0.10 ± 0.01	0.11 ± 0.01	0.25 ± 0.02
10	**3043**	6-MeC30	422 (M-15), 98/99, 364/365	0.07 ± 0.01	0.05 ± 0.00	0.06 ± 0.01	0.08 ± 0.01
11	**3074**	Unidentified1		0.10 ± 0.02	0.07 ± 0.00	0.08 ± 0.00	0.08 ± 0.01
12	**3081**	Z9C31	434	2.01 ± 0.49	0.04 ± 0.01	0.12 ± 0.08	0.56 ± 0.08
13	**3089**	Z7C31	434	0.33 ± 0.08	0.06 ± 0.01	0.08 ± 0.04	0.16 ± 0.02
14	**3100**	C31	436	4.67 ± 0.59	7.61 ± 0.35	7.23 ± 0.31	5.16 ± 0.19
15	**3104**	Unidentified2		0.07 ± 0.01	0.12 ± 0.01	0.10 ± 0.02	0.11 ± 0.01
16	**3126**	15-+13-MeC31	435 (M-15), 224/225, 252/253, 196/197, 280/281	0.28 ± 0.04	1.38 ± 0.04	1.45 ± 0.15	0.89 ± 0.06
17	**3128**	11-MeC31	435 (M-15), 168/169, 308/309	0.40 ± 0.04	2.17 ± 0.05	2.28 ± 0.08	1.48 ± 0.06
18	**3132**	9-MeC31	435 (M-15), 140/141, 336/337	0.99 ± 0.12	1.29 ± 0.04	1.19 ± 0.08	1.24 ± 0.04
19	**3137**	7-MeC31	435 (M-15), 112/113, 364/365	9.70 ± 0.59	4.74 ± 0.21	4.46 ± 0.38	7.92 ± 0.54
20	**3146**	5-MeC31	435 (M-15), 84/85, 392/393	3.85 ± 0.14	2.89 ± 0.09	2.54 ± 0.12	3.59 ± 0.11
21	**3150**	Unidentified3		0.15 ± 0.05	0.62 ± 0.04	0.74 ± 0.03	0.34 ± 0.02
22	**3157**	Unidentified4		0.20 ± 0.03	0.59 ± 0.07	0.61 ± 0.02	0.45 ± 0.01
23	**3161**	7,11-DiMeC31	449 (M-15), 112/113, 378/379, 182/183, 308/309	1.13 ± 0.10	1.21 ± 0.09	1.16 ± 0.08	1.28 ± 0.04
24	**3163**	7,x-DiMeC31	449 (M-15), 112/113, 378/379	0.45 ± 0.08	0.73 ± 0.20	0.39 ± 0.03	0.46 ± 0.03
25	**3167**	7,19-DiMeC31	449 (M-15), 112/113, 378/379, 196/197, 294/295	0.67 ± 0.29	0.86 ± 0.10	0.61 ± 0.07	0.55 ± 0.03
26	**3169**	7,21-DiMeC31	449 (M-15), 112/113, 378/379, 168/169, 322/323	3.50 ± 0.31	1.65 ± 0.10	1.44 ± 0.13	1.90 ± 0.07
27	**3175**	3-MeC31+ 7,23-DiMeC31	449 (M-15), 435 (M-15), 421 (M-29), 112/113, 378/379, 140/141, 350/351	3.95 ± 0.28	3.45 ± 0.17	3.59 ± 0.11	3.37 ± 0.07
28	**3180**	5,9-+7,25-DiMeC31	449 (M-15), 84/85, 406/407, 154/155, 336/337, 112/113, 378/379 (sym)	0.62 ± 0.07	0.45 ± 0.03	0.40 ± 0.04	0.48 ± 0.02
29	**3185**	5,25-DiMeC31	449 (M-15), 84/85, 406/407, 112/113, 378/379	1.05 ± 0.09	0.33 ± 0.02	0.30 ± 0.04	0.64 ± 0.02
30	**3188**	Unidentified5		0.18 ± 0.03	0.18 ± 0.02	0.13 ± 0.02	0.21 ± 0.01
31	**3193**	Unidentified6		0.13 ± 0.03	0.14 ± 0.02	0.08 ± 0.01	0.15 ± 0.01
32	**3200**	3,15-DiMeC31	449 (M-15), 435 (M-29), 238/239, 252/253	0.52 ± 0.02	0.77 ± 0.04	0.71 ± 0.04	0.68 ± 0.02

33	**3205**	3,7-DiMeC31	449 (M-15), 435 (M-29), 126/127, 364/365	1.06 ± 0.05	0.39 ± 0.05	0.30 ± 0.02	0.74 ± 0.03
34	**3212**	Unidentified7		0.15 ± 0.02	0.14 ± 0.08	0.01 ± 0.00	0.13 ± 0.01
35	**3228**	3,x,x-TriMeC31 A	463 (M-15), 449 (M-29), 126/127, 378/379	0.30 ± 0.03	0.68 ± 0.06	0.74 ± 0.04	0.48 ± 0.03
36	**3233**	3,x,x-TriMeC31 B	463 (M-15), 449 (M-29)	0.30 ± 0.03	0.12 ± 0.01	0.14 ± 0.01	0.21 ± 0.01
37	**3236**	3,x,x-TriMeC31 C	463 (M-15), 449 (M-29)	0.22 ± 0.01	0.05 ± 0.01	0.04 ± 0.00	0.12 ± 0.01
38	**3240**	6-MeC32	449 (M-15), 98/99, 392/393	0.23 ± 0.03	0.17 ± 0.04	0.12 ± 0.01	0.17 ± 0.02
39	**3246**	3,7,11,15-TetraMeC31	477 (M-15), 463 (M-29), 126/127, 392/393, 196/197, 322/323, 266/267, 252/253	0.11 ± 0.02	0.53 ± 0.05	0.55 ± 0.03	0.36 ± 0.02
40	**3255**	Unidentified8		0.05 ± 0.02	0.18 ± 0.02	0.07 ± 0.02	0.12 ± 0.01
41	**3262**	Unidentified9		0.14 ± 0.02	0.14 ± 0.01	0.10 ± 0.02	0.14 ± 0.01
42	**3266**	Unidentified10		0.19 ± 0.02	0.05 ± 0.00	0.04 ± 0.00	0.14 ± 0.02
43	**3273**	Unidentified11		0.13 ± 0.02	0.05 ± 0.00	0.07 ± 0.01	0.10 ± 0.01
44	**3281**	Z9C33	462	0.57 ± 0.11	0.10 ± 0.01	0.17 ± 0.03	0.33 ± 0.04
45	**3289**	Z7C33	462	0.59 ± 0.08	0.09 ± 0.01	0.11 ± 0.04	0.38 ± 0.03
46	**3293**	Unidentified12		0.13 ± 0.04	0.01 ± 0.01	0.01 ± 0.00	0.02 ± 0.00
47	**3300**	C33	464	0.60 ± 0.12	0.39 ± 0.02	0.35 ± 0.01	0.65 ± 0.05
48	**3324**	15-MeC33 + 13-MeC33	463 (M-15), 224/225, 280/281, 196/197, 308/309	1.39 ± 0.12	6.02 ± 0.10	5.67 ± 0.16	2.88 ± 0.11
49	**3327**	11-MeC33	463 (M-15), 168/169, 337/338	1.02 ± 0.10	2.37 ± 0.09	2.28 ± 0.08	1.60 ± 0.06
50	**3331**	9-MeC33	463 (M-15), 140/141, 364/365	0.44 ± 0.05	0.39 ± 0.01	0.42 ± 0.03	0.58 ± 0.03
51	**3336**	7-MeC33	463 (M-15), 112/113, 392/393	1.62 ± 0.15	0.84 ± 0.03	0.79 ± 0.04	1.96 ± 0.11
52	**3346**	5-MeC33	463 (M-15), 84/85, 420/421	0.84 ± 0.09	4.97 ± 0.11	5.36 ± 0.21	2.01 ± 0.07
53	**3353**	11,21-DiMeC33	479 (M-14), 168/169, 350/351, 196/197, 322/323	0.59 ± 0.09	3.33 ± 0.10	3.35 ± 0.15	1.75 ± 0.09
54	**3356**	9,23-DiMeC33	479 (M-14), 140/141, 378/379, 168/169, 350/351	0.79 ± 0.05	2.70 ± 0.09	2.67 ± 0.09	1.52 ± 0.05
55	**3360**	7,21-+7,19-DiMeC33	477 (M-15), 112/113, 406/407, 196/197, 322/323, 224/225, 294/295	3.36 ± 0.11	2.61 ± 0.04	2.65 ± 0.07	2.83 ± 0.05
56	**3365**	7,23-DiMeC33	477 (M-15), 112/113, 406/407, 168/169, 350/351	5.37 ± 0.29	1.66 ± 0.03	1.63 ± 0.04	3.76 ± 0.13
57	**3372**	5,19-+5,17-DiMeC33	477 (M-15), 84/85, 435/436, 252/253, 266/267, 224/225, 294/295	5.25 ± 0.32	3.10 ± 0.10	3.32 ± 0.10	4.08 ± 0.10
58	**3374**	5,9-DiMeC33	477 (M-15), 84/85, 435/436, 154/155, 364/365	2.16 ± 0.26	1.59 ± 0.07	1.83 ± 0.08	2.03 ± 0.07
59	**3378**	Unidentified13		0.83 ± 0.10	0.72 ± 0.03	0.80 ± 0.04	0.73 ± 0.03
60	**3386**	11,15,23-TriMeC33	491 (M-15), 168/169, 364/365, 238/239, 294/295,	0.45 ± 0.05	0.20 ± 0.01	0.24 ± 0.02	0.30 ± 0.02
61	**3389**	7,11,23-TriMeC33	491 (M-15), 112/113, 420/421, 182/183, 350/351, 168/169, 364/365	0.53 ± 0.07	0.18 ± 0.01	0.16 ± 0.01	0.34 ± 0.02
62	**3400**	3,15-DiMeC33	477 (M-15), 463 (M-29), 280/281, 266/267	2.04 ± 0.19	1.25 ± 0.05	1.43 ± 0.07	1.48 ± 0.04
63	**3402**	5,9,21-TriMeC33	491 (M-15), 84/85, 449, 154/155, 378/379, 196/197, 336/337	1.22 ± 0.10	0.21 ± 0.02	0.23 ± 0.02	0.67 ± 0.02
64	**3405**	5,9,25-TriMeC33	491 (M-15), 84/85, 449, 154/155, 378/379, 140/141, 392/393	0.41 ± 0.05	0.07 ± 0.01	0.05 ± 0.01	0.25 ± 0.02
65	**3426**	3,11,x-TriMeC33	477 (M-29), 182/183, 350/351	0.11 ± 0.02	0.36 ± 0.02	0.27 ± 0.02	0.21 ± 0.01
66	**3428**	3,7,17-+3,7,19-+3,7,21-TriMeC33	477 (M-29), 126/127, 406/407	0.62 ± 0.04	0.30 ± 0.02	0.30 ± 0.02	0.40 ± 0.01
67	**3432**	3,7,23-TriMeC33	477 (M-29), 126/127, 406/407, 168/169, 364/365	0.21 ± 0.02	0.02 ± 0.00	0.02 ± 0.00	0.10 ± 0.01

68	**3444**	3,7,11,15-TetraMeC33	505 (M-15), 491 (M-29), 126/127, 420/421, 196/197, 350/351, 266/267, 280/281	0.18 ± 0.03	0.62 ± 0.03	0.96 ± 0.03	0.51 ± 0.04
69	**3446**	Unidentified14		0.12 ± 0.03	0.35 ± 0.01	0.33 ± 0.02	0.21 ± 0.02
70	**3452**	Unidentified15		0.10 ± 0.03	0.27 ± 0.01	0.24 ± 0.01	0.17 ± 0.02
71	**3464**	Unidentified16		0.13 ± 0.02	0.08 ± 0.01	0.11 ± 0.01	0.13 ± 0.01
72	**3466**	Unidentified17		0.26 ± 0.04	0.03 ± 0.00	0.02 ± 0.00	0.24 ± 0.02
73	**3468**	Unidentified18		0.11 ± 0.02	0.04 ± 0.00	0.04 ± 0.00	0.10 ± 0.00
74	**3495**	Unidentified19		0.15 ± 0.02	0.03 ± 0.00	0.03 ± 0.00	0.09 ± 0.01
75	**3523**	17-+15-+13-+11-MeC35	491 (M-15), 252/253 (sym), 280/281, 224/225, 308/309, 196/197, 336/337, 168/169, 364/365	1.91 ± 0.14	3.31 ± 0.09	3.32 ± 0.11	2.88 ± 0.11
76	**3535**	7-MeC35	491 (M-15), 112/113, 420/421	0.18 ± 0.04	0.05 ± 0.00	0.04 ± 0.00	0.26 ± 0.02
77	**3543**	15,19-+13,17-DiMeC35	505 (M-15), 224/225, 322/323, 252/253, 294/295, 196/197, 350/351, 266/267, 280/281	0.30 ± 0.04	2.52 ± 0.09	2.42 ± 0.13	0.91 ± 0.07
78	**3546**	11,15-DiMeC35	505 (M-15), 168/169, 378/379, 238/239, 308/309	0.83 ± 0.08	4.36 ± 0.10	4.94 ± 0.22	2.66 ± 0.14
79	**3549**	11,19-+11,21-DiMeC35	505 (M-15), 168/169, 378/379, 224/225, 322/323, 196/197, 350/351	0.78 ± 0.09	3.17 ± 0.16	3.27 ± 0.12	1.86 ± 0.08
80	**3559**	7,19-+7,21-+7,23-DiMeC35	505 (M-15), 112/113, 434/435, 252/253, 294/295, 224/225, 322/323, 196/197, 350/351	9.36 ± 0.53	2.48 ± 0.05	2.45 ± 0.03	6.98 ± 0.23
81	**3569**	5,17-+5,19-+5,21-+5,23-DiMeC35	505 (M-15), 84/85, 462/463, 196/197, 350/351, 224/225, 322/323, 252/253, 294/295, 266/267, 280/281	5.88 ± 0.46	3.79 ± 0.11	3.89 ± 0.10	5.29 ± 0.13
82	**3581**	7,15,x-TriMeC35 A	519 (M-15), 112/113, 449/450, 238/239, 322/323	1.02 ± 0.14	0.41 ± 0.02	0.34 ± 0.03	0.78 ± 0.02
83	**3583**	7,15,x-TriMeC35 B	519 (M-15), 112/113, 449/450, 238/239, 322/323	0.37 ± 0.08	0.30 ± 0.02	0.19 ± 0.03	0.48 ± 0.01
84	**3591**	5,9,x-TriMeC35 A	519 (M-15), 84/85, 476/477, 254/155, 406/407	0.24 ± 0.09	0.20 ± 0.01	0.09 ± 0.03	0.29 ± 0.01
85	**3596**	5,9,x-TriMeC35 B	519 (M-15), 84/85, 476/477, 254/155, 406/407	0.73 ± 0.17	0.22 ± 0.02	0.08 ± 0.02	0.47 ± 0.03
86	**3596**	Unidentified20		0.63 ± 0.20	0.22 ± 0.02	0.25 ± 0.03	0.61 ± 0.08
87	**3610**	Unidentified21		0.05 ± 0.02	0.11 ± 0.01	0.11 ± 0.01	0.06 ± 0.00
88	**3626**	Unidentified22		0.18 ± 0.06	0.04 ± 0.00	0.04 ± 0.01	0.09 ± 0.01
89	**3640**	Unidentified23		0.09 ± 0.02	0.11 ± 0.01	0.13 ± 0.01	0.13 ± 0.00
90	**3643**	Unidentified24		0.12 ± 0.02	0.39 ± 0.02	0.45 ± 0.02	0.30 ± 0.01
91	**3658**	Unidentified25		0.09 ± 0.03	0.05 ± 0.01	0.04 ± 0.00	0.16 ± 0.01
92	**3663**	Unidentified26		0.30 ± 0.04	0.08 ± 0.01	0.08 ± 0.01	0.25 ± 0.02
93	**3692**	Unidentified27		0.15 ± 0.02	0.02 ± 0.00	0.01 ± 0.00	0.08 ± 0.01
94	**3727**	17-+15-MeC37	519 (M-15), 252/253, 322/323, 224/225, 350/351	0.32 ± 0.03	0.48 ± 0.01	0.44 ± 0.03	0.49 ± 0.03
95	**3752**	15,19-+13,17-DiMeC37	533 (M-15), 224/225, 322/323, 294/295, 252/253, 196/197, 350/351, 266/267, 280/281	0.31 ± 0.05	1.77 ± 0.05	1.75 ± 0.06	1.02 ± 0.06
96	**3754**	11,15-DiMeC37	533 (M-15), 168/169, 406/407, 238/239, 336/337	0.27 ± 0.05	1.75 ± 0.04	1.79 ± 0.09	1.17 ± 0.05
97	**3770**	7,19-+7,21-+7,23-DiMeC37	533 (M-15), 112/113, 462/463, 224/225, 350/351, 252/253, 322/323, 280/281, 294/295	2.62 ± 0.17	0.51 ± 0.02	0.47 ± 0.02	1.99 ± 0.10
98	**3782**	5,15-+5,17-+5,21-DiMeC37	533 (M-15), 84/85, 490/491, 336/337, 238/239, 308/309, 266/267, 252/253, 322/323	0.61 ± 0.06	0.69 ± 0.03	0.30 ± 0.03	0.69 ± 0.05

Multivariate analyses of the relative composition of CHCs

We performed a square-root transformation on the relative CHC peak areas prior to multivariate analyses. The NMDS analysis visualized the four CHC profiles of our four treatment groups (**Supplementary Figure 1**). The CHC profiles of *Gfp*-i and wild-type females clearly clustered together, indicating their high degree of similarity and the effectiveness of the *Gfp*-i treatment as a control. The CHC profile of *Tra*-i females, on the other hand, was positioned between the CHC profiles of wild-type males and *Gfp*-i females. The ANOSIM revealed a significant difference between the CHC profiles identified by the NMDS analysis ($R = 1$, $p < 0.001$), except between the CHC profiles of wild-type females and *Gfp*-i females ($R = 0.308$, $p < 0.01$) (**Supplementary Table 2**). We then conducted a SIMPER analysis on the square-root transformed data to calculate the average contribution of CHC compounds to the Bray-Curtis dissimilarity between the CHC profiles of wild-type males and wild-type females, and between *Gfp*-i females and *Tra*-i females (**Supplementary Table 3**). Square-root transformed data was used to include compounds that occur in low abundances, as these can also be important infochemicals. We analysed the CHCs that contributed most (with a cut-off set at 50%) to the Bray-Curtis dissimilarity between the various treatment groups so that those compounds that contributed least were excluded.

We first compared wild-type males to wild-type females and identified 20 CHC peaks (representing 29 compounds) contributing the most (cumulatively 50.78%) to the Bray-Curtis dissimilarity (23.54%) between the CHC profiles of these specimens (**Figure 2A, Supplementary Table 3**). The SIMPER analysis showed that the CHC compounds contributing more than 1% to the average dissimilarity included two alkanes (cumulatively 3.57%), seven monomethyl alkanes (13.58%), 18 dimethyl alkanes (28.54%), one trimethyl alkane (1.78%) and one alkene (3.31%). Dimethyl alkanes contributed the most (cumulatively 28.54%) to the average dissimilarity between the wild-type specimens. Eight compounds contributed more than 3% to the average dissimilarity, including four dimethyl alkanes (7,19-/7,21-/7,23-DiMeC35 and 11,15-DiMeC35), three monomethyl alkanes (5-/13-/15-MeC33) and one alkene (Z9-C31ene). These results confirm that MB-alkanes, and in particular dimethyl alkanes, are the compounds predominantly responsible for sexual dimorphism in the CHC profile between wild-type males and wild-type females.

We subsequently compared *Tra*-i females to *Gfp*-i females and identified 23 CHC peaks (representing 34 compounds) contributing the most (cumulatively 50.98%) to the Bray-Curtis dissimilarity (14.93%) between the CHC profiles of these specimens (**Figure 2B, Supplementary Table 3**). The CHC compounds contributing more than 1% to the average dissimilarity included two alkanes (cumulatively 4.04%), six monomethyl alkanes (13.24%), 21 dimethyl alkanes (25.37%), two trimethyl alkanes (3.25%), two alkenes (3.51%) and one unidentified compound (1.57%). Eight compounds contributed more than 3% to the average dissimilarity, including six dimethyl alkanes (7,19-/7,21-/7,23-DiMeC35 and 7,19-/7,21-/7,23-DiMeC37) and two monomethyl alkanes (7-MeC31 and 5-MeC33). The comparison between

Tra-i females and *Gfp*-i females identified 16 CHC peaks (representing 24 compounds) that also contributed the most to the average dissimilarity between wild-type males and wild-type females. These CHC compounds included two alkanes (C29, C31), four monomethyl alkanes (7-MeC31, 5-MeC33, 13-/15-MeC33), 16 dimethyl alkanes (7,23-DiMeC33, 9,23-DiMeC33, 11,21-DiMeC33, 7,19-/7,21-/7,23-DiMeC35, 11,15-DiMeC35, 11,19-/11,21-DiMeC35, 13,17-/15,19-DiMeC35, 7,19-/7,21-/7,23-DiMeC37, 13,17-/15,19-DiMeC37), one trimethyl alkane (5,9,21-TriMeC33) and one alkene (Z9-C31ene). The results of the SIMPER analysis confirm that *NvTra* plays an important role in regulating sexual differences in the relative composition of CHC compounds and therefore sexual dimorphism in the CHC profile. We propose that the compounds we identified have a sex-specific function in pheromone communication in *Nasonia vitripennis.*

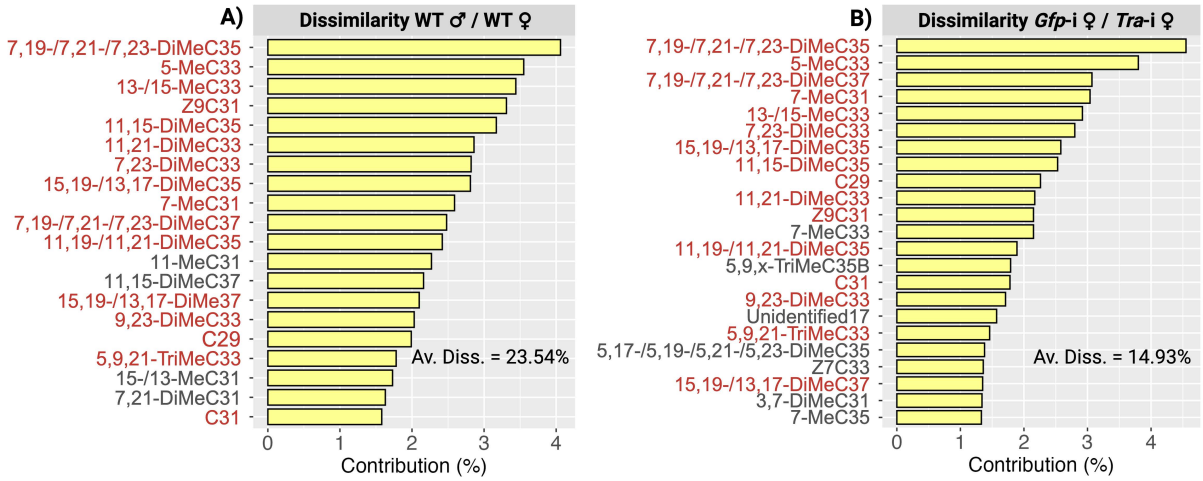

Figure 2: One-way SIMPER analysis on pair-wise comparisons of the four treatment groups.
The SIMPER analysis calculated the average dissimilarity in the relative peak area of each CHC substance and the contribution of each CHC peak to the average Bray-Curtis dissimilarity between the treatment groups. Bar graphs show the average contribution of each CHC peak in percentages to the average Bray-Curtis dissimilarity (Av. Diss.) between the CHC profiles of wild-type (WT) males and wild-type females (**A**), and *Gfp*-i females and *Tra*-i females (**B**). The compounds highlighted in red contributed to the average dissimilarity in both pair-wise comparisons. A 50% cut-off was set to exclude CHC compounds that contributed least to the average dissimilarity.

Silencing *NvTra* changes alkene absolute quantities

Previous research has shown that the alkenes Z7-C31ene, Z7-C33ene, Z9-C31ene and Z9-C33ene function as close-range pheromones in *N. vitripennis* to inhibit male-male courtship and are upregulated in males by NvDSX (Wang *et al*., 2022b). We therefore hypothesized that silencing *NvTra* would result in the upregulation of absolute alkene quantities in females. We related each alkene to the internal standard to determine the absolute quantities (**Supplementary Table 4**). We confirmed a significant difference in the total alkene absolute quantity between wild-type males and wild-type females (**Figure 3A**; Wilcoxon rank-sum test, $W = 0$, $p < 0.001$). Wild-type males produce significantly larger quantities of all four identified alkenes (**Figure 3B-3E**; Wilcoxon rank-sum test, $p < 0.001$). We then calculated the absolute

quantities of these alkenes in *Tra*-i females and compared these to wild-type females and *Gfp*-i females. Our results showed that *Tra*-i females possess a significantly larger total alkene absolute quantity (**Figure 3A**; Wilcoxon rank-sum test, W = 3, p < 0.001), as well as a larger absolute quantity of each of the four alkenes (**Figure 3B-3E**; Wilcoxon rank-sum test, p < 0.001), similar to the absolute quantities in wild-type males. Our results therefore confirm that *NvTra* plays an essential role in suppressing alkene production in female *N. vitripennis*, which is necessary for mate-recognition for males.

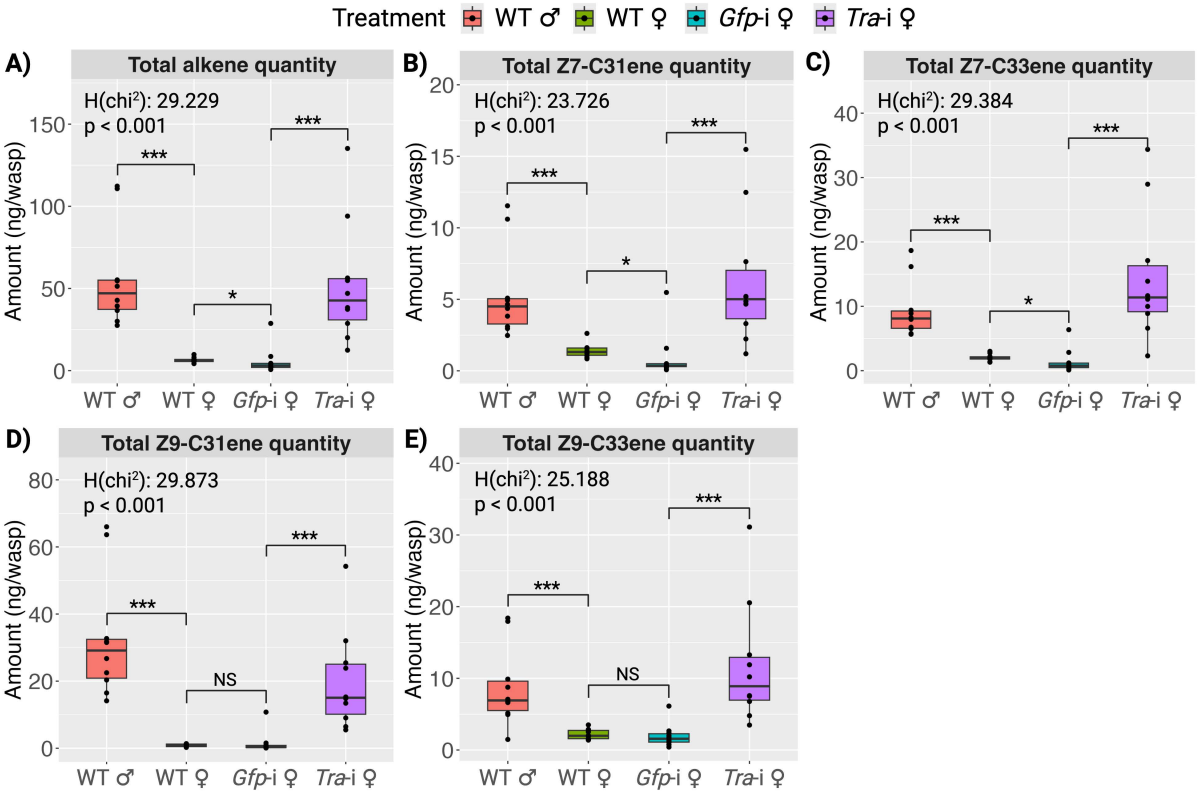

Figure 3: Changes in absolute quantity of alkenes after silencing *NvTra* in female *N. vitripennis*.
Absolute quantities are shown in boxplots for the total amount of alkenes (**A**) and the alkene compounds Z7-C31ene (**B**), Z7-C33ene (**C**), Z9-C31ene (**D**) and Z9-C33ene (**E**), after silencing *NvTra* in female *N. vitripennis*. *Gfp*-i females were used as a control group. The boxplots show the median (horizontal line), 25-75% quartiles (box), maximum/minimum range (whiskers) and outliers. Significant differences between groups were assessed with a Kruskal-Wallis H test. Pair-wise comparisons were assessed with Bonferroni-corrected Wilcoxon rank-sum tests. Significance levels: *** = p < 0.001, * = p < 0.05 and NS = not significant.

Silencing *NvTra* in females affects mating behaviour

We hypothesized that silencing *NvTra* in females would impact male mating behaviour. To verify this, we conducted a behavioural assay in which we quantified male mating behaviour in response to live *Tra*-i females (**Supplementary Table 5**). Wild-type males normally respond to female CHCs by mounting females, performing courtship to make the female sexually receptive and then attempting to copulate with them. We first exposed live females to virgin wild-type males and observed the duration of male mating behaviour: the time spent searching, mounting, copulating and performing post-copulatory courtship. We determined

the duration of male mating behaviour in response to live virgin *Tra*-i females (n = 17), using live virgin *Gfp*-i females (n = 19) as a control (**Figure 4A**). Males spent more time searching for the *Tra*-i females compared to searching for the *Gfp*-i control females (Wilcoxon rank-sum test, Z = −1.9271, p = 0.05). It is interesting to note that whereas 100% of males successfully mounted *Gfp*-i females, they were less successful (58%) when attempting to mount a *Tra*-i female within the five-minute observation period. Importantly, *Tra*-i females clearly showed a flight response to the mounting attempts of males. We also found that the duration of mounting and courtship was significantly longer with the *Tra*-i females (Wilcoxon rank-sum test, Z = −2.2942, p < 0.05). After the experiment, we calculated the mating success rate as the percentage of males that completed all stages of mating behaviour (searching, mounting, copulating and post-copulatory courtship) (**Figure 4B**). Of all the males that successfully mounted (58%) a *Tra*-i female, only one male specimen succeeded in completing all stages of mating behaviour (Pearson's Chi-squared test, χ^2 = 24.969, p < 0.001). The remaining male specimens failed to arrest the *Tra*-i females, which exhibited rejection behaviour and impeded successful courtship. These results demonstrate that silencing *NvTra* induces significant behavioural changes in females.

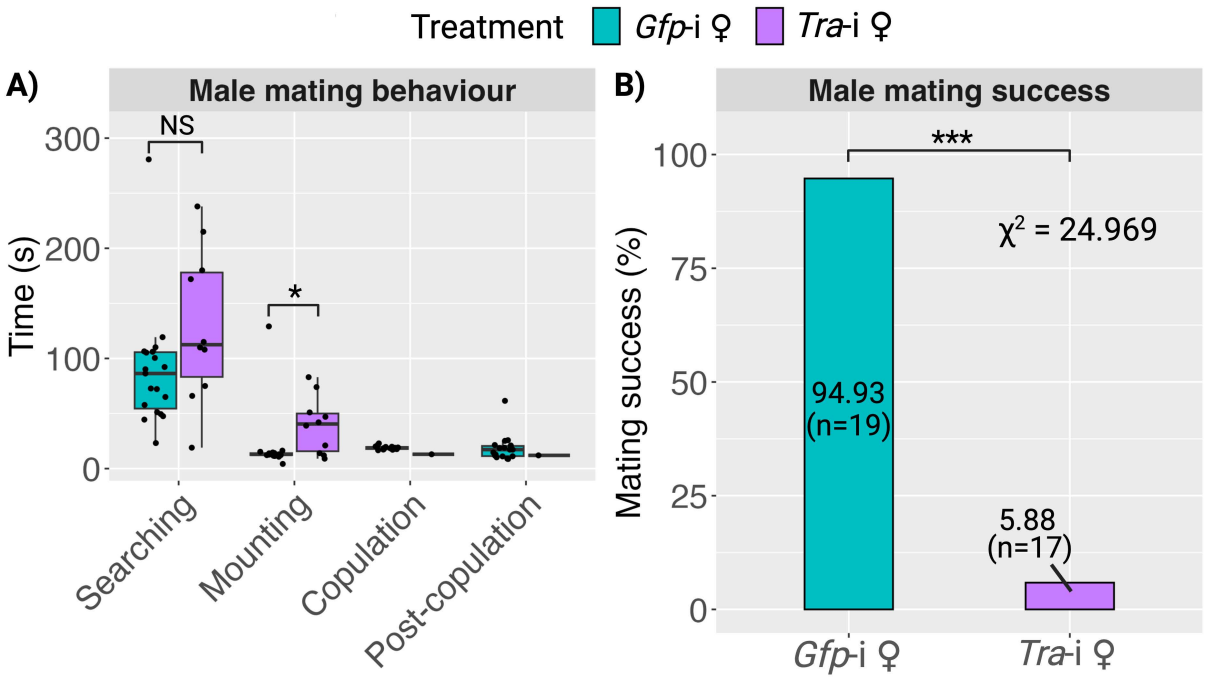

Figure 4: Male mating behaviour in response to live *Gfp*-i and *Tra*-i females.
A-B: Live virgin *Gfp*-i and *Tra*-i females were introduced to virgin wild-type males in a glass vial for a duration of five minutes. **A:** The duration wild-type males spent searching, mounting, copulating and performing post-copulatory courtship when exposed to *Gfp*-i and *Tra*-i females. Pair-wise comparisons were assessed with Bonferroni-corrected Wilcoxon rank-sum tests. Significance levels: * = p < 0.05 and NS = not significant. **B:** Mating success was calculated as the percentage of males that completed all stages of mating behaviour. Significant differences in mating success were assessed with a Pearson's Chi-squared test. Significance levels: *** = p < 0.001.

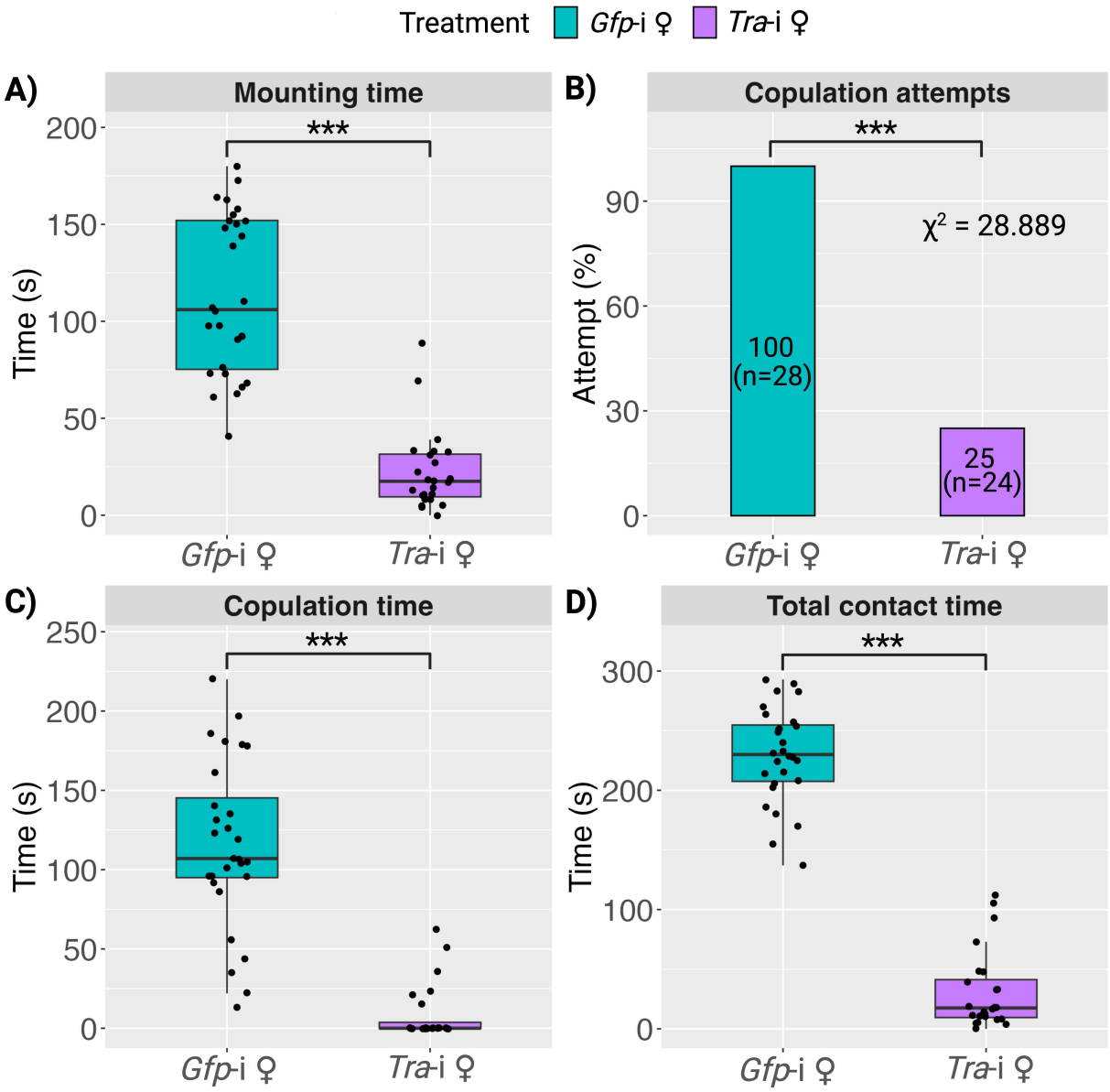

Figure 5: Male mating behaviour in response to dead *Gfp*-i and *Tra*-i females.
A-D: Dead virgin *Gfp*-i and *Tra*-i females were introduced to virgin wild-type males in a mating chamber bioassay for a duration of five minutes. **A:** The cumulative amount of time males spent mounting the *Gfp*-i and *Tra*-i females. **B:** The percentage of males attempting to copulate with these specimens. **C:** The cumulative copulation duration. **D:** The total time males spent mounting and copulating the female specimens. Significant differences in mounting and copulation duration were analysed with a Wilcoxon rank-sum test. Significant differences in the percentage of males attempting to copulate were analysed with a Pearson's Chi-squared test. Significance levels: *** = $p < 0.001$.

We also hypothesized that the changes we identified in the CHC profile of *Tra*-i females would impact male mating behaviour. To verify this, we conducted a behavioural assay in which we quantified male mating behaviour in response to dead *Tra*-i females (**Supplementary Table 6**). We exposed dead females (dummies) to virgin wild-type males to observe the duration of male mating behaviour specifically in response to CHCs and to minimize other potential mating signals (e.g. behavioural or vibrational signals). We determined the cumulative time

males spent mounting and copulating in response to virgin *Tra*-i female dummies (n = 24), using *Gfp*-i female dummies (n = 28) as a control. We found that the cumulative time males spent mounting *Tra*-i female dummies was significantly shorter than with *Gfp*-i female dummies (**Figure 5A**; Wilcoxon rank-sum test, $Z = 5.9304$, $p < 0.001$). This in turn resulted in a significantly lower percentage of males attempting to copulate with *Tra*-i female dummies (25%) compared to *Gfp*-i female dummies (100%) (**Figure 5B**; Pearson's Chi-squared test, $\chi^2 = 28.889$, $p < 0.001$). We also observed a significantly lower copulation duration with these *Tra*-i female dummies (**Figure 5C**; Wilcoxon rank-sum test, $Z = 5.9998$, $p < 0.001$). Overall, the total time males spent mounting and copulating was significantly shorter for all *Tra*-i specimens (**Figure 5D**; Wilcoxon rank-sum test, $Z = 6.1684$, $p < 0.001$). These results indicate that NvTRA regulates the production of those CHCs in females that are integral to male mating behaviour.

Discussion

The sex-determination pathway plays a key role in regulating the production of sexually dimorphic CHCs in insects (Chertemps *et al*., 2006, 2007; Ferveur *et al*., 1997; Jallon *et al*., 1988; Sun *et al*., 2023a; Tompkins & McRobert, 1989, 1995; Waterbury *et al*., 1999). These long-chain carbon chemicals are utilized by insects for close-range sexual communication (Chung *et al*., 2014; Chung & Carroll, 2015). Transformer (TRA) is a conserved splicing factor in the sex-determination pathway and has been shown to regulate sexually dimorphic CHC production (Savarit & Ferveur, 2002). Research on the way in which this specific splicing factor regulates CHC production has been limited to the model species *Drosophila melanogaster*. It would therefore be beneficial to investigate how sex determination influences the evolution of CHC sexual dimorphism in insects that use a different pheromone-coding system, such as Hymenoptera. In this chapter, we established the function of TRA in regulating sexual dimorphism in the CHC profile of the parasitoid wasp *Nasonia vitripennis*.

We successfully used dsRNA to silence *NvTra* expression in female *N. vitripennis.* We were able to establish that silencing *NvTra* masculinized the CHC profile of females by shifting the relative composition of CHCs from a female-specific to a male-like phenotype. This was particularly the case in the composition of dimethyl alkanes. Our results also corroborate previous research that showed that sex-determination transcription factors regulate alkene biosynthesis in males, which is necessary for inhibiting male-male courtship (Wang *et al*., 2022b). Masculinization of the female CHC profile also affected male mating behaviour, as demonstrated in the decreased duration males spent mounting and attempting to copulate with the silenced females. Silencing *NvTra* also masculinized the behaviour of females, which clearly rejected the mounting and courtship attempts of males. Moreover, these results support our findings in **Chapter 3**, where we established the role of *NvTra* in regulating female-specific neural circuits and the perception of male pheromones.

We determined that *Tra* is involved in the genetic regulation of sexually dimorphic CHC production in *N. vitripennis*. In *Drosophila*, *Tra* is expressed in adult female oenocytes to regulate *Dsx*, which in turn upregulates the expression of its downstream target *DesatF* (Chertemps *et al*., 2006). This results in feminization of the CHC profile and the production of the female-specific diene pheromones 7,11-HD and 7,11-ND that elicit courtship behaviour in males (Chertemps *et al*., 2006; Ferveur, 1997). Knocking down *Tra* in female oenocytes, however, masculinized the CHC profile and this triggered male-female aggression in *Drosophila* (Fernández *et al*., 2010). *Fruitless* (*Fru*), on the other hand, was shown not to be responsible for regulating sexually dimorphic CHCs, but rather for maintaining overall CHC production (Sun *et al*., 2023a). However, the specific functions of DSX and FRU in regulating CHC biosynthesis in Hymenoptera remain unknown. It would therefore be apposite to investigate the specific role of *Dsx* and *Fru* in CHC biosynthesis in *N. vitripennis*. The upregulation of biosynthetic genes by DSX for alkene production has already been confirmed in this species (Wang *et al*., 2022b). *Doublesex* is therefore an important candidate for

investigating the genetic regulation of the sexually dimorphic CHCs that we identified in our study.

We confirmed that the CHC profile of *N. vitripennis* comprises various MB-alkanes, *n*-alkanes and alkenes. We found that the MB-alkanes, in particular dimethyl alkanes, are primarily responsible for sexual dimorphism in the CHC profile between males and females. After silencing, we revealed that NvTRA is responsible for the regulation of these sexually dimorphic differences. MB-alkanes also dominate the CHC profile of other Hymenoptera, whereas these compounds only comprise a small fraction of the CHC profile in *Drosophila* (Kather & Martin, 2015; Martin & Drijfhout, 2009). The specific genes that regulate the production of MB-alkanes in Hymenoptera, however, still need to be identified. The results of our study now enable us to investigate the corresponding biosynthetic genes of these compounds in more detail.

A recent study on *N. vitripennis* found multiple biosynthetic candidate genes that are involved in the production of MB-alkanes in this species (Buellesbach *et al*., 2022). It would therefore be interesting to investigate whether these candidate genes are targeted by the sex-determination pathway for regulating MB-alkane biosynthesis in *N. vitripennis*. The genes *Fas5* and *Fas6* were found to be responsible for sex-specific MB-alkane biosynthesis (Sun *et al*., 2023b) and are therefore potential targets of the sex-determination pathway. Likewise, desaturases play an important role in producing unsaturated CHCs, such as alkenes. This makes desaturases also suitable candidates given the effects of silencing *NvTra* on the relative peak areas of alkenes in our study.

Nasonia parasitoids utilize CHCs for close-range sexual communication. These CHCs function as contact pheromones for males to recognize female mating partners and to initiate courtship behaviour. Our study confirmed that silencing *NvTra* modified the CHC composition in females and this affected male mating behaviour. Wild-type males were unsuccessful in arresting live *Tra*-i females in order to proceed with courtship behaviour. This in turn resulted in a prolonged mounting time and a significant decrease in male mating success. It is possible that male CHCs are also involved in the arrestment process of females, but this remains to be investigated. We already observed in **Chapter 3** that silencing *NvTra* in females has an effect on their perception of male pheromones. We also tested male mating behaviour in response to dead *Tra*-i females and found a significant decrease in the duration males spent mounting and attempting to copulate with these specimens. Alkene absolute quantities were significantly upregulated in *Tra*-i females. These CHCs function as pheromones in *N. vitripennis* that inhibit male-male courtship (Wang *et al*., 2022b) and indicate why males are less sexually attracted to the CHC profile of *Tra*-i females. Our results open up new avenues to investigate which biosynthetic genes are regulated by the sex-determination pathway to produce CHCs that function as mate-recognition pheromones in *N. vitripennis*.

Our study enables us to conclude for the first time that *Tra* plays a crucial role in developing the female-specific CHC phenotype in *N. vitripennis* and in regulating the biosynthesis of CHCs that induce male mating behaviour. We hypothesize that NvTRA regulation has played an important role in the evolution of sexually dimorphic CHC profiles in *Nasonia* species. Sexual dimorphism and species specificity of the CHC profile enables males to direct courtship to conspecific mating partners and this reinforces reproductive isolation. Our results now enable us to turn to identifying the corresponding biosynthetic genes targeted by the sex-determination pathway for producing sexually dimorphic CHCs. Variations in the way in which these genes are regulated form a potential mechanism for the diversification of CHC profiles between the closely related *Nasonia* species.

Acknowledgements

We are grateful for the feedback on this chapter provided by Marcel Dicke.

Supplementary information

Supplementary Figure 1: Non-metric multi-dimensional scaling (NMDS) analysis of the CHC profiles of the four treatment groups.
The NMDS analysis was performed on square-root transformed data using the Bray-Curtis similarity with 99,999 permutations. This figure can be accessed online at:
https://git.wur.nl/aidan.williams/chapter5/-/blob/main/Supplementary_Figure_1.png?ref_type=heads

Supplementary Table 1: Integrated peak areas of CHC compounds.
Table shows the integrated peak area values of CHCs for all wild-type and dsRNA-treated specimens. This table can be accessed online at:
https://git.wur.nl/aidan.williams/chapter5/-/blob/main/Supplementary_Table_1.csv?ref_type=heads

Supplementary Table 2: Pair-wise ANOSIM comparisons between the four treatment groups using square-root transformed data.
The ANOSIM showed a global R-value of 0.918 ($p < 0.001$) following 99,999 permutations.

Groups	R statistic	Significance level	Possible permutations	Actual permutations	Number ≥ observed
Gfp-i female / *Tra*-i female	1	$p < 0.001$	92378	92378	1
Gfp-i female / WT female	0.308	$p < 0.01$	92378	92378	139
Gfp-i female / WT male	1	$p < 0.001$	92378	92378	1
Tra-i female / WT female	1	$p < 0.001$	92378	92378	1
Tra-i female / WT male	1	$p < 0.001$	92378	92378	1
WT female / WT male	1	$p < 0.001$	92378	92378	1

Supplementary Table 3: One-way SIMPER analysis of the pair-wise comparison between wild-type (WT) males and wild-type females and between *Gfp*-i females and *Tra*-i females using square-root transformed data.
The analysis was performed using the Bray-Curtis dissimilarity index. For each CHC compound, the table shows the average relative peak area, average dissimilarity, standard deviation of the dissimilarity and the contribution to the average dissimilarity as a percentage. A 50% cut-off was set to exclude CHCs with a minor contribution to the average dissimilarity.

WT male / WT female	Average dissimilarity = 23.54%				
CHC compound	Average relative peak area WT female	Average relative peak area WT male	Average dissimilarity	Dissimilarity /SD	Contrib. %
7,19-/7,21-/7,23-DiMeC35	1.58	3.07	0.96	15.73	4.06
5-MeC33	2.23	0.92	0.83	13.70	3.55
13-/15-MeC33	2.45	1.18	0.81	15.58	3.44
Z9C31	0.19	1.41	0.78	7.08	3.31
11,15-DiMeC35	2.09	0.91	0.75	13.01	3.17

11,21-DiMeC33	1.82	0.77	0.67	10.58	2.86
7,23-DiMeC33	1.29	2.33	0.66	14.43	2.82
13,17-/15,19-DiMeC35	1.59	0.55	0.66	11.28	2.81
7-MeC31	2.17	3.13	0.61	5.59	2.59
7,19-/7,21-/7,23-DiMeC37	0.71	1.63	0.58	14.57	2.48
11,19-/11,21-DiMeC35	1.78	0.88	0.57	6.17	2.42
11-MeC31	1.47	0.63	0.53	13.39	2.27
11,15-DiMeC37	1.32	0.52	0.51	12.54	2.16
13,17-/15,19-DiMeC37	1.33	0.56	0.49	10.33	2.10
9,23-DiMeC33	1.64	0.89	0.48	8.96	2.03
C29	1.31	0.58	0.47	5.16	1.99
5,9,21-TriMeC33	0.46	1.11	0.42	8.43	1.78
13-/15-MeC31	1.17	0.53	0.41	10.13	1.73
7,21-DiMeC31	1.28	1.88	0.38	4.04	1.63
C31	2.75	2.17	0.37	2.55	1.58

***Gfp*-i female / *Tra*-i female**	**Average dissimilarity = 14.93%**				
CHC compound	Average relative peak area *Gfp*-i	Average relative peak area *Tra*-i	Average dissimilarity	Dissimilarity /SD	Contrib. %
7,19-/7,21-/7,23-DiMeC35	1.58	2.65	0.68	7.98	4.55
5-MeC33	2.33	1.43	0.57	5.82	3.80
7,19-/7,21-/7,23-DiMeC37	0.69	1.41	0.46	5.98	3.07
7-MeC31	2.11	2.82	0.45	2.00	3.04
13-/15-MeC33	2.39	1.70	0.44	4.96	2.92
7,23-DiMeC33	1.28	1.95	0.42	6.03	2.80
13,17-/15,19-DiMeC35	1.56	0.95	0.39	3.52	2.58
11,15-DiMeC35	2.23	1.63	0.38	2.98	2.53
C29	1.29	0.76	0.34	2.53	2.26
11,21-DiMeC33	1.84	1.32	0.32	3.11	2.17
7-MeC33	0.89	1.40	0.32	3.45	2.15
Z9C31	0.26	0.73	0.32	2.52	2.15
11,19-/11,21-DiMeC35	1.82	1.37	0.28	3.20	1.89
5,9,x-TriMeC35B	0.26	0.69	0.27	3.17	1.79
C31	2.70	2.28	0.27	2.03	1.78
9,23-DiMeC33	1.64	1.24	0.26	3.69	1.71
Unidentified17	0.12	0.49	0.24	4.66	1.57
5,9,21-TriMeC33	0.48	0.82	0.22	5.47	1.46
5,17-/5,19-/5,21-/5,23-DiMeC35	1.98	2.31	0.21	2.93	1.38
Z7C33	0.31	0.61	0.20	2.73	1.36
13,17-/15,19-DiMeC37	1.33	1.01	0.20	2.62	1.35
3,7-DiMeC31	0.55	0.87	0.20	4.64	1.34
7-MeC35	0.19	0.51	0.20	3.98	1.33

Supplementary Table 4: Average absolute quantities (in ng ± SE) of all alkenes identified in *Nasonia vitripennis.*

Treatment group	Z7-C31ene	Z7-C33ene	Z9-C31ene	Z9-C33ene	Sum of all alkenes
WT male	5.4 ± 1	9.4 ± 1.4	32.6 ± 5.7	8.7 ± 1.7	56 ± 9.7
WT female	6.2 ± 1.4	14.5 ± 3.2	20 ± 4.7	11.7 ± 2.7	52.4 ± 12
Gfp-i female	1.4 ± 0.2	2 ± 0.2	0.9 ± 0.1	2.2 ± 0.2	6.5 ± 0.5
Tra-i female	1 ± 0.5	1.5 ± 0.6	1.5 ± 1	2 ± 0.5	5.9 ± 2.6

Supplementary Table 5: Male mating behaviour in response to live *Gfp*-i and *Tra*-i females.
Table shows the time wild-type males spent searching, mounting, copulating and performing post-copulatory behaviour when exposed to live *Gfp*-i and *Tra*-i females. This table can be accessed online at:
https://git.wur.nl/aidan.williams/chapter5/-/blob/main/Supplementary_Table_5.csv?ref_type=heads

Supplementary Table 6: Male mating behaviour in response to dead *Gfp*-i and *Tra*-i females.
Table shows the cumulative time wild-type males spent mounting and attempting to copulate with *Gfp*-i and *Tra*-i female dummies. It also shows the total contact time males spent interacting with *Gfp*-i and *Tra*-i female dummies. This table can be accessed online at:
https://git.wur.nl/aidan.williams/chapter5/-/blob/main/Supplementary_Table_6.csv?ref_type=heads

Chapter 6

Decoding sexual dimorphism in cuticular hydrocarbon pheromones by fatty acyl-CoA reductases in the parasitoid *Nasonia vitripennis*

Aidan Williams[1], *Weizhao Sun*[2], *Filippo Guerra*[1], *Jan Büllesbach*[2] & *Eveline Verhulst*[1]

[1]Laboratory of Entomology, Wageningen University, PO Box 16, 6700 AA Wageningen, the Netherlands

[2]Institute for Evolution & Biodiversity, University of Münster, Hüfferstrasse 1, 48149 Münster, Germany

Abstract

Finding and choosing a potential mating partner is essential for all sexually reproducing animals. Many insects recognize mating partners based on contact pheromones called cuticular hydrocarbons (CHCs). These long-chain carbon chemicals are a major component of the waxy layer on the insect cuticle and form a pheromone signature unique to each insect species. Previous research on the biosynthetic genes involved in regulating CHC production in insects has been limited to *Drosophila melanogaster,* a model species for Diptera. In this species, sex-determination transcription factors, such as Doublesex, determine sexual dimorphism in the CHC profile. However, only limited research has been carried out on how Doublesex regulates genes for CHC production in other species, such as parasitoid wasps. In this study, we identified four candidate fatty acyl-CoA reductases (FARs) in the parasitoid *Nasonia vitripennis* that are regulated by the transcription factor Doublesex: *LOC100117683*, *LOC100117760*, *LOC100117837* and *LOC100117878*. These candidate FARs are sex-biased in their expression and show peak expression levels during specific developmental time windows. After successfully silencing the four candidate FARs using RNA interference, we confirmed their function in lipid metabolism and CHC production. Silencing these FARs coincided with the concomitant upregulation or downregulation of components of specific CHC compound classes, including methyl-branched alkanes, *n*-alkanes and alkenes. The modified CHC composition in FAR-silenced females affected mate recognition, including the duration males spent mounting and copulating. We can therefore conclude that our candidate FARs regulate sexual dimorphism in the CHC profile and play a specific role in producing CHCs that influence male mating behaviour in *N. vitripennis*.

Introduction

Sex-pheromone signalling is among the most ancient and universal forms of insect communication (Wyatt, 2003). Sex pheromones continue to evolve as a potent driver of mate choice to discriminate between sexes and potential mates (Johansson & Jones, 2007). Similarity in pheromone profiles between closely related species can lead to fitness reduction due to the risk of heterospecific mating and hybridization (Baker, 2002; Symonds & Elgar, 2008). Sexual selection acts on pheromone communication within and between sexes to reduce the risk of hybridization, resulting in sexually dimorphic traits, such as sex-specific signalling and perception (Buchinger & Li, 2023; Johansson & Jones, 2007; Ritchie & Noor, 2004; Smadja & Butlin, 2009; Steiger & Stökl, 2014; Svensson, 1996). These traits are genetically correlated between emitter and receiver, leading to a so-called Fisherian runaway process, which in turn causes rapid changes in pheromone signals and sensory preferences (Baker, 2002; Groot *et al*., 2016; Johansson & Jones, 2007; Shirangi *et al*., 2009; Symonds & Elgar, 2008). These evolutionary transitions epitomize how selection forces induce genetic divergence between insect species. In **Chapter 5**, we discussed the essential role of TRA in regulating sexual dimorphism in CHC production. We will now turn to the CHC biosynthetic genes downstream of the sex-determination pathway involved in this process. Understanding how pheromones evolve from a sexually monomorphic to a sexually dimorphic state would help explain the evolutionary transitions in insect sex-pheromone communication.

CHCs are of particular interest among researchers investigating the production and evolution of sexually dimorphic pheromone profiles (Chung & Carroll, 2015; Holze *et al*., 2021; Howard & Blomquist, 2005; Moris *et al*., 2023; Wang *et al*., 2025). These long carbon-chain chemicals provide insects with an efficient means to discriminate and choose potential mating partners (Chung *et al*., 2014; Chung & Carroll, 2015). CHCs form the major component of the waxy layer on the insect cuticle, alongside alcohols, esters, aldehydes, ketones and long-chain fatty acids (Blomquist *et al*., 1987; Lockey, 1988). CHCs are divided into various classes. In the majority of insects, linear straight-chain and methyl-branched alkanes are the most abundant classes and unsaturated alkenes and alkadienes the least abundant (Blomquist *et al*., 1987; Blomquist & Bagnères, 2010; Hamilton, 1995). A blend of all the CHC components form the pheromone signature, which is both sex- and species-specific. Sensory preferences to these pheromone signatures are themselves driven by gains and losses of individual hydrocarbons (Luo *et al*., 2019). Consequently, CHCs are a textbook example of how sexual selection induces a diverse range of sexually dimorphic pheromone profiles in insects. However, research on the genetic mechanisms regulating sex-specific CHC production has been predominately limited to the model species *Drosophila melanogaster*. In this species, CHCs are produced in specialized oenocyte cells in a chain of chemical reactions (**Figure 1**) involving fatty acid synthases, desaturases, elongases and reductases (Billeter *et al*., 2009). With regard to other insect species, there is a lack of knowledge on how these biosynthetic genes are regulated to produce sexually dimorphic CHCs.

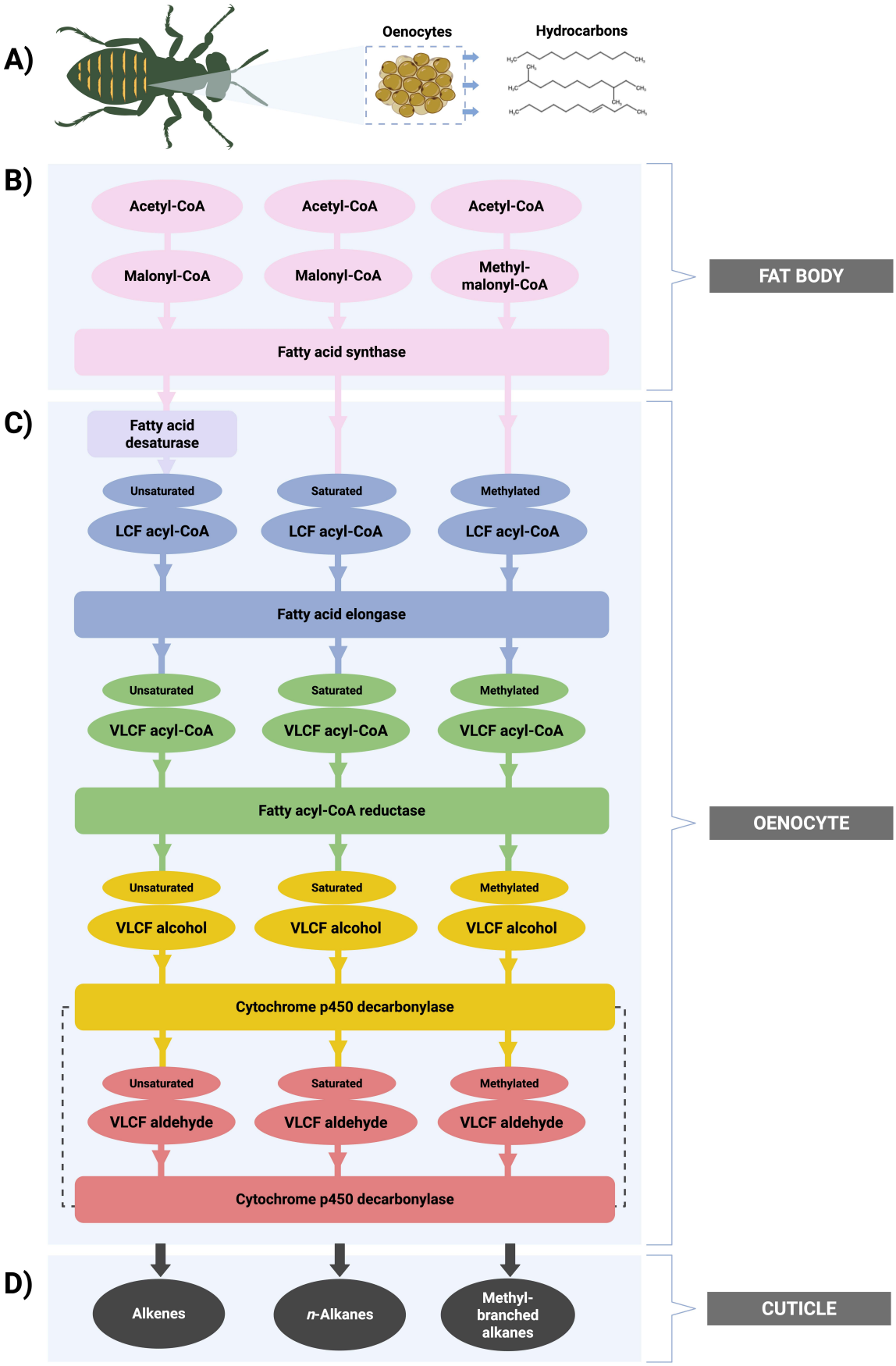
A)
Oenocytes
Hydrocarbons
B)
Acetyl-CoA
Acetyl-CoA
Acetyl-CoA
Malonyl-CoA
Malonyl-CoA
Methyl-malonyl-CoA
Fatty acid synthase
FAT BODY
C)
Fatty acid desaturase
Unsaturated
Saturated
Methylated
LCF acyl-CoA
LCF acyl-CoA
LCF acyl-CoA
Fatty acid elongase
Unsaturated
Saturated
Methylated
VLCF acyl-CoA
VLCF acyl-CoA
VLCF acyl-CoA
Fatty acyl-CoA reductase
Unsaturated
Saturated
Methylated
VLCF alcohol
VLCF alcohol
VLCF alcohol
Cytochrome p450 decarbonylase
Unsaturated
Saturated
Methylated
VLCF aldehyde
VLCF aldehyde
VLCF aldehyde
Cytochrome p450 decarbonylase
OENOCYTE
D)
Alkenes
n-Alkanes
Methyl-branched alkanes
CUTICLE

Figure 1: Schematic summary of the insect CHC production pathway (adapted from Holze *et al*. (2021)).
Ovals denote chemical compounds and rectangles the corresponding enzymes that catalyse their transitions. **A:** CHC production occurs in specialized secretory cells, called oenocytes, located underneath the cuticle of the insect abdomen (Blomquist & Ginzel, 2021; Chung & Carroll, 2015; Howard & Blomquist, 2005). **B:** The pathway starts in the insect fat body, in which fatty acid synthases bind acetyl-coenzyme A (CoA) with malonyl-CoA and methylmalonyl-CoA units. The consecutive elongation of the fatty acyl-CoA chain by the fatty acid synthase results in long-chain fatty (LCF) acyl-CoAs. It has been predicted that the production of methyl-branched alkanes depends on a specific fatty acid synthase that incorporates methylmalonyl-CoA (Blomquist & Bagnères, 2010) **C:** The LCF acyl-CoAs are further elongated to very long-chain fatty (VLCF) acyl-CoA by fatty acid elongases that add additional malonyl-CoA molecules to the LCF acyl-CoA. Before this step, double bonds can be inserted in the LCF acyl-CoAs by fatty acid desaturases, resulting in the production of unsaturated hydrocarbons. The VLCF acyl-CoAs are further reduced to VLCF alcohols by fatty acyl-CoA reductases and to VLCF aldehydes through oxidative decarbonylation. **D:** The final step involves decarbonylation of the aldehydes by cytochrome p450 into cuticular hydrocarbons, including alkenes, *n*-alkanes and methyl-branched alkanes.

The transcription factor Doublesex (DSX) has emerged as an important CHC regulator, contributing to the divergence of these pheromones between sexes in closely related species (Antony *et al*., 1985; Jallon *et al*., 1988; Shirangi *et al*., 2009; Sun *et al*., 2023a; Wang *et al*., 2022b). *Doublesex* was one the first genes shown to play a significant role in the production of CHC pheromones in *Drosophila*. Female flies produce the long-chain dienes 7,11-heptacosadiene and 7,11-nonacosadiene, also referred to as aphrodisiac molecules for males (Antony *et al*., 1985; Jallon *et al*., 1988; Toda *et al*., 2012). However, female flies in which *Dsx* has been disrupted lack their usual dienes and elicit a significantly lower level of courtship from males (Jallon *et al*., 1988). A female-specific desaturase, DESATF, was later identified to produce precursors for these diene pheromones (Chertemps *et al*., 2006). Researchers have now also found a DSX binding site in a *cis*-regulatory element upstream of *DesatF* that is responsible for the female-specific expression of this gene (Shirangi *et al*., 2009). Sexually dimorphic diene production occurs through the DSX-F isoform binding to this element and directly activating female-specific *DesatF* expression. Moreover, disrupting *Dsx* has also been shown to affect the CHC profile of male flies and results in so-called chaining behaviour (male-male attraction) (Sun *et al*., 2023a).

A considerable amount of research has been carried on the composition of CHCs in Hymenoptera. This insect order comprises many economically and environmentally important species (Kather & Martin, 2015). Hymenoptera have also evolved an extensive diversity of CHC profiles between species, in particular the methyl-branched alkanes that are believed to function as pheromones for recognizing both nest mates in social species and hosts in parasitoid wasps (Kather & Martin, 2015; Martin & Drijfhout, 2009; Sprenger & Menzel, 2020). Limited research, however, has been carried out on the genetic regulation of CHCs in these species. In parasitoid wasps, it has been shown that TRA and DSX feminize and masculinize the CHC profile respectively, in particular the CHCs involved in mate recognition (Wang *et al*., 2022b; **Chapter 5** of this dissertation). Nevertheless, research has yet to elucidate how sex-determination transcription factors regulate the genetic pathways for CHC

synthesis to produce sex-specific pheromones. Understanding how DSX regulates CHC biosynthetic genes in these species would therefore be of major interest.

Hymenoptera have evolved highly divergent CHC profiles between sexes and closely related species (Buellesbach *et al*., 2013; Kather & Martin, 2015). The biosynthetic genes underlying insect CHCs diverge rapidly between closely related species (Finck *et al*., 2016; Finet *et al*., 2019; Helmkampf *et al*., 2015; Shirangi *et al*., 2009; Tupec *et al*., 2019; Wang *et al*., 2023), enabling individual species to form mating barriers and adapt to novel ecological environments. A group of these potential genes belong to the fatty acyl-CoA reductases (FARs) that convert fatty acids into fatty alcohols, the precursors for CHC production (Riendeau & Meighen, 1985). Hymenoptera have experienced a considerable expansion of the FAR gene family, which has been linked to the diversification of pheromones in these species (Tupec *et al*., 2019). FARs expressed in oenocytes are known to evolve rapidly relative to those expressed in other insect tissues (Finet *et al*., 2019). The process of gene duplication and loss gives rise to novel FAR genes, which enables the diversification of CHCs between closely related species. Understanding whether these genes are sex biased and how they are regulated by DSX is therefore necessary for elucidating CHC diversification between male and female insects. Here, we analysed the role that FARs play in sexually dimorphic CHC profiles in *Nasonia vitripennis*, a suitable parasitoid model species for characterizing genes involved in CHC production.

Nasonia uses CHCs as contact pheromones to recognize potential mates (Mair & Ruther, 2019). CHCs have diverged in all *Nasonia* species and form unique profiles between the various species and sexes (Buellesbach *et al*., 2013). A recent study also identified numerous FAR candidates contributing to substantial CHC diversity, especially in the methyl-branched alkanes (Buellesbach *et al*., 2022). In addition, we confirmed that DSX regulates the expression of FARs in *N. vitripennis* in a transcriptomic survey following *NvDsx* silencing (Rougeot *et al*., 2025). The aim of our current study is to analyse the function of four of these FAR genes in producing sexually dimorphic CHC profiles: *LOC100117683* (*LOC683*), *LOC100117760* (*LOC760*), *LOC100117837* (*LOC837*) and *LOC100117878* (*LOC878*). We first determined sex-biased and temporal expression levels through RT-qPCR before silencing all four FARs at the fourth-instar larval stage with dsRNA. After silencing, we analysed changes in the CHC profile of both sexes and the behavioural significance of these changes for male-female pheromone communication. Our study confirmed a new complex of CHC-producing genes contributing to the diversification of parasitoid CHC pheromones. Our results open up new avenues to elucidate how the expansion of the FAR-gene family enabled the evolution of *cis*-regulatory elements in FARs to become potential targets for transcription factors like DSX and the resulting rapid diversification of CHCs in the evolutionary history of Hymenoptera.

Materials & Methods

Nasonia rearing

We used the lab strain AsymCX of *N. vitripennis* to silence FAR and *NvDsx* expression with dsRNA. The AsymCX wasps were reared on *Calliphora vomitoria* pupae obtained as larvae from a commercial manufacturer (Kreikamp & Zn, Hoevelaken, the Netherlands). The fly larvae were reared in sawdust at room temperature and stored at 4°C for a maximum duration of four weeks after pupation. Once they emerged, individual female wasps were placed together with a single host pupa in glass vials for 24 hours. Virgin females were used to produce male-only offspring (100% males) and mated females were used to produce mainly female offspring (90% females). After 24 hours, we followed the rearing protocol for strain maintenance as set out by Werren & Loehlin (2009a). This involved incubating the parasitized pupae at a constant temperature of 25°C using a 16-hour light, 8-hour dark cycle.

RNA extraction and cDNA synthesis

We extracted RNA from wasp pupae to generate cDNA for comparing FAR expression between sexes and pupal developmental stages. Accordingly, we collected male and female pupae eight, ten and twelve days after ovipositing. In total, 40 pupae were collected per sex and per developmental stage. Five pupae were pooled into one Eppendorf tube, forming one replicate, and eight replicates were used for each developmental stage. The samples were snap-frozen in liquid nitrogen and stored at −80°C until RNA was extracted. The frozen samples were ground up and homogenized with a sterile pellet pestle in 200 µl of Trizol (Invitrogen, Carlsbad, CA, USA). The RNA samples were then treated with DNase (Zymo Research, E1010) to form a total volume of 50 µl and subsequently purified with a phenol:chloroform:isoamyl alcohol solution (25:24:1, v/v) (15593031, Invitrogen). The resulting RNA was resuspended in 8 µl of autoclaved water and quantified with a spectrophotometer (DeNovix, DS-11 FX, Wilmington, Delaware, USA). 500 ng of RNA was used to synthesize cDNA using the 5x TransAmp buffer of the SensiFAST cDNA Synthesis Kit (Bioline Reagents Ltd, London, UK) containing a mixture of anchored oligo(dT) and random hexamer primers. The resulting cDNA was then diluted 1:16 before being used for reverse transcription quantitative real-time PCR (RT-qPCR).

FAR expression levels between sexes and developmental stages

RT-qPCR was performed with a solution of 2 µl of cDNA diluted 1:16 and a 400 nM SensiFAST SYBR Lo-ROX mix (Bioline Reagents Ltd, London, UK) on a BIORAD CFX-Opus96 machine (Bio-Rad, Veenendaal, the Netherlands). Primers were designed with Geneious Prime (Dotmatics, Boston, MA, USA) (see **Supplementary Table 1** for all qPCR primer sequences). The qPCR thermocycling conditions were 95°C 3’; 39x 95°C 15’’, 55°C 30’’, 72°C 30’’, followed by a post-melt curve to check the degree of non-specific amplification. After generating the raw fluorescence data, a baseline threshold was manually set by using the Single Threshold mode

in the CFX Manager software (v3.1). The housekeeping genes *Ribosomal protein 49* (*Rp49*), *Elongation factor 1-alfa* (*Ef1a*) and *LOC100119962* (*Ak3*) were used for gene expression normalization. We performed the analysis of the data in RStudio (v2024.12.1+563, Posit PBC). We used the delta-delta Ct method ($2^{-\Delta\Delta Ct}$) to calculate relative gene expression (Livak & Schmittgen, 2001), in which delta-delta Ct is the calculated difference in cycle threshold values of housekeeping genes and reference samples. The sample with the lowest gene expression was used as a reference and the average of this sample was therefore set to one. The influence of sex and developmental stage on gene expression was tested with a two-way ANOVA (log2(FAR expression)~sex*day) and the difference between sexes at each developmental stage was tested with Tukey's honest significance test (THSD). Graphs were generated with the R package ggplot2 in RStudio (v2024.12.1+563, Posit PBC).

Synthesis of FAR and *NvDsx* dsRNA

We used the MEGAscript RNAi Kit (Thermo Fisher, Waltham, MA, USA) to generate FAR and *NvDsx* dsRNA from *N. vitripennis* cDNA. Primers were designed in Geneious Prime to yield amplicons with a target size of ~533 bp (*LOC683*), ~660 bp (*LOC760*), ~617 bp (*LOC878*) and ~536 bp (*LOC837*). We also designed a T7 RNA polymerase promotor [TAATACGACTCACTATAGGG] version of these primers. *Gfp* dsRNA was used as an exogenous control in all our experiments and was generated from the pOPINEneo-3C-GFP vector (Addgene plasmid #53534; https://www.addgene.org/53534/; RRID: Addgene_53534) to produce a 460 bp amplicon, which covered 64% of the Emerald GFP CDS. (See **Supplementary Table 1** for all dsRNA primer sequences). The dsRNA template fragments were synthesized in a PCR using the GoTaq Flexi DNA polymerase (Promega, Madison, WI, USA) and the relevant primers without the T7 addition. These PCR products were used as templates in two separate PCRs to add the T7 promotors to either end of the amplicon. The resulting two templates were then used in separate reactions to transcribe both sense and antisense RNA molecules in accordance with the MEGAscript RNAi Kit protocol (16 hours at 37°C). The synthesized dsRNA was measured for its purity and concentration on a spectrophotometer (DeNovix, DS-11 FX, Wilmington, Delaware, USA) and subsequently diluted with RNase-free water to a concentration of 4 µg/µl.

Micro-injection of FAR dsRNA

FAR and *Gfp* dsRNA was injected in male and female L4 larvae and eight-day-old pupae. This was carried out before and just after the onset of adult oenocyte development and CHC production that occur during the pupal stage (Carlson *et al*., 1999; Johnson & Butterworth, 1985; Lawrence & Johnston, 1982). The larvae and pupae were aligned on a 1x phosphate-buffered saline (PBS) agar plate and a mixture of 4.5 µl dsRNA and 0.5 µl food dye was injected in their posterior using a FemtoJet 4i microinjection pump (Eppendorf, Hamburg, Germany) according to the protocols set out by Lynch & Desplan (2006) and Werren *et al*. (2009). The dsRNA-injected larvae and pupae were incubated at 25°C until further use. We used pupae

three days post-larval injection to analyse FAR expression. Adults treated at both the larval and pupal stage were used to analyse changes in CHC composition. Females treated at the larval stage were subsequently used for analysing male mating behaviour. Male and female specimens for chemical and behavioural analyses were separated at the pupal stage based on sex-specific traits (forewing size and presence/absence of the ovipositor). Due to difficulty with eclosure, the pupal cases of the *LOC683* dsRNA-injected specimens were removed with sharp forceps (Dumont No. 5) under a stereomicroscope.

Analysis of FAR expression levels after RNA interference (RNAi)

The same procedures for RNA extraction, cDNA synthesis and RT-qPCR were used as set out above to assess FAR expression after silencing. FAR expression was analysed on nine-day-old female pupae with RT-qPCR. FAR relative expression was then analysed with a Benjamini-Hochberg-corrected Wilcoxon rank-sum test in RStudio (v2024.12.1+563, Posit PBC).

Assessing *Nasonia vitripennis* morphology after FAR RNAi

We assessed external morphological changes after silencing FAR expression in female adults. Photographs were taken of legs, antennae, wings and cuticle pigmentation with a Dino-Lite Edge 5 MP digital microscope (Dino-Lite Digital Microscope, New Taipei City, Taiwan).

Chemical analysis

CHC extraction

The adult CHC profile was analysed with GC-MS after silencing the candidate FARs in male and female L4 larvae and eight-day-old pupae. Wild-type and *Gfp* RNA interference (*Gfp*-i) specimens were used as controls. We extracted the CHCs of individual male and female wasps by immersing them in 50 µl HPLC-grade *n*-hexane (Merck, KGaA, Darmstadt, Germany) in 2 ml glass vials (Agilent Technologies, Waldbronn, Germany) on an orbital shaker (IKA KS 130 Basic, Staufen, Germany) for ten minutes. The *n*-hexane was then evaporated under a constant stream of gaseous CO_2 and the extracted profile was then resuspended in a 10 µl *n*-hexane solution containing 7.5 ng/µl dodecane used as the internal standard. Subsequently, 3 µl of the resuspended extract was injected in splitless mode with an automated liquid sampler (PAL RSI 120, CTC Analytics AG, Zwingen, Switzerland) into a gas chromatograph (GC: 7890B) coupled to a flame ionization detector (FID: G3440B) and a tandem mass spectrometer (MS/MS: 7010B, all provided by Agilent Technologies, Waldbronn, Germany). This setup was equipped with a fused silica column (DB-5MS ultra inert; 30 m × 250 µm × 0.25 µm; Agilent J&W GC columns, Santa Clara, CA, USA) using helium as a carrier gas at a constant flow of 1.8 ml/min. The column was split at an auxiliary electronic pressure control module into a deactivated fused silica column (0.9 m × 150 µm) leading to the FID at a flow rate of 0.8 ml/min and another deactivated fused silica column (1.33 m × 150 µm) leading to the mass spectrometer at a flow rate of 1.33 ml/min. The FID had a temperature of 300°C and used

nitrogen as make-up gas at a flow rate of 20 ml/min and hydrogen as fuel gas at a flow rate of 30 ml/min. The column temperature profile started at 60°C and was held for one minute, increasing 40°C per minute up to 200°C and then increasing 5°C per minute to the final temperature of 320°C, which was held for five minutes.

CHC identification and quantification

CHC peak detection, integration, quantification and identification were all carried out with Quantitative Analysis MassHunter Workstation software (vB.09.00/Build 9.0.647.0, Agilent Technologies, Santa Clara, CA, USA). CHCs were identified according to their retention indices, diagnostic ions and mass spectra as provided by the total ion count chromatograms, whereas their quantifications were obtained from the FID chromatograms. Absolute CHC quantities (in ng) were obtained by calibrating each compound according to a dilution series based on the closest eluting *n*-alkane from a C21-40 standard series (Merck, KGaA, Darmstadt, Germany) at 0.5, 1, 2, 5, 10, 20 and 40 ng/µl, respectively. Differences in the absolute quantities between the treatments were analysed in accordance with the method set out in Sun *et al*. (2023b)

Mating trials following FAR RNAi

We tested the mating responses of virgin male wasps to the CHCs of FAR- and *Gfp*-silenced females in a mating chamber bioassay in accordance with the setup adopted by Mair *et al*. (2017). Silenced females were freeze-killed in liquid nitrogen before the experiment and used as dummies to minimize potential mating signals (e.g. behavioural and vibrational signals), excluding CHCs (Buellesbach *et al*., 2013, 2018). The female dummies were then presented to newly emerged (0-48 hour old) virgin wild-type males in an acrylic mating chamber (ø10 mm) placed on a glass plate and covered with a glass microscope slide. The mating behaviour was then analysed under a stereomicroscope. Males typically show mating behaviour in response to female CHCs by mounting and copulating with the females. For mounting behaviour, we recorded the amount of time a male spent positioning and performing courtship (i.e. head nodding, antennal sweeping and wing twitching, etc.) on a female dummy. For copulation behaviour, we recorded the amount of time a male spent attempting to copulate with the female dummy. We recorded the cumulative time of this behaviour for five minutes. After testing six replicates, the acrylic mating chamber was cleaned with detergent (TORK Mild Liquid Soap, 420501) and the glass plate with 70% ethanol. The differences in male mating behaviour were analysed with a Wilcoxon rank-sum test of the Coin package in RStudio (v2024.12.1+563, Posit PBC). Significant differences in mating success were assessed with a Pearson's Chi-squared test with Yates's continuity correction.

Results

FAR expression levels

Temporal and sex-biased expression levels

We postulated that fatty acyl-CoA reductases are expressed during *N. vitripennis* pupal development, as they contribute to the production of fatty alcohols that are subsequently metabolized into adult CHCs (**Figure 1**). Since these FARs are targeted by DSX in *N. vitripennis* (Rougeot *et al*., 2025), we also hypothesized that their expression should be sex biased, which in turn results in the production of sexually dimorphic CHC pheromones. To verify this, we first analysed the relative expression levels of four candidate FARs (*LOC683*, *LOC760*, *LOC837* and *LOC878*) during pupal development of male and female *N. vitripennis* (**Supplementary Table 2**).

We determined that all four FARs were expressed throughout pupal development of both males and females (**Figure 2**). We carried out a two-way ANOVA to analyse the effect of the developmental stage, sex and the interaction between these variables on the relative expression levels of all four FARs (**Supplementary Table 3**). We confirmed that the developmental stage had a significant main effect on the relative expression of three FARs (*LOC760*, *LOC837* and *LOC878*), and that sex and the interaction between sex and the developmental stage had a significant main effect on the expression levels of all four FARs. The expression level of *LOC683* (**Figure 2A**) remained relatively stable between day 8 and day 10 of both males and females. At day 12, however, *LOC683* expression was significantly male biased (THSD, $p < 0.001$), whereas in females it decreased (THSD, $p < 0.01$). *LOC760* expression (**Figure 2B**) was consistently female biased and showed stable expression levels throughout pupal development. *LOC760* expression in males, on the other hand, significantly decreased after day 8 (THSD, $p < 0.001$). *LOC837* (**Figure 2C**) was significantly female biased at day 10 (THSD, $p < 0.05$) and showed a ~45-fold increase in expression level (THSD, $p < 0.001$). It then significantly decreased in females at day 12 and switched to a male-biased expression (THSD, $p < 0.001$). *LOC878* expression (**Figure 2D**) was significantly male biased at day 8 (THSD, $p < 0.001$) before switching to a female-biased expression at day 10 (THSD, $p < 0.001$). It then significantly decreased in both sexes at day 12 (THSD, $p < 0.001$).

These results show that the expression of all four FARs is highly dynamic throughout pupal development and it is expected that the specific time of upregulation observed in each of the FARs in males and females corresponds to the production of CHC precursors.

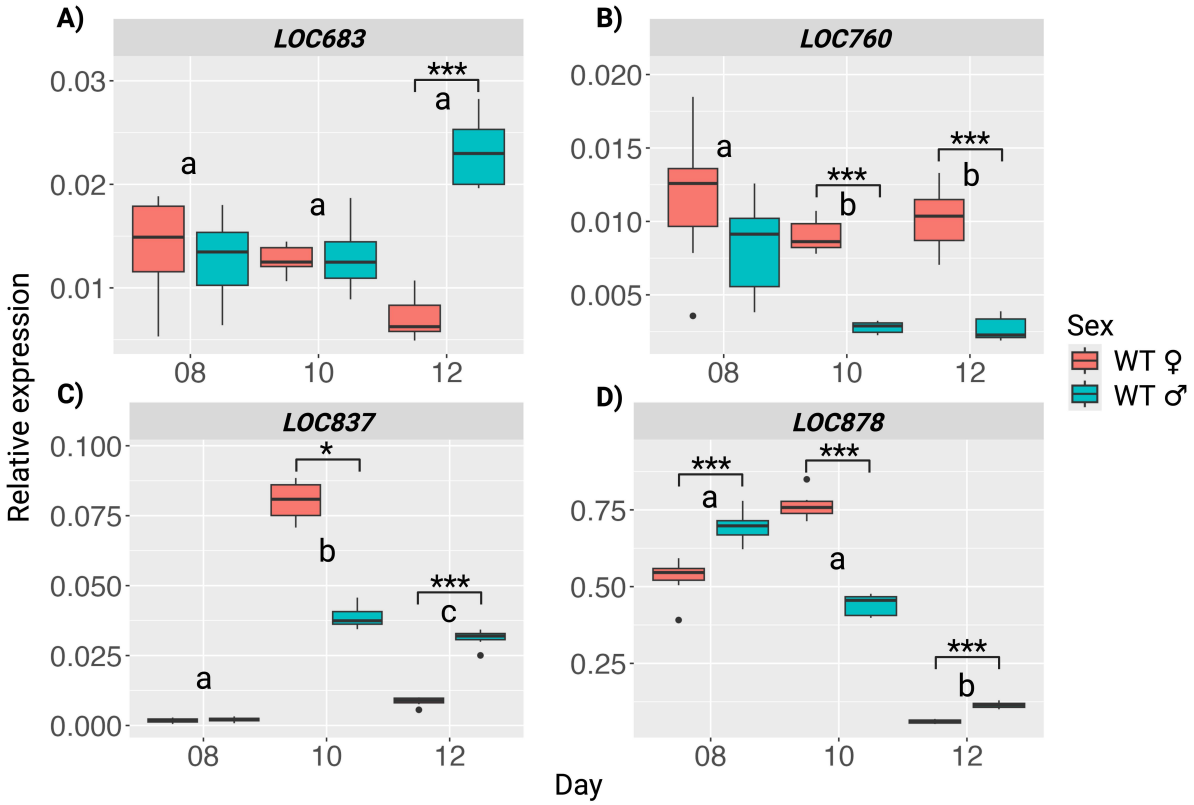

Figure 2: Relative expression of the four candidate FARs throughout pupal development of wild-type (WT) male and female *N. vitripennis*.
Developmental stage is displayed on the x-axis in days after oviposition. Normalized, relative expression is shown for *LOC683* (n = 7), *LOC760* (n = 7), *LOC837* (n = 7) and *LOC878* (n = 7) on the y-axis. Note: panels **A**, **B** and **D** do not start at 0. The effect of developmental stage, sex and the interaction between these variables on the relative expression levels was analysed using a two-way ANOVA. Significance values of the main effects are provided in **Supplementary Table 3**. Significant differences in relative expression between days and sex were analysed with a Tukey's Honestly Significant Difference (THSD) test (**Supplementary Table 4**). Significant differences in relative expression between days are depicted by letters, whereas significant differences between sexes are depicted by asterisks. Significance levels: *** = $p < 0.001$ and * = $p < 0.05$.

Efficiency test of dsRNA on FAR expression

We assessed the efficiency of our synthesized dsRNA on FAR expression with RT-qPCR (**Supplementary Table 5**). We injected L4 female larvae with dsRNA and collected these silenced samples three days later as white-stage pupae to assess FAR expression. All four FARs were significantly reduced in their expression relative to *Gfp*-i control samples (**Figure 3**), with almost complete reduction of three of the FARs (*LOC760, LOC837* and *LOC878)*, confirming that our dsRNA successfully silenced FAR expression in our samples.

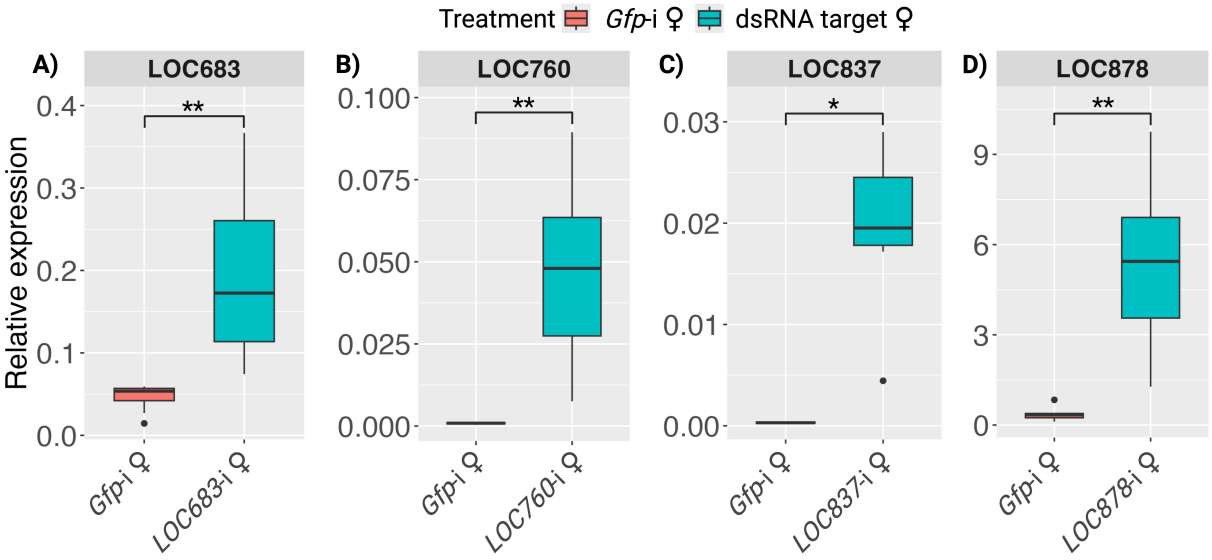

Figure 3: Relative expression of the four candidate FARs after dsRNA treatment.
Normalized, relative expression of FARs in white-stage female pupae three days after dsRNA treatment of L4 larvae. Relative quantification of expression shows a significant reduction of *LOC683* (n = 8), *LOC760* (n = 7), *LOC837* (n = 4) and *LOC878* (n = 8), compared to the *Gfp*-i control (n = 7). Significant differences in FAR expression between the dsRNA and *Gfp*-i control group were analysed with a Wilcoxon rank-sum test. P-values were Benjamini-Hochberg corrected for multiple comparisons. Significance levels: ** = $p < 0.01$ and * = $p < 0.05$.

Morphological changes after FAR RNAi

We observed morphological changes in males and females after silencing *LOC683* at the L4 stage. *Gfp*-i specimens were able to shed their exuviae and showed normal eclosure after six days incubation, identical to wild-type wasps (**Figure 4A, 4C**). *LOC683*-i specimens, however, were unable to shed their exuviae and therefore did not eclose properly after six days incubation (**Figure 4B, 4D**). To facilitate eclosure, we dissected the pupal case of the *LOC683*-i specimens and observed that the cuticle of these specimens lacked the normal rigidity found in wild types. The abdomen and wings of these specimens also appeared underdeveloped (**Figure 4B, 4D**). Moreover, we observed changes in the coloration of the cuticle, most notably on the sides of the thorax (**Figure 4B**). The cuticle of our *Gfp*-i specimens was metallic green in colour, identical to wild-type wasps, whereas the cuticle of the *LOC683*-i specimens was metallic blue in colour. The pigmentation of the antennae and legs in the silenced specimens remained unchanged (**Figure 4E, 4F**). These results indicate that silencing *LOC683*-i affects the production of crucial chemical components influencing the formation of the cuticular waxy layer. These modifications to the waxy layer hamper the normal hardening of the cuticle itself (Hendricks & Hadley, 1983; Kawase, 1961; Wigglesworth, 1970), which in turn affects the ability of the wasp to shed its exuviae and therefore to eclose.

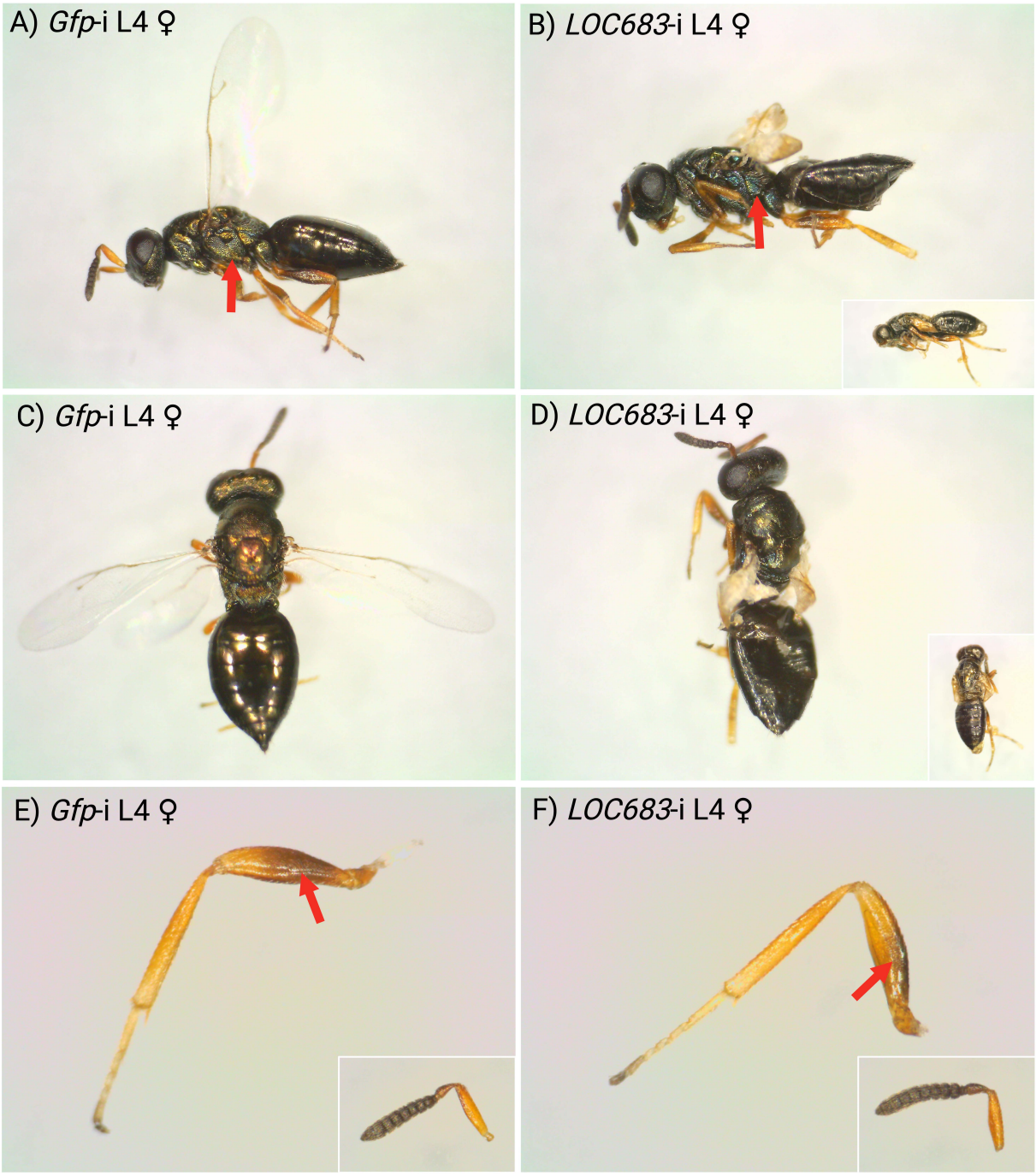

Figure 4: Pigmentation of cuticle, hind legs and antennae of adult females after *LOC683*-i and *Gfp*-i at the larval stage.

Pigmentation of the cuticle (see red arrows) changed from metallic green in *Gfp*-i females (**A**) to metallic blue in *LOC683*-i females (**B**). *Gfp*-i females eclosed properly after six days incubation, whereas *LOC683*-i were unable to shed their exuviae (inserts in **B** and **D**). Wings and abdomen developed normally in *Gfp*-i females (**C**), whereas these were underdeveloped in *LOC683*-i females (**D**). Pigmentation on the legs (depicted by red arrows) and antennae (inserts in **E** and **F**) remained unaffected in both *Gfp*-i (**E**) and *LOC683*-i (**F**) females.

CHC profile changes

Fatty acyl-CoA reductases (FARs) are important enzymes for metabolizing fatty alcohols. Fatty alcohols are the precursors of CHCs in insects. FARs therefore contribute to the production of these CHCs. We hypothesized that silencing the candidate FARs would differentially affect CHC compound classes of both male and female *N. vitripennis*. This would indicate the specific roles of these FARs in converting fatty-acid precursors at various developmental stages for CHC biosynthesis. To verify this, we analysed and quantified the CHC compounds of methyl-branched alkanes (MB-alkanes), linear straight-chain alkanes (*n*-alkanes) and alkenes by GC-MS (**Supplementary Table 6**). We analysed the FAR-silenced specimens and compared these with wild-type and *Gfp*-i specimens to identify significant differences. The chemical analyses of the *LOC837*-i and *LOC683*-i at the eight-day pupal stage proved incomplete and were therefore not included in our results.

Silencing *LOC683*, *LOC760* and *LOC878* changed the CHC profile of adult female *N. vitripennis* (**Figure 5**). Changes in the overall quantity of CHC compounds are represented in **Figure 5A**, **5E** and **5I**. Silencing these candidate FARs affected the absolute quantities of the individual CHC compound classes.

MB-alkanes, the dominant CHC compound class in female *N. vitripennis*, significantly increased after *LOC683*-i at the larval stage when compared to wild-type and *Gfp*-i females (**Figure 5B**). Specifically, *LOC683*-i resulted in a significant increase in the absolute quantities of MB-alkanes with their first methyl branches positioned on the 3rd, 5th, 7th, 9th, 11th and 13th C-atom (**Supplementary Figure 1A-1D**). *LOC760*-i did not significantly affect the total quantity of MB-alkanes (**Figure 5F**), although MB-alkanes with their first methyl branches positioned on the 9th, 11th and 13th C-atom were significantly upregulated (**Supplementary Figure 1E-1H**). *LOC878*-i, on the other hand, showed a significant decrease in the absolute quantities of all MB-alkane types after silencing at both the larval and pupal stage (**Figure 5J, Supplementary Figure 1I-1L**). The absolute quantities of *n*-alkanes, the second most abundant CHC compound class in females, were also affected after *LOC683*-i and *LOC878*-i, and showed a significant increase after *LOC683*-i (**Figure 5C**) and a significant decrease after *LOC878*-i, specifically when silenced at the larval stage (**Figure 5K**). Interestingly, *Gfp*-i appears to have a generally upregulating effect on *n*-alkanes as opposed to the wild-type control. Alkenes are the least abundant CHC compound class in female *N. vitripennis*, yet play an important role in male mating behaviour (Wang *et al*., 2022b). *Gfp*-i appears to have a generally downregulating effect on these CHCs as opposed to the wild-type control. Alkene quantity significantly increased in females after *LOC683*-i (**Figure 5D**), whereas they significantly decreased after *LOC760*-i (**Figure 5H**) and *LOC878*-i (**Figure 5L**). *LOC760*-i only affected alkene absolute quantity after silencing at the pupal stage, whereas *LOC878*-i affected alkene absolute quantity after silencing at both the larval and pupal stage. Silencing *LOC760* specifically decreased the compounds Z9-C31ene and Z9-C33ene (**Supplementary Figure 3E-3H**), alkenes that have a *cis* double bond at the ninth carbon atom.

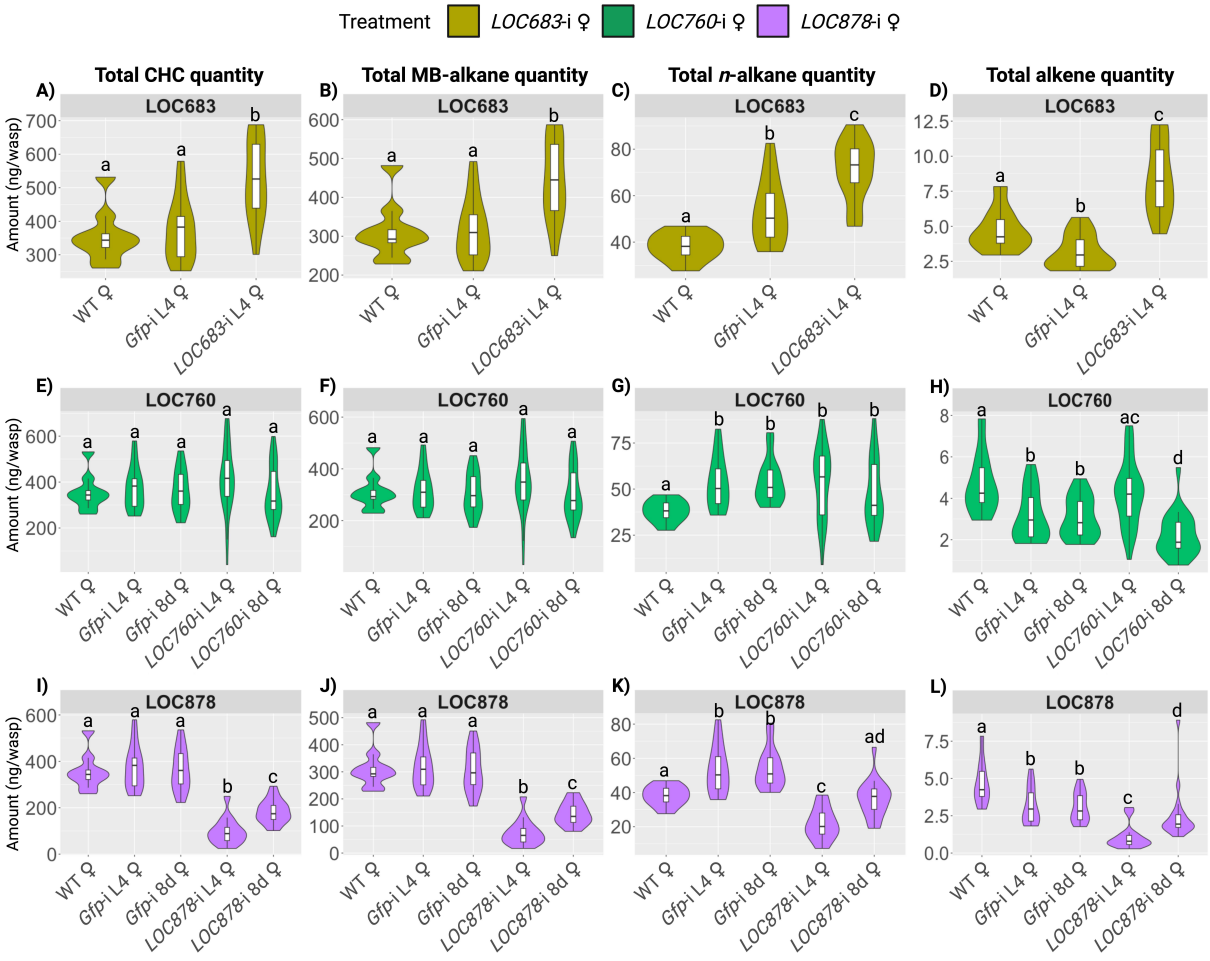

Figure 5: Changes in absolute quantity of CHC compound classes after candidate FAR knockdown in female *N. vitripennis*.

Absolute quantities are shown in violin plots for the total amount of CHCs, methyl-branched alkanes (MB-alkanes), *n*-alkanes and alkenes after silencing *LOC683* (**A-D**), *LOC760* (**E-H**) and *LOC878* (**I-L**) in female *N. vitripennis*. *LOC683* was silenced at the fourth larval (L4) stage (n = 15), and *LOC760* and *LOC878* were silenced at both the L4 stage (n = 36 and n = 14) and eighth-day pupal (8d) stage (n = 22 and n = 19). Wild-type (WT) and *Gfp*-i females (n = 9 and n = 15) were used as control groups. Significant differences ($p < 0.05$) between the treatment groups were assessed with Benjamini-Hochberg corrected Wilcoxon rank-sum tests and are depicted by letters.

Silencing *LOC683*, *LOC760* and *LOC878* also changed the CHC profile of adult male *N. vitripennis* (**Figure 6**). Changes in the overall quantity of CHC compounds are represented in **Figure 6A**, **6E** and **6I**. However, silencing these candidate FARs affected the absolute quantities of the individual CHC compound classes differently when compared with female silenced specimens, depending on the developmental stage at which they were silenced.

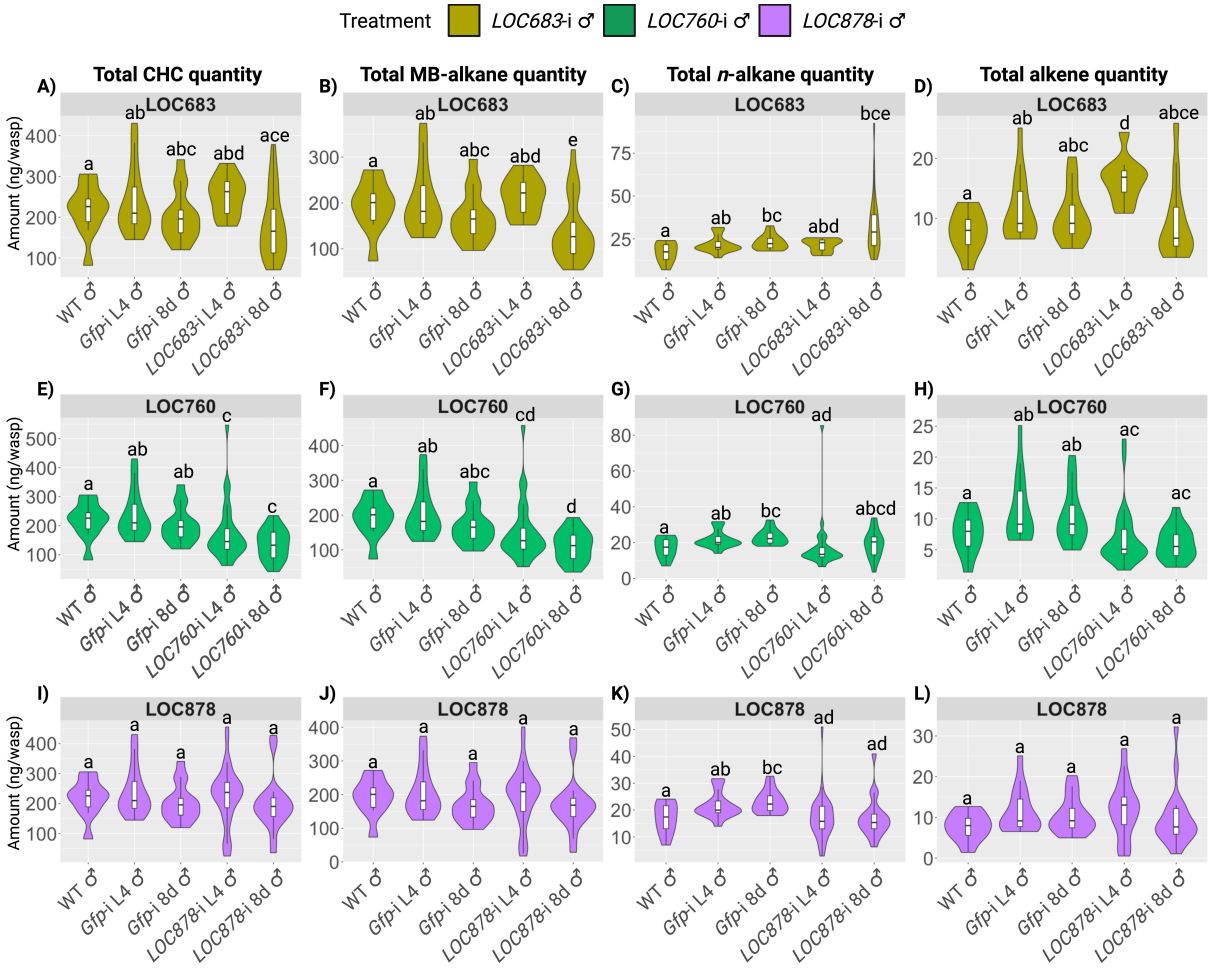

Figure 6: Changes in absolute quantity of CHC compound classes after candidate FAR knockdown in male *N. vitripennis*.

Absolute quantities are shown in violin plots for the total amount of CHCs, methyl-branched alkanes (MB-alkanes), *n*-alkanes and alkenes after silencing *LOC683* (**A-D**), *LOC760* (**E-H**) and *LOC878* (**I-L**) in male *N. vitripennis*. All three candidate FARs were silenced at the fourth larval (L4) stage (n = 10, 28 and 35, respectively) and eighth-day pupal (8d) stage (n = 27, 17 and 19, respectively). Wild-type (WT), *Gfp*-i L4 and *Gfp*-i 8d males (n = 15, 14 and 10, respectively) were used as control groups. Significant differences ($p < 0.05$) between the treatment groups were assessed with Benjamini-Hochberg corrected Wilcoxon rank-sum tests and are depicted by letters.

MB-alkanes, also the dominant CHC compound class in male *N. vitripennis*, remained unaffected after *LOC683*-i at the larval stage, whereas they significantly decreased after silencing at the pupal stage (**Figure 6B**). Specifically, *LOC683*-i at the pupal stage resulted in a significant decrease in the absolute quantities of MB-alkanes with their first methyl branches positioned on the 3rd, 5th, 7th, 9th, 11th and 13th C-atom (**Supplementary Figure 2A-2D**). Unlike in females, *LOC760*-i in males significantly decreased MB-alkanes after silencing at the larval and pupal stage (**Figure 6F**). The downregulation of MB-alkanes in *LOC760*-i also corresponded to lower absolute quantities of MB-alkanes with their first methyl branches positioned on the 3rd, 5th, 7th, 9th, 11th and 13th C-atom (**Supplementary Figure 2E-2H**). *LOC878*-i individuals, on the other hand, remained unaffected in the absolute quantities of

MB-alkanes (**Figure 6J, Supplementary Figure 2I-1L**). The *n*-alkanes, also the second most abundant CHC compound class in males, changed in absolute quantity after silencing the three candidate FARs, although these changes were not significant when compared to either wild-type or *Gfp*-i males (**Figure 6C**, **6G** and **6K**). Alkenes are also the least abundant CHC compound class in male *N. vitripennis*. It has been shown, however, that they are sexually dimorphic (Wang *et al*., 2022b) and occur in greater quantities in males (3.48 ± 1.87 ng) compared to females (2.06 ± 0.68 ng). Interestingly, the absolute quantities of alkenes also significantly increased in males after *LOC683*-i at the larval stage (**Figure 6D**), whereas they remained unaffected after *LOC760*-i (**Figure 6H**) and *LOC878*-i (**Figure 6L**) at both the larval and pupal stage when compared to wild-type or *Gfp*-i males. Silencing *LOC683* significantly increased the absolute quantities of the compounds Z7-C31ene, Z9-C31ene and Z9-C33ene (**Supplementary Figure 4A-4D**).

These results show varying effects on the CHC profile after silencing each candidate FAR and indicate that each FAR plays a sex-specific role at various developmental stages in *N. vitripennis*. Silencing *LOC683* conspicuously upregulates the absolute quantities of all CHC compound classes in females at the larval stage. Silencing this FAR in males, however, specifically affects the alkenes after silencing at the larval stage and the MB-alkanes after silencing at the pupal stage. Silencing *LOC760* at the pupal stage specifically downregulates the absolute quantities of alkenes in females, but has a minor effect on other CHC compound classes. In males, on the other hand, silencing this FAR at the larval and pupal stage specifically downregulated the MB-alkanes. Silencing *LOC878* at the larval and pupal stage conspicuously downregulates the absolute quantities of all CHC compound classes in females, whereas silencing this FAR in males plays only a minor role. These varying effects on the male and female CHC profile after silencing our candidate FARs show that these genes are important components in the CHC biosynthesis pathway for regulating sexual dimorphism in the CHC compound classes of *N. vitripennis*.

Male mating behaviour

Mate recognition in *N. vitripennis* males is initiated through the female CHC profile, which in turn elicits male mating behaviour. We hypothesized that changes to the female CHC profile after silencing each of the four candidate FARs affected male mating behaviour. To verify this, we conducted behavioural assays in which we quantified male mating behaviour in response to the CHCs of dead FAR-silenced female dummies (**Supplementary Table 7**). Wild-type males normally respond to female CHCs by mounting females (through positioning and performing courtship) and then copulating with them. We first confirmed this behaviour in response to *Gfp*-i females (n = 33) and then compared these results with male mating behaviour in response to FAR-silenced females (**Figure 7**).

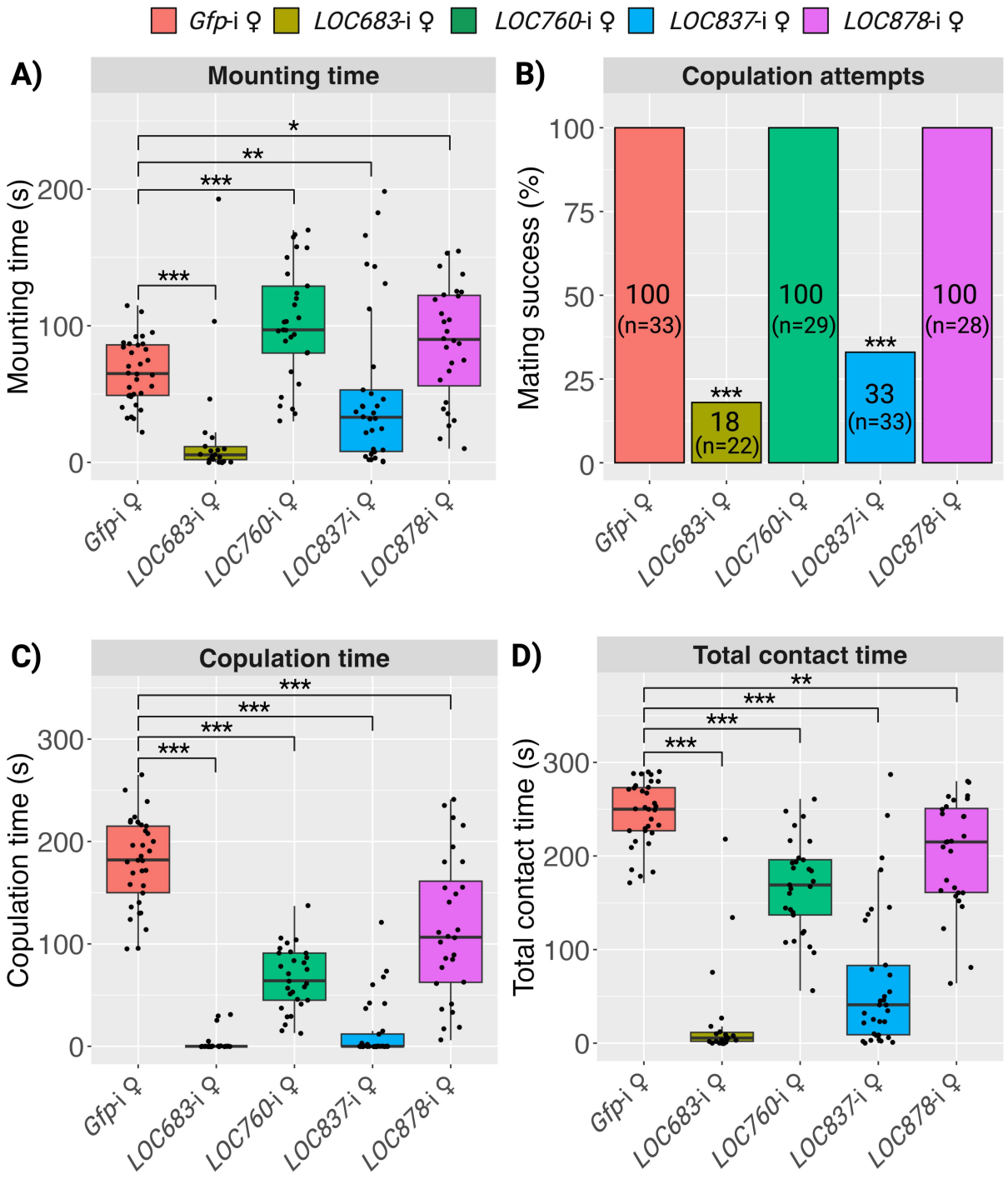

Figure 7: Male mating behaviour in response to CHCs of FAR-silenced females.
Dead FAR-silenced female dummies were introduced to wild-type males in a mating chamber bioassay for a duration of five minutes. Male mating behaviour was quantified and compared with the *Gfp*-i control. **A:** The cumulative amount of time males spent mounting the *Gfp*-i and FAR-silenced females. **B:** The percentage of males attempting to copulate with these specimens. **C:** The cumulative copulation duration. **D:** The total time males spent mounting and copulating the female specimens. Significant differences in mounting and copulation duration were analysed with a Wilcoxon rank-sum test. Significant differences in the percentage of males attempting to copulate were analysed with a Pearson's Chi-squared test. Significance levels: *** = $p < 0.001$, ** = $p < 0.01$ and * = $p < 0.05$.

We determined a change in the duration males spent mounting and copulating in response to the CHC profile of FAR-silenced females. Silencing *LOC683* (n = 22) and *LOC837* (n = 33) in females resulted in a significantly less amount of time males spent mounting (**Figure 7A**; Wilcoxon rank-sum test, $Z = 5.0097$, $p < 0.001$ and $Z = 2.9568$, $p < 0.01$, respectively), which was particularly evident with the *LOC683*-i specimens. This in turn resulted in, firstly, a significantly lower percentage of males attempting to copulate with *LOC683*-i and *LOC837*-i females (**Figure 7B**). In total, 18% of wild-type males attempted to copulate with *LOC683*-i females (Pearson's Chi-squared test, $\chi^2 = 36.505$, $p < 0.001$) and 33% with *LOC837*-i females ($\chi^2 = 30.068$, $p < 0.001$), compared to 100% with *Gfp*-i females. And, secondly, a significantly lower copulation duration for both of these FAR-silenced females (**Figure 7C**; Wilcoxon rank-sum test, $Z = 6.3487$, $p < 0.001$ and $Z = 7.0768$, $p < 0.001$, respectively). Silencing *LOC760* (n = 29) and *LOC878* (n = 28) in females, on the other hand, resulted in a longer amount of time males spent mounting in comparison with the *Gfp*-i control (**Figure 7A**; $Z = -3.6053$, $p < 0.001$ and $Z = -2.2436$, $p < 0.05$, respectively). However, silencing these FARS also resulted in a significantly shorter copulation duration (**Figure 7C**; $Z = 6.5466$, $p < 0.001$ and $Z = 3.6766$, $p < 0.001$, respectively), despite the fact that all males attempted to copulate with these FAR-silenced females (**Figure 7B**). Overall, the total time males spent mounting and copulating was significantly shorter for all FAR-silenced specimens (**Figure 7D**), indicating that all four FARs regulate the production of CHC pheromones and that these genes are integral to male mating behaviour. *LOC683* and *LOC837* clearly have a significant function in producing CHC pheromones that initiate female recognition and courtship behaviour (i.e. mounting, head nodding, etc) in males, whereas the expression of *LOC760* and *LOC878* play a different role, specifically in producing CHC pheromones that affect the duration of the copulatory process.

Discussion

Sex pheromones are chemical substances produced and released into the environment and are used by insects to recognize potential mating partners of the opposite sex and to elicit courtship behaviour (Wyatt, 2014). Many insects, including parasitoids of the genus *Nasonia*, recognize conspecific mating partners based on contact pheromones on the cuticle, known as cuticular hydrocarbons (CHCs) (Blomquist & Ginzel, 2021; Kather & Martin, 2015). Together these chemicals form a specific pheromone, which differs between males and females and is believed to contribute to reproductive isolation between species (Chung & Carroll, 2015). To date, the main focus of research has been aimed at identifying the genes involved in insect CHC production (Holze *et al*., 2021), but only limited research has been carried out into how these genes are specifically regulated to produce sexually dimorphic CHC profiles for mate recognition (Wang *et al*., 2025). In order to produce sexually dimorphic CHC profiles, genes that biosynthesize CHCs are more prone to rapid evolutionary change (Chung *et al*., 2014; Combs *et al*., 2018; Shirangi *et al*., 2009). Within the CHC production pathway, a group of candidate genes that are more inclined to undergo such evolutionary change belong to the fatty acyl-CoA reductases (FARs) (Finet *et al*., 2019). These are key enzymes in the synthesis of fatty alcohols, the precursors for CHC production (Riendeau & Meighen, 1985). In this chapter, we identified four candidate FARs in *N. vitripennis* that are potentially targeted by Doublesex, a transcription factor of the sex-determination pathway.

After analysing gene expression, we successfully used RNAi to silence four candidate FARs in male and female *N. vitripennis*. After silencing, we determined a change in the overall CHC composition in both males and females. The change in female CHC composition also clearly affected male mating behaviour. As a result, our study demonstrates for the first time that FARs play a crucial role in *Nasonia*, not only in the production process of CHCs, but also specifically in producing the pheromone compounds that elicit male mating behaviour. Our results have identified a group of genes in *N. vitripennis* that are targeted by the sex-determination pathway and which are potentially responsible for the evolution of sexually dimorphic CHC profiles and by extension for the specific variations between closely related *Nasonia* species.

We determined that the candidate FARs in our study are sex biased and showed peak expression levels during specific developmental time windows. Many insect FARs are known to catalyse distinct fatty acyl-CoA substrates, which show variation in chain length and degree of saturation (Zhang *et al*., 2021). Many moth species, for example, express FARs in pheromone glands that act on fatty acyls of various chain lengths to produce pheromone precursors (Carot-Sans *et al*., 2015; Lassance *et al*., 2010; Liénard *et al*., 2010; Moto *et al*., 2003). We can therefore conclude that the timing of FAR activity is dependent on the presence of their associated fatty acyl-CoA substrates. Moreover, FAR expression in *Nasonia* should also correspond to the catalytic activity of the FARs in order to convert their particular fatty acyl-CoA substrates. Consequently, we can now investigate which fatty acyl-CoA

substrates are processed in *Nasonia* and how FARs coordinate their function with each other and other enzymes in the CHC production pathway.

After successfully silencing the four candidate FARs, we confirmed a lethal phenotype following suppression of *LOC683* expression. The *LOC683*-silenced specimens failed to shed their pupal exuviae, and consequently expand their wings and develop the typically rigid abdomen of an adult wasp. Our observations are in line with a study on the planthopper *Nilaparvata lugens*, which failed to shed its exuviae during moulting after supressing the expression of various FARs (Li *et al*., 2020). The cuticle of insects is made up of a waxy layer, composed of lipids. These lipids include hydrocarbons, fatty acids, alcohols, aldehydes, ketones and esters (Gołębiowski & Stepnowski, 2022). In many insects, these lipids contribute to cuticular hardening and rigidity by impregnating the inner layers of the cuticle (Hendricks & Hadley, 1983; Kawase, 1961; Wigglesworth, 1970). After silencing *LOC683*, we also observed a change in the coloration of the cuticle from a normal metallic green colour in wild-types to a blueish hue in our silenced specimens. The lipid composition of the insect waxy layer is able to form light-scattering structures with strong reflective properties (Futahashi *et al*., 2019). It is therefore reasonable to assume that silencing *LOC683* in *N. vitripennis* modified the lipid composition of the waxy layer that is normally required for cuticle integrity. We hypothesize that *LOC683* affects cuticular properties by producing long-chain lipids incorporated into the waxy layer for cuticular hardening and rigidity.

Fatty acyl-CoA reductases play an integral part in the CHC production pathway, by metabolizing long-chain fatty acids into fatty alcohols (Holze *et al*., 2021). In this study, we demonstrated the function of *LOC683, LOC760* and *LOC878* in generating sexual dimorphism in the CHC profile of *N. vitripennis*. Knocking down these FARs coincided with the concomitant upregulation or downregulation of components of the specific CHC compound classes. Each knockdown affected the CHC profile differently between sexes and therefore demonstrates that each FAR plays a sex-specific role in metabolizing CHC compounds. Silencing *LOC683* and *LOC760* in males specifically affected MB-alkanes and alkenes, depending on the developmental stage of silencing, whereas silencing *LOC878* had no significant effect at all. In females, most notable was the upregulation and downregulation of all the CHC compound classes after silencing *LOC683* and *LOC878*, respectively. Silencing *LOC760*, on the other hand, affected only a number of MB-alkane and alkene compounds. MB-alkanes form the predominant component of the CHC profile in *Nasonia* (Buellesbach *et al*., 2022) and other parasitoid wasps (Kather & Martin, 2015). The universal effect of silencing *LOC683* and *LOC878* in females and *LOC683* and *LOC760* in males on all MB-alkanes indicates that all three FARs play a major role in determining the CHC composition in *N. vitripennis*. Our results are in line with other studies on *Nasonia* and *Drosophila* that emphasize the important function of FARs in determining CHC composition (Buellesbach *et al*., 2022; Rusuwa *et al*., 2022). We hypothesize that our candidate FARs are important in the CHC production pathway for producing a sexually dimorphic CHC profile in *N. vitripennis*.

Many Hymenoptera, including *Nasonia* parasitoids, rely on CHCs for close-range sexual communication (Kather & Martin, 2015; Mair & Ruther, 2019). They function as contact pheromones used for attracting conspecific mating partners, initiating courtship and copulation (Buellesbach *et al*., 2018) and as a means to signal receptivity, mating status and fertility (Billeter & Wolfner, 2018). Silencing our candidate FARs modified the CHC composition in females and affected mate recognition for males. The most prominent effect on male mating behaviour was observed after silencing *LOC683* and *LOC837* in females. These female specimens were mounted significantly less when compared to our control. Although we failed to quantify the CHC profile in females after silencing *LOC837*, we hypothesize a change in CHC composition in these specimens similar to *LOC683*-silenced females. MB-alkanes were considerably upregulated in our *LOC683*-silenced specimens and are known to function as mate-recognition pheromones in female *N. vitripennis* (Sun *et al*., 2023b). In our study, however, alkenes also increased in females after silencing *LOC683,* mirroring the alkene profile in wild-type males. Interestingly, these CHCs are also known to function as pheromones for inhibiting male-male courtship (Wang *et al*., 2022b). We therefore conclude that the significantly shorter time males spent mounting the *LOC683*- and *LOC837*-silenced specimens was due to the increase in alkenes rather than the increase in MB-alkanes. The opposite effect was observed after silencing *LOC760* and *LOC878* in females, which were mounted for a significantly longer time by males when compared to control females. Alkenes were significantly decreased in these female specimens, which made the CHC profile more sexually attractive for males. Surprisingly, we also observed that males spent a significantly shorter time attempting to copulate with these specimens when compared to control females. It has been observed that in Diptera, including *Drosophila*, CHCs also influence the time males spend copulating (Jois *et al*., 2022). We can therefore confirm that each of our four candidate FARs plays a specific role in regulating the CHCs that influence male mating behaviour in *N. vitripennis*.

We conclude that the fatty acyl-CoA reductases LOC683, LOC760, LOC837 and LOC878, regulate sexual dimorphism in the CHC profile of *N. vitripennis*. The CHCs that these enzymes regulate play an important role in mate recognition and the initiation of male courtship and copulation. To our knowledge, our study is the first to identify the function of FARs in the CHC production pathway in Hymenoptera species. Our results serve as a basis for future studies investigating the specific function of these FARs in metabolizing lipids for CHC production and their role in development and survival. We hypothesize that these genes provide an important mechanism for producing a sexually dimorphic CHC profile to ensure reproductive isolation between closely related parasitoid species. Future studies should address how sex-determination transcription factors, such as Doublesex, influence the process of CHC diversification by analysing the precise mechanism by which this transcription factor regulates the expression of these FARs between sexes. Investigating the genetic pathways involved in the production of CHCs in parasitoid wasps is important as these species are invaluable for both natural and agriculture ecosystems.

Acknowledgements

We would like to thank the research assistants at the Institute for Evolution and Biodiversity at the University of Münster, Germany, for carrying out extractions of cuticular hydrocarbons and GC-MS analysis on our FAR-silenced specimens. We are also grateful for the feedback on this chapter provided by Marcel Dicke.

Supplementary information

Supplementary Table 1: FAR-specific primers used in this study.
Table shows the sequences for the FAR-specific primers used in our dsRNA and qPCR experiments.

Target	Region	Primer	Sequence
LOC100117683	Exon3-4	F_RNAi_L683	5-TGGATGGACGACAGTCTC-3
		F_RNAi_L683_T7	5-[TAATACGACTCACTATAGGG]ACGACAGTCTCGTGG-3
		R_RNAi_L683	5-GGGACGATGTGCTGGAA-3
		R_RNAi_L683_T7	5-[TAATACGACTCACTATAGGG]AGACCACCATGTCCA-3
	Exon1-2	Fq_LOC683	5-TTGCTCAATGCTCCCCTGTT-3
		Rq_LOC683	5-CCACCGGCACGATTTTCAAC-3
LOC100117760	Exon2-4	F_RNAi_L760	5-CAGGATCAACTTGTGCGG-3
		F_RNAi_L760_T7	5-[TAATACGACTCACTATAGGG]ATCAACTTGTGCGGA-3
		R_RNAi_L760	5-CGTGGATACCAGGCTACG-3
		R_RNAi_L760_T7	5-[TAATACGACTCACTATAGGG]ATACCAGGCTACGGA-3
	Exon5-6	Fq_LOC760	5-GCACCAGGACCTACTTCCAC-3
		Rq_LOC760	5-AGCCCGGTGAAACTCAAGAC-3
LOC100117837	Exon4-6	F_RNAi_L837	5-CGAATGGATGGAAGACGAG-3
		F_RNAi_L837_T7	5-[TAATACGACTCACTATAGGG]ATGGAAGACGAGGTC-3
		R_RNAi_L837	5-GTATCATGTGGAAGAAGAGC-3
		R_RNAi_L837_T7	5-[TAATACGACTCACTATAGGG]AAGAAGAGCACGCAG-3
	Exon1-2	Fq_LOC683	5-CAGGCCGAAAAAGGGCAAAG-3
		Rq_LOC683	5-CCTTTTCGAACAACGCCGAG-3
LOC100117878	Exon2-5	F_RNAi_L878	5-TCTGGATATGGCAAAGAC-3
		F_RNAi_L878_T7	5-[TAATACGACTCACTATAGGG]ATATGGCAAAGACAC-3
		R_RNAi_L878	5-CTGGATACCATATTGCAC-3
		R_RNAi_L878_T7	5-[TAATACGACTCACTATAGGG]ATACCATATTGCACC-3
	Exon3-4	Fq_LOC878	5-CGCACGTCCTTCAATCGTTAC-3
		Rq_LOC878	5-CGAAGCTCCTTGGAAATTGCT-3
GFP		GFP_RNAi_F	5-GTGACCACCTTGACCTACG-3
		GFP_RNAi_F_T7	5-[TAATACGACTCACTATAGGG]GTGACCACCTTGACCTACG-3
		GFP_RNAi_R	5-TCTCGTTGGGGTCTTTGCT-3
		GFP_RNAi_R_T7	5-[TAATACGACTCACTATAGGG]TCTCGTTGGGGTCTTTGCT-3

Supplementary Table 2: Relative expression of the four candidate FARs between sexes and developmental stages.
Relative expression of the four candidate FARs was calculated using the delta-delta Ct method. *EF1α*, *AK3* and *RP49* were used as reference genes. This table can be accessed online at:
https://git.wur.nl/aidan.williams/chapter6/-/blob/main/Supplementary_Table_2.csv?ref_type=heads

Supplementary Table 3: Statistical output of a two-way ANOVA on FAR relative expression.
Table shows the influence of sex and developmental time on the relative expression of the four candidate FARs. Significance levels: *** = p < 0.001, * = p < 0.05.

LOC683	Df	Sum Sq	Mean Sq	F value	Pr(>F)	
day	2	0.004	0.002	0.011	0.989327	
sex	1	3.009	3.009	16.027	0.000299	***
day:sex	2	7.422	3.711	19.769	0.00000161	***
Residuals	36	6.758	0.188			

LOC760	Df	Sum Sq	Mean Sq	F value	Pr(>F)	
day	2	6.226	3.113	13.061	0.0000543340406	***
sex	1	19.845	19.845	83.264	0.0000000000676	***
day:sex	2	4.250	2.125	8.916	0.000716	***
Residuals	36	8.580	0.238			

LOC837	Df	Sum Sq	Mean Sq	F value	Pr(>F)	
day	2	180.76	90.38	388.529	< 0.0000000000000002	***
sex	1	1.60	1.60	6.885	0.0127	*
day:sex	2	15.00	7.50	32.240	0.00000000946	***
Residuals	36	8.37	0.23			

LOC878	Df	Sum Sq	Mean Sq	F value	Pr(>F)	
Day	2	74.89	37.45	2015.84	< 0.0000000000000002	***
Sex	1	0.31	0.31	16.59	0.000244	***
Day:sex	2	5.40	2.70	145.37	< 0.0000000000000002	***
Residuals	36	0.67	0.02			

Supplementary Table 4: Statistical output of a THSD test on FAR relative expression.
Table shows the significancy of the differences in relative expression of the candidate FARs between sexes and developmental stages. This table can be accessed online at:
https://git.wur.nl/aidan.williams/chapter6/-/blob/main/Supplementary_Table_4.csv?ref_type=heads

Supplementary Table 5: Relative expression of the four candidate FARs after RNAi.
Relative expression of the four candidate FARs was calculated using the delta-delta Ct method and compared to the *Gfp*-i control. *EF1α* and *RP49* were used as reference genes. This table can be accessed online at:
https://git.wur.nl/aidan.williams/chapter6/-/blob/main/Supplementary_Table_5.csv?ref_type=heads

Supplementary Table 6: Absolute quantities of CHC compounds.
Absolute quantities of all CHC compounds identified in all dsRNA-treated male and female specimens. This table can be accessed online at:
https://git.wur.nl/aidan.williams/chapter6/-/blob/main/Supplementary_Table_6.csv?ref_type=heads

Supplementary Table 7: Male mating behavioural data.
Table shows the cumulative time males spent mounting and attempting to copulate a FAR-silenced female dummy. It also shows the number of males that attempted to copulate and the total contact time males spent interacting with the FAR-silenced female dummy. This table can be accessed online at:
https://git.wur.nl/aidan.williams/chapter6/-/blob/main/Supplementary_Table_7.csv?ref_type=heads

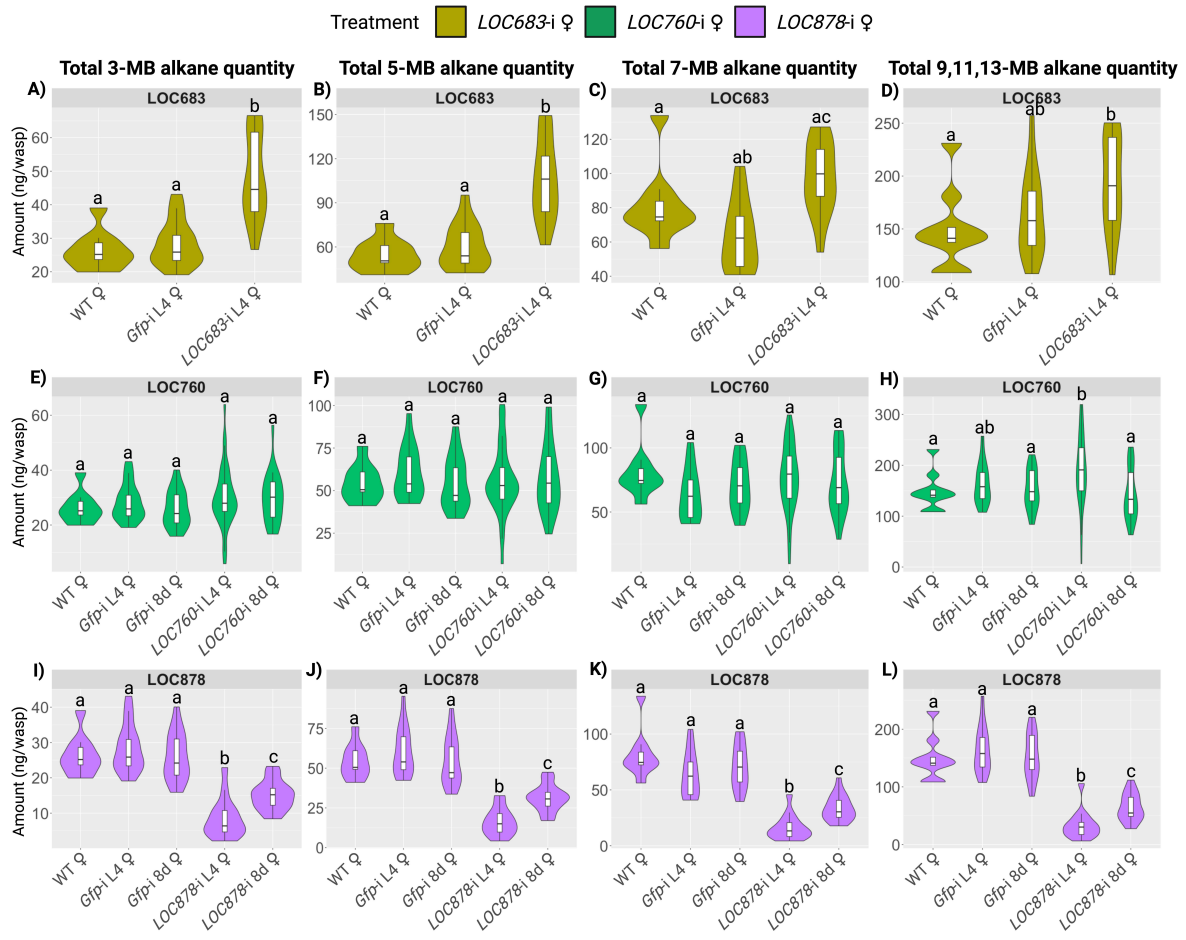

Supplementary Figure 1: Changes in absolute quantity of methyl-branched alkanes after candidate FAR knockdown in female *N. vitripennis.*

Absolute quantities are shown in violin plots for the total amount of methyl-branched alkanes with their first methyl branches positioned on the 3rd, 5th, 7th, 9th, 11th and 13th C-atom, after silencing *LOC683* (**A-D**), *LOC760* (**E-H**) and *LOC878* **(I-L**) in female *N. vitripennis. LOC683* was silenced at the fourth larval (L4) stage, and *LOC760* and *LOC878* were silenced at the fourth larval and eighth-day pupal (8d) stages. Wild-type (WT) and *Gfp*-i females were used as control groups. Significant differences ($p < 0.05$) between the treatment groups were assessed with Benjamini-Hochberg corrected Wilcoxon rank-sum tests and are depicted by letters.

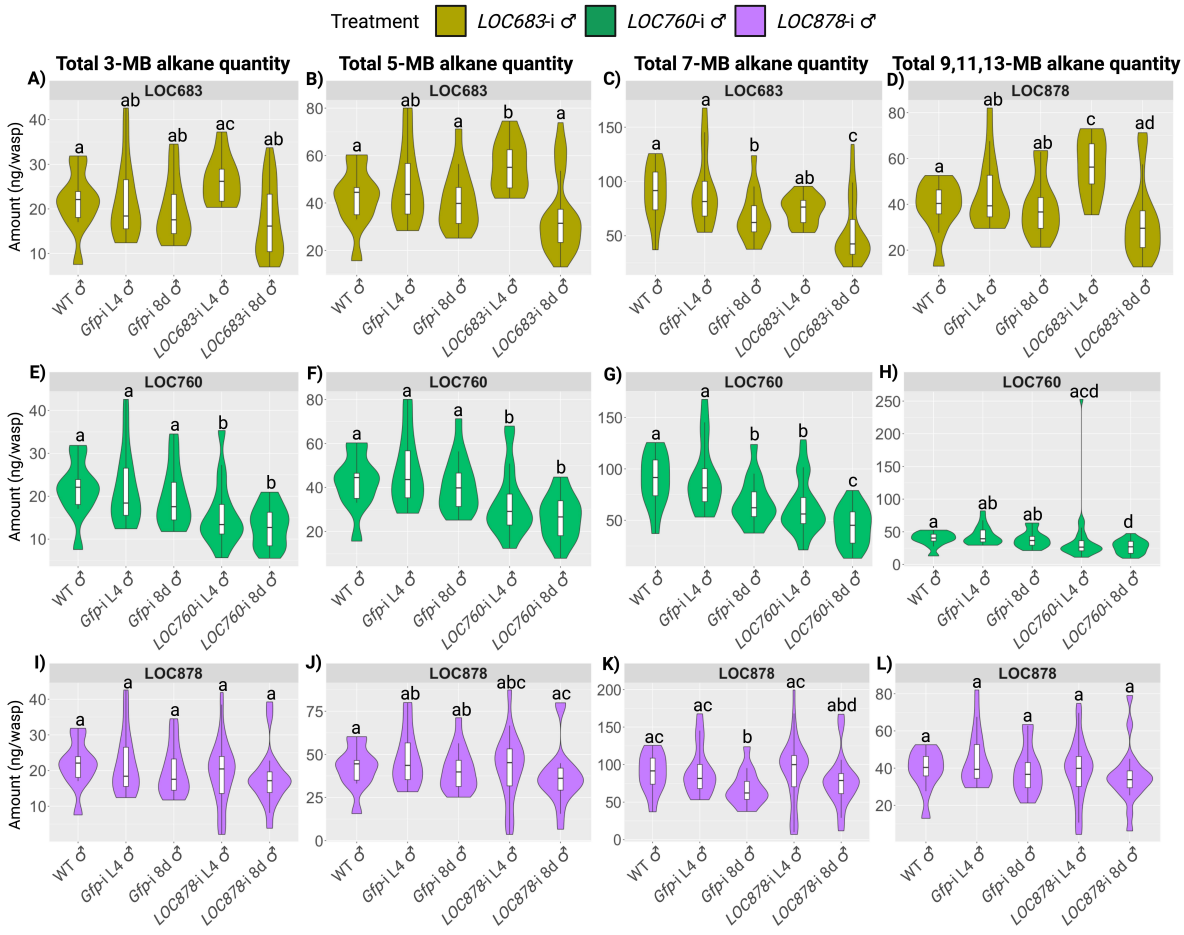

Supplementary Figure 2: Changes in absolute quantity of methyl-branched alkanes after candidate FAR knockdown in male *N. vitripennis*.

Absolute quantities are shown in violin plots for the total amount of methyl-branched alkanes with their first methyl branches positioned on the 3rd, 5th, 7th, 9th, 11th and 13th C-atom, after silencing *LOC683* (**A-D**), *LOC760* (**E-H**) and *LOC878* (**I-L**) in male *N. vitripennis*. All three candidate FARs were silenced at the fourth larval (L4) and eighth-day pupal (8d) stages. Wild-type (WT) and *Gfp*-i males were used as control groups. Significant differences ($p < 0.05$) between the treatment groups were assessed with Benjamini-Hochberg corrected Wilcoxon rank-sum tests and are depicted by letters.

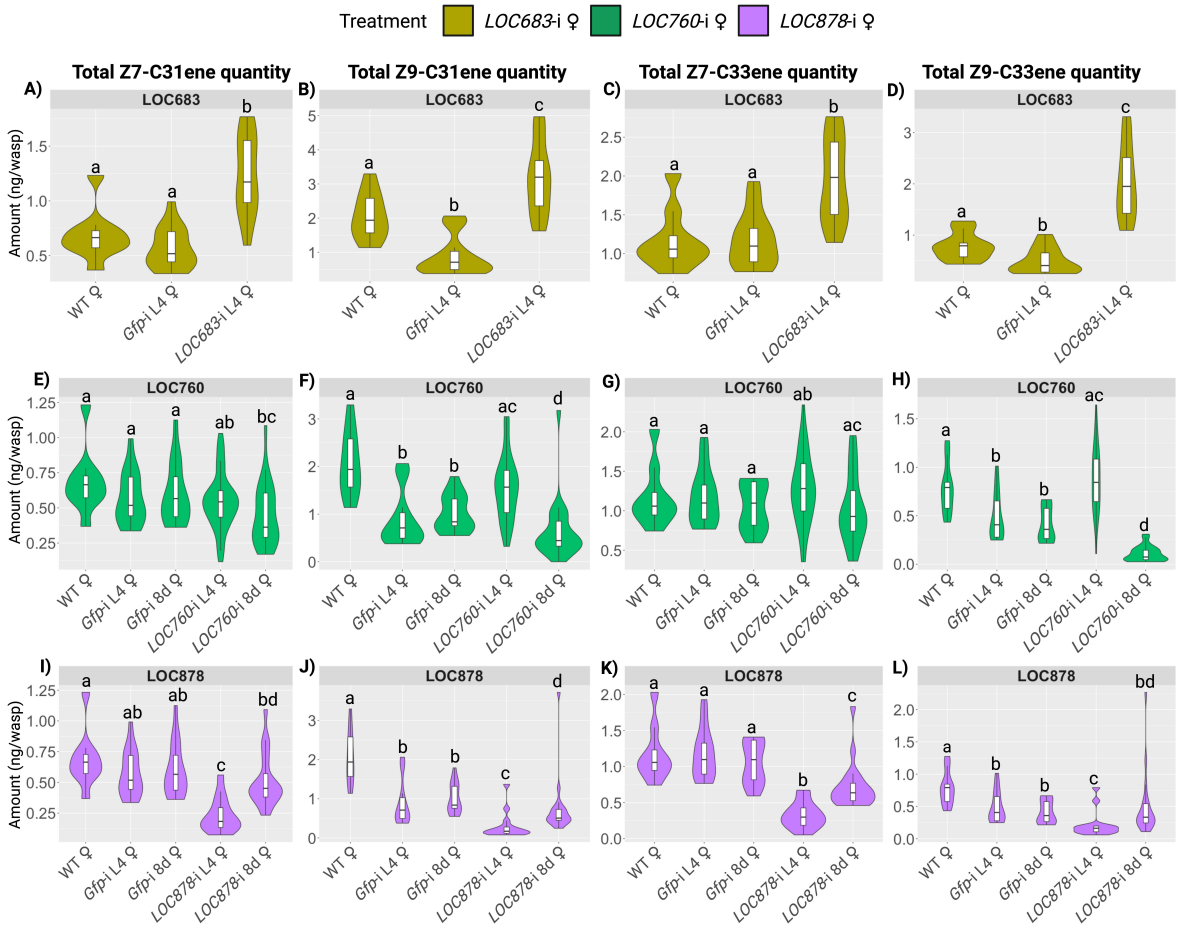

Supplementary Figure 3: Changes in absolute quantity of alkenes after candidate FAR knockdown in female *N. vitripennis*.

Absolute quantities are shown in violin plots for the total amount of the alkene compounds Z7-C31ene, Z9-C31ene, Z7-C33ene and Z9-C33ene, after silencing *LOC683* (**A-D**), *LOC760* (**E-H**) and *LOC878* **(I-L**) in female *N. vitripennis. LOC683* was silenced at the fourth larval (L4) stage, and *LOC760* and *LOC878* were silenced at the fourth larval and eighth-day pupal (8d) stages. Wild-type (WT) and *Gfp*-i females were used as control groups. Significant differences ($p < 0.05$) between the treatment groups were assessed with Benjamini-Hochberg corrected Wilcoxon rank-sum tests and are depicted by letters.

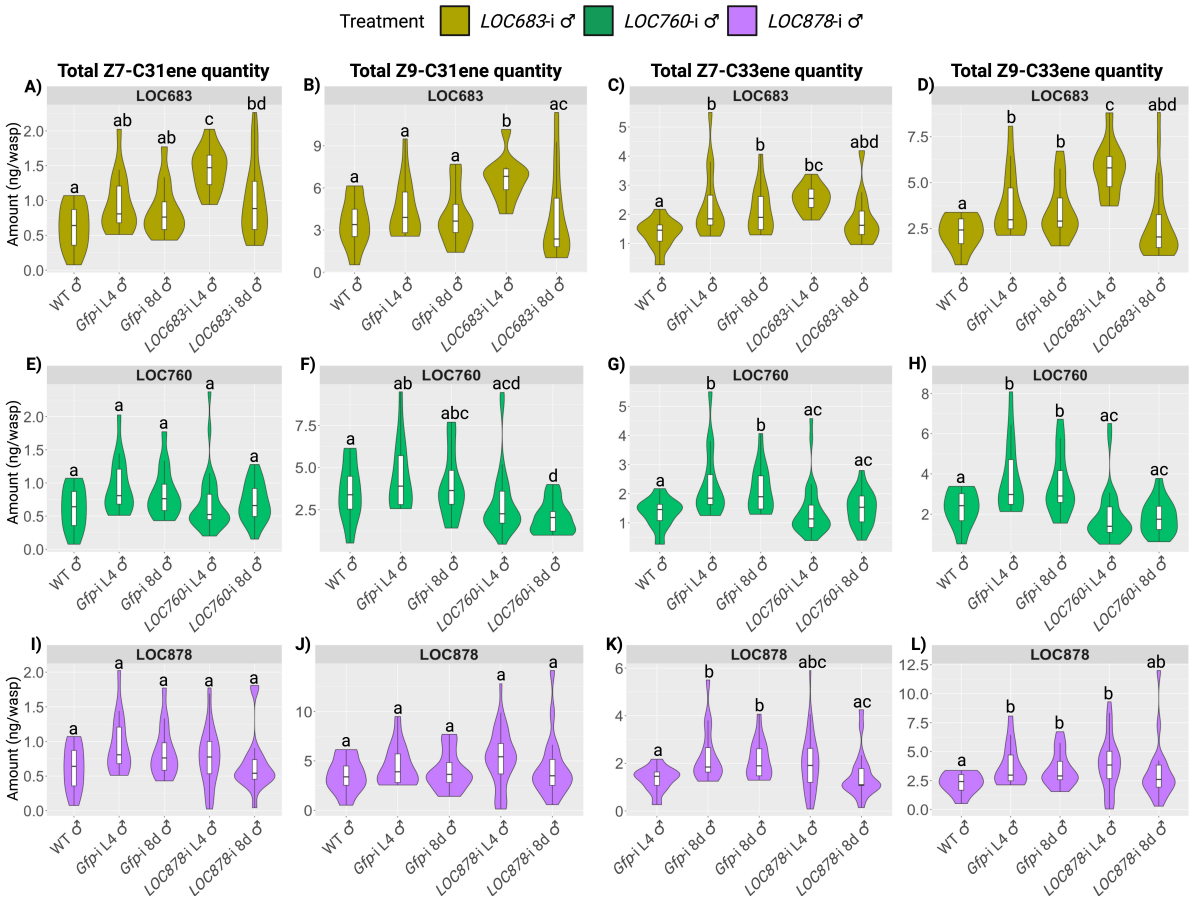

Supplementary Figure 4: Changes in absolute quantity of alkenes after candidate FAR knockdown in male *N. vitripennis*.

Absolute quantities are shown in violin plots for the total amount of the alkene compounds Z7-C31ene, Z9-C31ene, Z7-C33ene and Z9-C33ene, after silencing *LOC683* (**A-D**), *LOC760* (**E-H**) and *LOC878* (**I-L**) in male *N. vitripennis*. All three candidate FARs were silenced at the fourth larval (L4) and eighth-day pupal (8d) stages. Wild-type (WT) and *Gfp*-i males were used as control groups. Significant differences ($p < 0.05$) between the treatment groups were assessed with Benjamini-Hochberg corrected Wilcoxon rank-sum tests and are depicted by letters.

Chapter 7

General discussion

General discussion

Chemical signalling is the most ancient and universal form of animal communication (Wyatt, 2014). It continues to evolve and remains a potent driver of mate choice and speciation (Johansson & Jones, 2007). However, we are only now beginning to grasp how the production and perception of chemical signals are actually coordinated as a coevolutionary process (Steiger *et al*., 2011). Insects use sex pheromones to choose potential mates and to distinguish these from closely related species through variations in their specific pheromone blends (Baker, 2002; Fleischer & Krieger, 2018; Johansson & Jones, 2007; Steiger *et al*., 2011; Symonds & Elgar, 2008). Pheromones can evolve from any chemical precursor compound that is released by one individual and detected by another individual of the same species. These compounds were either by-products of normal metabolic pathways or had a non-communicative function (Stökl & Steiger, 2017; Tillman *et al*., 1999). If perceiving these compounds leads to greater reproductive success, sexual selection can act on improving selectivity and sensitivity in the receiver and on increasing pheromone production in the sender. This process results in assortative mating and sexual dimorphism in pheromone signalling, where mate choice is based on sender-receiver preferences (Buchinger & Li, 2023; Johansson & Jones, 2007; Steiger & Stökl, 2014). However, we currently have only a limited understanding of the underlying genetic mechanisms on which the forces of sexual selection operate. It is therefore necessary to investigate the sex-specific regulation of pheromone production and perception in order to explain the evolutionary transitions in insect male-female pheromone communication.

Insect pheromone communication is typically sexually dimorphic. Males and females may produce different pheromones and have distinct chemosensory receptors to perceive them, or they may produce the same pheromone and have the same receptor, but a sexually dimorphic neural circuit to process the information. Sexual differentiation in these traits is regulated by the sex-determination pathway (Billeter *et al*., 2006a; Ferveur *et al*., 1997; Savarit & Ferveur, 2002). Most insects share a common sex-determination mechanism, comprising a conserved binary switch or splicing-factor gene, called *Transformer* (*Tra*), and the transcription-factor gene, *Doublesex* (*Dsx*) (Verhulst *et al*., 2010b; Verhulst & van de Zande, 2015). Sex-determination transcription factors are important for regulating biosynthesis, chemoreception and neurodevelopment in insect pheromone communication (Bray & Amrein, 2003; Kimura *et al*., 2008; Kurtovic *et al*., 2007; Shirangi *et al*., 2009; Sun *et al*., 2023a; Zhou *et al*., 2014). Research on how these transcription factors regulate these pathways has primarily focused on the model organism *Drosophila*. These insects perceive pheromones through dedicated neural circuits, called labelled lines. Insects such as Hymenoptera, on the other hand, have evolved a combinatorial-coding system to discriminate pheromones (Brandstaetter & Kleineidam, 2011; Carcaud *et al*., 2015; Couto *et al*., 2017, 2023; d'Ettorre *et al*., 2017; Galizia & Rössler, 2010; Joerges *et al*., 1997; Marty *et al*., 2025; McKenzie *et al*., 2016; McKenzie & Kronauer, 2018; Sandoz *et al*., 2007; Wang *et al*.,

2008; Yamagata *et al*., 2006; Zube *et al*., 2008). However, how this coding system evolves at the molecular level of sex determination remains unknown in these species.

The central objective of this thesis was to elucidate the genetic mechanisms by which sex-determination genes are involved in regulating sexual dimorphism in the pheromone communication system of the parasitoid wasp *Nasonia vitripennis*. I first presented a comprehensive literature review and explored the underlying sex-determination mechanisms that regulate the development of sexually dimorphic neural circuits in insects. I also discussed the neurodevelopmental mechanisms unique to Hymenoptera before turning to the model organism *N. vitripennis* (**Chapter 2**). In this species, I silenced the genes responsible for male and female differentiation with RNA interference (RNAi): *Dsx* in males and *Tra* in females. I focused on sexual dimorphism in both pheromone perception and processing by investigating the sex-determination mechanisms that regulate the development of sensory organs and glomeruli in the antennal lobe (AL) (**Chapters 3 and 4**). I subsequently examined the regulation of sexually dimorphic cuticular hydrocarbon (CHC) production (**Chapter 5**) and the role of biosynthetic genes downstream of the sex-determination pathway (**Chapter 6**). The key findings of this thesis will now be interpreted and contextualized within the existing body of knowledge on insect sexual differentiation.

A unique sense of smell

Based on the current consensus of published research, I presented a theoretical framework in **Chapter 2** in which sexual dimorphism in the insect olfactory system evolves in the light of sexual differentiation (Williams *et al*., 2022). My review showed that the development of sexually dimorphic pheromone circuits is most likely initiated in the peripheral nervous system through the expression of pheromone receptors in specialized sensilla. Subsequently, during neuronal development, the process of programmed cell-death regulation determines olfactory sensory neuron (OSN) survival, which is necessary for establishing functional connections in the AL and other brain regions (Prieto-Godino *et al*., 2020). I highlighted the importance of *Dsx* and *Fruitless* (*Fru*) for determining sexual dimorphism of these neurons by regulating downstream genes, such as programmed cell-death-inducing genes for neuronal survival and axon-guidance genes for neurite development (Kimura *et al*., 2005, 2008). I propose investigating whether these sex-specific mechanisms are conserved in species that use different pheromone-coding systems from *Drosophila*, such as Hymenoptera.

My published review also presented the perceptional and processing properties unique to Hymenoptera (Williams *et al*., 2022). These species typically use a specialized sensillum subsystem consisting of basiconic sensilla for perceiving CHCs as cues for recognizing nestmates, mating partners and hosts (Couto *et al*., 2017; Kropf *et al*., 2014; Ozaki *et al*., 2005). The intricate life histories of Hymenoptera also served as a driver for the expansion of their OR repertoire (Legan *et al*., 2021; McKenzie *et al*., 2016; McKenzie & Kronauer, 2018; Robertson *et al*., 2010; Zhou *et al*., 2015) and the number of glomeruli in the AL (Arnold *et al*.,

1985; Couto *et al*., 2023; Groothuis *et al*., 2019; McKenzie *et al*., 2016; Zube & Rössler, 2008). It has been shown that one such subfamily of the OR repertoire, the 9-exon ORs, has dramatically expanded in ants, social wasps and parasitoids, including *Nasonia* (Engsontia *et al*., 2015; Legan *et al*., 2021; McKenzie *et al*., 2016; Slone *et al*., 2017; Zhou *et al*., 2015). These ORs are exclusively expressed in basiconic sensilla and respond to CHCs (Ozaki *et al*., 2005; Renthal *et al*., 2003). Sensory neurons expressing these ORs innervate a glomerular subsystem specialized in processing CHCs (Couto *et al*., 2017; Legan *et al*., 2021; McKenzie *et al*., 2016). These evolutionary transitions were necessary in order to meet the increased demand for olfactory discrimination and enabled the development of specific pheromone-processing adaptations in Hymenoptera species (**Figure 1**).

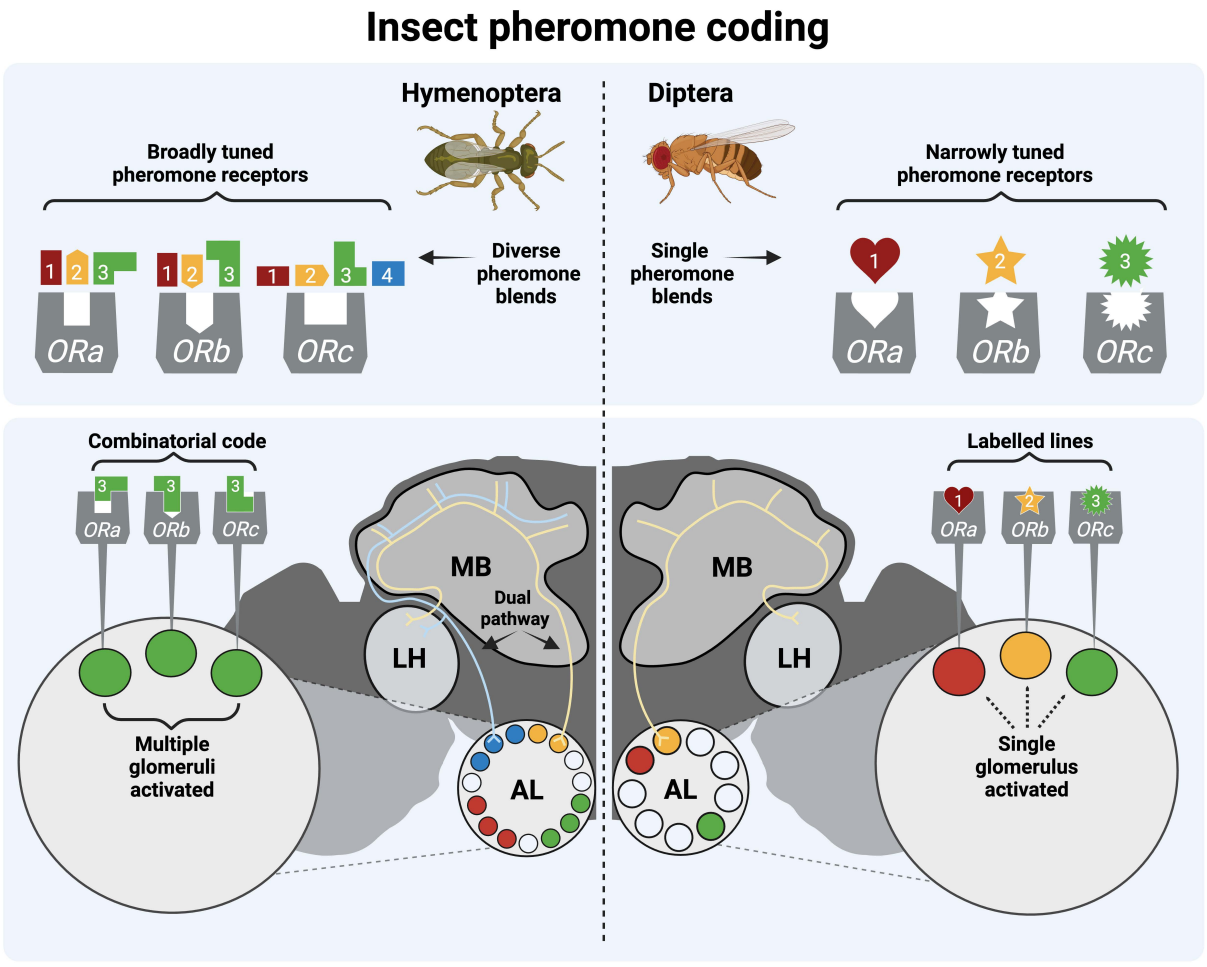

Figure 1: Pheromone-coding in Hymenoptera and Diptera.
Hymenoptera, such as *N. vitripennis*, have evolved broadly tuned pheromone receptors to perceive a wide variety of pheromone blends, whereas Diptera, such as *Drosophila,* utilize narrowly tuned pheromone receptors to perceive single pheromone blends. The relatively high number of olfactory receptors (ORs) in Hymenoptera is reflected in the higher number of glomeruli in the antennal lobe (AL) of these species. Hymenoptera process pheromones through combinatorial codes, where a single pheromone compound can activate multiple ORs and glomeruli. Diptera utilize labelled lines for pheromones, where a single OR and glomerulus are tuned to a single pheromone compound. Moreover, Hymenoptera possess a dual olfactory pathway connecting the AL with the lateral horn (LH) and mushroom body (MB). This enables olfactory information to be processed in parallel and provide enhanced odour-processing capabilities in these species.

Drosophila, on the other hand, typically process pheromones through so-called dedicated labelled lines, where a single receptor and glomerulus are specifically tuned to a single pheromone (Keesey & Hansson, 2021; Kurtovic *et al*., 2007). Complex pheromones in Hymenoptera, conversely, require olfactory discrimination through combinatorial codes, where combinations of receptors and glomeruli are tuned to a specific pheromone (Carcaud *et al*., 2015; Couto *et al*., 2023; d'Ettorre *et al*., 2017; Joerges *et al*., 1997; Marty *et al*., 2025; Sandoz *et al*., 2007; Yamagata *et al*., 2006; Zube *et al*., 2008).

In **Chapter 2**, I also compared the specific processes responsible for AL formation in Diptera, Lepidoptera and Hymenoptera. I concluded that Hymenoptera have evolved unique neurodevelopmental mechanisms. I discussed how these species rely on OSN innervation for refining glomerular development necessary for combinatorial coding. This evolutionary adaptation increases the likelihood of modifications in AL morphology, specifically in the number of glomeruli. The *Olfactory-receptor co-receptor* (*Orco*) plays a crucial role in this adaptation in regulating OSN development (Sieriebriennikov *et al*., 2024). These novel adaptations therefore make Hymenoptera ideal model species for investigating how sexual differentiation and neurodevelopment are closely interlinked with the evolution of pheromone communication. The experimental research in this thesis on the parasitoid *N. vitripennis* provides compelling evidence that sex-determination transcription factors are integral to this evolutionary process.

Neuroplasticity

Insects have developed specialized sensory systems with distinct physiological features to perceive pheromones (Hansson & Stensmyr, 2011). Sensilla on the antennae possess OSNs that express ORs tuned to these pheromones (Ozaki *et al*., 2005; Van der Goes van Naters & Carlson, 2007; Zacharuk, 1980). Like all insects, *N. vitripennis* has evolved a specific set of sensilla necessary for its chemical ecology. Although the physiological responses of sensilla to odours have yet to be determined in parasitoids, I used electron microscopy scans to identify olfactory sensilla based on their morphological characteristics. The predominance of a certain sensillum type corresponds to its relative importance for perceiving ecologically relevant chemicals, such as pheromones or host cues (**Chapter 2**). The type and morphology of sensilla are regulated by neurodevelopmental pathways, which in themselves can be sexually dimorphic (Luecke *et al*., 2022; Mellert *et al*., 2010, 2012). The most abundant olfactory sensilla on the antennae of *N. vitripennis* are the sexually dimorphic trichoid and placoid sensilla. My experimental results in **Chapter 3** determined for the first time in a hymenopteran species how TRA and DSX regulate the number and morphology of these two types of olfactory sensilla.

After silencing *Dsx* in males, I confirmed that a large number of trichoid sensilla developed into an intermediate state between a trichoid and a placoid. This demonstrates that DSX regulates the morphology of these sensilla in the peripheral nervous system of *N. vitripennis*.

My results also provide conclusive evidence that trichoid sensilla in parasitoids are homologs of the placoid sensilla and that DSX controls the switch between these homologs in males and females. The intermediate phenotype I identified closely resembles the *sensilla trichodea curvata* found in the majority of ant species (Dumpert, 1972; Hashimoto, 1990; McKenzie *et al*., 2016; Ramirez-Esquivel *et al*., 2014, 2017; Renthal *et al*., 2003). This sensillum is also described as a homolog of plate-like placoid sensilla and is claimed to be unique to ants (Hashimoto, 1990). In these species, this sensillum detects alarm pheromones and its presence serves as an indicator for advanced social communication (Taniguchi *et al*., 2024). However, the presence of this intermediate sensillum after silencing *Dsx* sheds new light on its evolution in Hymenoptera. The evolution of parasitoidism in Hymenoptera predates the vast radiation of eusocial species, such as ants. Therefore, rather than being an adaptation to eusociality, I have shown evidence that this sensillum precedes the evolution of eusocial hymenopteran species. Moreover, the identification of the intermediate sensillum demonstrates an interesting case of neuroplasticity regulated by DSX in the sensory system of *N. vitripennis*. This neuroplasticity would enable *N. vitripennis* to adapt to novel sensory challenges in a dynamic chemical environment.

The insect antennae emerge from antennal imaginal discs. This larval tissue is composed of progenitor cells that develop during metamorphosis (Ray & Rodrigues, 1995). Sensory organ precursors (SOPs) within the antennal imaginal discs undergo asymmetrical cell divisions to produce various types of sensilla, such as tactile, gustatory and olfactory (Roegiers *et al*., 2001). The type of sensillum is in turn determined by the level of proneural genes expressed in the SOPs (Barad *et al*., 2011; Gómez-Skarmeta *et al*., 2003; Goulding *et al*., 2000; Gupta & Rodrigues, 1997; Jhaveri *et al*., 2000; Troost *et al*., 2023; zur Lage *et al*., 2003). In *Drosophila*, DSX has been shown to regulate proneural genes required for the formation of the SOPs of gustatory sensilla (Luecke *et al*., 2022). My experiments in **Chapter 3** show that *Dsx* functions after the formation of the SOPs to determine subtypes of olfactory sensilla in *N. vitripennis*, such as the trichoids and the placoids. The intermediate sensillum I identified after silencing *Dsx* was particularly widened at the base of the hair, indicating an increase in innervating neurons in this sensillum. I therefore postulate that DSX regulates the proliferation of neurons to determine the trichoid and placoid homologs. However, it remains unclear which genes downstream of *Dsx* are responsible for this process in *N. vitripennis*. In *Drosophila*, the process of programmed cell death has been shown to be essential for regulating the number of neurons in the peripheral nervous system (Prieto-Godino *et al*., 2020). DSX has also been shown to be an important regulator of genes that induce programmed cell death to control sexually dimorphic neural clusters in the brain (Kimura *et al*., 2008). I therefore propose that DSX also targets these genes to regulate the number of neurons in the olfactory sensilla of *N. vitripennis*. My results provide a novel opportunity to investigate these downstream target genes in more detail.

Rewiring pheromone circuits

My experiments presented in **Chapter 3** elucidated how sex determination shapes pheromone circuits in the brain of *N. vitripennis*. The neural tracings revealed the number, organizational complexity and sexual dimorphism of glomeruli in the AL of this species. The AL of *N. vitripennis* corresponds to the ALs of other Hymenoptera that use combinatorial coding to process sex pheromones. The lack of a clear macroglomerulus or macroglomerular complex and the relatively large number of glomeruli in the AL of *N. vitripennis* are representative adaptations to this specific coding strategy (Carcaud *et al*., 2015; Couto *et al*., 2023; d'Ettorre *et al*., 2017; Joerges *et al*., 1997; Marty *et al*., 2025; Sandoz *et al*., 2007; Yamagata *et al*., 2006; Zube *et al*., 2008). Due to their life histories, *Nasonia* species must navigate a highly complex chemical environment, which necessitates discriminating numerous host odours and sex pheromones, such as CHCs used for mate recognition (Mair *et al*., 2017). Males not only need to locate suitable mating partners, but also distinguish these from closely related species. Moreover, parasitoid species must often compete for the same host, lay multiple eggs and develop in a gregarious environment (Harvey *et al*., 2013). These challenges can have considerable consequences for their reproductive success and impose strong selection pressures on their pheromone communication system. I postulate that these olfactory demands drove the diversification and complexity of the AL, which resulted in the combinatorial coding of pheromones in parasitoid Hymenoptera. My research determined how the genetic mechanisms of sex determination have played an important role in this evolutionary process.

The insect AL is organized into clusters of glomeruli. These clusters are innervated by sensory-neuron tracts that project from specific types of sensilla on the antennae (Couto *et al*., 2005; Gao *et al*., 2000; Grabe *et al*., 2016). After silencing *Tra* in female *N. vitripennis* larvae, my neural tracings showed dramatic changes in glomerular organization (**Chapter 3**). Silencing this gene induced masculinization of the AL by changing the splicing of *Dsx* from female-specific to male-specific isoforms. This in turn resulted in the loss of glomerular clusters in the silenced female AL. The loss of these clusters therefore indicates that TRA regulates the OSNs of specific sensilla for glomerular development. This is consistent with my findings that TRA and DSX determine the type and morphology of sensilla on the antennae of *N. vitripennis*. From my results, I therefore conclude that sexual dimorphism in the AL of *N. vitripennis* originates from neuroplasticity regulated in the peripheral nervous system and that, by targeting downstream transcription factors in the peripheral nervous system, TRA determines which glomerular clusters are expressed in males and females for their sex-specific life histories.

During development, the insect AL forms large neuropils consisting of protoglomeruli (Jefferis, 2005; Oland & Tolbert, 2011). These protoglomeruli are in turn innervated by the axons of OSNs. In Hymenoptera, these innervations are necessary for the protoglomeruli to divide and form the glomerular organization of the adult AL (**Chapter 2**). In **Chapter 4**, I

elucidated the downstream genetic mechanism underlying sexual dimorphism in this developmental process. I identified the *Olfactory-receptor co-receptor* (*Orco*) gene as a candidate target for TRA and DSX for regulating glomerular development. Silencing this gene in female *N. vitripennis* caused a significant decrease in the number of glomeruli and an increase in glomerular volume due to the inability of protoglomeruli to subdivide into multiple glomeruli. My experiments on *N. vitripennis* therefore confirm that the expression of *Orco* in OSNs is necessary for the formation of the adult AL. These results are consistent with studies on ant species, which show the crucial role that *Orco* plays in glomerular development (Trible *et al*., 2017; Yan *et al*., 2017). In these species, the expression of *Orco* prevents programmed cell death for the development of OSNs (Sieriebriennikov *et al*., 2024). In line with my findings in **Chapter 3**, I therefore propose that *Orco* is the likely target for sex-determination transcription factors, such as DSX and/or FRU, for regulating the number of neurons in the trichoid and placoid homologs of *N. vitripennis* (**Figure 2**). Moreover, the regulation of this gene in the OSNs of specific sensilla would enable the development of the sex-specific clusters of glomeruli I identified in the female AL. Changes in the expression of this gene during evolution can be an important mechanism for inducing novel pheromone circuits.

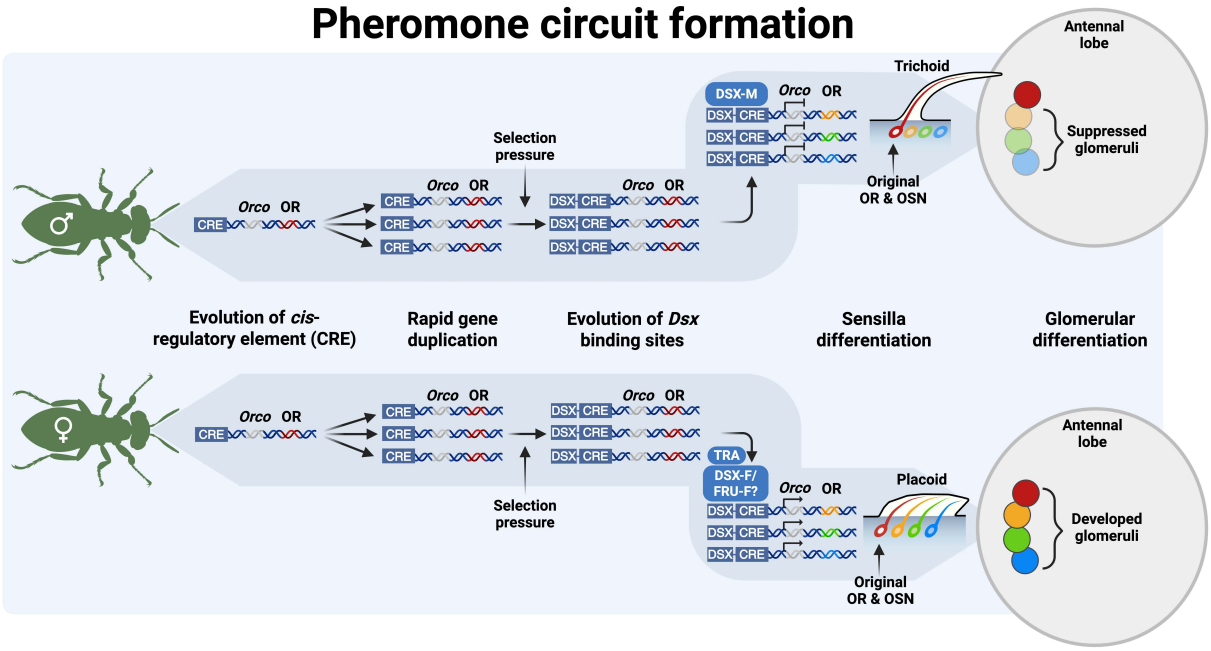

Figure 2: Hypothetical evolution of pheromone circuits in parasitoid wasps through sexual differentiation. Olfactory receptor (OR) genes in the antennae have evolved *cis*-regulatory elements (CREs) for transcription factors that regulate the expression of these genes in olfactory sensory neurons (OSNs). Each OR is expressed together with *Olfactory-receptor co-receptor* (*Orco*), a conserved gene which regulates the development of OSNs in Hymenoptera. The process of gene duplication gives rise to novel OR genes. Sexual-selection pressures can subsequently induce the formation of binding sites in CREs for sex-determination transcription factors, such as Doublesex (DSX) and/or Fruitless (FRU). Sex-specific isoforms of these transcription factors regulate the expression of *Orco*, which in turn results in the development of neurons expressing the newly evolved OR genes. Regulation of neuronal development induces sexual dimorphism in olfactory sensilla. *Dsx* suppression of *Orco* results in normal trichoid development in males, whereas silencing *Dsx* in males induces neuronal proliferation and the development of placoid-like sensilla. The OSNs of these sensilla project to sex-specific glomeruli in the antennal lobe.

Pheromone profile complexity

The experiments presented in **Chapter 5** elucidated how sex determination shapes sexual dimorphism in the pheromone profile of *N. vitripennis*. I confirmed sexual dimorphism in the CHC profile and provided evidence for the important role of the splicing-factor gene *Tra*. The CHC profile of *N. vitripennis* possesses all the main CHC compound classes (*n*-alkanes, alkenes, and methyl-branched alkanes), of which the methyl-branched (MB) alkanes is the most predominant. This is consistent with the majority of parasitoid Hymenoptera (Kather & Martin, 2015). Together, the CHCs form a pheromone profile, which is utilized by males to discriminate between sexes of con- and heterospecific species and to direct courtship to suitable mating partners (Mair *et al*., 2017; Mair & Ruther, 2019; Steiner *et al*., 2006). Competition to parasitize the same host among closely related species not only limits the availability of food resources, but can also result in hybridization. I hypothesize that these selection pressures influenced the CHC production pathway of parasitoid species and resulted in the development of distinct and diverse CHC profiles. My research has now determined the upstream and downstream sex-determination mechanisms that play an essential role in shaping individual CHC profiles.

Male and female *N. vitripennis* have evolved an extensive diversity of MB-alkanes in their CHC profile. My experiments verified sexual dimorphism in the relative abundance of all the MB-alkanes (mono-, di-, tri- and tetramethyl alkanes), including the position of their methyl branches. Research has identified mono- and dimethyl alkanes as sex pheromones for mate recognition in *N. vitripennis* and other related species . Whether this is also the case with tri- and tetramethyl alkanes remains to be determined. After silencing *Tra,* my results show that this gene regulates considerable variation in MB-alkanes and I propose that this variation also affects male mating behaviour. My results now enable us to identify the CHCs utilized by females as species-specific sex pheromones. The MB-alkanes regulated by TRA are therefore ideal candidates for investigating their potential role in mate discrimination. Moreover, my experiments have also identified TRA as a potential candidate for regulating interspecific variation in CHC pheromones between the four *Nasonia* species.

Parasitoids, such as *N. vitripennis*, possess one of the most diverse and complex CHC profiles of Hymenoptera. This degree of complexity has also been shown in basal parasitoids, as they also produce almost all types of MB-alkanes and alkenes (Kather & Martin, 2015). This would imply that the majority of CHC classes and their biosynthetic pathways were already present early in hymenopteran evolutionary history. This also indicates that complexity in the CHC profile of Hymenoptera evolved from a life history of parasitoidism rather than sociality. This is supported by a comprehensive literature review, which showed that basal parasitoids already possessed a complex CHC profile before the vast radiation of the social Hymenoptera (Kather & Martin, 2015). It has therefore been hypothesized that this pre-existing complexity in parasitoids served as a spring-loaded system, in which the diversity of CHCs needed for advanced social communication found in social species was already present for natural

selection to act upon, rather than evolving independently (Kather & Martin, 2015; Nowak *et al*., 2010). This is also consistent with the evolution of the OR repertoire for CHC perception, which evolved independently of eusociality (Gautam *et al*., 2024). My research has now elucidated the genetic mechanisms that are responsible for the diversification of the CHC profile in parasitoid Hymenoptera. *Transformer* plays an essential role in the sex-specific splicing of downstream transcription factors that regulate biosynthetic genes to generate the sex-specific diversity of CHC profiles in these species. It has also been hypothesized that the absence of certain CHC classes in a number of Hymenoptera is a consequence of gene regulation rather than gene gain and loss (Kather & Martin, 2015). My research has conclusively provided evidence of the important role that sex-determination transcription factors play in this process.

Rapid combinatorial biosynthesis

Genes that are conserved are generally constrained in the degree of their functionality (Finet *et al*., 2019; Thomas, 2007). Genes with a higher degree of functionality are less subject to selection pressure and therefore have a slower rate of mutation. Genes that evolve rapidly, on the other hand, are subject to greater selection pressure and have a faster rate of mutation. The biosynthetic genes underlying insect CHCs diverge rapidly between closely related species (Finck *et al*., 2016; Finet *et al*., 2019; Helmkampf *et al*., 2015; Shirangi *et al*., 2009; Tupec *et al*., 2019; Wang *et al*., 2023), enabling individual species to form mating barriers and adapt to novel ecological environments. Moreover, the sex-biased expression of these genes also plays an important role in the formation of sexually dimorphic CHC profiles (Shirangi *et al*., 2009). A group of rapidly evolving biosynthetic genes are the fatty acyl-CoA reductases (FARs), which are responsible for converting very long-chain fatty acids into fatty alcohols, the precursors of insect hydrocarbons (Finet *et al*., 2019). Understanding whether these genes are sex biased and how they are regulated is therefore necessary to elucidate the process of CHC diversification between male and female insects. In **Chapter 6**, I identified four FAR genes targeted by DSX involved in regulating sexual dimorphism in the CHC profiles of both male and female *N. vitripennis*.

As described above, the CHC profile of male and female *N. vitripennis* comprises a diversity of CHC compound classes, including *n*-alkanes, mono-, di-, tri- and tetramethyl alkanes, as well as a number of alkenes. Silencing the candidate FARs resulted in the concomitant up- and downregulation of these compound classes. The up- and downregulation of entire CHC classes means that the enzymes these genes encode possess a broad selectivity for a wide variety of fatty-acyl precursors. This has also been shown in other insect species, such as moths, in which FARs convert a wide range of fatty-acyl precursors for the production of multi-component pheromone blends (Hagström *et al*., 2012; Liénard *et al*., 2010). My results therefore establish the important position and function of the candidate FARs in the CHC biosynthetic pathway for generating the sex-specific diversity in the CHC profile of male and female *N. vitripennis*.

A recent study on *N. vitripennis* showed that this species utilizes a relatively large set of FAR genes for CHC biosynthesis (Buellesbach *et al*., 2022). This was associated to the degree of diversity and complexity of the CHC profile of *N. vitripennis*. As previously indicated, the diversity and complexity of the CHC profile in Hymenoptera evolved from a life history of parasitoidism rather than eusociality. I therefore hypothesize that in order to develop these complex CHC profiles, parasitoids already possessed a large set of FAR genes before the evolution of eusocial species. I also propose that the expansion of this gene family enabled the evolution of *cis*-regulatory elements in FARs to become potential targets for transcription factors like DSX (**Figure 3**), resulting in the rapid diversification and complexity of CHCs in the evolutionary history of Hymenoptera.

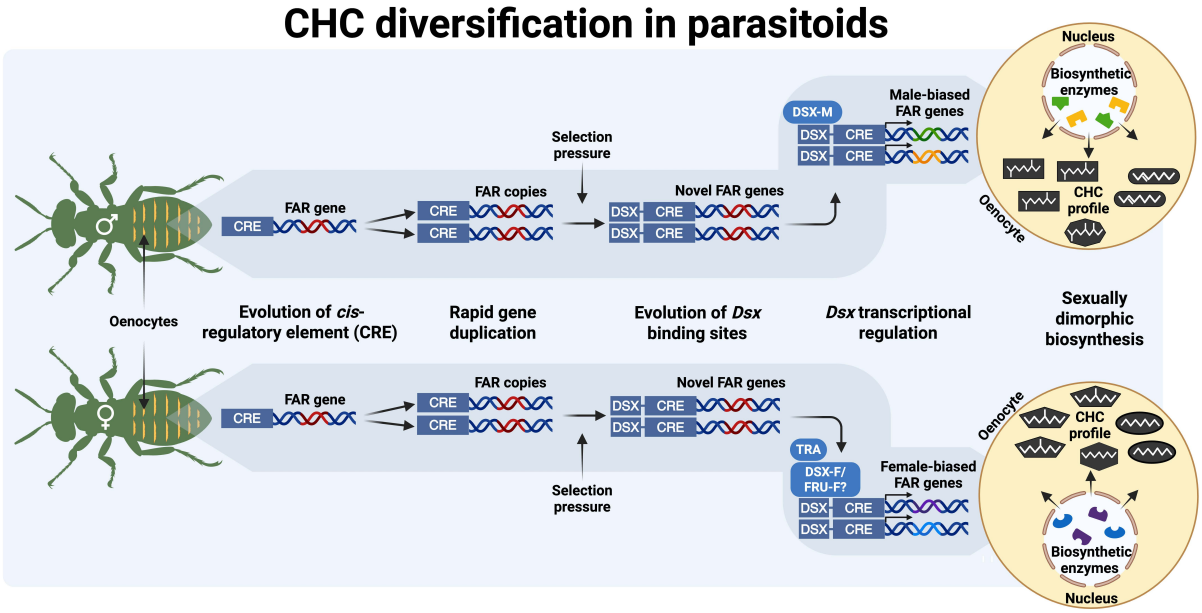

Figure 3: Hypothetical evolution of cuticular hydrocarbon diversification in parasitoid wasps through sexual differentiation.
Cuticular hydrocarbon (CHC) biosynthesis in insects takes place in specialized cells called oenocytes below the cuticle. Biosynthetic genes have evolved *cis*-regulatory elements (CREs) for transcription factors that regulate the expression of these genes in the oenocytes. The process of gene duplication gives rise to novel biosynthetic genes, which enables the diversification of CHCs between closely related species. Sexual-selection pressures can induce the formation of binding sites in CREs for sex-determination transcription factors, such as DSX and FRU. Sex-specific isoforms of transcription factors subsequently regulate the sex-biased expression of the newly evolved biosynthetic genes in the oenocytes of males and females. The sex-biased expression of these newly evolved genes leads to the creation of enzymes that produce a sexually dimorphic CHC profile.

As gene family expansion favours a combinatorial strategy of gene regulation, rather than a single master regulator coordinating the expression of individual genes (Bhattacharjee *et al*., 2013), this would provide a mechanism by which a relatively small number of transcription factors regulates a much larger number of genes with finely tuned temporal expression patterns, such as the FAR genes in my experiments. A similar strategy is also employed for regulating the fine-tuned expression pattern of ORs in the insect peripheral nervous system (Li *et al*., 2013; Ray *et al*., 2007). I therefore propose that DSX is among a group of transcription

factors involved in the combinatorial control of FAR expression in the CHC biosynthetic pathway of Hymenoptera. This would in turn enable a form of combinatorial synthesis for the rapid diversification of CHCs needed for the specific life histories of these species.

Conclusion and future directions

The research and evidence I present in my thesis elucidate how sexual differentiation, neurodevelopment and biosynthesis are interlinked in the evolution of parasitoid pheromone communication. Parasitoids possess an elaborate neural network to perceive and process a complex pheromone profile necessary for their specific life histories. I showed how sexual differentiation is a major driver of complex pheromone circuits in these species. This involves sex-determination transcription factors targeting conserved neurodevelopmental genes that regulate neuroplasticity in the peripheral nervous system. I also determined that *Tra* and *Dsx* play a major role in the diversification of the CHC profile in parasitoids. The transcription factors spliced by TRA target rapidly evolving genes in the CHC biosynthetic pathway for generating diversity in the CHC profile of these species. My thesis provides evidence that these genetic mechanisms evolved early in hymenopteran evolutionary history and that this resulted in the degree of diversification and complexity of their pheromone communication system.

Having elucidated the genetic mechanisms that regulate sexual dimorphism in the pheromone communication system of the parasitoid *Nasonia vitripennis*, I can now turn to the implications and potential future directions of my research. My key findings have paved the way for further investigation into the sex-specific mechanisms shaping the coevolution of pheromone production and perception in insects. Sexual differentiation in pheromone communication arises through *cis*-regulatory mechanisms, such as gene regulation by DSX and FRU. Accordingly, biosynthetic and chemosensory genes evolve rapidly through gene family expansion and the subsequent gain, loss and modification of *cis*-regulatory elements. Sex-determination transcription factors are known to bind to multiple *cis*-regulatory elements of genes to regulate both pheromone production (Chertemps *et al*., 2006, 2007; Shirangi *et al*., 2009) and perception (Luecke *et al*., 2022; Mellert *et al*., 2012). This creates a pleiotropic constraint on transcription-factor evolution and generates genetic covariance, which in turn results in the co-evolution of the production and perception of pheromones. My research has now provided a solid framework for investigating how this process results in the production of complex CHC profiles and the formation of their corresponding coding mechanisms.

I have also provided significant insight into the neurodevelopmental mechanisms shaping the evolution of insect pheromone processing. Research into the downstream molecular mechanisms of sex determination will provide a much better understanding of the evolution of complex pheromone coding systems. Hymenoptera in particular have evolved elaborate receptor repertoires (Legan *et al*., 2021; McKenzie *et al*., 2016; McKenzie & Kronauer, 2018; Robertson *et al*., 2010; Zhou *et al*., 2015) and antennal lobes (Arnold *et al*., 1985; Couto *et al*.,

2023; Groothuis *et al*., 2019; McKenzie *et al*., 2016; Zube & Rössler, 2008) for the combinatorial coding of complex pheromone blends. I therefore propose further investigation into how sex determination regulates neurodevelopmental processes for the combinatorial coding of pheromones in these species. Research on these sex-specific mechanisms in Hymenoptera would enable us to draw comparisons with other well-studied pheromone communication systems, such as those of the Lepidoptera (Groot *et al*., 2016; Löfstedt, 1993). The *Nasonia* genus is an ideal model system for this, as these species have evolved a diversity of cuticular pheromones as important determinants for their complex life histories (Kather & Martin, 2015). I would also recommend carrying out research into the sex-specific coding mechanisms behind these specific pheromones. This knowledge can then be extrapolated to additional studies into identifying the specific genetic mechanisms and neural circuits involved in host-odour perception.

Parasitoid wasps are invaluable biocontrol agents and play a crucial role in agricultural and natural ecosystems to reduce invasive pests in an ecologically sustainable way (Floate, 2002; Leung *et al*., 2020; Pilkington *et al*., 2010; Stouthamer, 1993; Van Lenteren *et al*., 2018). Pheromones and other chemicals are used by parasitoids for orientation and to detect potential mates, hosts and competing species (Cusumano *et al*., 2020; Giunti *et al*., 2015). Specific insight into the genetic regulation of parasitoid pheromone communication is therefore integral to pheromone-based pest-control strategies (Leung *et al*., 2020), including push-pull technologies (Cook *et al*., 2007) and pheromone traps (Suckling *et al*., 2002). Understanding how sex-determination transcription factors regulate genes responsible for pheromone perception can also be utilized in selective breeding strategies to optimize parasitoid life-history traits, such as for locating mates and hosts. My research therefore provides significant groundwork for comparative studies and future research into sex determination regulating insect olfaction and the role that *Tra* and *Dsx* play in the evolution of parasitoid behaviour.

Acknowledgements

I am grateful for the feedback on this chapter provided by Marcel Dicke and Eveline Verhulst.

Bibliography

A

Agarwal, G., & Isacoff, E. (2011). Specializations of a pheromonal glomerulus in the *Drosophila* olfactory system. *Journal of Neurophysiology*, *105*(4), 1711–1721. https://doi.org/10.1152/jn.00591.2010

Ai, M., Min, S., Grosjean, Y., Leblanc, C., Bell, R., Benton, R., & Suh, G. S. B. (2010). Acid sensing by the *Drosophila* olfactory system. *Nature*, *468*(7324), 691–695. https://doi.org/10.1038/nature09537

Anton, S., & Homberg, U. (1999). Antennal lobe structure. In B. S. Hansson (Ed.), *Insect olfaction* (pp. 97–124). Springer Berlin Heidelberg. https://doi.org/10.1007/978-3-662-07911-9_5

Anton, S., Ignell, R., & Hansson, B. S. (2002). Developmental changes in the structure and function of the central olfactory system in gregarious and solitary desert locusts. *Microscopy Research and Technique*, *56*(4), 281–291. https://doi.org/10.1002/jemt.10032

Antony, C., Davis, T. L., Carlson, D. A., Pechine, J.-M., & Jallon, J.-M. (1985). Compared behavioral responses of male *Drosophila melanogaster* (Canton S) to natural and synthetic aphrodisiacs. *Journal of Chemical Ecology*, *11*(12), 1617–1629. https://doi.org/10.1007/BF01012116

Araújo, S. J., & Tear, G. (2003). Axon guidance mechanisms and molecules: Lessons from invertebrates. *Nature Reviews Neuroscience*, *4*(11), 910–922. https://doi.org/10.1038/nrn1243

Arnold, G., Masson, C., & Budharugsa, S. (1984). Demonstration of a sexual dimorphism in the olfactory pathways of the drones of *Apis mellifica* L. (Hymenoptera, Apidae). *Experientia*, *40*(7), 723–725. https://doi.org/10.1007/BF01949744

Arnold, G., Masson, C., & Budharugsa, S. (1985). Comparative study of the antennal lobes and their afferent pathway in the worker bee and the drone (*Apis mellifera*). *Cell and Tissue Research*, *242*(3), 593–605. https://doi.org/10.1007/BF00225425

Asahina, K. (2018). Sex differences in *Drosophila* behavior: Qualitative and quantitative dimorphism. *Current Opinion in Physiology*, *6*, 35–45. https://doi.org/10.1016/j.cophys.2018.04.004

Auer, T. O., & Benton, R. (2016). Sexual circuitry in *Drosophila*. *Current Opinion in Neurobiology*, *38*, 18–26. https://doi.org/10.1016/j.conb.2016.01.004

B

Baker, B. S., & Ridge, K. A. (1980). Sex and the single cell. I. On the action of major loci affecting sex determination in *Drosophila melanogaster*. *Genetics*, *94*(2), 383–423. https://doi.org/10.1093/genetics/94.2.383

Baker, B. S., Taylor, B. J., & Hall, J. C. (2001). Are complex behaviors specified by dedicated regulatory genes? Reasoning from *Drosophila*. *Cell*, *105*(1), 13–24. https://doi.org/10.1016/s0092-8674(01)00293-8

Baker, T. C. (2002). Mechanism for saltational shifts in pheromone communication systems. *Proceedings of the National Academy of Sciences of the United States of America*, *99*(21), 13368–13370. https://doi.org/10.1073/pnas.222539799

Barad, O., Hornstein, E., & Barkai, N. (2011). Robust selection of sensory organ precursors by the Notch-Delta pathway. *Current Opinion in Cell Biology*, *23*(6), 663–667. https://doi.org/10.1016/j.ceb.2011.09.005

Barrass, R. (1960). The Courtship behaviour of *Mormoniella Vitripennis* Walk. (Hymenoptera, Pteromalidae). *Behaviour*, *15*(3–4), 185–208. https://doi.org/10.1163/156853960X00223

Bellonci, G. (1883). Intorno alla struttura e alle connessioni dei lobi olfattorii negli Artropodi superiori e nei Vertebrati. *Atti Della Reale Accademia Dei Lincei*, 1882–1883.

Benton, R., Sachse, S., Michnick, S. W., & Vosshall, L. B. (2006). Atypical membrane topology and heteromeric function of *Drosophila* odorant receptors in vivo. *PLOS Biology*, *4*(2), e20. https://doi.org/10.1371/journal.pbio.0040020

Bertossa, R. C., van de Zande, L., & Beukeboom, L. W. (2009). The *Fruitless* gene in *Nasonia* displays complex sex-specific splicing and contains new zinc finger domains. *Molecular Biology and Evolution*, *26*(7), 1557–1569. https://doi.org/10.1093/molbev/msp067

Bhattacharjee, S., Renganaath, K., Mehrotra, R., & Mehrotra, S. (2013). Combinatorial control of gene expression. *BioMed Research International*, *2013*, 407263. https://doi.org/10.1155/2013/407263

Billeter, J.-C., Atallah, J., Krupp, J. J., Millar, J. G., & Levine, J. D. (2009). Specialized cells tag sexual and species identity in *Drosophila melanogaster*. *Nature*, *461*(7266), 987–991. https://doi.org/10.1038/nature08495

Billeter, J.-C., Rideout, E. J., Dornan, A. J., & Goodwin, S. F. (2006a). Control of male sexual behavior in *Drosophila* by the sex determination pathway. *Current Biology*, *16*(17), R766–R776. https://doi.org/10.1016/j.cub.2006.08.025

Billeter, J.-C., Villella, A., Allendorfer, J. B., Dornan, A. J., Richardson, M., Gailey, D. A., & Goodwin, S. F. (2006b). Isoform-specific control of male neuronal differentiation and

behavior in *Drosophila* by the *Fruitless* gene. *Current Biology*, *16*(11), 1063–1076. https://doi.org/10.1016/j.cub.2006.04.039

Billeter, J.-C., & Wolfner, M. F. (2018). Chemical cues that guide female reproduction in *Drosophila melanogaster*. *Journal of Chemical Ecology*, *44*(9), 750–769. https://doi.org/10.1007/s10886-018-0947-z

Blaul, B., & Ruther, J. (2011). How parasitoid females produce sexy sons: A causal link between oviposition preference, dietary lipids and mate choice in *Nasonia*. *Proceedings of the Royal Society B: Biological Sciences*, *278*(1722), 3286–3293. https://doi.org/10.1098/rspb.2011.0001

Blomquist, G. J., & Bagnères, A.-G. (Eds) (2010). *Insect hydrocarbons: Biology, biochemistry, and chemical ecology* (1st ed.). Cambridge University Press, Cambridge. https://doi.org/10.1017/CBO9780511711909

Blomquist, G. J., & Ginzel, M. D. (2021). Chemical ecology, biochemistry, and molecular Biology of insect hydrocarbons. *Annual Review of Entomology*, *66*(1), 45–60. https://doi.org/10.1146/annurev-ento-031620-071754

Blomquist, G. J., Nelson, D. R., & De Renobales, M. (1987). Chemistry, biochemistry, and physiology of insect cuticular lipids. *Archives of Insect Biochemistry and Physiology*, *6*(4), 227–265. https://doi.org/10.1002/arch.940060404

Boeckh, J., & Boeckh, V. (1979). Threshold and odor specificity of pheromone-sensitive neurons in the deutocerebrum of *Antheraea pernyi* and *A. polyphemus* (Saturnidae). *Journal of Comparative Physiology*, *132*(3), 235–242. https://doi.org/10.1007/BF00614495

Boeckh, J., Ernst, K. D., & Selsam, P. (1987). Neurophysiology and neuroanatomy of the olfactory pathway in the cockroach. *Annals of the New York Academy of Sciences*, *510*, 39–43. https://doi.org/10.1111/j.1749-6632.1987.tb43464.x

Boeckh, J., Kaissling, K. E., & Schneider, D. (1960). Sensillen und bau der antennengeißel von *Telea polyphemus*. *Zoologische Jahrbücher: Abteilung Für Anatomie Und Ontogenie Der Tiere*, *78*, 559–584.

Boeckh, J., & Tolbert, L. P. (1993). Synaptic organization and development of the antennal lobe in insects. *Microscopy Research and Technique*, *24*(3), 260–280. https://doi.org/10.1002/jemt.1070240305

Bopp, D., Saccone, G., & Beye, M. (2014). Sex determination in insects: Variations on a common theme. *Sexual Development*, *8*(1–3), 20–28. https://doi.org/10.1159/000356458

Brandstaetter, A. S., & Kleineidam, C. J. (2011). Distributed representation of social odors indicates parallel processing in the antennal lobe of ants. *Journal of Neurophysiology*, *106*(5), 2437–2449. https://doi.org/10.1152/jn.01106.2010

Bray, S., & Amrein, H. (2003). A putative *Drosophila* pheromone receptor expressed in male-specific taste neurons is required for efficient courtship. *Neuron*, *39*(6), 1019–1029. https://doi.org/10.1016/s0896-6273(03)00542-7

Bretschneider, F. (1924). Über die gehirne des eichenspinners und des seidenspinners (*Lasiocampa quercus* L. und *Bombyx mori* L.). *Jenaische Zeitschriften Für Naturwissenschaften*, *60*, 563–578.

Brill, M. F., Rosenbaum, T., Reus, I., Kleineidam, C. J., Nawrot, M. P., & Rössler, W. (2013). Parallel processing via a dual olfactory pathway in the honeybee. *Journal of Neuroscience*, *33*(6), 2443–2456. https://doi.org/10.1523/JNEUROSCI.4268-12.2013

Brockmann, A., & Brückner, D. (2001). Structural differences in the drone olfactory system of two phylogenetically distant *Apis* species, *A. florea* and *A. mellifera*. *Naturwissenschaften*, *88*(2), 78–81. https://doi.org/10.1007/s001140000199

Buchinger, T. J., & Li, W. (2023). Chemical communication and its role in sexual selection across Animalia. *Communications Biology*, *6*(1), 1178. https://doi.org/10.1038/s42003-023-05572-w

Buellesbach, J., Gadau, J., Beukeboom, L. W., Echinger, F., Raychoudhury, R., Werren, J. H., & Schmitt, T. (2013). Cuticular hydrocarbon divergence in the jewel wasp *Nasonia*: Evolutionary shifts in chemical communication channels? *Journal of Evolutionary Biology*, *26*(11), 2467–2478. https://doi.org/10.1111/jeb.12242

Buellesbach, J., Holze, H., Schrader, L., Liebig, J., Schmitt, T., Gadau, J., & Niehuis, O. (2022). Genetic and genomic architecture of species-specific cuticular hydrocarbon variation in parasitoid wasps. *Proceedings of the Royal Society B: Biological Sciences*, *289*(1976), 20220336. https://doi.org/10.1098/rspb.2022.0336

Buellesbach, J., Vetter, S. G., & Schmitt, T. (2018). Differences in the reliance on cuticular hydrocarbons as sexual signaling and species discrimination cues in parasitoid wasps. *Frontiers in Zoology*, *15*, 22. https://doi.org/10.1186/s12983-018-0263-z

Butenandt, A., Beckmann, R., & Hecker, E. (1961). Über den sexuallockstoff des seidenspinners, I. Der biologische test und die Isolierung des reinen sexuallockstoffes Bombykol. *Hoppe-Seyler´s Zeitschrift Für Physiologische Chemie*, *324*, 71–83. https://doi.org/10.1515/bchm2.1961.324.1.71

C

Cachero, S., Ostrovsky, A. D., Yu, J. Y., Dickson, B. J., & Jefferis, G. S. X. E. (2010). Sexual dimorphism in the fly brain. *Current Biology*, *20*(18), 1589–1601. https://doi.org/10.1016/j.cub.2010.07.045

Cao, S., Shi, C., Wang, B., Xiu, P., Wang, Y., Liu, Y., & Wang, G. (2023). Evolutionary shifts in pheromone receptors contribute to speciation in four *Helicoverpa* species. *Cellular and Molecular Life Sciences*, *80*(8), 199. https://doi.org/10.1007/s00018-023-04837-1

Carcaud, J., Giurfa, M., & Sandoz, J.-C. (2015). Differential combinatorial coding of pheromones in two olfactory subsystems of the honey bee brain. *Journal of Neuroscience*, *35*(10), 4157–4167. https://doi.org/10.1523/JNEUROSCI.0734-14.2015

Cardé, R. T., & Baker, T. C. (1984). Sexual communication with pheromones. In W. J. Bell & R. T. Cardé (Eds.), *Chemical ecology of insects* (pp. 355–383). Springer US, Boston, MA. https://doi.org/10.1007/978-1-4899-3368-3_13

Carey, A. F., Wang, G., Su, C.-Y., Zwiebel, L. J., & Carlson, J. R. (2010). Odorant reception in the malaria mosquito *Anopheles gambiae*. *Nature*, *464*(7285), 66–71. https://doi.org/10.1038/nature08834

Carlson, D. A., Geden, C. J., & Bernier, U. R. (1999). Identification of pupal exuviae of *Nasonia vitripennis* and *Muscidifurax raptorellus* parasitoids Using cuticular hydrocarbons. *Biological Control*, *15*(2), 97–106. https://doi.org/10.1006/bcon.1999.0708

Carot-Sans, G., Muñoz, L., Piulachs, M. D., Guerrero, A., & Rosell, G. (2015). Identification and characterization of a fatty acyl reductase from a *Spodoptera littoralis* female gland involved in pheromone biosynthesis. *Insect Molecular Biology*, *24*(1), 82–92. https://doi.org/10.1111/imb.12138

Chaffiol, A., Kropf, J., Barrozo, R. B., Gadenne, C., Rospars, J.-P., & Anton, S. (2012). Plant odour stimuli reshape pheromonal representation in neurons of the antennal lobe macroglomerular complex of a male moth. *Journal of Experimental Biology*, *215*(Pt 10), 1670–1680. https://doi.org/10.1242/jeb.066662

Chambille, I., Masson, C., & Rospars, J. P. (1980). The deutocerebrum of the cockroach *Blaberus craniifer* Burm. Spatial organization of the sensory glomeruli. *Journal of Neurobiology*, *11*(2), 135–157. https://doi.org/10.1002/neu.480110202

Chambille, I., & Pierre Rospars, I. (1985). Neurons and identified glomeruli of antennal lobes during postembryonic development in the cockroach *Blaberus craniifer* burm. (Dictyoptera: Blaberidae). *International Journal of Insect Morphology and Embryology*, *14*(4), 203–226. https://doi.org/10.1016/0020-7322(85)90055-8

Chen, Z., Traniello, I. M., Rana, S., Cash-Ahmed, A. C., Sankey, A. L., Yang, C., & Robinson, G. E. (2021). Neurodevelopmental and transcriptomic effects of CRISPR/Cas9-induced

somatic *Orco* mutation in honey bees. *Journal of Neurogenetics*, *35*(3), 320–332. https://doi.org/10.1080/01677063.2021.1887173

Chertemps, T., Duportets, L., Labeur, C., Ueda, R., Takahashi, K., Saigo, K., & Wicker-Thomas, C. (2007). A female-biased expressed elongase involved in long-chain hydrocarbon biosynthesis and courtship behavior in *Drosophila melanogaster*. *Proceedings of the National Academy of Sciences of the United States of America*, *104*(11), 4273–4278. https://doi.org/10.1073/pnas.0608142104

Chertemps, T., Duportets, L., Labeur, C., Ueyama, M., & Wicker-Thomas, C. (2006). A female-specific desaturase gene responsible for diene hydrocarbon biosynthesis and courtship behaviour in *Drosophila melanogaster*. *Insect Molecular Biology*, *15*(4), 465–473. https://doi.org/10.1111/j.1365-2583.2006.00658.x

Chou, Y.-H., Spletter, M. L., Yaksi, E., Leong, J. C. S., Wilson, R. I., & Luo, L. (2010a). Diversity and wiring variability of olfactory local interneurons in the *Drosophila* antennal lobe. *Nature Neuroscience*, *13*(4), 439–449. https://doi.org/10.1038/nn.2489

Chou, Y.-H., Zheng, X., Beachy, P. A., & Luo, L. (2010b). Patterning axon targeting of olfactory receptor neurons by coupled hedgehog signaling at two distinct steps. *Cell*, *142*(6), 954–966. https://doi.org/10.1016/j.cell.2010.08.015

Christensen, T. A., Harrow, I. D., Cuzzocrea, C., Randolph, P. W., & Hildebrand, J. G. (1995). Distinct projections of two populations of olfactory receptor axons in the antennal lobe of the sphinx moth *Manduca sexta*. *Chemical Senses*, *20*(3), 313–323. https://doi.org/10.1093/chemse/20.3.313

Christensen, T. A., & Hildebrand, J. G. (2002). Pheromonal and host-odor processing in the insect antennal lobe: How different? *Current Opinion in Neurobiology*, *12*(4), 393–399. https://doi.org/10.1016/s0959-4388(02)00336-7

Chung, H., & Carroll, S. B. (2015). Wax, sex and the origin of species: Dual roles of insect cuticular hydrocarbons in adaptation and mating. *BioEssays*, *37*(7), 822–830. https://doi.org/10.1002/bies.201500014

Chung, H., Loehlin, D. W., Dufour, H. D., Vaccarro, K., Millar, J. G., & Carroll, S. B. (2014). A single gene affects both ecological divergence and mate choice in *Drosophila*. *Science*, *343*(6175), 1148–1151. https://doi.org/10.1126/science.1249998

Clarke, K. R. (1993). Non-parametric multivariate analyses of changes in community structure. *Australian Journal of Ecology*, *18*(1), 117–143. https://doi.org/10.1111/j.1442-9993.1993.tb00438.x

Clarke, K. R., & Gorley, R. N. (2006). *PRIMER v6: User Manual/Tutorial, (PRIMER-E, Plymouth)*. https://www.researchgate.net/publication/285668711_PRIMER_v6_user_manualtutorial_PRIMER-E_Plymouth

Cline, T. W., & Meyer, B. J. (1996). Vive la différence: Males vs females in flies vs worms. *Annual Review of Genetics*, *30*, 637–702. https://doi.org/10.1146/annurev.genet.30.1.637

Clough, E., Jimenez, E., Kim, Y.-A., Whitworth, C., Neville, M. C., Hempel, L. U., Pavlou, H. J., Chen, Z.-X., Sturgill, D., Dale, R. K., Smith, H. E., Przytycka, T. M., Goodwin, S. F., Van Doren, M., & Oliver, B. (2014). Sex- and tissue-specific functions of *Drosophila Doublesex* transcription factor target genes. *Developmental Cell*, *31*(6), 761–773. https://doi.org/10.1016/j.devcel.2014.11.021

Clyne, P. J., Warr, C. G., Freeman, M. R., Lessing, D., Kim, J., & Carlson, J. R. (1999). A novel family of divergent seven-transmembrane proteins: Candidate odorant receptors in *Drosophila*. *Neuron*, *22*(2), 327–338. https://doi.org/10.1016/s0896-6273(00)81093-4

Combs, P. A., Krupp, J. J., Khosla, N. M., Bua, D., Petrov, D. A., Levine, J. D., & Fraser, H. B. (2018). Tissue-specific cis-regulatory divergence implicates *EloF* in Inhibiting Interspecies Mating in *Drosophila*. *Current Biology*, *28*(24), 3969-3975.e3. https://doi.org/10.1016/j.cub.2018.10.036

Conchou, L., Lucas, P., Meslin, C., Proffit, M., Staudt, M., & Renou, M. (2019). Insect odorscapes: From plant volatiles to natural olfactory scenes. *Frontiers in Physiology*, *10*, 972. https://doi.org/10.3389/fphys.2019.00972

Cook, S. M., Khan, Z. R., & Pickett, J. A. (2007). The use of push-pull strategies in integrated pest management. *Annual Review of Entomology*, *52*, 375–400. https://doi.org/10.1146/annurev.ento.52.110405.091407

Couto, A., Alenius, M., & Dickson, B. J. (2005). Molecular, anatomical, and functional organization of the *Drosophila* olfactory system. *Current Biology*, *15*(17), 1535–1547. https://doi.org/10.1016/j.cub.2005.07.034

Couto, A., Lapeyre, B., Thiéry, D., & Sandoz, J.-C. (2016). Olfactory pathway of the hornet *Vespa velutina*: New insights into the evolution of the hymenopteran antennal lobe. *Journal of Comparative Neurology*, *524*(11), 2335–2359. https://doi.org/10.1002/cne.23975

Couto, A., Marty, S., Dawson, E. H., d'Ettorre, P., Sandoz, J.-C., & Montgomery, S. H. (2023). Evolution of the neuronal substrate for kin recognition in social Hymenoptera. *Biological Reviews*, *98*(6), 2226–2242. https://doi.org/10.1111/brv.13003

Couto, A., Mitra, A., Thiéry, D., Marion-Poll, F., & Sandoz, J.-C. (2017). Hornets have it: A conserved olfactory subsystem for social recognition in Hymenoptera? *Frontiers in Neuroanatomy*, *11*, 48. https://doi.org/10.3389/fnana.2017.00048

Coyne, J. A., Crittenden, A. P., & Mah, K. (1994). Genetics of a pheromonal difference contributing to reproductive isolation in *Drosophila*. *Science*, *265*(5177), 1461–1464. https://doi.org/10.1126/science.8073292

Cusumano, A., Harvey, J. A., Bourne, M. E., Poelman, E. H., & G de Boer, J. (2020). Exploiting chemical ecology to manage hyperparasitoids in biological control of arthropod pests. *Pest Management Science*, *76*(2), 432–443. https://doi.org/10.1002/ps.5679

d'Ettorre, P., Deisig, N., & Sandoz, J.-C. (2017). Decoding ants' olfactory system sheds light on the evolution of social communication. *Proceedings of the National Academy of Sciences of the United States of America*, *114*(34), 8911–8913. https://doi.org/10.1073/pnas.1711075114

D

Dalla Benetta, E., Antoshechkin, I., Yang, T., Nguyen, H. Q. M., Ferree, P. M., & Akbari, O. S. (2020). Genome elimination mediated by gene expression from a selfish chromosome. *Science Advances*, *6*(14), eaaz9808. https://doi.org/10.1126/sciadv.aaz9808

Darling, D. C., & Werren, J. H. (1990). Biosystematics of *Nasonia* (Hymenoptera: Pteromalidae): Two new species reared from birds' nests in North America. *Annals of the Entomological Society of America*, *83*(3), 352–370. https://doi.org/10.1093/aesa/83.3.352

Darwin, C. (1871). *The descent of man, and selection in relation to sex, vol 1.* John Murray. https://doi.org/10.1037/12293-000

Das, P., & Fadamiro, H. Y. (2013). Species and sexual differences in antennal lobe architecture and glomerular organization in two parasitoids with different degree of host specificity, *Microplitis croceipes* and *Cotesia marginiventris*. *Cell and Tissue Research*, *352*(2), 227–235. https://doi.org/10.1007/s00441-013-1568-z

Das, S., Trona, F., Khallaf, M. A., Schuh, E., Knaden, M., Hansson, B. S., & Sachse, S. (2017). Electrical synapses mediate synergism between pheromone and food odors in *Drosophila melanogaster*. *Proceedings of the National Academy of Sciences of the United States of America*, *114*(46), E9962–E9971. https://doi.org/10.1073/pnas.1712706114

Datta, S. R., Vasconcelos, M. L., Ruta, V., Luo, S., Wong, A., Demir, E., Flores, J., Balonze, K., Dickson, B. J., & Axel, R. (2008). The *Drosophila* pheromone cVA activates a sexually dimorphic neural circuit. *Nature*, *452*(7186), 473–477. https://doi.org/10.1038/nature06808

de Bruyne, M., Foster, K., & Carlson, J. R. (2001). Odor coding in the *Drosophila* antenna. *Neuron*, *30*(2), 537–552. https://doi.org/10.1016/s0896-6273(01)00289-6

DeGennaro, M., McBride, C. S., Seeholzer, L., Nakagawa, T., Dennis, E. J., Goldman, C., Jasinskiene, N., James, A. A., & Vosshall, L. B. (2013). *Orco* mutant mosquitoes lose strong preference for humans and are not repelled by volatile DEET. *Nature*, *498*(7455), 487–491. https://doi.org/10.1038/nature12206

Deisig, N., Kropf, J., Vitecek, S., Pevergne, D., Rouyar, A., Sandoz, J.-C., Lucas, P., Gadenne, C., Anton, S., & Barrozo, R. (2012). Differential interactions of sex pheromone and plant odour in the olfactory pathway of a male moth. *PLOS One*, *7*(3), e33159. https://doi.org/10.1371/journal.pone.0033159

Dekker, T., Ibba, I., Siju, K. P., Stensmyr, M. C., & Hansson, B. S. (2006). Olfactory shifts parallel superspecialism for toxic fruit in *Drosophila melanogaster* sibling, *D. sechellia*. *Current Biology*, *16*(1), 101–109. https://doi.org/10.1016/j.cub.2005.11.075

Dembeck, L. M., Böröczky, K., Huang, W., Schal, C., Anholt, R. R. H., & Mackay, T. F. C. (2015). Genetic architecture of natural variation in cuticular hydrocarbon composition in *Drosophila melanogaster*. *eLife*, *4*, e09861. https://doi.org/10.7554/eLife.09861

Demir, E., & Dickson, B. J. (2005). *Fruitless* splicing specifies male courtship behavior in *Drosophila*. *Cell*, *121*(5), 785–794. https://doi.org/10.1016/j.cell.2005.04.027

Dicke, M., & Sabelis, M. W. (1988). Infochemical terminology: Based on cost-benefit analysis rather than origin of compounds? *Functional Ecology*, *2*(2), 131–139. https://doi.org/10.2307/2389687

Dietl, M. J. (1876). Die organisation des arthropodengehirns. *Zeitschrift Für Wissenschaftliche Zoologie*, *27*, 488–517.

Dobritsa, A. A., van der Goes van Naters, W., Warr, C. G., Steinbrecht, R. A., & Carlson, J. R. (2003). Integrating the molecular and cellular basis of odor coding in the *Drosophila* antenna. *Neuron*, *37*(5), 827–841. https://doi.org/10.1016/s0896-6273(03)00094-1

Dujardin, F. (1850). Mémoire sur le système nerveux des insectes. *Annales Des Sciences Naturelles Biodiversity*, *14*, 195–206.

Dumpert, K. (1972). Bau und verteilung der sensillen auf der antennengeißel von *Lasius fuliginosus* (Latr.) (Hymenoptera, Formicidae). *Zeitschrift für Morphologie der Tiere*, *73*(2), 95–116. https://doi.org/10.1007/BF00280771

Dweck, H. K. M. (2009). Antennal sensory receptors of *Pteromalus puparum* female (Hymenoptera: Pteromalidae), a gregarious pupal endoparasitoid of *Pieris rapae*. *Micron*, *40*(8), 769–774. https://doi.org/10.1016/j.micron.2009.07.012

Dweck, H. K. M., & Gadallah, N. S. (2008). Description of the antennal sensilla of *Habrobracon Hebetor*. *BioControl*, *53*(6), 841–856. https://doi.org/10.1007/s10526-007-9145-6

E

Elmore, T., Ignell, R., Carlson, J. R., & Smith, D. P. (2003). Targeted mutation of a *Drosophila* odor receptor defines receptor requirement in a novel class of sensillum. *Journal of Neuroscience*, *23*(30), 9906–9912. https://doi.org/10.1523/JNEUROSCI.23-30-09906.2003

Engsontia, P., Sangket, U., Robertson, H. M., & Satasook, C. (2015). Diversification of the ant odorant receptor gene family and positive selection on candidate cuticular hydrocarbon receptors. *BMC Research Notes*, *8*(1), 380. https://doi.org/10.1186/s13104-015-1371-x

Esslen, J., & Kaissling, K.-E. (1976). Zahl und verteilung antennaler sensillen bei der honigbiene (*Apis mellifera* L.). *Zoomorphologie*, *83*(3), 227–251. https://doi.org/10.1007/BF00993511

Evans, T. A., & Bashaw, G. J. (2010). Axon guidance at the midline: Of mice and flies. *Current Opinion in Neurobiology*, *20*(1), 79–85. https://doi.org/10.1016/j.conb.2009.12.006

F

Fan, X.-B., Mo, B.-T., Li, G.-C., Huang, L.-Q., Guo, H., Gong, X.-L., & Wang, C.-Z. (2022). Mutagenesis of the odorant receptor co-receptor (*Orco*) reveals severe olfactory defects in the crop pest moth *Helicoverpa armigera*. *BMC Biology*, *20*(1), 214. https://doi.org/10.1186/s12915-022-01411-2

Fandino, R. A., Haverkamp, A., Bisch-Knaden, S., Zhang, J., Bucks, S., Nguyen, T. A. T., Schröder, K., Werckenthin, A., Rybak, J., Stengl, M., Knaden, M., Hansson, B. S., & Große-Wilde, E. (2019). Mutagenesis of odorant coreceptor *Orco* fully disrupts foraging but not oviposition behaviors in the hawkmoth *Manduca sexta*. *Proceedings of the National Academy of Sciences of the United States of America*, *116*(31), 15677–15685. https://doi.org/10.1073/pnas.1902089116

Fernández, M. de la P., Chan, Y.-B., Yew, J. Y., Billeter, J.-C., Dreisewerd, K., Levine, J. D., & Kravitz, E. A. (2010). Pheromonal and behavioral cues trigger male-to-female aggression in *Drosophila*. *PLOS Biology*, *8*(11), e1000541. https://doi.org/10.1371/journal.pbio.1000541

Ferveur, J. F. (1997). The pheromonal role of cuticular hydrocarbons in *Drosophila melanogaster*. *BioEssays*, *19*(4), 353–358. https://doi.org/10.1002/bies.950190413

Ferveur, J. F., Savarit, F., O'Kane, C. J., Sureau, G., Greenspan, R. J., & Jallon, J. M. (1997). Genetic feminization of pheromones and its behavioral consequences in *Drosophila* males. *Science*, *276*(5318), 1555–1558. https://doi.org/10.1126/science.276.5318.1555

Ferveur, J. F., & Sureau, G. (1996). Simultaneous influence on male courtship of stimulatory and inhibitory pheromones produced by live sex-mosaic *Drosophila melanogaster*. *Proceedings of the Royal Society of London B: Biological Sciences*, *263*(1373), 967–973. https://doi.org/10.1098/rspb.1996.0143

Ferveur, J.-F. (2005). Cuticular hydrocarbons: Their evolution and roles in *Drosophila* pheromonal communication. *Behavior Genetics*, *35*(3), 279–295. https://doi.org/10.1007/s10519-005-3220-5

Finck, J., Berdan, E. L., Mayer, F., Ronacher, B., & Geiselhardt, S. (2016). Divergence of cuticular hydrocarbons in two sympatric grasshopper species and the evolution of fatty acid synthases and elongases across insects. *Scientific Reports*, *6*(1), 33695. https://doi.org/10.1038/srep33695

Finet, C., Slavik, K., Pu, J., Carroll, S. B., & Chung, H. (2019). Birth-and-death evolution of the fatty acyl-coA reductase (FAR) gene family and diversification of cuticular hydrocarbon synthesis in *Drosophila*. *Genome Biology and Evolution*, *11*(6), 1541–1551. https://doi.org/10.1093/gbe/evz094

Fishilevich, E., & Vosshall, L. B. (2005). Genetic and functional subdivision of the *Drosophila* antennal lobe. *Current Biology*, *15*(17), 1548–1553. https://doi.org/10.1016/j.cub.2005.07.066

Fleischer, J., & Krieger, J. (2018). Insect pheromone receptors—Key elements in sensing intraspecific chemical signals. *Frontiers in Cellular Neuroscience*, *12*, 425. https://doi.org/10.3389/fncel.2018.00425

Floate, K. D. (2002). Production of filth fly parasitoids (Hymenoptera: Pteromalidae) on fresh and on freeze-killed and stored house fly pupae. *Biocontrol Science and Technology*, *12*(5), 595–603. https://doi.org/10.1080/0958315021000016252

Flögel, J. H. L. (1878). Über den einheitlichen bau des gehirns in den verschiedenen insektenordnungen. *Zeitschrift Für Wissenschaftliche Zoologie*, *30*, 556–592.

Frederickx, C., Dekeirsschieter, J., Verheggen, F. J., & Haubruge, E. (2014). Host-habitat location by the parasitoid, *Nasonia vitripennis* Walker (Hymenoptera: Pteromalidae). *Journal of Forensic Sciences*, *59*(1), 242–249. https://doi.org/10.1111/1556-4029.12267

Futahashi, R., Yamahama, Y., Kawaguchi, M., Mori, N., Ishii, D., Okude, G., Hirai, Y., Kawahara-Miki, R., Yoshitake, K., Yajima, S., Hariyama, T., & Fukatsu, T. (2019). Molecular basis of wax-based color change and UV reflection in dragonflies. *eLife*, *8*, e43045. https://doi.org/10.7554/eLife.43045

G

Gailey, D. A., Billeter, J.-C., Liu, J. H., Bauzon, F., Allendorfer, J. B., & Goodwin, S. F. (2006). Functional conservation of the *Fruitless* Male sex-determination gene across 250 myr of insect evolution. *Molecular Biology and Evolution*, *23*(3), 633–643. https://doi.org/10.1093/molbev/msj070

Galizia, C. G. (2014). Olfactory coding in the insect brain: Data and conjectures. *European Journal of Neuroscience*, *39*(11), 1784–1795. https://doi.org/10.1111/ejn.12558

Galizia, C. G., & Rössler, W. (2010). Parallel olfactory systems in insects: Anatomy and function. *Annual Review of Entomology*, *55*(1), 399–420. https://doi.org/10.1146/annurev-ento-112408-085442

Gamble, T., & Zarkower, D. (2012). Sex determination. *Current Biology*, *22*(8), R257–R262. https://doi.org/10.1016/j.cub.2012.02.054

Gao, Q., Yuan, B., & Chess, A. (2000). Convergent projections of *Drosophila* olfactory neurons to specific glomeruli in the antennal lobe. *Nature Neuroscience*, *3*(8), 780–785. https://doi.org/10.1038/77680

Gardiner, A., Barker, D., Butlin, R. K., Jordan, W. C., & Ritchie, M. G. (2008). *Drosophila* chemoreceptor gene evolution: Selection, specialization and genome size. *Molecular Ecology*, *17*(7), 1648–1657. https://doi.org/10.1111/j.1365-294X.2008.03713.x

Gautam, S., McKenzie, S., Katzke, J., Hita Garcia, F., Yamamoto, S., & Economo, E. P. (2024). Evolution of odorant receptor repertoires across Hymenoptera is not linked to the evolution of eusociality. *Proceedings of the Royal Society B: Biological Sciences*, *291*(2031). https://doi.org/10.1098/rspb.2024.1280

Getahun, M. N., Olsson, S. B., Lavista-Llanos, S., Hansson, B. S., & Wicher, D. (2013). Insect odorant response sensitivity is tuned by metabotropically autoregulated olfactory receptors. *PLOS One*, *8*(3), e58889. https://doi.org/10.1371/journal.pone.0058889

Geuverink, E., & Beukeboom, L. W. (2014). Phylogenetic distribution and evolutionary dynamics of the sex determination genes *Doublesex* and *Transformer* in insects. *Sexual Development*, *8*(1–3), 38–49. https://doi.org/10.1159/000357056

Ghosh, N., Bakshi, A., Khandelwal, R., Rajan, S. G., & Joshi, R. (2019). The Hox gene *Abdominal-B* uses DoublesexF as a cofactor to promote neuroblast apoptosis in the *Drosophila* central nervous system. *Development*, *146*(16), dev175158. https://doi.org/10.1242/dev.175158

Gibson, N. J., & Tolbert, L. P. (2006). Activation of epidermal growth factor receptor mediates receptor axon sorting and extension in the developing olfactory system of the moth *Manduca sexta*. *Journal of Comparative Neurology*, *495*(5), 554–572. https://doi.org/10.1002/cne.20890

Gibson, N. J., Tolbert, L. P., & Oland, L. A. (2012). Activation of glial FGFRs is essential in glial migration, proliferation, and survival and in glia-neuron signaling during olfactory system development. *PLOS One*, *7*(4), e33828. https://doi.org/10.1371/journal.pone.0033828

Gill, K. S. (1963). A mutation causing abnormal courtship and mating behavior in males of *Drosophila melanogaster*. *American Zoologist*, *3*, 507.

Giunti, G., Canale, A., Messing, R. H., Donati, E., Stefanini, C., Michaud, J. P., & Benelli, G. (2015). Parasitoid learning: Current knowledge and implications for biological control. *Biological Control*, *90*, 208–219. https://doi.org/10.1016/j.biocontrol.2015.06.007

Goldman, A. L., Van der Goes van Naters, W., Lessing, D., Warr, C. G., & Carlson, J. R. (2005). Coexpression of two functional odor receptors in one neuron. *Neuron*, *45*(5), 661–666. https://doi.org/10.1016/j.neuron.2005.01.025

Gołębiowski, M., & Stepnowski, P. (2022). Chemical composition of insect surface waxes: Biological functions and analytics. In B. Buszewski & I. Baranowska (Eds.), *Handbook of bioanalytics* (pp. 647–664). Springer International Publishing, Cham. https://doi.org/10.1007/978-3-030-95660-8_29

Gómez-Skarmeta, J. L., Campuzano, S., & Modolell, J. (2003). Half a century of neural prepatterning: The story of a few bristles and many genes. *Nature Reviews Neuroscience*, *4*(7), 587–598. https://doi.org/10.1038/nrn1142

Goto, J., Mikawa, Y., Koganezawa, M., Ito, H., & Yamamoto, D. (2011). Sexually dimorphic shaping of interneuron dendrites involves the Hunchback transcription factor. *Journal of Neuroscience*, *31*(14), 5454–5459. https://doi.org/10.1523/JNEUROSCI.4861-10.2011

Goulding, S. E., zur Lage, P., & Jarman, A. P. (2000). *Amos*, a proneural gene for *Drosophila* olfactory sense organs that is regulated by Lozenge. *Neuron*, *25*(1), 69–78. https://doi.org/10.1016/s0896-6273(00)80872-7

Goyal, G., Zierau, A., Lattemann, M., Bergkirchner, B., Javorski, D., Kaur, R., & Hummel, T. (2019). Inter-axonal recognition organizes *Drosophila* olfactory map formation. *Scientific Reports*, *9*(1), 11554. https://doi.org/10.1038/s41598-019-47924-9

Grabe, V., Baschwitz, A., Dweck, H. K. M., Lavista-Llanos, S., Hansson, B. S., & Sachse, S. (2016). Elucidating the neuronal architecture of olfactory glomeruli in the *Drosophila* antennal Lobe. *Cell Reports*, *16*(12), 3401–3413. https://doi.org/10.1016/j.celrep.2016.08.063

Groot, A. T., Dekker, T., & Heckel, D. G. (2016). The genetic basis of pheromone evolution in moths. *Annual Review of Entomology*, *61*(1), 99–117. https://doi.org/10.1146/annurev-ento-010715-023638

Groothuis, J., Pfeiffer, K., El Jundi, B., & Smid, H. M. (2019). The jewel wasp standard brain: Average shape atlas and morphology of the female *Nasonia vitripennis* brain. *Arthropod Structure & Development*, *51*, 41–51. https://doi.org/10.1016/j.asd.2019.100878

Guerra, F. (2024). *The role of* Doublesex *in shaping temporal, spatial and species specific sex differentiation in* Nasonia *Wasps*. PhD dissertation, Wageningen University, Wageningen. https://edepot.wur.nl/651636

Gupta, B. P., & Rodrigues, V. (1997). *Atonal* is a proneural gene for a subset of olfactory sense organs in *Drosophila*. *Genes to Cells*, *2*(3), 225–233. https://doi.org/10.1046/j.1365-2443.1997.d01-312.x

H

Ha, T. S., & Smith, D. P. (2006). A pheromone receptor mediates 11-cis-vaccenyl acetate-induced responses in *Drosophila*. *Journal of Neuroscience*, *26*(34), 8727–8733. https://doi.org/10.1523/JNEUROSCI.0876-06.2006

Hagström, Å. K., Liénard, M. A., Groot, A. T., Hedenström, E., & Löfstedt, C. (2012). Semi–selective fatty acyl reductases from four Heliothine moths influence the specific pheromone composition. *PLOS One*, *7*(5), e37230. https://doi.org/10.1371/journal.pone.0037230

Hallem, E. A., & Carlson, J. R. (2006). Coding of odors by a receptor repertoire. *Cell*, *125*(1), 143–160. https://doi.org/10.1016/j.cell.2006.01.050

Hamilton, R. J. (1995). *Waxes: Chemistry, molecular biology and functions*. Oily Press, Dundee.

Hansson, B. S., & Anton, S. (2000). Function and morphology of the antennal lobe: New developments. *Annual Review of Entomology*, *45*(1), 203–231. https://doi.org/10.1146/annurev.ento.45.1.203

Hansson, B. S., Christensen, T. A., & Hildebrand, J. G. (1991). Functionally distinct subdivisions of the macroglomerular complex in the antennal lobe of the male sphinx moth *Manduca sexta*. *Journal of Comparative Neurology*, *312*(2), 264–278. https://doi.org/10.1002/cne.903120209

Hansson, B. S., Ljungberg, H., Hallberg, E., & Löfstedt, C. (1992). Functional specialization of olfactory glomeruli in a Moth. *Science*, *256*(5061), 1313–1315. https://doi.org/10.1126/science.1598574

Hansson, B. S., & Stensmyr, M. C. (2011). Evolution of insect olfaction. *Neuron*, *72*(5), 698–711. https://doi.org/10.1016/j.neuron.2011.11.003

Harvey, J. A., Poelman, E. H., & Tanaka, T. (2013). Intrinsic inter- and intraspecific competition in parasitoid wasps. *Annual Review of Entomology*, *58*(1), 333–351. https://doi.org/10.1146/annurev-ento-120811-153622

Hashimoto, Y. (1990). Unique features of sensilla on the antennae of formicidae (Hymenoptera). *Applied Entomology and Zoology*, *25*(4), 491–501. https://doi.org/10.1303/aez.25.491

Haverkamp, A., Hansson, B. S., & Knaden, M. (2018). Combinatorial codes and labeled lines: How insects use olfactory cues to find and judge food, mates, and oviposition sites in

complex environments. *Frontiers in Physiology*, *9*, 49. https://doi.org/10.3389/fphys.2018.00049

Heinrichs, V., Ryner, L. C., & Baker, B. S. (1998). Regulation of sex-specific selection of *Fruitless* 5' splice sites by Transformer and Transformer-2. *Molecular and Cellular Biology*, *18*(1), 450–458. https://doi.org/10.1128/MCB.18.1.450

Helmkampf, M., Cash, E., & Gadau, J. (2015). Evolution of the insect desaturase gene family with an emphasis on social Hymenoptera. *Molecular Biology and Evolution*, *32*(2), 456–471. https://doi.org/10.1093/molbev/msu315

Hendricks, G. M., & Hadley, N. F. (1983). Structure of the cuticle of the common house cricket with reference to the location of lipids. *Tissue & Cell*, *15*(5), 761–779. https://doi.org/10.1016/0040-8166(83)90049-6

Hildebrand, J. G., Matsumoto, S. G., Camazine, S. M., Tolbert, L. P., & Blank, S. (1980). Organisation and physiology of antennal centres in the brain of the moth *Manduca sexta*. In *Insect neurobiology and pesticide action (Neurotox 79)* (pp. 375–382). Society of Chemical Industry, London.

Hildebrand, J. G., & Shepherd, G. M. (1997). Mechanisms of olfactory discrimination: Converging evidence for common principles across phyla. *Annual Review of Neuroscience*, *20*(1), 595–631. https://doi.org/10.1146/annurev.neuro.20.1.595

Holze, H., Schrader, L., & Buellesbach, J. (2021). Advances in deciphering the genetic basis of insect cuticular hydrocarbon biosynthesis and variation. *Heredity*, *126*(2), 219–234. https://doi.org/10.1038/s41437-020-00380-y

Homberg, U., Christensen, T. A., & Hildebrand, J. G. (1989). Structure and function of the deutocerebrum in insects. *Annual Review of Entomology*, *34*(1), 477–501. https://doi.org/10.1146/annurev.en.34.010189.002401

Howard, R. W., & Blomquist, G. J. (2005). Ecological, behavioral, and biochemical aspects of insect hydrocarbons. *Annual Review of Entomology*, *50*(1), 371–393. https://doi.org/10.1146/annurev.ento.50.071803.130359

I

Ignell, R., Anton, S., & Hansson, B. S. (2001). The antennal lobe of orthoptera—Anatomy and evolution. *Brain, Behavior and Evolution*, *57*(1), 1–17. https://doi.org/10.1159/000047222

Ito, H., Fujitani, K., Usui, K., Shimizu-Nishikawa, K., Tanaka, S., & Yamamoto, D. (1996). Sexual orientation in *Drosophila* is altered by the satori mutation in the sex-determination gene *Fruitless* that encodes a zinc finger protein with a BTB domain. *Proceedings of the National Academy of Sciences of the United States of America*, *93*(18), 9687–9692. https://doi.org/10.1073/pnas.93.18.9687

J

Jallon, J.-M., Lauge, G., Orssaud, L., & Antony, C. (1988). Female pheromones in *Drosophila melanogaster* are controlled by the *Doublesex* locus. *Genetical Research*, *51*(1), 17–22. https://doi.org/10.1017/S0016672300023892

Jawlowski, H. (1948). Studies on the insect brain. *Annales Universitatis Mariae Curie-Sklodowska C*, *3*, 1–30.

Jefferis, G. S. X. E. (2005). Development of wiring specificity of the *Drosophila* olfactory System. *Chemical Senses*, *30*(Supplement 1), i94–i94. https://doi.org/10.1093/chemse/bjh130

Jefferis, G. S. X. E., Marin, E. C., Stocker, R. F., & Luo, L. (2001). Target neuron prespecification in the olfactory map of *Drosophila*. *Nature*, *414*(6860), 204–208. https://doi.org/10.1038/35102574

Jefferis, G. S. X. E., Vyas, R. M., Berdnik, D., Ramaekers, A., Stocker, R. F., Tanaka, N. K., Ito, K., & Luo, L. (2004). Developmental origin of wiring specificity in the olfactory system of *Drosophila*. *Development*, *131*(1), 117–130. https://doi.org/10.1242/dev.00896

Jhaveri, D., & Rodrigues, V. (2002). Sensory neurons of the *Atonal* lineage pioneer the formation of glomeruli within the adult *Drosophila* olfactory lobe. *Development*, *129*(5), 1251–1260. https://doi.org/10.1242/dev.129.5.1251

Jhaveri, D., Sen, A., & Rodrigues, V. (2000). Mechanisms underlying olfactory neuronal connectivity in *Drosophila*-the *Atonal* lineage organizes the periphery while sensory neurons and glia pattern the olfactory lobe. *Developmental Biology*, *226*(1), 73–87. https://doi.org/10.1006/dbio.2000.9855

Joerges, J., Küttner, A., Galizia, C. G., & Menzel, R. (1997). Representations of odours and odour mixtures visualized in the honeybee brain. *Nature*, *387*(6630), 285–288. https://doi.org/10.1038/387285a0

Johansson, B. G., & Jones, T. M. (2007). The role of chemical communication in mate choice. *Biological Reviews*, *82*(2), 265–289. https://doi.org/10.1111/j.1469-185X.2007.00009.x

Johnson, M. B., & Butterworth, F. M. (1985). Maturation and aging of adult fat body and oenocytes in *Drosophila* as revealed by light microscopic morphometry. *Journal of Morphology*, *184*(1), 51–59. https://doi.org/10.1002/jmor.1051840106

Jois, S., Chan, Y.-B., Fernandez, M. P., Pujari, N., Janz, L. J., Parker, S., & Leung, A. K.-W. (2022). Sexually dimorphic peripheral sensory neurons regulate copulation duration and persistence in male *Drosophila*. *Scientific Reports*, *12*(1), 6177. https://doi.org/10.1038/s41598-022-10247-3

Jones, W. D., Nguyen, T.-A. T., Kloss, B., Lee, K. J., & Vosshall, L. B. (2005). Functional conservation of an insect odorant receptor gene across 250 million years of evolution. *Current Biology*, *15*(4), R119–R121. https://doi.org/10.1016/j.cub.2005.02.007

K

Kaissling, K.-E., Kasang, G., Bestmann, H. J., Stransky, W., & Vostrowsky, O. (1978). A new pheromone of the silkworm moth *Bombyx mori*: Sensory pathway and behavioral effect. *Naturwissenschaften*, *65*(7), 382–384. https://doi.org/10.1007/BF00439702

Kaissling, K.-E., & Priesner, E. (1970). Die riechschwelle des seidenspinners. *Naturwissenschaften*, *57*(1), 23–28. https://doi.org/10.1007/BF00593550

Kaissling, K.-E., & Renner, M. (1968). Antennale rezeptoren für queen substance und sterzelduft bei der honigbiene. *Zeitschrift für Vergleichende Physiologie*, *59*(4), 357–361. https://doi.org/10.1007/BF00365967

Kalberer, N. M., Reisenman, C. E., & Hildebrand, J. G. (2010). Male moths bearing transplanted female antennae express characteristically female behaviour and central neural activity. *Journal of Experimental Biology*, *213*(8), 1272–1280. https://doi.org/10.1242/jeb.033167

Kandel, E. R. (2001). The molecular biology of memory storage: A dialogue between genes and synapses. *Science*, *294*(5544), 1030–1038. https://doi.org/10.1126/science.1067020

Kather, R., & Martin, S. J. (2015). Evolution of cuticular hydrocarbons in the Hymenoptera: A meta-Analysis. *Journal of Chemical Ecology*, *41*(10), 871–883. https://doi.org/10.1007/s10886-015-0631-5

Kawase, S. (1961). Role of lipid in the hardening of the cuticle in the silkworm, *Bombyx mori*. *Nature*, *191*, 279. https://doi.org/10.1038/191279a0

Keesey, I. W., & Hansson, B. S. (2021). The neuroethology of labeled lines in insect olfactory systems. In G. J. Blomquist & R. G. Vogt (Eds.), *Insect pheromone biochemistry and molecular Biology* (pp. 285–327). Elsevier, Amsterdam. https://doi.org/10.1016/B978-0-12-819628-1.00010-9

Keil, T. A. (1999). Morphology and development of the peripheral olfactory organs. In B. S. Hansson (Ed.), *Insect olfaction* (pp. 5–47). Springer Berlin Heidelberg. https://doi.org/10.1007/978-3-662-07911-9_2

Kenyon, F. C. (1896). The brain of the bee. A preliminary contribution to the morphology of the nervous system of the Arthropoda. *Journal of Comparative Neurology*, *6*, 133–210.

Kimura, K.-I., Hachiya, T., Koganezawa, M., Tazawa, T., & Yamamoto, D. (2008). *Fruitless* and *Doublesex* coordinate to generate male-specific neurons that can initiate courtship. *Neuron*, *59*(5), 759–769. https://doi.org/10.1016/j.neuron.2008.06.007

Kimura, K.-I., Ote, M., Tazawa, T., & Yamamoto, D. (2005). *Fruitless* specifies sexually dimorphic neural circuitry in the *Drosophila* brain. *Nature*, *438*(7065), 229–233. https://doi.org/10.1038/nature04229

King, P. E., & Rafai, J. (1970). Host discrimination in a gregarious parasitoid *Nasonia Vitripennis* (Walker) (Hymenoptera: Pteromalidae). *Journal of Experimental Biology*, *53*(1), 245–254. https://doi.org/10.1242/jeb.53.1.245

Kleineidam, C. J., Obermayer, M., Halbich, W., & Rössler, W. (2005). A macroglomerulus in the antennal lobe of leaf-cutting ant workers and its possible functional significance. *Chemical Senses*, *30*(5), 383–392. https://doi.org/10.1093/chemse/bji033

Koganezawa, M., Kimura, K.-I., & Yamamoto, D. (2016). The neural circuitry that functions as a switch for courtship versus aggression in *Drosophila* males. *Current Biology*, *26*(11), 1395–1403. https://doi.org/10.1016/j.cub.2016.04.017

Kohl, J., Ostrovsky, A. D., Frechter, S., & Jefferis, G. S. X. E. (2013). A bidirectional circuit switch reroutes pheromone signals in male and female brains. *Cell*, *155*(7), 1610–1623. https://doi.org/10.1016/j.cell.2013.11.025

Kollmann, M., Schmidt, R., Heuer, C. M., & Schachtner, J. (2016). Variations on a theme: Antennal lobe architecture across Coleoptera. *PLOS One*, *11*(12), e0166253. https://doi.org/10.1371/journal.pone.0166253

Komiyama, T., & Luo, L. (2006). Development of wiring specificity in the olfactory system. *Current Opinion in Neurobiology*, *16*(1), 67–73. https://doi.org/10.1016/j.conb.2005.12.002

Kondoh, Y., Kaneshiro, K. Y., Kimura, K., & Yamamoto, D. (2003). Evolution of sexual dimorphism in the olfactory brain of Hawaiian *Drosophila*. *Proceedings of the Royal Society B: Biological Sciences*, *270*(1519), 1005–1013. https://doi.org/10.1098/rspb.2003.2331

Koontz, M. A., & Schneider, D. (1987). Sexual dimorphism in neuronal projections from the antennae of silk moths (*Bombyx mori*, Antheraea polyphemus) and the gypsy moth (*Lymantria dispar*). *Cell and Tissue Research*, *249*(1), 39–50.

Koutroumpa, F. A., Monsempes, C., François, M.-C., De Cian, A., Royer, C., Concordet, J.-P., & Jacquin-Joly, E. (2016). Heritable genome editing with CRISPR/Cas9 induces anosmia in a crop pest moth. *Scientific Reports*, *6*(1), 29620. https://doi.org/10.1038/srep29620

Kropf, J., Kelber, C., Bieringer, K., & Rössler, W. (2014). Olfactory subsystems in the honeybee: Sensory supply and sex specificity. *Cell and Tissue Research*, *357*(3), 583–595. https://doi.org/10.1007/s00441-014-1892-y

Kühbandner, S., Sperling, S., Mori, K., & Ruther, J. (2012). Deciphering the signature of cuticular lipids with contact sex pheromone function in a parasitic wasp. *Journal of Experimental Biology*, *215*(14), 2471–2478. https://doi.org/10.1242/jeb.071217

Kurtovic, A., Widmer, A., & Dickson, B. J. (2007). A single class of olfactory neurons mediates behavioural responses to a *Drosophila* sex pheromone. *Nature*, *446*(7135), 542–546. https://doi.org/10.1038/nature05672

L

Larsson, M. C., Domingos, A. I., Jones, W. D., Chiappe, M. E., Amrein, H., & Vosshall, L. B. (2004). Or83b encodes a broadly expressed odorant receptor essential for *Drosophila* olfaction. *Neuron*, *43*(5), 703–714. https://doi.org/10.1016/j.neuron.2004.08.019

Laslo, M., Just, J., & Angelini, D. R. (2023). Theme and variation in the evolution of insect sex determination. *Journal of Experimental Zoology Part B: Molecular and Developmental Evolution*, *340*(2), 162–181. https://doi.org/10.1002/jez.b.23125

Lassance, J.-M., Groot, A. T., Liénard, M. A., Antony, B., Borgwardt, C., Andersson, F., Hedenström, E., Heckel, D. G., & Löfstedt, C. (2010). Allelic variation in a fatty-acyl reductase gene causes divergence in moth sex pheromones. *Nature*, *466*(7305), 486–489. https://doi.org/10.1038/nature09058

Lawrence, P. A., & Johnston, P. (1982). Cell lineage of the *Drosophila* abdomen: The epidermis, oenocytes and ventral muscles. *Journal of Embryology and Experimental Morphology*, *72*(1), 197–208.

Leal, W. S. (2013). Odorant reception in insects: Roles of receptors, binding proteins, and degrading enzymes. *Annual Review of Entomology*, *58*(1), 373–391. https://doi.org/10.1146/annurev-ento-120811-153635

Leary, G. P., Allen, J. E., Bunger, P. L., Luginbill, J. B., Linn, C. E., Macallister, I. E., Kavanaugh, M. P., & Wanner, K. W. (2012). Single mutation to a sex pheromone receptor provides adaptive specificity between closely related moth species. *Proceedings of the National Academy of Sciences of the United States of America*, *109*(35), 14081–14086. https://doi.org/10.1073/ pnas.1204661109

Lebreton, S., Trona, F., Borrero-Echeverry, F., Bilz, F., Grabe, V., Becher, P. G., Carlsson, M. A., Nässel, D. R., Hansson, B. S., Sachse, S., & Witzgall, P. (2015). Feeding regulates sex pheromone attraction and courtship in *Drosophila* females. *Scientific Reports*, *5*(1), 13132. https://doi.org/10.1038/srep13132

Lee, G., Foss, M., Goodwin, S. F., Carlo, T., Taylor, B. J., & Hall, J. C. (2000). Spatial, temporal, and sexually dimorphic expression patterns of the *Fruitless* gene in the *Drosophila* central nervous system. *Journal of Neurobiology*, *43*(4), 404–426. https://doi.org/10.1002/1097-4695(20000615)43:4<404::aid-neu8>3.0.co;2-d

Lee, G., Hall, J. C., & Park, J. H. (2002). *Doublesex* gene expression in the central nervous system of *Drosophila* melanogaster. *Journal of Neurogenetics*, *16*(4), 229–248. https://doi.org/10.1080/01677060216292

Legan, A. W., Jernigan, C. M., Miller, S. E., Fuchs, M. F., & Sheehan, M. J. (2021). Expansion and accelerated evolution of 9-exon odorant receptors in *Polistes* paper wasps. *Molecular Biology and Evolution*, *38*(9), 3832–3846. https://doi.org/10.1093/molbev/msab023

Leonhardt, S. D., Menzel, F., Nehring, V., & Schmitt, T. (2016). Ecology and evolution of communication in social insects. *Cell*, *164*(6), 1277–1287. https://doi.org/10.1016/j.cell.2016.01.035

Leung, K., Ras, E., Ferguson, K. B., Ariëns, S., Babendreier, D., Bijma, P., Bourtzis, K., Brodeur, J., Bruins, M. A., Centurión, A., Chattington, S. R., Chinchilla-Ramírez, M., Dicke, M., Fatouros, N. E., González-Cabrera, J., Groot, T. V. M., Haye, T., Knapp, M., Koskinioti, P., … Pannebakker, B. A. (2020). Next-generation biological control: The need for integrating genetics and genomics. *Biological Reviews*, *95*(6), 1838–1854. https://doi.org/10.1111/brv.12641

Leydig, F. (1864). *Vom bau des thierischen körpers: Handbuch der vergleichenden anatomie (Vol. 1)*. Verlag der H. Laupp'schen Buchhandlung, Tübingen.

Li, D., Dai, Y., Chen, X., Wang, X., Li, Z., Moussian, B., & Zhang, C. (2020). Ten fatty acyl-CoA reductase family genes were essential for the survival of the destructive rice pest, *Nilaparvata lugens*. *Pest Management Science*, *76*(7), 2304–2315. https://doi.org/10.1002/ps.5765

Li, Q., Ha, T. S., Okuwa, S., Wang, Y., Wang, Q., Millard, S. S., Smith, D. P., & Volkan, P. C. (2013). Combinatorial rules of precursor specification underlying olfactory neuron diversity. *Current Biology*, *23*(24), 2481–2490. https://doi.org/10.1016/j.cub.2013.10.053

Li, Y., Hoxha, V., Lama, C., Dinh, B. H., Vo, C. N., & Dauwalder, B. (2011). The hector G-protein coupled receptor is required in a subset of *Fruitless* neurons for male courtship behavior. *PLOS One*, *6*(11), e28269. https://doi.org/10.1371/journal.pone.0028269

Li, Y., Zhang, J., Chen, D., Yang, P., Jiang, F., Wang, X., & Kang, L. (2016). CRISPR/Cas9 in locusts: Successful establishment of an olfactory deficiency line by targeting the mutagenesis of an odorant receptor co-receptor (*Orco*). *Insect Biochemistry and Molecular Biology*, *79*, 27–35. https://doi.org/10.1016/j.ibmb.2016.10.003

Liénard, M. A., Hagström, Å. K., Lassance, J.-M., & Löfstedt, C. (2010). Evolution of multicomponent pheromone signals in small ermine moths involves a single fatty-acyl reductase gene. *Proceedings of the National Academy of Sciences of the United States of America*, *107*(24), 10955–10960. https://doi.org/10.1073/pnas.1000823107

Lin, C.-C., Prokop-Prigge, K. A., Preti, G., & Potter, C. J. (2015). Food odors trigger *Drosophila* males to deposit a pheromone that guides aggregation and female oviposition decisions. *eLife*, *4*, e08688. https://doi.org/10.7554/eLife.08688

Linz, J., Baschwitz, A., Strutz, A., Dweck, H. K. M., Sachse, S., Hansson, B. S., & Stensmyr, M. C. (2013). Host plant-driven sensory specialization in *Drosophila erecta*. *Proceedings of the Royal Society B: Biological Sciences*, *280*(1760), 20130626. https://doi.org/10.1098/rspb.2013.0626

Liu, L., Wei, K., Ren, Z., & Wang, X. (2024). Ultrastructure and distribution of antennal sensilla of parasitic wasp, *Cotesia gregalis* (Hymenoptera: Braconidae). *Microscopy Research and Technique*, *87*(12), jemt.24666. https://doi.org/10.1002/jemt.24666

Liu, Q., Liu, W., Zeng, B., Wang, G., Hao, D., & Huang, Y. (2017). Deletion of the *Bombyx mori* odorant receptor co-receptor (*BmOrco*) impairs olfactory sensitivity in silkworms. *Insect Biochemistry and Molecular Biology*, *86*, 58–67. https://doi.org/10.1016/j.ibmb.2017.05.007

Livak, K. J., & Schmittgen, T. D. (2001). Analysis of relative gene expression data using real-time quantitative PCR and the 2(-Delta Delta C(T)) method. *Methods*, *25*(4), 402–408. https://doi.org/10.1006/meth.2001.1262

Lockey, K. H. (1988). Lipids of the insect cuticle: Origin, composition and function. *Comparative Biochemistry and Physiology Part B: Comparative Biochemistry*, *89*(4), 595–645. https://doi.org/10.1016/0305-0491(88)90305-7

Löfstedt, C. (1993). Moth pheromone genetics and evolution. *Philosophical Transactions of the Royal Society B: Biological Sciences*, *340*(1292), 167–177. https://doi.org/10.1098/rstb.1993.0055

Luecke, D., Rice, G., & Kopp, A. (2022). Sex-specific evolution of a *Drosophila* sensory system via interacting cis- and trans-regulatory changes. *Evolution & Development*, *24*(1–2), 37–60. https://doi.org/10.1111/ede.12398

Luo, Y., Zhang, Y., Ferveur, J.-F., Ramírez, S., & Kopp, A. (2019). Evolution of sexually dimorphic pheromone profiles coincides with increased number of male-specific chemosensory organs in *Drosophila prolongata*. *Ecology and Evolution*, *9*(23), 13608–13618. https://doi.org/10.1002/ece3.5819

Lynch, J. A. (2015). The expanding genetic toolbox of the wasp *Nasonia vitripennis* and its relatives. *Genetics*, *199*(4), 897–904. https://doi.org/10.1534/genetics.112.147512

Lynch, J. A., & Desplan, C. (2006). A method for parental RNA interference in the wasp *Nasonia vitripennis*. *Nature Protocols*, *1*(1), 486–494. https://doi.org/10.1038/nprot.2006.70

M

Mair, M. M., Kmezic, V., Huber, S., Pannebakker, B. A., & Ruther, J. (2017). The chemical basis of mate recognition in two parasitoid wasp species of the genus *Nasonia*. *Entomologia Experimentalis et Applicata*, *164*(1), 1–15. https://doi.org/10.1111/eea.12589

Mair, M. M., & Ruther, J. (2019). Chemical ecology of the parasitoid wasp genus *Nasonia* (Hymenoptera, Pteromalidae). *Frontiers in Ecology and Evolution*, *7*, 184. https://doi.org/10.3389/fevo.2019.00184

Manoli, D. S., Fan, P., Fraser, E. J., & Shah, N. M. (2013). Neural control of sexually dimorphic behaviors. *Current Opinion in Neurobiology*, *23*(3), 330–338. https://doi.org/10.1016/j.conb.2013.04.005

Manoli, D. S., Foss, M., Villella, A., Taylor, B. J., Hall, J. C., & Baker, B. S. (2005). Male-specific *Fruitless* specifies the neural substrates of *Drosophila* courtship behaviour. *Nature*, *436*(7049), 395–400. https://doi.org/10.1038/nature03859

Martin, S., & Drijfhout, F. (2009). A review of ant cuticular hydrocarbons. *Journal of Chemical Ecology*, *35*(10), 1151–1161. https://doi.org/10.1007/s10886-009-9695-4

Marty, S., Couto, A., Dawson, E. H., Brard, N., d'Ettorre, P., Montgomery, S. H., & Sandoz, J.-C. (2025). Ancestral complexity and constrained diversification of the ant olfactory system. *Proceedings of the Royal Society B: Biological Sciences*, *292*(2045), 20250662. https://doi.org/10.1098/rspb.2025.0662

Masse, N. Y., Turner, G. C., & Jefferis, G. S. X. E. (2009). Olfactory information processing in *Drosophila*. *Current Biology*, *19*(16), R700–R713. https://doi.org/10.1016/j.cub.2009.06.026

McKenzie, S. K., Fetter-Pruneda, I., Ruta, V., & Kronauer, D. J. C. (2016). Transcriptomics and neuroanatomy of the clonal raider ant implicate an expanded clade of odorant receptors in chemical communication. *Proceedings of the National Academy of Sciences of the United States of America*, *113*(49), 14091–14096. https://doi.org/10.1073/pnas.1610800113

McKenzie, S. K., & Kronauer, D. J. C. (2018). The genomic architecture and molecular evolution of ant odorant receptors. *Genome Research*, *28*(11), 1757–1765. https://doi.org/10.1101/gr.237123.118

Meiners, T., Wäckers, F., & Lewis, W. J. (2003). Associative learning of complex odours in parasitoid host location. *Chemical Senses*, *28*(3), 231–236. https://doi.org/10.1093/chemse/28.3.231

Mellert, D. J., Knapp, J.-M., Manoli, D. S., Meissner, G. W., & Baker, B. S. (2010). Midline crossing by gustatory receptor neuron axons is regulated by *Fruitless*, *Doublesex* and

the *Roundabout* receptors. *Development*, *137*(2), 323–332. https://doi.org/10.1242/dev.045047

Mellert, D. J., Robinett, C. C., & Baker, B. S. (2012). *Doublesex* functions early and late in gustatory sense organ development. *PLOS One*, *7*(12), e51489. https://doi.org/10.1371/journal.pone.0051489

Missbach, C., Dweck, H., Vogel, H., Vilcinskas, A., Stensmyr, M. C., Hansson, B. S., & Grosse-Wilde, E. (2014). Evolution of insect olfactory receptors. *eLife*, *3*, e02115. https://doi.org/10.7554/eLife.02115

Moris, V. C., Podsiadlowski, L., Martin, S., Oeyen, J. P., Donath, A., Petersen, M., Wilbrandt, J., Misof, B., Liedtke, D., Thamm, M., Scheiner, R., Schmitt, T., & Niehuis, O. (2023). Intrasexual cuticular hydrocarbon dimorphism in a wasp sheds light on hydrocarbon biosynthesis genes in Hymenoptera. *Communications Biology*, *6*(1), 147. https://doi.org/10.1038/s42003-022-04370-0

Moto, K., Yoshiga, T., Yamamoto, M., Takahashi, S., Okano, K., Ando, T., Nakata, T., & Matsumoto, S. (2003). Pheromone gland-specific fatty-acyl reductase of the silkmoth, *Bombyx mori*. *Proceedings of the National Academy of Sciences of the United States of America*, *100*(16), 9156–9161. https://doi.org/10.1073/pnas.1531993100

N

Nakagawa, T., Pellegrino, M., Sato, K., Vosshall, L. B., & Touhara, K. (2012). Amino acid residues contributing to function of the heteromeric insect olfactory receptor complex. *PLOS One*, *7*(3), e32372. https://doi.org/10.1371/journal.pone.0032372

Nakanishi, A., Nishino, H., Watanabe, H., Yokohari, F., & Nishikawa, M. (2010). Sex-specific antennal sensory system in the ant *Camponotus japonicus*: Glomerular organizations of antennal lobes. *Journal of Comparative Neurology*, *518*(12), 2186–2201. https://doi.org/10.1002/cne.22326

Namiki, S., Iwabuchi, S., & Kanzaki, R. (2008). Representation of a mixture of pheromone and host plant odor by antennal lobe projection neurons of the silkmoth *Bombyx mori*. *Journal of Comparative Physiology A*, *194*(5), 501–515. https://doi.org/10.1007/s00359-008-0325-3

Neder, R. (1959). Allomerrisches wachstum von hirnteilen bei drei verschieden grossen schabenarten. *Zoologische Jahrbücher – Abteilung Für Anatomie Und Ontogenie Der Tiere*, *4*, 411–464.

Netschitailo, O., Wang, Y., Wagner, A., Sommer, V., Verhulst, E. C., & Beye, M. (2023). The function and evolution of a genetic switch controlling sexually dimorphic eye differentiation in honeybees. *Nature Communications*, *14*(1), 463. https://doi.org/10.1038/s41467-023-36153-4

Neville, M. C., Nojima, T., Ashley, E., Parker, D. J., Walker, J., Southall, T., Van de Sande, B., Marques, A. C., Fischer, B., Brand, A. H., Russell, S., Ritchie, M. G., Aerts, S., & Goodwin, S. F. (2014). Male-specific *Fruitless* isoforms target neurodevelopmental genes to specify a sexually dimorphic nervous system. *Current Biology*, *24*(3), 229–241. https://doi.org/10.1016/j.cub.2013.11.035

Nichols, A. S., Chen, S., & Luetje, C. W. (2011). Subunit contributions to insect olfactory receptor function: Channel block and odorant recognition. *Chemical Senses*, *36*(9), 781–790. https://doi.org/10.1093/chemse/bjr053

Niehuis, O., Buellesbach, J., Gibson, J. D., Pothmann, D., Hanner, C., Mutti, N. S., Judson, A. K., Gadau, J., Ruther, J., & Schmitt, T. (2013). Behavioural and genetic analyses of *Nasonia* shed light on the evolution of sex pheromones. *Nature*, *494*(7437), 345–348. https://doi.org/10.1038/nature11838

Niehuis, O., Büllesbach, J., Judson, A. K., Schmitt, T., & Gadau, J. (2011). Genetics of cuticular hydrocarbon differences between males of the parasitoid wasps *Nasonia giraulti* and *Nasonia vitripennis*. *Heredity*, *107*(1), 61–70. https://doi.org/10.1038/hdy.2010.157

Nishikawa, M., Nishino, H., Misaka, Y., Kubota, M., Tsuji, E., Satoji, Y., Ozaki, M., & Yokohari, F. (2008). Sexual dimorphism in the antennal lobe of the ant *Camponotus japonicus*. *Zoological Science*, *25*(2), 195–204. https://doi.org/10.2108/zsj.25.195

Nojima, T., Rings, A., Allen, A. M., Otto, N., Verschut, T. A., Billeter, J.-C., Neville, M. C., & Goodwin, S. F. (2021). A sex-specific switch between visual and olfactory inputs underlies adaptive sex differences in behavior. *Current Biology*, *31*(6), 1175–1191. https://doi.org/10.1016/j.cub.2020.12.047

Nowak, M. A., Tarnita, C. E., & Wilson, E. O. (2010). The evolution of eusociality. *Nature*, *466*(7310), 1057–1062. https://doi.org/10.1038/nature09205

O

Ochieng, S. A., Park, K. C., Zhu, J. W., & Baker, T. C. (2000). Functional morphology of antennal chemoreceptors of the parasitoid *Microplitis croceipes* (Hymenoptera: Braconidae). *Arthropod Structure & Development*, *29*(3), 231–240. https://doi.org/10.1016/s1467-8039(01)00008-1

Oland, L. A., Biebelhausen, J. P., & Tolbert, L. P. (2008). Glial investment of the adult and developing antennal lobe of *Drosophila*. *Journal of Comparative Neurology*, *509*(5), 526–550. https://doi.org/10.1002/cne.21762

Oland, L. A., & Tolbert, L. P. (1987). Glial patterns during early development of antennal lobes of *Manduca sexta*: A comparison between normal lobes and lobes deprived of antennal axons. *Journal of Comparative Neurology*, *255*(2), 196–207. https://doi.org/10.1002/cne.902550204

Oland, L. A., & Tolbert, L. P. (1998). Glomerulus development in the absence of a set of mitral-like neurons in the insect olfactory lobe. *Journal of Neurobiology*, *36*(1), 41–52. https://doi.org/10.1002/(sici)1097-4695(199807)36:1<41::aid-neu4>3.0.co;2-a

Oland, L. A., & Tolbert, L. P. (2011). Roles of glial cells in neural circuit formation: Insights from research in insects. *Glia*, *59*(9), 1273–1295. https://doi.org/10.1002/glia.21096

Oliveira, C. C. D., Manfrin, M. H., Sene, F. D. M., Jackson, L. L., & Etges, W. J. (2011). Variations on a theme: Diversification of cuticular hydrocarbons in a clade of cactophilic *Drosophila*. *BMC Evolutionary Biology*, *11*(1), 179. https://doi.org/10.1186/1471-2148-11-179

Oliveira, D. C. S. G., Werren, J. H., Verhulst, E. C., Giebel, J. D., Kamping, A., Beukeboom, L. W., & van de Zande, L. (2009). Identification and characterization of the *Doublesex* gene of *Nasonia*. *Insect Molecular Biology*, *18*(3), 315–324. https://doi.org/10.1111/j.1365-2583.2009.00874.x

Onagbola, E. O., & Fadamiro, H. Y. (2008). Scanning electron microscopy studies of antennal sensilla of *Pteromalus cerealellae* (Hymenoptera: Pteromalidae). *Micron*, *39*(5), 526–535. https://doi.org/10.1016/j.micron.2007.08.001

Ozaki, M., Wada-Katsumata, A., Fujikawa, K., Iwasaki, M., Yokohari, F., Satoji, Y., Nisimura, T., & Yamaoka, R. (2005). Ant nestmate and non-nestmate discrimination by a chemosensory sensillum. *Science*, *309*(5732), 311–314. https://doi.org/10.1126/science.1105244

P

Pask, G. M., Jones, P. L., Rützler, M., Rinker, D. C., & Zwiebel, L. J. (2011). Heteromeric Anopheline odorant receptors exhibit distinct channel properties. *PLOS One*, *6*(12), e28774. https://doi.org/10.1371/journal.pone.0028774

Pei, X.-J., Fan, Y.-L., Bai, Y., Bai, T.-T., Schal, C., Zhang, Z.-F., Chen, N., Li, S., & Liu, T.-X. (2021). Modulation of fatty acid elongation in cockroaches sustains sexually dimorphic hydrocarbons and female attractiveness. *PLOS Biology*, *19*(7), e3001330. https://doi.org/10.1371/journal.pbio.3001330

Pettersson, E. M., Hallberg, E., & Birgersson, G. (2001). Evidence for the importance of odour-perception in the parasitoid *Rhopalicus tutela* (Walker) (Hym., Pteromalidae). *Journal of Applied Entomology*, *125*(6), 293–301. https://doi.org/10.1046/j.1439-0418.2001.00550.x

Pilkington, L. J., Messelink, G., Van Lenteren, J. C., & Le Mottee, K. (2010). "Protected biological control" – biological pest management in the greenhouse industry. *Biological Control*, *52*(3), 216–220. https://doi.org/10.1016/j.biocontrol.2009.05.022

Polaszek, A., & Vilhemsen, L. (2023). Biodiversity of hymenopteran parasitoids. *Current Opinion in Insect Science*, *56*, 101026. https://doi.org/10.1016/j.cois.2023.101026

Prieto-Godino, L. L., Silbering, A. F., Khallaf, M. A., Cruchet, S., Bojkowska, K., Pradervand, S., Hansson, B. S., Knaden, M., & Benton, R. (2020). Functional integration of "undead" neurons in the olfactory system. *Science Advances*, *6*(11), eaaz7238. https://doi.org/10.1126/sciadv.aaz7238

R

Rabl-Rückhard, H. (1875). Studien über insektengehirne. *Reichert Und Du Bois Reymond's Archiv Für Anatomie*, 488–489.

Ramirez-Esquivel, F., Leitner, N. E., Zeil, J., & Narendra, A. (2017). The sensory arrays of the ant, *Temnothorax rugatulus*. *Arthropod Structure & Development*, *46*(4), 552–563. https://doi.org/10.1016/j.asd.2017.03.005

Ramirez-Esquivel, F., Zeil, J., & Narendra, A. (2014). The antennal sensory array of the nocturnal bull ant *Myrmecia pyriformis*. *Arthropod Structure & Development*, *43*(6), 543–558. https://doi.org/10.1016/j.asd.2014.07.004

Ray, A., van Naters, W. van der G., Shiraiwa, T., & Carlson, J. R. (2007). Mechanisms of odor receptor gene choice in *Drosophila*. *Neuron*, *53*(3), 353–369. https://doi.org/10.1016/j.neuron.2006.12.010

Ray, K., & Rodrigues, V. (1995). Cellular events during development of the olfactory sense organs in *Drosophila melanogaster*. *Developmental Biology*, *167*(2), 426–438. https://doi.org/10.1006/dbio.1995.1039

Raychoudhury, R., Desjardins, C. A., Buellesbach, J., Loehlin, D. W., Grillenberger, B. K., Beukeboom, L., Schmitt, T., & Werren, J. H. (2010). Behavioral and genetic characteristics of a new species of *Nasonia*. *Heredity*, *104*(3), 278–288. https://doi.org/10.1038/hdy.2009.147

Reddy, G. V. P., & Guerrero, A. (2004). Interactions of insect pheromones and plant semiochemicals. *Trends in Plant Science*, *9*(5), 253–261. https://doi.org/10.1016/j.tplants.2004.03.009

Reisenman, C. E., Christensen, T. A., Francke, W., & Hildebrand, J. G. (2004). Enantioselectivity of projection neurons innervating identified olfactory glomeruli. *Journal of Neuroscience*, *24*(11), 2602–2611. https://doi.org/10.1523/JNEUROSCI.5192-03.2004

Reisenman, C. E., Dacks, A. M., & Hildebrand, J. G. (2011). Local interneuron diversity in the primary olfactory center of the moth *Manduca sexta*. *Journal of Comparative Physiology A*, *197*(6), 653–665. https://doi.org/10.1007/s00359-011-0625-x

Renthal, R., Velasquez, D., Olmos, D., Hampton, J., & Wergin, W. P. (2003). Structure and distribution of antennal sensilla of the red imported fire ant. *Micron*, *34*(8), 405–413. https://doi.org/10.1016/S0968-4328(03)00050-7

Rideout, E. J., Billeter, J.-C., & Goodwin, S. F. (2007). The sex-determination genes *Fruitless* and *Doublesex* specify a neural substrate required for courtship song. *Current Biology*, *17*(17), 1473–1478. https://doi.org/10.1016/j.cub.2007.07.047

Riendeau, D., & Meighen, E. (1985). Enzymatic reduction of fatty acids and acyl-CoAs to long chain aldehydes and alcohols. *Experientia*, *41*(6), 707–713. https://doi.org/10.1007/BF02012564

Ritchie, M. G., & Noor, M. A. F. (2004). Evolutionary genetics: Gene replacement and the genetics of speciation. *Heredity*, *93*(1), 1–2. https://doi.org/10.1038/sj.hdy.6800456

Robertson, H. M., Gadau, J., & Wanner, K. W. (2010). The insect chemoreceptor superfamily of the parasitoid jewel wasp *Nasonia vitripennis*. *Insect Molecular Biology*, *19*, 121–136. https://doi.org/10.1111/j.1365-2583.2009.00979.x

Roegiers, F., Younger-Shepherd, S., Jan, L. Y., & Jan, Y. N. (2001). Two types of asymmetric divisions in the *Drosophila* sensory organ precursor cell lineage. *Nature Cell Biology*, *3*(1), 58–67. https://doi.org/10.1038/35050568

Roselino, A. C., Hrncir, M., da Cruz Landim, C., Giurfa, M., & Sandoz, J.-C. (2015). Sexual dimorphism and phenotypic plasticity in the antennal lobe of a stingless bee, *Melipona scutellaris*. *Journal of Comparative Neurology*, *523*(10), 1461–1473. https://doi.org/10.1002/cne.23744

Rospars, J. P. (1988). Structure and development of the insect antennodeutocerebral system. *Journal of Insect Morphology and Embryology*, *17*(3), 243–294. https://doi.org/10.1016/0020-7322(88)90041-4

Rospars, J. P., & Chambille, I. (1981). Deutocerebrum of the cockroach *Blaberus craniifer* Burm. Quantitative study and automated identification of the glomeruli. *Journal of Neurobiology*, *12*(3), 221–247. https://doi.org/10.1002/neu.480120304

Rospars, J. P., & Hildebrand, J. G. (2000). Sexually dimorphic and isomorphic glomeruli in the antennal lobes of the sphinx moth *Manduca sexta*. *Chemical Senses*, *25*(2), 119–129. https://doi.org/10.1093/chemse/25.2.119

Rospars, J.-P., & Chambille, I. (1989). Identified glomeruli in the antennal lobes of insects: In variance, sexual variation and postembryonic development. In R. N. Singh & N. J. Strausfeld (Eds.), *Neurobiology of sensory systems* (pp. 355–375). Springer US, Boston, MA. https://doi.org/10.1007/978-1-4899-2519-0_23

Rössler, W., & Brill, M. F. (2013). Parallel processing in the honeybee olfactory pathway: Structure, function, and evolution. *Journal of Comparative Physiology*, *199*(11), 981–996. https://doi.org/10.1007/s00359-013-0821-y

Rössler, W., Oland, L. A., Higgins, M. R., Hildebrand, J. G., & Tolbert, L. P. (1999). Development of a glia-rich axon-sorting zone in the olfactory pathway of the moth *Manduca sexta*. *Journal of Neuroscience*, *19*(22), 9865–9877. https://doi.org/10.1523/JNEUROSCI.19-22-09865.1999

Rössler, W., Tolbert, L. P., & Hildebrand, J. G. (2000). Importance of timing of olfactory receptor-axon outgrowth for glomerulus development in *Manduca sexta*. *Journal of Comparative Neurology*, *425*(2), 233–243.

Rössler, W., & Zube, C. (2011). Dual olfactory pathway in Hymenoptera: Evolutionary insights from comparative studies. *Arthropod Structure & Development*, *40*(4), 349–357. https://doi.org/10.1016/j.asd.2010.12.001

Rougeot, J., Guerra, F., & Verhulst, E. C. (2025). A transcriptional control model for *Doublesex*-dependent sex differentiation in *Nasonia* wasps. *BioRxiv*. https://doi.org/10.1101/2025.02.03.636189

Rusuwa, B. B., Chung, H., Allen, S. L., Frentiu, F. D., & Chenoweth, S. F. (2022). Natural variation at a single gene generates sexual antagonism across fitness components in *Drosophila*. *Current Biology*, *32*(14), 3161–3169. https://doi.org/10.1016/j.cub.2022.05.038

Ruther, J., & Hammerl, T. (2014). An oral male courtship pheromone terminates the response of *Nasonia vitripennis* females to the male-produced sex attractant. *Journal of Chemical Ecology*, *40*(1), 56–62. https://doi.org/10.1007/s10886-013-0372-2

Ruther, J., Stahl, L. M., Steiner, S., Garbe, L. A., & Tolasch, T. (2007). A male sex pheromone in a parasitic wasp and control of the behavioral response by the female's mating status. *Journal of Experimental Biology*, *210*(12), 2163–2169. https://doi.org/10.1242/jeb.02789

Ruther, J., Steiner, S., & Garbe, L. A. (2008). 4-methylquinazoline is a minor component of the male sex pheromone in *Nasonia vitripennis*. *Journal of Chemical Ecology*, *34*(1), 99–102. https://doi.org/10.1007/s10886-007-9411-1

Ruther, J., Thal, K., Blaul, B., & Steiner, S. (2010). Behavioural switch in the sex pheromone response of *Nasonia vitripennis* females is linked to receptivity signalling. *Animal Behaviour*, *80*(6), 1035–1040. https://doi.org/10.1016/j.anbehav.2010.09.008

Ruther, J., Thal, K., & Steiner, S. (2011). Pheromone communication in *Nasonia vitripennis*: Abdominal sex attractant mediates site fidelity of releasing males. *Journal of Chemical Ecology*, *37*(2), 161–165. https://doi.org/10.1007/s10886-010-9898-8

Ryba, A. R., McKenzie, S. K., Olivos-Cisneros, L., Clowney, E. J., Pires, P. M., & Kronauer, D. J. C. (2020). Comparative development of the ant chemosensory system. *Current Biology*, *30*(16), 3223–3230. https://doi.org/10.1016/j.cub.2020.05.072

Ryner, L. C., Goodwin, S. F., Castrillon, D. H., Anand, A., Villella, A., Baker, B. S., Hall, J. C., Taylor, B. J., & Wasserman, S. A. (1996). Control of male sexual behavior and sexual orientation in *Drosophila* by the *Fruitless* gene. *Cell*, *87*(6), 1079–1089. https://doi.org/10.1016/s0092-8674(00)81802-4

S

Saccone, G. (2022). A history of the genetic and molecular identification of genes and their functions controlling insect sex determination. *Insect Biochemistry and Molecular Biology*, *151*, 103873. https://doi.org/10.1016/j.ibmb.2022.103873

Sachse, S., Rappert, A., & Galizia, C. G. (1999). The spatial representation of chemical structures in the antennal lobe of honeybees: Steps towards the olfactory code. *European Journal of Neuroscience*, *11*(11), 3970–3982. https://doi.org/10.1046/j.1460-9568.1999.00826.x

Sanchez, G. M., Alkhori, L., Hatano, E., Schultz, S. W., Kuzhandaivel, A., Jafari, S., Granseth, B., & Alenius, M. (2016). Hedgehog signaling regulates the ciliary transport of odorant receptors in *Drosophila*. *Cell Reports*, *14*(3), 464–470. https://doi.org/10.1016/j.celrep.2015.12.059

Sánchez, L. (2008). Sex-determining mechanisms in insects. *International Journal of Developmental Biology*, *52*(7), 837–856. https://doi.org/10.1387/ijdb.072396ls

Sandoz, J.-C., Deisig, N., de Brito Sanchez, M. G., & Giurfa, M. (2007). Understanding the logics of pheromone processing in the honeybee brain: From labeled-lines to across-fiber patterns. *Frontiers in Behavioral Neuroscience*, *1*, 156. https://doi.org/10.3389/neuro.08.005.2007

Sato, K., Ito, H., & Yamamoto, D. (2020). *Teiresias*, a *Fruitless* target gene encoding an immunoglobulin-superfamily transmembrane protein, is required for neuronal feminization in *Drosophila*. *Communications Biology*, *3*(1), 598. https://doi.org/10.1038/s42003-020-01327-z

Sato, K., & Yamamoto, D. (2020). The mode of action of *Fruitless*: Is it an easy matter to switch the sex? *Genes, Brain, and Behavior*, *19*(2), e12606. https://doi.org/10.1111/gbb.12606

Savarit, F., & Ferveur, J.-F. (2002). Genetic study of the production of sexually dimorphic cuticular hydrocarbons in relation with the sex-determination gene *Transformer* in *Drosophila melanogaster*. *Genetical Research*, *79*(1), 23–40. https://doi.org/10.1017/s0016672301005481

Savarit, F., Sureau, G., Cobb, M., & Ferveur, J. F. (1999). Genetic elimination of known pheromones reveals the fundamental chemical bases of mating and isolation in *Drosophila*. *Proceedings of the National Academy of Sciences of the United States of America*, *96*(16), 9015–9020. https://doi.org/10.1073/pnas.96.16.9015

Schneider, D. (1964). Insect antennae. *Annual Review of Entomology*, *9*(1), 103–122. https://doi.org/10.1146/annurev.en.09.010164.000535

Schneider, D., & Steinbrecht, R. A. (1968). Checklist of insect olfactory sensilla. *Symposia of the Zoological Society London*, *23*, 279–297.

Schneiderman, A. M., Matsumoto, S. G., & Hildebrand, J. G. (1982). Trans-sexually grafted antennae influence development of sexually dimorphic neurones in moth brain. *Nature*, *298*(5877), 844–846. https://doi.org/10.1038/298844a0

Scott, D., & Jackson, L. L. (1988). Interstrain comparison of male-predominant antiaphrodisiacs in *Drosophila melanogaster*. *Journal of Insect Physiology*, *34*(9), 863–871. https://doi.org/10.1016/0022-1910(88)90120-5

Sen, A., Kuruvilla, D., Pinto, L., Sarin, A., & Rodrigues, V. (2004). Programmed cell death and context dependent activation of the EGF pathway regulate gliogenesis in the *Drosophila* olfactory system. *Mechanisms of Development*, *121*(1), 65–78. https://doi.org/10.1016/j.mod.2003.10.002

Sen, A., Shetty, C., Jhaveri, D., & Veronica Rodrigues. (2005). Distinct types of glial cells populate the *Drosophila* antenna. *BMC Developmental Biology*, *5*(1), 25. https://doi.org/10.1186/1471-213X-5-25

Shirangi, T. R., Dufour, H. D., Williams, T. M., & Carroll, S. B. (2009). Rapid evolution of sex pheromone-producing enzyme expression in *Drosophila*. *PLOS Biology*, *7*(8), e1000168. https://doi.org/10.1371/journal.pbio.1000168

Shirangi, T. R., Taylor, B. J., & McKeown, M. (2006). A double-switch system regulates male courtship behavior in male and female *Drosophila melanogaster*. *Nature Genetics*, *38*(12), 1435–1439. https://doi.org/10.1038/ng1908

Sieriebriennikov, B., Sieber, K. R., Kolumba, O., Mlejnek, J., Jafari, S., & Yan, H. (2024). *Orco*-dependent survival of odorant receptor neurons in ants. *Science Advances*, *10*(23), eadk9000. https://doi.org/10.1126/sciadv.adk9000

Silbering, A. F., Rytz, R., Grosjean, Y., Abuin, L., Ramdya, P., Jefferis, G. S. X. E., & Benton, R. (2011). Complementary function and integrated wiring of the evolutionarily distinct *Drosophila* olfactory subsystems. *Journal of Neuroscience*, *31*(38), 13357–13375. https://doi.org/10.1523/JNEUROSCI.2360-11.2011

Silva, I. M. D., Pereira, K. D. S., Spranghers, T., Zanuncio, J. C., & Serrão, J. E. (2016). Antennal sensilla and sexual dimorphism of the parasitoid *Trichospilus pupivorus*

(Hymenoptera: Eulophidae). *Microscopy and Microanalysis*, *22*(4), 913–921. https://doi.org/10.1017/S1431927616011314

Siwicki, K. K., & Kravitz, E. A. (2009). *Fruitless*, *Doublesex* and the genetics of social behavior in *Drosophila melanogaster*. *Current Opinion in Neurobiology*, *19*(2), 200–206. https://doi.org/10.1016/j.conb.2009.04.001

Slifer, E. H. (1969). Sense organs on the antenna of a parasitic wasp, *Nasonia vitripennis* (Hymenoptera, Pteromalidae). *The Biological Bulletin*, *136*(2), 253–263.

Slone, J. D., Pask, G. M., Ferguson, S. T., Millar, J. G., Berger, S. L., Reinberg, D., Liebig, J., Ray, A., & Zwiebel, L. J. (2017). Functional characterization of odorant receptors in the ponerine ant, *Harpegnathos saltator*. *Proceedings of the National Academy of Sciences of the United States of America*, *114*(32), 8586–8591. https://doi.org/10.1073/pnas.1704647114

Smadja, C., & Butlin, R. K. (2009). On the scent of speciation: The chemosensory system and its role in premating isolation. *Heredity*, *102*(1), 77–97. https://doi.org/10.1038/hdy.2008.55

Smid, H. M., Bleeker, M. A. K., van Loon, J. J. A., & Vet, L. E. M. (2003). Three-dimensional organization of the glomeruli in the antennal lobe of the parasitoid wasps *Cotesia glomerata* and *C. rubecula*. *Cell and Tissue Research*, *312*(2), 237–248. https://doi.org/10.1007/s00441-002-0659-z

Sprenger, P. P., & Menzel, F. (2020). Cuticular hydrocarbons in ants (Hymenoptera: Formicidae) and other insects: how and why they differ among individuals, colonies, and species. *Myrmecological News*, *30*, 1–26. https://doi.org/10.25849/MYRMECOL.NEWS_030:001

Steiger, S., Schmitt, T., & Schaefer, H. M. (2011). The origin and dynamic evolution of chemical information transfer. *Proceedings of the Royal Society B: Biological Sciences*, *278*(1708), 970–979. https://doi.org/10.1098/rspb.2010.2285

Steiger, S., & Stökl, J. (2014). The role of sexual selection in the evolution of chemical signals in insects. *Insects*, *5*(2), 423–438. https://doi.org/10.3390/insects5020423

Steinbrecht, R. A. (1970). Zur morphometrie der antenne des seidenspinners, *Bombyx mori* L.: Zahl und verteilung der riechsensillen (Insecta, Lepidoptera). *Zeitschrift für Morphologie der Tiere*, *68*(2), 93–126. https://doi.org/10.1007/BF00277500

Steinbrecht, R. A. (1987). Functional morphology of pheromone-sensitive sensilla. In G. D. Prestwich & G. J. Blomquist (Eds.), *Pheromone biochemistry* (pp. 353–384). Elsevier, Amsterdam. https://doi.org/10.1016/B978-0-12-564485-3.50016-6

Steinbrecht, R. A. (1997). Pore structures in insect olfactory sensilla: A review of data and concepts. *International Journal of Insect Morphology and Embryology*, *26*(3–4), 229–245. https://doi.org/10.1016/S0020-7322(97)00024-X

Steiner, S., Hermann, N., & Ruther, J. (2006). Characterization of a female-produced courtship pheromone in the parasitoid *Nasonia vitripennis*. *Journal of Chemical Ecology*, *32*(8), 1687–1702. https://doi.org/10.1007/s10886-006-9102-3

Steiner, S., & Ruther, J. (2009). Mechanism and behavioral context of male sex pheromone release in *Nasonia vitripennis*. *Journal of Chemical Ecology*, *35*(4), 416–421. https://doi.org/10.1007/s10886-009-9624-6

Stensmyr, M. C., Giordano, E., Balloi, A., Angioy, A.-M., & Hansson, B. S. (2003). Novel natural ligands for *Drosophila* olfactory receptor neurones. *Journal of Experimental Biology*, *206*(4), 715–724. https://doi.org/10.1242/jeb.00143

Stocker, R. F. (2001). *Drosophila* as a focus in olfactory research: Mapping of olfactory sensilla by fine structure, odor specificity, odorant receptor expression, and central connectivity. *Microscopy Research and Technique*, *55*(5), 284–296. https://doi.org/10.1002/jemt.1178

Stockinger, P., Kvitsiani, D., Rotkopf, S., Tirián, L., & Dickson, B. J. (2005). Neural circuitry that governs *Drosophila* male courtship behavior. *Cell*, *121*(5), 795–807. https://doi.org/10.1016/j.cell.2005.04.026

Stökl, J., & Steiger, S. (2017). Evolutionary origin of insect pheromones. *Current Opinion in Insect Science*, *24*, 36–42. https://doi.org/10.1016/j.cois.2017.09.004

Stouthamer, R. (1993). The use of sexual versus asexual wasps in biological control. *Entomophaga*, *38*(1), 3–6. https://doi.org/10.1007/BF02373133

Stowers, L., & Logan, D. W. (2010). Sexual dimorphism in olfactory signaling. *Current Opinion in Neurobiology*, *20*(6), 770–775. https://doi.org/10.1016/j.conb.2010.08.015

Strausfeld, N. J., Sinakevitch, I., Brown, S. M., & Farris, S. M. (2009). Ground plan of the insect mushroom body: Functional and evolutionary implications. *Journal of Comparative Neurology*, *513*(3), 265–291. https://doi.org/10.1002/cne.21948

Streinzer, M., Kelber, C., Pfabigan, S., Kleineidam, C. J., & Spaethe, J. (2013). Sexual dimorphism in the olfactory system of a solitary and a eusocial bee species. *Journal of Comparative Neurology*, *521*(12), 2742–2755. https://doi.org/10.1002/cne.23312

Suckling, D. M., Gibb, A. R., Burnip, G. M., & Delury, N. C. (2002). Can parasitoid sex pheromones help in insect biocontrol? A case study of codling moth (Lepidoptera: Tortricidae) and its parasitoid *Ascogaster quadridentata* (Hymenoptera: Braconidae). *Environmental Entomology*, *31*(6), 947–952. https://doi.org/10.1603/0046-225X-31.6.947

Suh, G. S. B., Wong, A. M., Hergarden, A. C., Wang, J. W., Simon, A. F., Benzer, S., Axel, R., & Anderson, D. J. (2004). A single population of olfactory sensory neurons mediates an innate avoidance behaviour in *Drosophila*. *Nature*, *431*(7010), 854–859. https://doi.org/10.1038/nature02980

Sun, H., Liu, F., Ye, Z., Baker, A., & Zwiebel, L. J. (2020). Mutagenesis of the *Orco* odorant receptor co-receptor impairs olfactory function in the malaria vector *Anopheles coluzzii*. *Insect Biochemistry and Molecular Biology*, *127*, 103497. https://doi.org/10.1016/j.ibmb.2020.103497

Sun, J., Liu, W.-K., Ellsworth, C., Sun, Q., Pan, Y., Huang, Y.-C., & Deng, W.-M. (2023a). Integrating lipid metabolism, pheromone production and perception by *Fruitless* and *Hepatocyte Nuclear Factor 4*. *Science Advances*, *9*(26), eadf6254. https://doi.org/10.1126/sciadv.adf6254

Sun, W., Lange, M. I., Gadau, J., & Buellesbach, J. (2023b). Decoding the genetic and chemical basis of sexual attractiveness in parasitic wasps. *eLife*, *12*, e86182. https://doi.org/10.7554/eLife.86182

Svensson, M. (1996). Sexual selection in moths: The role of chemical communication. *Biological Reviews*, *71*(1), 113–135. https://doi.org/10.1111/j.1469-185X.1996.tb00743.x

Syed, Z., Kopp, A., Kimbrell, D. A., & Leal, W. S. (2010). Bombykol receptors in the silkworm moth and the fruit fly. *Proceedings of the National Academy of Sciences of the United States of America*, *107*(20), 9436–9439. https://doi.org/10.1073/pnas.1003881107

Symonds, M. R. E., & Elgar, M. A. (2008). The evolution of pheromone diversity. *Trends in Ecology & Evolution*, *23*(4), 220–228. https://doi.org/10.1016/j.tree.2007.11.009

T

Taniguchi, R., Grimaldi, D. A., Watanabe, H., & Iba, Y. (2024). Sensory evidence for complex communication and advanced sociality in early ants. *Science Advances*, *10*(24), eadp3623. https://doi.org/10.1126/sciadv.adp3623

Taylor, B. J., & Truman, J. W. (1992). Commitment of abdominal neuroblasts in *Drosophila* to a male or female fate is dependent on genes of the sex-determining hierarchy. *Development*, *114*(3), 625–642. https://doi.org/10.1242/dev.114.3.625

Taylor, B. J., Villella, A., Ryner, L. C., Baker, B. S., & Hall, J. C. (1994). Behavioral and neurobiological implications of sex-determining factors in *Drosophila*. *Developmental Genetics*, *15*(3), 275–296. https://doi.org/10.1002/dvg.1020150309

Thomas, J. H. (2007). Rapid birth-death evolution specific to xenobiotic cytochrome P450 genes in vertebrates. *PLOS Genetics*, *3*(5), e67. https://doi.org/10.1371/journal.pgen.0030067

Tillman, J. A., Seybold, S. J., Jurenka, R. A., & Blomquist, G. J. (1999). Insect pheromones—An overview of biosynthesis and endocrine regulation. *Insect Biochemistry and Molecular Biology*, *29*(6), 481–514. https://doi.org/10.1016/s0965-1748(99)00016-8

Tissot, M., & Stocker, R. F. (2000). Metamorphosis in *Drosophila* and other insects: The fate of neurons throughout the stages. *Progress in Neurobiology*, *62*(1), 89–111. https://doi.org/10.1016/s0301-0082(99)00069-6

Toda, H., Zhao, X., & Dickson, B. J. (2012). The *Drosophila* female aphrodisiac pheromone activates ppk23+ sensory neurons to elicit male courtship behavior. *Cell Reports*, *1*(6), 599–607. https://doi.org/10.1016/j.celrep.2012.05.007

Tolbert, L. P., Oland, L. A., Tucker, E. S., Gibson, N. J., Higgins, M. R., & Lipscomb, B. W. (2004). Bidirectional influences between neurons and glial cells in the developing olfactory system. *Progress in Neurobiology*, *73*(2), 73–105. https://doi.org/10.1016/j.pneurobio.2004.04.004

Tompkins, L., & McRobert, S. P. (1989). Regulation of behavioral and pheromonal aspects of sex determination in *Drosophila melanogaster* by the *Sex-lethal* gene. *Genetics*, *123*(3), 535–541. https://doi.org/10.1093/genetics/123.3.535

Tompkins, L., & McRobert, S. P. (1995). Behavioral and pheromonal phenotypes associated with expression of loss-of-function mutations in the *Sex-lethal* gene of *Drosophila Melanogaster*. *Journal of Neurogenetics*, *9*(4), 219–226. https://doi.org/10.3109/01677069509084158

Touhara, K., & Vosshall, L. B. (2009). Sensing odorants and pheromones with chemosensory receptors. *Annual Review of Physiology*, *71*(1), 307–332. https://doi.org/10.1146/annurev.physiol.010908.163209

Trible, W., Olivos-Cisneros, L., McKenzie, S. K., Saragosti, J., Chang, N.-C., Matthews, B. J., Oxley, P. R., & Kronauer, D. J. C. (2017). *Orco* mutagenesis causes loss of antennal lobe glomeruli and impaired social behavior in ants. *Cell*, *170*(4), 727–735. https://doi.org/10.1016/j.cell.2017.07.001

Troost, T., Binshtok, U., Sprinzak, D., & Klein, T. (2023). *Cis*-inhibition suppresses basal Notch signaling during sensory organ precursor selection. *Proceedings of the National Academy of Sciences of the United States of America*, *120*(23), e2214535120. https://doi.org/10.1073/ pnas.2214535120

Tupec, M., Buček, A., Janoušek, V., Vogel, H., Prchalová, D., Kindl, J., Pavlíčková, T., Wenzelová, P., Jahn, U., Valterová, I., & Pichová, I. (2019). Expansion of the fatty acyl reductase gene family shaped pheromone communication in Hymenoptera. *eLife*, *8*, e39231. https://doi.org/10.7554/eLife.39231

U

Usui-Aoki, K., Ito, H., Ui-Tei, K., Takahashi, K., Lukacsovich, T., Awano, W., Nakata, H., Piao, Z. F., Nilsson, E. E., Tomida, J., & Yamamoto, D. (2000). Formation of the male-specific muscle in female *Drosophila* by ectopic *Fruitless* expression. *Nature Cell Biology*, *2*(8), 500–506. https://doi.org/10.1038/35019537

V

Van Den Assem, J., Jachmann, F., & Simbolotti, P. (1980). Courtship behaviour of *Nasonia vitripennis* (Hym., Pteromalidae): Some qualitative, experimental evidence for the role of pheromones. *Behaviour*, *75*(3–4), 301–307. https://doi.org/10.1163/156853980X00456

Van der Goes van Naters, W., & Carlson, J. R. (2007). Receptors and neurons for fly odors in *Drosophila*. *Current Biology*, *17*(7), 606–612. https://doi.org/10.1016/j.cub.2007.02.043

Van Lenteren, J. C., Bolckmans, K., Köhl, J., Ravensberg, W. J., & Urbaneja, A. (2018). Biological control using invertebrates and microorganisms: Plenty of new opportunities. *BioControl*, *63*(1), 39–59. https://doi.org/10.1007/s10526-017-9801-4

Van Schooten, B., Meléndez-Rosa, J., Van Belleghem, S. M., Jiggins, C. D., Tan, J. D., McMillan, W. O., & Papa, R. (2020). Divergence of chemosensing during the early stages of speciation. *Proceedings of the National Academy of Sciences of the United States of America*, *117*(28), 16438–16447. https://doi.org/10.1073/pnas.1921318117

Vareschi, E. (1971). Duftunterscheidung bei der honigbiene—Einzelzell-ableitungen und verhaltensreaktionen. *Zeitschrift für vergleichende Physiologie*, *75*(2), 143–173. https://doi.org/10.1007/BF00335260

Verhulst, E. C., Beukeboom, L. W., & van de Zande, L. (2010a). Maternal control of haplodiploid sex determination in the wasp *Nasonia*. *Science*, *328*(5978), 620–623. https://doi.org/10.1126/science.1185805

Verhulst, E. C., & van de Zande, L. (2015). Double nexus—*Doublesex* is the connecting element in sex determination. *Briefings in Functional Genomics*, *14*(6), 396–406. https://doi.org/10.1093/bfgp/elv005

Verhulst, E. C., van de Zande, L., & Beukeboom, L. W. (2010b). Insect sex determination: It all evolves around *Transformer*. *Current Opinion in Genetics & Development*, *20*(4), 376–383. https://doi.org/10.1016/j.gde.2010.05.001

Vernes, S. C. (2014). Genome wide identification of *Fruitless* targets suggests a role in upregulating genes important for neural circuit formation. *Scientific Reports*, *4*(1), 4412. https://doi.org/10.1038/srep04412

Viallanes, H. (1887). Etudes histologiques et organologiques sur les centres nerveux et les organs des sens des animaux articulés. I. Le cerveau du criquet (Oedipoda coerulesence et *Caloptenus italicus*). *Annales Des Sciences Naturelles, Zoologie 7e Série*, *2*, 1–98.

Villella, A., & Hall, J. C. (1996). Courtship anomalies caused by *Doublesex* mutations in *Drosophila melanogaster*. *Genetics*, *143*(1), 331–344. https://doi.org/10.1093/genetics/143.1.331

Vogt, R. G., Prestwich, G. D., & Lerner, M. R. (1991). Odorant-binding-protein subfamilies associate with distinct classes of olfactory receptor neurons in insects. *Journal of Neurobiology*, *22*(1), 74–84. https://doi.org/10.1002/neu.480220108

von Philipsborn, A. C., Jörchel, S., Tirian, L., Demir, E., Morita, T., Stern, D. L., & Dickson, B. J. (2014). Cellular and behavioral functions of *Fruitless* isoforms in *Drosophila* courtship. *Current Biology*, *24*(3), 242–251. https://doi.org/10.1016/j.cub.2013.12.015

Vosshall, L. B. (2000). Olfaction in *Drosophila*. *Current Opinion in Neurobiology*, *10*(4), 498–503. https://doi.org/10.1016/s0959-4388(00)00111-2

Vosshall, L. B., Amrein, H., Morozov, P. S., Rzhetsky, A., & Axel, R. (1999). A spatial map of olfactory receptor expression in the *Drosophila* antenna. *Cell*, *96*(5), 725–736. https://doi.org/10.1016/s0092-8674(00)80582-6

W

Walther, J. R. (1981). *Die morphologie und feinstruktur der sinnesorgane auf den antennengeisse in der männchen, weibchen und arbeiterinnen der roten waldameise* Formica rufa *Linne 1758 mit einem vergleich der antennalen sensillenmuster weiterer Formicoidea (Hymenoptera)*. PhD dissertation, Free University, Berlin.

Wang, S., Sato, K., Giurfa, M., & Zhang, S. (2008). Processing of sting pheromone and its components in the antennal lobe of the worker honeybee. *Journal of Insect Physiology*, *54*(5), 833–841. https://doi.org/10.1016/j.jinsphys.2008.03.004

Wang, Y., Rensink, A. H., Fricke, U., Riddle, M. C., Trent, C., van de Zande, L., & Verhulst, E. C. (2022a). *Doublesex* regulates male-specific differentiation during distinct developmental time windows in a parasitoid wasp. *Insect Biochemistry and Molecular Biology*, *142*, 103724. https://doi.org/10.1016/j.ibmb.2022.103724

Wang, Y., Sun, W., Fleischmann, S., Millar, J. G., Ruther, J., & Verhulst, E. C. (2022b). Silencing *Doublesex* expression triggers three-level pheromonal feminization in *Nasonia vitripennis* males. *Proceedings of the Royal Society B: Biological Sciences*, *289*(1967), 20212002. https://doi.org/10.1098/rspb.2021.2002

Wang, Z., Andika, I. P., & Chung, H. (2025). Regulation of insect cuticular hydrocarbon biosynthesis. *Current Opinion in Insect Science*, *67*, 101287. https://doi.org/10.1016/j.cois.2024.101287

Wang, Z., Pu, J., Richards, C., Giannetti, E., Cong, H., Lin, Z., & Chung, H. (2023). Evolution of a fatty acyl–CoA elongase underlies desert adaptation in *Drosophila*. *Science Advances*, *9*(35), eadg0328. https://doi.org/10.1126/sciadv.adg0328

Watanabe, H., Haupt, S. S., Nishino, H., Nishikawa, M., & Yokohari, F. (2012). Sensillum-specific, topographic projection patterns of olfactory receptor neurons in the antennal lobe of the cockroach *Periplaneta americana*. *The Journal of Comparative Neurology*, *520*(8), 1687–1701. https://doi.org/10.1002/cne.23007

Watanabe, T. (2019). Evolution of the neural sex-determination system in insects: Does *Fruitless* homologue regulate neural sexual dimorphism in basal insects? *Insect Molecular Biology*, *28*(6), 807–827. https://doi.org/10.1111/imb.12590

Waterbury, J. A., Jackson, L. L., & Schedl, P. (1999). Analysis of the *Doublesex* female protein in *Drosophila melanogaster*: Role on sexual differentiation and behavior and dependence on *Intersex*. *Genetics*, *152*(4), 1653–1667. https://doi.org/10.1093/genetics/152.4.1653

Wcislo, W. T. (1995). Sensilla numbers and antennal morphology of parasitic and non-parasitic bees (Hymenoptera: Apoidea). *International Journal of Insect Morphology and Embryology*, *24*(1), 63–81. https://doi.org/10.1016/0020-7322(94)E0006-B

Weiss, I., Hofferberth, J., Ruther, J., & Stökl, J. (2015). Varying importance of cuticular hydrocarbons and iridoids in the species-specific mate recognition pheromones of three closely related *Leptopilina* species. *Frontiers in Ecology and Evolution*, *3*. https://doi.org/10.3389/fevo.2015.00019

Werren, J. H., & Loehlin, D. W. (2009a). Strain maintenance of *Nasonia vitripennis* (parasitoid wasp). *Cold Spring Harbor Protocols*, *2009*(10), pdb.prot5307. https://doi.org/10.1101/pdb.prot5307

Werren, J. H., & Loehlin, D. W. (2009b). The parasitoid wasp *Nasonia:* an emerging model system with haploid male genetics. *Cold Spring Harbor Protocols*, *2009*(10), pdb.emo134. https://doi.org/10.1101/pdb.emo134

Werren, J. H., Loehlin, D. W., & Giebel, J. D. (2009). Larval RNAi in *Nasonia* (parasitoid wasp). *Cold Spring Harbor Protocols*, *2009*(10), pdb.prot5311. https://doi.org/10.1101/pdb.prot5311

Werren, J. H., Richards, S., Desjardins, C. A., Niehuis, O., Gadau, J., Colbourne, J. K., The Nasonia Genome Working Group. (2010). Functional and evolutionary insights from the genomes of three parasitoid *Nasonia* species. *Science*, *327*(5963), 343–348. https://doi.org/10.1126/science.1178028

Whiting, A. R. (1967). The biology of the parasitic wasp *Mormoniella vitripennis* [=*Nasonia brevicornis*] (Walker). *The Quarterly Review of Biology*, *42*(3), 333–406. https://doi.org/10.1086/405402

Wibel, R. G., Cassidy, J. D., Buhse, H. E., Cummings, M. R., Bindokas, V. P., Charlesworth, J., & Baumgartner, D. L. (1984). Scanning electron microscopy of antennal sense organs of *Nasonia vitripennis* (Hymenoptera: Pteromalidae). *Transactions of the American Microscopical Society*, *103*(4), 329–340. https://doi.org/10.2307/3226468

Wigglesworth, V. B. (1970). Structural lipids in the insect cuticle and the function of the oenocytes. *Tissue and Cell*, *2*(1), 155–179. https://doi.org/10.1016/s0040-8166(70)80013-1

Wilkins, A. S. (1995). Moving up the hierarchy: A hypothesis on the evolution of a genetic sex determination pathway. *BioEssays*, *17*(1), 71–77. https://doi.org/10.1002/bies.950170113

Williams, A. T., Verhulst, E. C., & Haverkamp, A. (2022). A unique sense of smell: Development and evolution of a sexually dimorphic antennal lobe – a review. *Entomologia Experimentalis et Applicata*, *170*(4), 303–318. https://doi.org/10.1111/eea.13145

Wilson, E. O. (1965). Chemical communication in the social insects. *Science*, *149*(3688), 1064–1071. https://doi.org/10.1126/science.149.3688.1064

Wilson, E. O., & Bossert, W. H. (1963). Chemical communication among animals. *Recent Progress in Hormone Research*, *19*, 673–716.

Würf, J., Pokorny, T., Wittbrodt, J., Millar, J. G., & Ruther, J. (2020). Cuticular hydrocarbons as contact sex pheromone in the parasitoid wasp *Urolepis rufipes*. *Frontiers in Ecology and Evolution*, *8*, 180. https://doi.org/10.3389/fevo.2020.00180

Wyatt, T. D. (2003). *Pheromones and animal behaviour: Communication by smell and taste* (1st ed.). Cambridge University Press, Cambridge. https://doi.org/10.1017/CBO9780511615061

Wyatt, T. D. (2014). *Pheromones and animal behavior: Chemical signals and signatures* (2nd ed.). Cambridge University Press, Cambridge. https://doi.org/10.1017/CBO9781139030748

X

Xu, P., Atkinson, R., Jones, D. N. M., & Smith, D. P. (2005). Drosophila OBP LUSH is required for activity of pheromone-sensitive neurons. *Neuron*, *45*(2), 193–200. https://doi.org/10.1016/j.neuron.2004.12.031

Y

Yamagata, N., Nishino, H., & Mizunami, M. (2006). Pheromone-sensitive glomeruli in the primary olfactory centre of ants. *Proceedings of the Royal Society B: Biological Sciences*, *273*(1598), 2219–2225. https://doi.org/10.1098/rspb.2006.3565

Yamamoto, D. (2007). The neural and genetic substrates of sexual behavior in *Drosophila*. *Advances in Genetics*, *59*, 39–66. https://doi.org/10.1016/S0065-2660(07)59002-4

Yamamoto, D., & Koganezawa, M. (2013). Genes and circuits of courtship behaviour in *Drosophila* males. *Nature Reviews Neuroscience*, *14*(10), 681–692. https://doi.org/10.1038/nrn3567

Yan, H., Opachaloemphan, C., Mancini, G., Yang, H., Gallitto, M., Mlejnek, J., Leibholz, A., Haight, K., Ghaninia, M., Huo, L., Perry, M., Slone, J., Zhou, X., Traficante, M., Penick, C. A., Dolezal, K., Gokhale, K., Stevens, K., Fetter-Pruneda, I., … Desplan, C. (2017). An engineered *Orco* mutation produces aberrant social behavior and defective neural development in ants. *Cell*, *170*(4), 736–747. https://doi.org/10.1016/j.cell.2017.06.051

Z

Zacharuk, R. Y. (1980). Ultrastructure and function of insect chemosensilla. In *Annual Review of Entomology*, 25, 27–47. https://doi.org/10.1146/ annurev.en.25.010180.000331

Zhang, Q., Chen, J., Wang, Y., Lu, Y., Dong, Z., Shi, W., Pang, L., Ren, S., Chen, X., & Huang, J. (2023). The *Odorant receptor co-receptor* gene contributes to mating and host-searching behaviors in parasitoid wasps. *Pest Management Science*, *79*(1), 454–463. https://doi.org/10.1002/ps.7214

Zhang, X., Miao, Q., Xu, X., Ji, B., Qu, L., & Wei, Y. (2021). Developments in fatty acid-derived insect pheromone production using engineered yeasts. *Frontiers in Microbiology*, *12*, 759975. https://doi.org/10.3389/fmicb.2021.759975

Zhou, C., Pan, Y., Robinett, C. C., Meissner, G. W., & Baker, B. S. (2014). Central brain neurons expressing *Doublesex* regulate female receptivity in *Drosophila*. *Neuron*, *83*(1), 149–163. https://doi.org/10.1016/j.neuron.2014.05.038

Zhou, X., Rokas, A., Berger, S. L., Liebig, J., Ray, A., & Zwiebel, L. J. (2015). Chemoreceptor evolution in Hymenoptera and its implications for the evolution of eusociality. *Genome Biology and Evolution*, *7*(8), 2407–2416. https://doi.org/10.1093/gbe/evv149

Zhu, H., Hummel, T., Clemens, J. C., Berdnik, D., Zipursky, S. L., & Luo, L. (2006). Dendritic patterning by Dscam and synaptic partner matching in the *Drosophila* antennal lobe. *Nature Neuroscience*, *9*(3), 349–355. https://doi.org/10.1038/nn1652

Zhu, H., & Luo, L. (2004). Diverse functions of N-cadherin in dendritic and axonal terminal arborization of olfactory projection neurons. *Neuron*, *42*(1), 63–75. https://doi.org/10.1016/s0896-6273(04)00142-4

Zou, Y., Geuverink, E., Beukeboom, L. W., Verhulst, E. C., & van de Zande, L. (2020). A chimeric gene paternally instructs female sex determination in the haplodiploid wasp *Nasonia*. *Science*, *370*(6520), 1115–1118. https://doi.org/10.1126/science.abb8949

Zube, C., Kleineidam, C. J., Kirschner, S., Neef, J., & Rössler, W. (2008). Organization of the olfactory pathway and odor processing in the antennal lobe of the ant *Camponotus floridanus*. *Journal of Comparative Neurology*, *506*(3), 425–441. https://doi.org/10.1002/cne.21548

Zube, C., & Rössler, W. (2008). Caste- and sex-specific adaptations within the olfactory pathway in the brain of the ant *Camponotus floridanus*. *Arthropod Structure & Development*, *37*(6), 469–479. https://doi.org/10.1016/j.asd.2008.05.004

zur Lage, P. I., Prentice, D. R. A., Holohan, E. E., & Jarman, A. P. (2003). The *Drosophila* proneural gene *Amos* promotes olfactory sensillum formation and suppresses bristle formation. *Development*, *130*(19), 4683–4693. https://doi.org/10.1242/dev.00680

Summary

The sex-determination system of animals regulates sexual differentiation, the development of sexual dimorphism between sexes of the same species. These distinct sexual characteristics can vary enormously. Compare the tail feathers of the male peacock, the mane of a male lion, the bright coloration of male guppies or the extreme size variation in angler fish. But also the production and perception of sex pheromones in insects. The sex-determination pathway in insects comprises a cascade of sex-determination genes. This pathway is initiated by a primary signal, which is transduced by instructor genes to conserved transcription factors required for sexual differentiation.

Most insects share a core sex-determination mechanism, comprising a splicing-factor gene, called *Transformer* (*Tra*), and the transcription-factor genes *Doublesex* (*Dsx*) and *Fruitless* (*Fru*). *Dsx* and *Fru* are responsible for morphological and behavioural sexual differentiation. These transcription-factor genes play a significant role in regulating biosynthesis, chemoreception and neurodevelopment in pheromone communication. Males and females may produce different pheromones and have distinct chemosensory receptors to perceive them, or they may produce the same pheromone and have the same receptor, but a different neural circuit to process the information. However, research on how these transcription factors regulate these traits has primarily been limited to the fruit fly *Drosophila melanogaster*, which utilizes a so-called dedicated labelled-line system to perceive and process pheromones. Other insects, including Hymenoptera, have evolved a different coding system to discriminate pheromones.

Hymenoptera utilize a system in which a single pheromone compound can activate combinations of pheromone receptors and glomeruli in the insect antennal lobe (AL). This system is called combinatorial coding and has evolved in Hymenoptera to meet the increased demand for olfactory discrimination to negotiate their intricate life histories, such as parasitoidism and sociality. Combinatorial coding is used in these species to process their complex pheromone blends, in particular their cuticular hydrocarbon (CHC) profiles. However, how sex-determination mechanisms regulate the specific pheromone-coding systems in these species remains unknown. Understanding how these genetic mechanisms operate would therefore provide more insight into the forces driving evolutionary transitions in insect pheromone communication.

The aim of my thesis was to elucidate the genetic mechanisms by which sexual differentiation regulates pheromone communication of the parasitoid wasp *Nasonia vitripennis*. To do this, I investigated the role that sex-determination transcription factors play in regulating pheromone production and perception in this model species. I silenced the genes responsible for male and female differentiation with RNA interference (RNAi): *Dsx* in males and *Tra* in females. I first determined the function of these genes in regulating pheromone perception

by analysing (1) the development of sensilla on the insect antennae, (2) the formation of glomeruli in the AL and (3) the downstream neurodevelopmental genes involved. I then turned to pheromone production and analysed (4) sexual dimorphism in the CHC profile and (5) the downstream biosynthetic genes.

In **Chapter 2**, I present a comprehensive literature review in which I reflect on the diversity of chemosensory adaptations that have evolved in insects to increase the sensitivity to sex pheromones. This chapter also explores the underlying sex-determination mechanisms that regulate the development of sexually dimorphic neural circuits. My review shows that the development of these circuits starts in the peripheral nervous system through the expression of pheromone receptors in specialized sensilla. Subsequently, during neuronal development, the process of programmed cell death determines the survival of olfactory sensory neurons (OSNs), which is necessary for establishing functional connections in the AL and higher brain regions. My review highlights the importance of DSX and FRU in determining sexual dimorphism of neurons by regulating programmed cell-death genes for neuronal survival and axon-guidance genes for neurite development. I also discuss the perceptional and processing properties unique to Hymenoptera. These species typically use specialized sensilla and glomeruli for perceiving CHCs as signals for recognizing mating partners, nestmates and hosts. My review compares the specific processes responsible for glomerular formation in Diptera, Lepidoptera and Hymenoptera. From this comparison, I conclude that Hymenoptera have evolved unique neurodevelopmental mechanisms. Essentially, these species depend heavily on OSN innervation for glomerular development necessary for combinatorial coding.

In **Chapter 3**, I focus on sexual dimorphism in the olfactory system of *N. vitripennis* and the role of the sex-determination genes *Tra* and *Dsx*. I analysed the sex-specific regulation of olfactory sensilla and the organization of glomeruli in the AL. My experimental results determine for the first time in a hymenopteran species how sex-determination transcription factors regulate the sex-specific number and morphology of olfactory sensilla. My electron microscopy scans provide conclusive evidence that trichoid sensilla in parasitoids are homologs of the placoid sensilla and that DSX controls the switch between these homologs in males and females. My neural tracings of OSNs reveal the number, organizational complexity and sexual dimorphism of glomeruli in the AL. These experiments show for the first time that TRA is responsible for regulating sexual dimorphism in the AL of a parasitoid wasp. Silencing *Tra* in females resulted in the loss of glomerular clusters in the AL, which indicates that TRA regulates the OSNs of specific sensilla for glomerular development. From my results, I can therefore conclude that sexual dimorphism in the AL of *N. vitripennis* originates from neuroplasticity regulated in the peripheral nervous system. In this way, TRA determines which glomerular clusters are expressed in females for perceiving sex pheromones.

In insects, there is a one-to-one relationship between the number of olfactory receptor (OR) genes and the number of glomeruli in the AL. The intricate life histories of Hymenoptera served as a driver for the expansion of their OR repertoire and the number of glomeruli in the AL. These species have evolved unique neurodevelopmental mechanisms to match the number of glomeruli to the number of expressed ORs. In **Chapter 4**, I analysed the function of the *Olfactory-receptor co-receptor* (*Orco*), a conserved chemosensory gene downstream of *Dsx*, which is known to play an important role in glomerular development in Hymenoptera. My neural tracing experiments on *N. vitripennis* confirm that the expression of *Orco* in OSNs is necessary for the formation of the adult AL. These results are consistent with studies on ant species, which show the crucial role *Orco* plays in glomerular formation. I therefore propose that *Orco* is the likely target for DSX for regulating OSN development in specific sensilla. The regulation of this gene in the OSNs of specific sensilla would enable the development of the sex-specific clusters of glomeruli I identified in **Chapter 3**.

Parasitoid wasps have evolved some of the most complex CHC profiles among insects. Species such as *N. vitripennis* depend on CHCs for close-range pheromone communication. In **Chapter 5**, I investigated how the sex-determination pathway regulates sexual dimorphism in the CHC profile of this species. My experiments verify sexual dimorphism in the relative abundance of methyl-branched (MB) alkanes, including mono-, di-, tri- and tetramethyl alkanes. My experiments show that *Tra* plays an essential role in the sex-specific splicing of downstream transcription factors that regulate considerable variation in the relative abundance of MB-alkanes in females. Silencing this gene also had a direct influence on male mating behaviour. My results provide the opportunity to identify the female CHCs that are utilized by males as species-specific mating signals. Moreover, my research elucidates the genetic mechanisms that are responsible for the diversification of the sex-specific CHC profile in parasitoid Hymenoptera.

Sexual dimorphism in the insect CHC profile originates from the sex-specific regulation of biosynthetic genes. The biosynthetic genes underlying insect CHCs diverge rapidly between closely related species, enabling individual species to form mating barriers and adapt to novel ecological environments. In **Chapter 6**, I investigated a group of such biosynthetic genes downstream of *Dsx*. These genes are called fatty acyl-CoA reductases (FARs), which are responsible for converting very long-chain fatty acids into fatty alcohols, the precursors of insect CHCs. Silencing these candidate FARs resulted in the concomitant up- and downregulation of CHC compound classes, including the MB-alkanes. My experiments therefore establish the important position and function of these genes in the CHC biosynthetic pathway for generating sex-specific diversity in the CHC profile of male and female *N. vitripennis*. I propose that the expansion of this gene family enabled the evolution of *cis*-regulatory elements in FARs to become potential targets for transcription factors like DSX, resulting in the rapid diversification and complexity of CHCs in the evolutionary history of Hymenoptera.

In **Chapter 7**, I interpret the key findings of this thesis and contextualize them within the existing body of knowledge on insect sexual differentiation. My research elucidates how sexual differentiation, neurodevelopment and biosynthesis are interlinked in the evolution of parasitoid pheromone communication. I discuss how sexual differentiation is a major driver of complex pheromone circuits in these species and the significance of *Tra* and *Dsx* in the diversification of the parasitoid pheromone profile. I elaborate on the implications and future directions of my research within the areas of evolutionary developmental biology, neuroethology and biological control.

My key findings have paved the way for further investigation into the sex-specific mechanisms shaping the coevolution of pheromone production and perception in insects. I recommend investigating how modifications in *cis*-regulatory elements can lead to the production of novel complex pheromones and the formation of their corresponding coding mechanisms. I provide significant insight into the neurodevelopmental mechanisms shaping the evolution of pheromone coding in parasitoids and advise further investigation into how *Tra* and *Dsx* have facilitated the evolution of neurodevelopmental mechanisms and combinatorial coding in these species. Parasitoid wasps have become increasingly invaluable biocontrol agents and play a crucial role in agricultural and natural ecosystems to reduce invasive pests in an ecologically sustainable way. My research has provided significant groundwork for comparative studies and future research into how sex determination regulates insect olfaction and the role that *Tra* and *Dsx* play in the evolution of parasitoid behaviour.

Acknowledgements

The title of my PhD thesis is Pathways to Perception. My own pathway to complete it has taken many hours of deliberation, research, analysis, writing the results and drawing conclusions. There have been many highs and quite a few lows along the way. However, what I have learned on my journey is that such an undertaking would never have been finished without the generous efforts, support and constructive criticism of friends, colleagues and family. Nothing stands in isolation. So, in light of this, I would like to take this opportunity to say something about some of the people who I had the great fortune to meet along the way: people who helped me and who left a positive impression on me while following my own personal pathway.

Firstly, I would like to thank my wonderful parents for their unwavering and loving support. They were there for me during every step I took on my journey towards becoming a scientific researcher. Not only in the role of loving parents, but also in the development of my passion for the natural environment and for entomology, stimulating my aspirations and providing guidance and a listening ear right up to finalizing my PhD. They showed more than a keen interest in my research topic and provided critical feedback to keep me on my toes. As their son, I have always felt very fortunate and could not have asked for anything more.

Happy coincidence enables some pathways to cross at just the right time and bring us into contact with individuals who help determine the course and direction of our future careers. I feel extremely blessed to have come into contact with my supervisor **Eveline Verhulst**. Eveline is one of those rare individuals who draws out the best in people. She delights in your high points and offers the necessary advice and support in times of adversity. She provided the flexibility that enabled me to pursue my interests and encouraged me to develop my own niche. For this I am eternally grateful. Thank you Eveline for giving me this wonderful opportunity and I look forward to working with you long into the future.

Another such inspirational figure for me is **Hans Smid**, who introduced me to the Entomology chair group in Wageningen and the subject of insect neurobiology. Together with Eveline, you diligently supervised my MSc thesis, which ultimately sowed the seed that would blossom into my PhD research project. Thank you Hans for your friendship, encouragement and expertise, you continue to be a mentoring figure for me.

Marcel Dicke introduced me to the subject of parasitoidism for the first time during his lecture on ecological aspects of bio-interactions. I was immediately hooked. His steadfast support, guidance and advice throughout my entire PhD cannot be overstated and I am grateful for having joined the chair group when I did. Thank you Marcel for being an inspirational figure to us all and for fostering a sense of community within the chair group where we could all feel at home.

This major endeavour could not have been accomplished without the substantial support of motivated and gifted BSc and MSc students. **Karthick Gajendiran**, you were my first thesis student. Your dedication and determination during my experimental research serve as an example to us all. It comes as no surprise to learn that you have gone on to further your research career in plant sciences. I wish you all the best. **Gabriel Charvalakis**, I remember how I was positively taken aback to actually meet someone who was just as eager to discuss insect neurobiology as I am. Working with you during your thesis project, Gabriel, was a real highlight of my PhD. **Jimmie Zeelenberg**, it was both surprising and inspiring to see how the dedication of a single person could make such a substantial contribution to my project, especially during all the constraints during Covid. **Jade van Doorn**, I thank you not only for your amazing work ethic, but also for your jolly and bubbly character, which is a must for every workplace. It was a great pleasure working with you. **Jeldert Dam**, I was immediately struck by your independence and resourcefulness: a great example to everyone pursuing an academic career. **Anna Haaring**, you were amazing in carrying out many behavioural assays. Your dedication saved me a lot of time in my experimental research. Thank you. **Lex Koekkoek**, carrying out the laborious 3D reconstructions of parasitoid brain samples was an unenviable task. I am extremely grateful for your perseverance.

A PhD project is anything but a solo enterprise, but a joint effort involving collaborators who provide additional expertise and resources. I would particularly like to thank my collaborators at the universities of Münster and Regensburg in Germany for sharing their knowledge and contributing to the advancement of my research. **Jan Büllesbach** and **Weizhao Sun**, thank you for hosting me at your department and for carrying out GC-MS analyses. But also for showing me around in the vibrant city of Münster. I not only enjoyed my stay and visits to the local pubs, but also sharing ideas and our many discussions. **Joachim Ruther**, although we have only met online, you have always been a ready and willing participant in my research. You have been an inspiring figure for me in the field of parasitoid chemical ecology. I would like to thank you heartily for our long-lasting collaboration and for your help in advancing my research into discovering the mysteries of parasitoid pheromone communication.

I was also very fortunate to be surrounded by supportive colleagues who share a common interest in pursuing the molecular mechanisms underlying sex determination in parasitoid wasps. **Yidong Wang**, as one of the first members of the InSexDet team, you helped me become quickly familiarized with the more nitty-gritty aspects of *Nasonia* molecular biology. Thank you sincerely for passing on this valuable knowledge, which I could often fall back on during my own research. **Filippo Guerra**, your continuous positive attitude in the team has benefited us all. Thank you for generously assisting me during my own molecular experiments throughout my PhD, but especially for all the fun moments in the lab and during our joint conference visits. **Julien Rougeot**, you are a real people person, who right from the start made me feel comfortable within the team. I am extremely grateful for all your advice and practical experience on the finer points of molecular biology. And **Saminathan Sivaprakasham**

Murugesan, you may have recently left the team, but your outgoing personality and friendly, approachable nature will live with me for a long time. Thank you and good luck with your endeavours in Malaysia and Thailand.

At the Entomology chair group in Wageningen there is always a sense of belonging and community. I cannot think of a better place to have carried out my research. Everybody at Entomology has the best intentions at heart. So I would simply like to thank everyone who has in one way or other assisted or facilitated me during this period. My fellow PhD colleagues **Parth Shah**, **Mitchel Bourne**, **Thibault Costaz** and **Katherine Barragán Fonseca**, I really appreciated our discussions and your motivational pep talks. To all the teaching and research staff at Entomology, thank you all. I am sure I must have called on your help or advice at one time or another. That is certainly the case with **Alexander Haverkamp**, who I first met when he joined Entomology as a post-doctoral researcher. We were immediately drawn together because of our related areas of research and our shared common ground. Thank you Alex for the numerous extensive discussions we have had over the years. I have always valued your insightful input, ideas and critical thinking. It was also a pleasure to work with you on our joint article and I trust this will be the first of many to come. And last, but certainly not least, I would like to extend my gratitude to all the support staff at Entomology, whose important contribution is often overlooked, but who work tirelessly to ensure everything runs smoothly. In particular, I would like to thank **Hariëtte Nijnens**, who possesses the incredible ability of putting a smile on a face and generating a good atmosphere. Thank you Hariëtte for all the nice moments and I hope it is not the last I see of you.

Over the past years, I have also been fortunate enough to develop close friendships, many of which have provided me with emotional support and encouragement during my PhD journey. **Jeroen Alkema**, you were already at the Entomology chair group when I joined as an MSc student and you became an inspiring figure for me in the field of insect behaviour. We had many stimulating discussions on insect mate choice, sexual selection and evolution. And you were a great source of support when I was still establishing myself during the initial stages of my project. Carrying out experiments late into the evening can be a solitary and often stressful exercise. Thankfully, however, I was fortunate enough to share many an evening in the company of **Alessandro Roman**. I am grateful that we could keep each other company during these late hours in the molecular lab and for our friendship. But also for your good taste in pizza and pasta, which we have enjoyed together on numerous occasions. Thank you for being such a great sounding board and I hope our friendship will continue for a long time. **Gabriel Charvalakis**, from thesis student, to close friend, to best man at my wedding. Thank you, Gabriel, you are one in a million.

And finally to my loving wife, words alone can never express how grateful I will always be that our pathways crossed. Thank you dear Lotte for being there during all my ups and downs. You are my beacon of light.

About the author

Aidan Williams was born in Roermond in the Netherlands on the 14th of January 1992 to a Dutch mother and an English father. His parents felt it important not to impose any particular aspirations on their son, but to provide him with the space and encouragement to develop his own particular interests and ambitions. Already at a young age, he felt an instinctive affinity with the natural environment, albeit after having an unpleasant encounter with dung beetles! By his early teens, while still at school, when his peers were spending most of their free time on the football field, Aidan was spending every opportunity running around flower meadows and wading through ponds and streams chasing after and identifying everything that caught his eye. He became a member of the regional natural history society, carried out field research and published articles and reports on subjects ranging from moths and butterflies, grasshoppers, dragonflies, an invasive harvestman and water bugs. He even (re)discovered a population of a rare leaf beetle, thought to have long disappeared from the Netherlands. It was a passion that would lead him to the conclusion that there was only one discipline he wanted to study and pursue his career in.

Aidan received his Bachelor's degree in Biology and Ecology from HAS University of Applied Sciences, the highlight of which was spending a six-month internship at the Senckenberg Deutsches Entomologisches Institut under the supervision of Prof. Thomas Schmitt researching the population ecology of butterflies. He then moved to Wageningen to undertake his Master's degree in biology. He was immediately drawn to the international standing of the university in life sciences and its credo of 'exploring the potential of nature to improve the quality of life'. Most importantly it offered him the flexibility to choose his own study programme and specialisation, which for him would be evolution and biodiversity.

Aidan had a clear vision of the direction he wanted to follow. However, this meant seeking out a suitable research topic for his thesis that was not only exciting and challenging, but also novel. He had the good fortune to find his way to Hans Smid and Eveline Verhulst from the Laboratory of Entomology. Hans was studying the neurobiology of parasitoid wasps and Eveline was researching the molecular pathways governing sexual dimorphism in insects. These two inspiring figures would introduce him to a specialisation which he would go on to embrace and fill him with passion. His Master's thesis on sexual dimorphism in the antennal

lobe of the parasitoid wasp *Nasonia vitripennis* would go on to win the annual Darwin Award from the National Congress Biology Students. Following on from this internship, Aidan travelled to the prestigious Max Planck Institute for Chemical Ecology in Jena to research the processing properties of excitatory local interneurons in the antennal lobe of *Drosophila melanogaster* under the supervision of Prof. Silke Sachse of the Olfactory Coding Group. It was an intensive period of concentrated dedication.

On his return to Wageningen, Aidan was rewarded for all his stamina and hard work with the opportunity of continuing his research as a PhD candidate under the expert guidance of Eveline Verhulst. The subject area would encompass the fields of genetics, molecular biology, biochemistry and neurobiology. His research focuses on the neural mechanisms and molecular pathways underlying odour perception, processing and communication in insects and the evolutionary forces that shape sexually dimorphic traits. Aidan is a consummate researcher and recently wrote a grant proposal aimed at continuing his work in this exciting field.

Aidan's journey has not always been plain sailing and he has had to overcome more than his fair share of hurdles in life. But he has always met these with a sense of perseverance and inner strength. His experiences have shaped him into the person he is, someone who meets adversity with quiet determination and resilience. His pleasant disposition and humility make him both approachable and engaging. He has a kind, respectful and cooperative nature and a readiness to help others when needed. Qualities he hopes will serve him well in his future academic career.

Aidan's story continues to be written, both professionally and personally. In 2024, Aidan married Lotte. They look forward to building and enjoying a wonderful life together.

Education statement

PE&RC Training and Education Statement

With the training and education activities listed below the PhD candidate has complied with the requirements set by the Graduate School for Production Ecology and Resource Conservation (PE&RC) which comprises of a minimum total of 30 ECTS (= 20 weeks of activities)

Review/project proposal (6 ECTS)

- Review: A unique sense of smell: development and evolution of a sexually dimorphic antennal lobe–a review.
- Project proposal: Variations on a common theme: evolutionary transitions in the Nasonia pheromone communication system.

Post-graduate courses (4.5 ECTS)

- Functional imaging, LCAM, UvA (2022)
- qBase+, qbasePLUS (2020)
- Tidy data transformation and visualization with R, WGS (2022)

Laboratory training and working visits (3 ECTS)

- Genes involved in cuticular hydrocarbon biosynthesis in parasitoids, University of Münster (2022)

Invited review of journal manuscripts (3 ECTS)

- Entomologia Experimentalis et Applicata, Cuticular hydrocarbons in honeybees (2021)
- Proceedings of the Royal society B: Biological Sciences, Cuticular hydrocarbons in parasitoid wasps (2022)
- PeerJ, Sex-specific splicing of genes involved in Drosophila male mating behaviour (2022)
- Peer Community in Zoology, High-throughput techniques for quantifying behavioural traits in Drosophila (2023)
- Insects, Sex-determination genes in planthoppers (2024)

Competence, skills and career-oriented activities (3.3 ECTS)

- Project and time management, WGS (2022)
- Scientific writing, WGS (2023)

Scientific Integrity/Ethics in science activities (0.6 ECTS)

- Scientific integrity, WGS (2022)

PE&RC Annual meetings, seminars and PE&RC weekend/retreat (1.5 ECTS)

- PE&RC First year retreat (2019)
- PE&RC Day (2019, 2021)

National scientific meetings, local seminars, and discussion groups (5.5 ECTS)

- Annual meeting of the Netherlands Entomological Society (2019, 2022, 2023, 2024)
- Insect Plant Interactions (IPI) / Ento seminars (2019-2023)
- National Conference Biology Students (winner of the Darwin Award) (2019)
- Netherlands Annual Ecology Meeting (presented during the meeting) (2020)
- Olfactomics: a comparative olfactome platform connecting and accelerating research in insect olfaction (2021)
- National Conference Biology students (invited to chair the conference) (2021)
- National Conference Biology students (elected as jury member for the Darwin Award) (2023)

International symposia, workshops and conferences (4.6 ECTS)

- 36th Annual Meeting of the International Society of Chemical Ecology, Stellenbosch (2021)
- Meeting of the European non-drosophilid sex determination researchers, Schiermonnikoog (2022)
- 5th International Nasonia meeting, Münster (2023)

Societally relevant exposure (0.3 ECTS)

- Interview for article in Dutch magazine Bionieuws (2019)

Lecturing/Supervision of practicals/tutorials (4.5 ECTS)

- Behavioural Ecology (2020 – 2022)
- Ecological Aspects of Bio-interactions (2020 – 2022)

BSc/MSc thesis supervision (6 ECTS)

- Research topic 1: Genetic regulation of pheromone production and mating behaviour in parasitoid wasps.
- Research topic 2: Developing new methods for tracing neurons in the brain of parasitoid wasps.
- Research topic 3: Characterizing and quantifying sensory organs on the antennae of parasitoid wasps.
- Research topic 4: Identifying genes involved in the biosynthesis of pheromones in parasitoid wasps.
- Research topic 5: Genetic regulation of mate-recognition behaviour in parasitoid wasps.
- Research topic 6: Sex-specific regulation of pheromone perception in parasitoid wasps.
- Research topic 7: Identifying genes involved in brain development in parasitoid wasps.

The research presented in this thesis was performed at the Laboratory of Entomology of Wageningen University & Research (WUR) and was supported by the Dutch Research Council (NWO VIDI Talent grant 016.Vidi.189.099 to Eveline C. Verhulst).

Printed by ProefschriftMaken, Wageningen, the Netherlands